HTR-TN 2002

Transactions

Oral Presentations and Posters

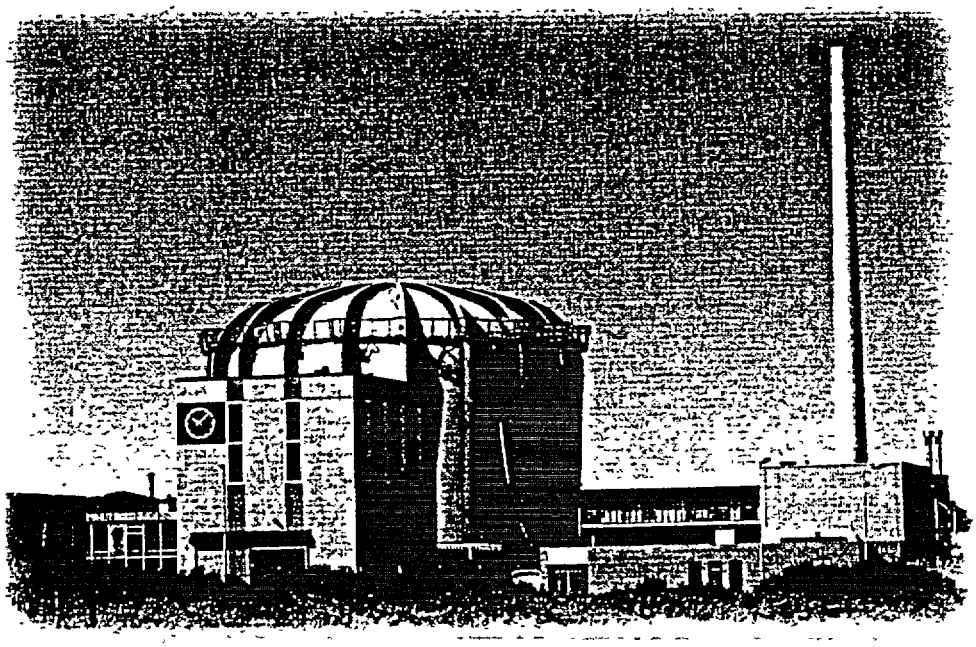

1st International Topical Meeting on
High Temperature Reactor Technology (HTR)
April 22–24, 2002, Petten, The Netherlands
Organised by the European Nuclear Society

C-12

European Nuclear Society
Belpstrasse 23
P. O. Box 5032
CH-3001 Berne/Switzerland

Phone Number: +41 58 286 61 11
Fax Number: +41 58 286 68 45

E-mail: htr2002@to.aey.ch
http://www.euronuclear.org/meetings

Shanlai Shi

HTR-TN 2002

1st International Topical Meeting on

High Temperature Reactor Technology (HTR)

Petten, The Netherlands

April 22 - 24, 2002

Organised by the European Nuclear Society

in cooperation with the International Atomic Energy Agency

Invited and Contributed Papers

Oral and Poster Presentations

HTR-TN 2002 Programme Committee

J. Guidez	(JRC), Chairman
T. Abram	(BNFL)
M. Chapelot	(CEA)
G.Greyvenstein	(Potchefstroom University)
D. Hittner	(Framatome ANP)
A. Kadak	(MIT)
M. Methnani	(IAEA)
M. Kiryushkin	(OKB)
G.Lohnert	(Stuttgart University)
M Hugon	(DG RTD)
D. Nicholls	(PBMR)
E. Rodwell	(EPRI)
S. Shiozawa	(JAERI)
T. Van der Hagen	(IRI/Delft)
A. Van Heek	(NRG)
R. Versluis	(DOE)
W. Von Lensa	(FZ Julich)
Yuanhui Xu	(INET)
Anthony Hunter	(ENS), Secretary

Published by the European Nuclear Society (ENS)

Belpstrasse 23, P.O. Box 5032, CH-3001 Berne (Switzerland)

Phone: +41 58 286 61 11 Fax: +41 58 286 68 45

Session 1: HTR Projects and Programmes

Page

USA Programme Status 1
R.M. Versluis, US Department of Energy, USA

Japanese Position and Status 3
S. Shiozawa, Department of Advanced Nuclear Technology, JAERI, Japan

Chinese Point and Status 5
Y. Xu, INET, Tsinghua University, China

The PBMR Project 7
NN, Eskom, South Africa

The GTHMR Project 9
A. Kiryushin, N. G. Kodochigov, OKB Mechanical Engineering , Russia

European Position in HTR-TN 14
D. Hittner, FRAMATOME-ANP, France

Session 2: Fuel and Fuel Cycle

Key Differences in the Fabrication of U.S. and German TRISO-coated Particle Fuel, and their Implications on Fuel Performance 17
D. A. Petti, J. Bongiorno, J. T. Maki and G. K. MillerIdaho National Engineering & Environmental Laboratory, Idaho National Engineering and Environmental Laboratory, USA

High Temperature Reactor Fuel Technology Programme in Europe 24
A. Languille, C. Perrais, M. Perez*, P. Obry, CEA Cadarache, Grenoble*, R. Conrad, CEC/JRC/IE Petten, P. Guillermier, FRAMATOME-ANP/Lyon, H. Nabielek, H. Werner, FZJ/Jülich, D. Haas, J. Somers, H. Toscano, JRC/ITU Karlsruhe, K. Bakker, NRG/Petten, T. Abram, BNFL

Microspheres of UO2, THO2 and PUO2 for the High Termperature Reactor 29
E. Brandau, Brace GmbH, Germany

Development of an Integrated Performance Model for TRISO-Coated Gas Reactor Particle Fuel 34
G. K. Miller, D. A. Petti and J. T. Maki, Idaho National Engineering and Environmental Laboratory, USA

Prospective Studies of HTR Fuel Cycles Involving Plutonium 40
B. Bonin and D. Grenache, Cogema, F. Carré, F. Damian and J. Y. Doriath, CEA Direction de l'Energie Nucléaire, France

Examination of the Potential for Diversion or Clandestine Dual Use of a Pebble-Bed Reactor to produce Plutonium 52
A. Ougouag, W. K. Terry and H. D. Gougar, Idaho National Engineering and Environmental Laboratory, USA

Deep Burn Transmutation of Nuclear Waste 58
C. Rodriguez, A. Baxter and D. McEachern, General Atomics, Francesco Venneri, Los Alamos National Laboratory and General Atomics and D. Williams, Oak Ridge National Laboratory, USA

Session 3: Physics and Neutronics

Analysis of the European Results on the HTTR's Core Physics Benchmarks 65
X. Raepsaet, F. Damian, CEN Saclay, France, U. A. Ohlig, H. J. Brockmann, Research Centre Jülich, Germany, J. B. M. De Haas, NRG/Petten and E. M. Wallerboss, Interfaculty Reactor Institute, Delft, The Netherlands

Investigation of Criticality Parameters of High-Temperature Reactors at the Kurchatov Institute's ASTRA Critical Facility 70
N. E. Kukharkin, E. S. Glushkov, G. V. Kompaniets, V. A. Lobyntsev, D. N. Polyakov, O. N. Smirnov, Institute of Nuclear Reactors, RRC Kurchatov Institute, Russia

Design of Spherical and "Hollow" Burnable Particles for UO_2 Fuels in High Temperature Reactors 75
J. L. Kloosterman, H. van Dam and T. H. J. J. van der Hagen, Interfaculty Reactor Institute, Technical University, Delft, The Netherlands

Matrix Formulation of Pebble Circulation in the PEBBED Code 80
H. D. Gougar, W. K. Terry and A. M. Ougouag, Idaho National Engineering and Environmental Laboratory, USA

Physics Studies for a Particle-Bed Gas Cooled Fast Reactor Core Design 86
T. A. Taiwo, M. Fatone, G. Palmiotti and R. N. Hill, Reactor Analysis and Engineering Division, Argonne National Laboratory, USA

Models for Neutronics Calculations for HTR Pebble Bed Modular Reactors 91
W. Bernnat and W. Feltes, University of Stuttgart, Germany

An Evaluation of the Control Rod Modelling Approach used in VSOP by Comparing its Results to the Experiments Performed in the ASTRA Critical Facility 93
F. Reitsma, D. Naidoo and Z. Karriem, Radiation and Reactor Theory, NECSA, Pretoria, South Africa

Creation of the Equilibrium Core PBMR ORIGEN-S Cross Section Library 100
C. C. Stoker, F. Reitsma and Z. Karriem, Radiation and Reactor Theory, NECSA, South Africa

HTR core physics analysis at NRG 106
J. C. Kuiper, J. B. M. de Haas and J. Oppe, Fuels, Actinides & Isotopes Department, NRG, The Netherlands

Neutronic Features of the GT-MHR Reactor 111
N. Kodochigov, Yu. Sukharev, E. Marova, OKB Mechanical Engineering, N. Ponomarev-Stepnoy, E. Glushkov and P. Fomichenko, RRC Kurchatov Institute, Russia

Session 4: Thermohydraulic Calculation

Three-dimensional Numerical Simulation of Flow and Heat Transport in a High-Temperature Reactor 119
S. Becker and E. Laurien, Institute for Nuclear Technology & Energy Systems, Germany (IKE), University of Stuttgart, Germany

Decay heat removal by passive means in case of a block type HTR reactor core - CFD Analysis 124
A. Woaye-Hune and S. Ehster, FRAMATOME-ANP, France

Thermal Hydraulic Simulations on High Temperature Reactors 126
N. Tauveron, M. Elmo, O. Cioni, T. Chataing, CEA/Grenoble, France

Steady-state and Accident Analyses of PBMR with the Computer Code SPECTRA 131
M. M. Stempniewicz, NRG/Arnhem, The Netherlands

Design of a Physical Model of the PBMR with the Aid of Flownet 141
G. P. Greyvenstein and P. G. Rousseau, Department of Mechanical Engineering, Potchefstroom University, South Africa

Flow Distribution of Pebble Bed High Temperature Gas Cooled Reactors Using Large Eddy Simulation 148
Y. A. Hassan and G. Gokhan Yesilut, Department of Nuclear Engineering, Texas A&M University, USA

Session 5: Engineering, Design and Applications

GTHTR300 System Design Features and Performance 157
X. Yan, K. Kunitomi, T. Nakata and S. Shiozawa, Japan Atomic Energy Research Institute, Japan

Design of a Power Conversion System for an Indirect Cycle, Helium Cooled Pebble Bed Reactor System 164
C. Wang, R. G. Ballinger and P. W. Stahle, Department of Nuclear Engineering, Massachusetts Institute of Technology, USA

Thermodynamic assessment of plant efficiencies for HTR power conversion systems 175
W. Fröhling, H.–M. Unger, Research Centre Jülich, Germany and Y. Dong, Institute of Nuclear Energy Technology, Tsinghua University, China

Load Analysis and Safety Evaluation of HTR-10's Hot-Gas Duct Vessel 180
H. Shu-Yan, Z. Zheng-Ming, Y. Su-Yuan, Division of Reactor Structure & Mechanics, Institute of Nuclear Energy Technology, NET, Tsinghua University, China

ACACIA-Indirect: A Small Scale Nuclear Plant for New Markets 185
D. F. Da Cruz, J. B. M. de Haas and A. I. van Heek, NRG/Petten, The Netherlands

The Concept Design of the Power Conversion Unit for HTR-10 with Direct Gas Cycle 190
S. Yu, Z. Zhang, Z. Wu, Y. Xu and Y. Sun, Institute of Nuclear Energy Technology, Tsinghua University, China

Burn-up Dependent Core Neutronic Analysis for PBMR 194
Y. Cecen, U. Colak and O. K. Kadiroglu, Department of Nuclear Engineering, Hacettepe University, Turkey

Economic Study of Seawater Desalination for 300MW(E) High Temperature Gas-Cooled Reactor (HTR) by Reverses Osmosis (RO) 201
L. Tian, J. Guo and Y. Sun, Institute of Nuclear Energy Technology, Tsinghua University, China

Session 6: Materials and Components

Operating Experience with the Dragon High Temperature Reactor Experiment 205
R. A. Simon, DRAGON Operation Branch/EC (retired), Belgium and P. D. Capp, DRAGON Operations Branch/UKAEA (retired), United Kingdom

The relation between irradiation induced dimensional change and the coefficient of thermal expansion: A new look 210
G. Hall, B. J. Marsden, A. Fok and J. Smart, Nuclear Graphite Technology Group, University of Manchester. United Kingdom

Comparison of Cycle Efficiency, Turbine Efficiency and Recuperator Heat Transfer Surface Area between Direct Cycles of Carbon Dioxide and Helium 215
Y. Kato, T. Nitawaki and Y. Muto, Research Laboratory for Nuclear Reactors, Tokyo Institute of Technology, Japan

Session 7: Safety and Licensing

Studies on Air Ingress for Pebble Bed Reactors 223
R. L. Moore, C. H. Oh, B. J. Merrill and D. A. Petti, Idaho National Engineering and Environmental Laboratory, USA

Nuclear Emergency Planning and Preparedness for the HTR-10 228
J. Qu and Z. Wu, Institute of Nuclear Energy Technology, Tsinghua University, China

HTR Confinement/Containment Question 233
G. Brinkmann, Framatome ANP GmbH, Germany and S. Esther, FRAMATOME-ANP, France

Lessons learned during the Safety Assessment of the THTR for further Developments and Assessments of HTR 236
R. Sartori, Department of Machine Technology, Stress Analysis, Nuclear Technology and K. Hofman, Subdivision Energy and Environment, RWTÜV Anlagetechnik GmbH, Germany

Posters

Thermal Characteristics Research of Circular High Temperature Gas-Cooled Reactors under Loss-Cooling and Depressurisation Crisis 241
T. Qin and Z. Gao, Institute of Nuclear Energy Technology, Tsinghua University, China

A Combined Experimental and Finite Element Analysis of MANETII Steel Fracture Proporties 247
K. Ahmed and M. Ghonim, Atomic Energy Authority, Egypt

HTR-E Project. High temperature Components and Systems 249
E. Breuil, FRAMATOME-ANP, France and R. Exner, Borsig Energy GmbH, Germany

Graphite Materials Testing in the ATR for Lifetime Management of Magnox Reactors 329
S.B. Grover, Idaho National Engineering and Environmental Laboratory, USA and M. P. Metcalfe, British Nuclear Fuels plc, Research and Technology, Berkeley Centre, United Kingdom

Energy Storage and Release Calculations for HTR-10 Reflector 336
U. Colak, H. Dikmen and U. E. Sikik, Nuclear Energy Department, Hacettepe University, Turkey

CEA methods improvement in HTTR modelling 343
F. Damian and X. Raepsaet, CEA, France

The Behaviour of Fission Products in the HTGR Fuel Irradiated in the IVV-2M Reactor 345
K. N. Koscheyev, Sverdlovsk Branch of R&D Institute of Power Engineering Zarechny and A. S. Chernikov, RPA "Lutch", Russia

Conceptual Design of a Simultaneous Hydrogen and Heavy Water Production System for High Temperature Reactors 350
H. Chung, D. H. Ahn, M. Lee, S. Paek and J. H. Chang, Korea Atomic Energy Research Institute, Korea

Thermodynamic Analysis of PBMR Plant 355
S. Sen and O. K. Kadıroglu, Nuclear Energy Department, Hacettepe University, Turkey

The measurement of burn-up level in HTR-10 261
L. Zhengpei, I. Wenfeng, H. Song and L. Fu, Institute of Nuclear Energy Technology, Tsinghua University, China

Overview of LEI investigations on heat transfer and flow structure in gas-cooled packed beds of spheres and channels 266
J. Vilemas, E. Uspurus, S. Rimkevicius, A. kaliatka, P. Pabarcius, Lithuanian Energy Institute, Lithuania

A High Temperature Reactor for ship propulsion 276
P. Lobet, R.Seigel, Ecole de application militaries de l'energie atomique, France and A. C. Thompson, R. M. Beadnell and P. A. Beeley, HMS Sultan, Nuclear Department, United Kingdom

Materials for the High Temperature Reactor 282
D. Buckthorpe, NNC, United Kingdom, R. Couturier, CEA/Grenoble, France, B. van der Schaaf,, NRG/Petten, The Netherlands, B. Riou, FRAMATOME-ANP, France, H. Rantala, JRC/Petten, The Netherlands, K. Kuehn, Research Centre Jülich, Germany, A. Buenventura, Empresarios Agrupados Internacional SA, Spain and B-C. Friedrich, Framatome ANP GmbH, Germany

The numerical determination of the variation in the porosity of Pebble-bed core 287
C. du Toit, School for Mechanical and Materials Engineering, Potchefstroom University, South Africa

Analysis of Operational Transients in a Fluidized Bed Nuclear Reactor 292
A. Agung, D. Lathouwers, T. H. J. J. van der Hagen, H. van Dam, Interfaculty Research Institute, Delft University of Technology, The Netherlands and C. C. Pain, C. R. E. Oliviera, A. J. H. Goddard, Department of Earth Science and Engineering, Imperial Colleage of Science, Technology and Medicine, United Kingdom

Conceptual design of a passive, inherently safe emergency shutdown rod for High Temperature Reactor applications 297
A. M. Ougouag, W. K. Terry and R. R. Schultz, Idaho National Engineering and Environmental Laboratory, USA

An inherent safe HTGR power plant: An innovative design concept 303
A. Hodzic, Environment & Energy Engineering EEE, Germany

An In-Depth Study on Oscillation Peculiarities by Step-Input of Reactivity and Frequency of Helium Fan's Transducer of 10 MW High Temperature Gas-Cooled Reactor and its Control Strategy 305
X. Huang, Institute of Nuclear Energy Technology, Tsinghua University, China

Thermal Insulation for Hot Gas Ducts 311
P. Bröckerhoff, Forschungszentrum Jülich, Germany

Stress and Seismic Calculation of HTR-10 SG Accident Discharge System 313
J. Dong, J. Fu and S. Yu, Institute of Nuclear Energy Technology, Tsinghua University, China

Modelling of the HTTR in Flownet 318
P. Rousseau and G. P. Greyvenstein, School of Mechanical & Ematerials Engineering, Faculty of Engineering, Potchefstroom University, South Africa

EC-Funded Project (HTR-L) for the Definition of a European Safety Approach for HTR's 323
S. Ehster, FRAMATOME-ANP, France, M. T. Dominguez, Empresarios Agrupados Internacional SA, I. Coe, NNC Ltd, United Kingdom, G. Brinkmann, Framatome ANP GmbH, Germany, W. von Lensa, Research Vcentre Jülich, Germany, W. van der Mheen, Nuclear Research and Consultancy Group, The Netherlands, C. Allessandroni, Ansaldo Nucleare, Italy and J. Pirson, Tractebel Energy Engineering, Belgium

Session 1

HTR Projects and Programmes

USA PROGRAMME STATUS

R.M. Versluis, US Department of Energy, USA

Paper will be handed out separately

JAPANESE POSITION AND STATUS

S. Shiozawa, Department of Advanced Nuclear Technology, JAERI, Japan

Paper will be handed out separately

CHINESE POINT AND STATUS

Y. Xu, Institute of Nuclear Energy Technology, Tsinghua University, China

Paper will be handed out separately

THE PBMR PROJECT

Eskom, South Africa

Paper will be handed out separately

GTMHR PROJECT

A. I. KIRYUSHIN, N.G. KODOCHIGOV
OKB Mechanical Engineering
15, Burnakovsky proezd, 603074 Nizhny Novgorod,
Russian Federation

ABSTRACT

The paper presents new generation reactor - modular helium reactor with gas turbine (GT-MHR), which satisfies the requirements of the developing nuclear power.
The paper describes the reactor plant and peculiarities of GT-MHR technical concept, such as high efficiency (about 48%) of electric power generation, increased safety of the plant, etc.
The technologies, which are the innovative essence of GT-MHR project, are:
- ceramic design of plutonium oxide fuel based on multilayer fuel particles, which confine fission products at high temperatures (~1600 °);
- the advances in large gas turbines;
- electromagnetic bearings;
- high effective compact recuperators.

Also, main technical and economical indices of GT-MHR project are presented.

1. Introduction

One of new generation power plants meeting the requirements of developing wide-scale atomic energy is gas turbine modular helium reactor plant (GT-MHR). GT-MHR Project is included into "Strategy for atomic power development in Russia for the first half of the XXI century". GT-MHR Conceptual Design was developed in 1997, adopted by Minatom of Russia and supported by international review in Paris.
Survey of the GT-MHR fuel cycles showed good capabilities of this reactor for weapon-grade plutonium burnup. Therefore, in 1999 the activities on development of the prototype plant Preliminary Design were carried out within the framework of Agreement between the Russian Federation and USA governments on research cooperation as for handling of plutonium extracted from military programs dated July 24, 1998. Load design and research institutes of Russia participated in Preliminary Design activities, such as: OKBM, RRC "KI", VNIPIET, VNIINM, SCC, NPO "Luch", etc. USA participants of the Project were: General Atomics, Oak Ridge National Laboratory, Framatome ANP (France) and Fuji Electric (Japan).

2. GT-MHR concept description

GT-MHR of modular reactor design and direct gas-turbine cycle ensures:
- high efficiency of electric power generation (efficiency ~ 50%)
- safety upgrade stipulated by inherent properties of the plant safety
- effective utilization of nuclear fuel and opportunity to implement various fuel cycles (uranium, plutonium, thorium)
- reduction of thermal and radiation impact to environment per unit of electric power generation
- possibility to use water hydrogen fabrication, for example, for process purposes.

Main indices of the GT-MHR prototype plant are presented below.

Description	Indices
1 Plant capacity: - thermal, MW - electric, MW	 600 285
2 Power conversion cycle	Brayton, with gas turbine in the primary circuit
3 Power conversion system efficiency	47.54%
4 Capacity factor	0.85
5 Core type	Annular of prizmatic FA
6 Fuel type	Microspheres of multi-layer ceramic coating
7 Fuel rating	6.5 MW/m^3
8 Average fuel burn up	640 MW·day/kg Pu-239
9 Fuel life duration	840 days – for plutonium fuel
10 Operation duration between refueling	280 days
11 Refueling duration	25 days
12 Refueling ratio	3
13 Design service life of basic equipment	60 years
14 Basic construction date	3 years
15 Total construction cost	355 US M $
16 Specific construction cost	1245 $/kW
17 Electric power prime cost	1.62 cent/kW

GT-MHR reactor unit consists of two integrated units: modular high-temperature and power conversion system with direct gas-turbine cycle (Fig. 1).

The modular helium reactor concept is based on the use of the core with graphite, fuel in form of microspheres with multi-layer ceramic coating and helium as the coolant. There are no metalwork in the core, at all. It allows helium temperature at reactor outlet of 850 °C and more that provides high efficiency of electric power generation in direct gas-turbine cycle, as well as GT-MHR to be used as the source of high-temperature process heat. Fuel particles with multi-layer ceramic coating allow high burnup to be ensured at very high temperatures of fuel element coating, which can not be achieved in other reactor plants.

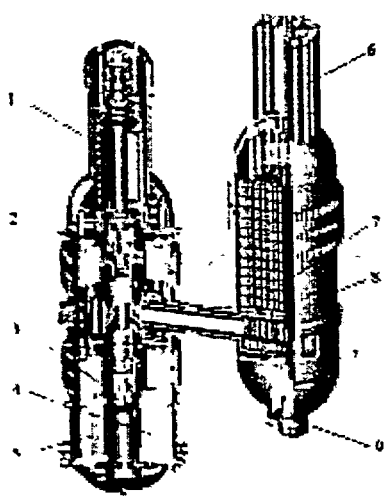

The power conversion system implementing closed gas-turbine cycle is completely arranged in PCS vessel. The turbomachine consists of generator, gas turbine, and two compressor sections mounted in a single-shaft structure completely suspended on electromagnets. PCS includes three compact heat exchangers: high efficiency recuperator, water-cooled precooler and intercooler.

Fig.1 GT-MHR reactor unit: 1 – generator; 2 – recuperator module; 3 – turbocompressor; 4 – intercooler module; 5 – precooler module; 6 – CPS assembly; 7 – core; 8 – vessel system; 9 – reactor shutdown cooling system

The reactor unit and associated primary systems are arranged in the underground building (Fig 2).

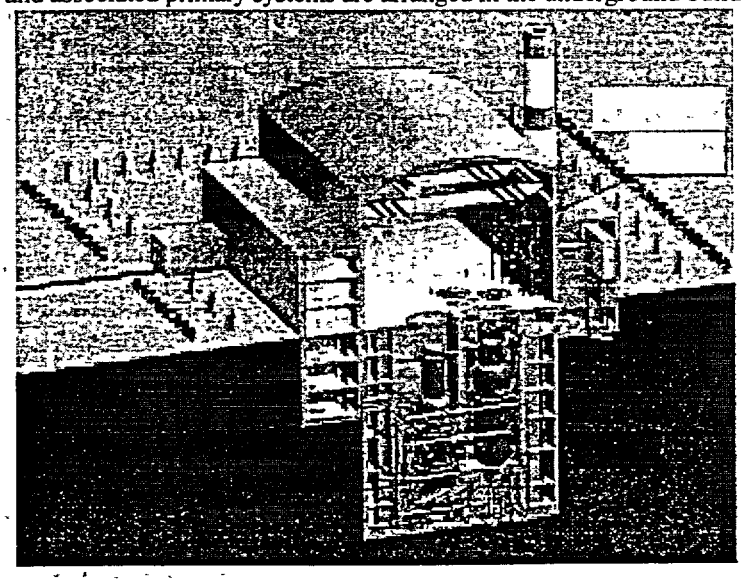

Fig. 2. GT-MHR module.

The schematic diagram of GT-MHR plant is given in Fig. 3.

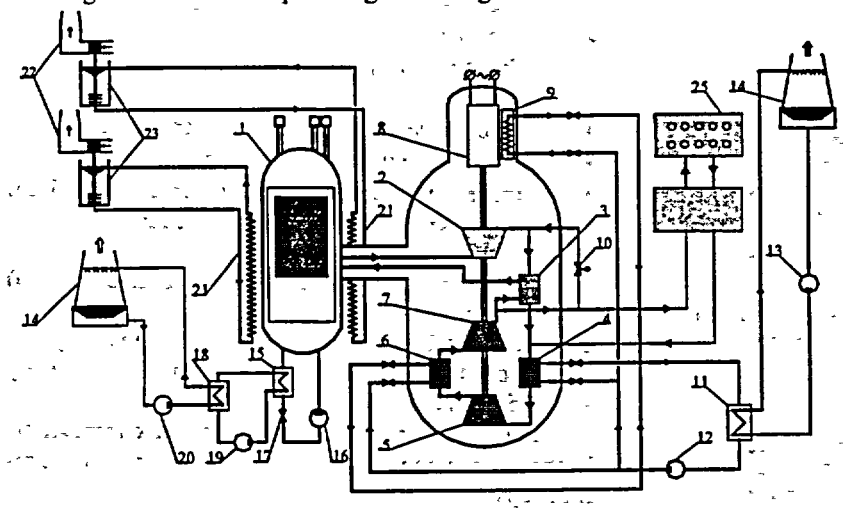

Fig. 3 – Schematic diagram of GT-MHR NPP: 1 - reactor; 2 - turbine; 3 - recuperator; 4 - precooler; 5 - LPC; 6 - intercooler; 7 - HPC; 8 - generator; 9 – generator cooler; 10 – bypass valve; 11 – PCU CWS heat exchanger; 12 – PCU CWS pump; 13 – recirculation water supply system pump; 14 – cooling tower; 15 – SCS unit heat exchanger; 16 – SCS unit gas circulator; 17 – SCS unit circulator shut-off valve; 18 – SCS CWS heat exchanger; 19 – SCS CWC pump; 20 – reliable recirculation water supply system pump; 21 – RCCS surface cooler; 22 – air duct; 23 - RCCS heat exchanger with heat pipes; 24 – primary circuit purification system; 25 – helium storage and transportation system

Technical concept of the GT-MHR is based on the following innovative technologies:

- ceramic fuel design in the form of small particles with thermal radiation resistance coating;
- modern technologies on large gas turbines;
- electromagnetic bearings;
- high efficiency compact recuperators;
- use of high-temperature strength materials.

Fuel (Fig. 4)

- Laboratory-scale technologies have been developed for Pu-kernels fabrication, coating and compacting.
- 200 g Pu-kernels are fabricated.
- Construction of the bench-scale fuel fabrication facility (BSF) for the fuel testing in reactor.
- A portion of BSF equipment and technical documentation are received from "General Atomics".
- Fuel exposure.
- Transfer of fuel fabrication technologies from NPO "Lutch", VNIINM, RRS "Kurchatov Institute" to SCC.
- Construction of facilities for implementation of GT-MHR plutonium fuel fabrication technology at SCC.

The GT-MHR fuel design uses kernels of plutonium oxide with multi-layer coatings of carbon and silicon carbide (fuel particles) dispersed in graphite matrix having a form of cylindrical compact. The compacts are placed into channels of graphite blocks which are similar to FSV reactor fuel assemblies (USA).

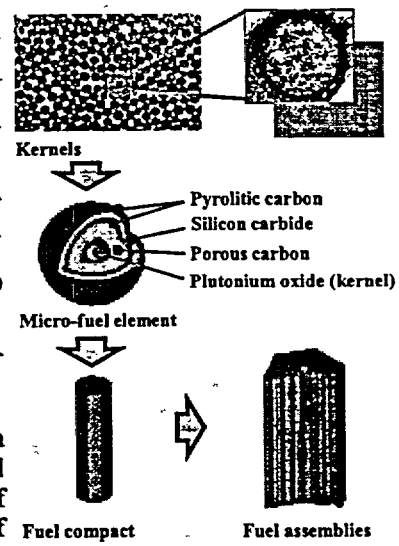

Fig. 4 Fuel components with Plutonium charge

Turbomachine

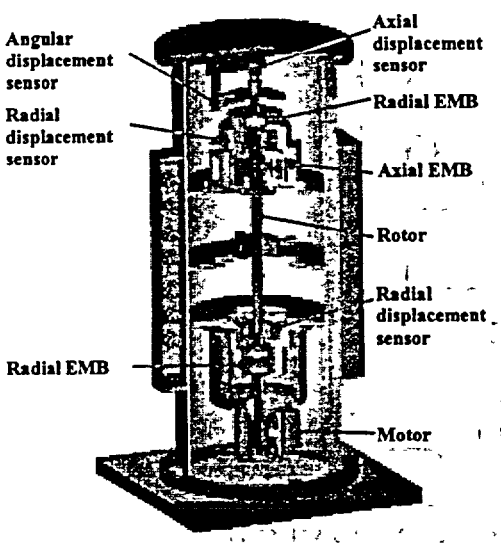

Fig. 5 GT-MHR components test facility

Turbomachine (TM) structural features :

- Vertical orientation;
- Turbocompressor and generator rotors form a single shaft;
- Electromagnetic bearings (EMB) are used;
- Slide seals are used in TM stator;
- Turbine and compressors operate in helium environment. Generator is cooled by helium.

Testing of TM and its components (Fig. 5, Fig. 6) models are needed.

The following is foreseen to validate the reliability and safety of the turbomachine operation completely suspended on electromagnets:

- testing of rotor model and electromagnetic bearings provided with control system on mini-mockups;
- testing of rotor scaled model to verify the software;
- testing of full-size electromagnetic bearings;
- testing of the entire set of electromagnetic bearings with control system.

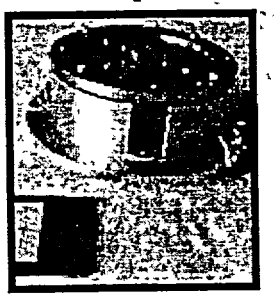

Fig. 6 Electromagnetic bearing

Recuperator (Fig. 7, Fig. 8)

- Recuperator considerably influences the GT-MHR plant efficiency.
- It shall provide high thermal effectiveness (~ 95 %) and compactness (~ 1500 m^2/m^3).
- Compact heat-exchange surface fabrication technology has been developed.
- Full-scaled heat exchange element has been manufactured
- The element is tested in a "cold" rig and in helium rig under working temperature and pressure conditions
- There is a powerful test facility (15 MW) at OKBM

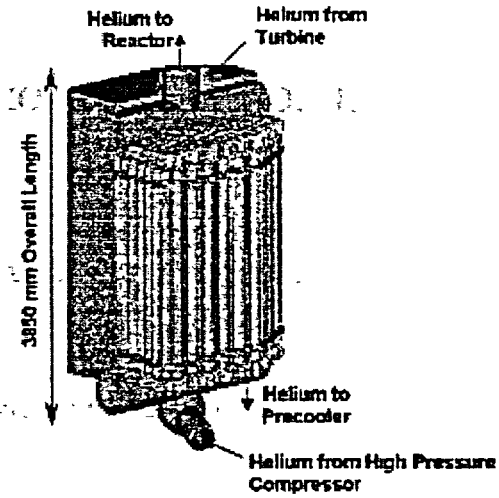

Fig.7 Recuperator module

Fig. 8 Recuperator mock-up

3. Advantages of GT-MHR PROJECT implementation

- Creation of a nuclear power plant, which meets the requirements of agreement about non-proliferation of nuclear materials due to high design indices of fuel burnup (up to 90 %)
- Future construction and operation of competitive nuclear power plants in various countries using uranium and MOX fuel with low enrichment as fuel
- Creation of up-to-date technologies which later on can be implemented in other industries
- Reduction of cost during creation of the GT-MHR project under international cooperation conditions
- Integration of international long-term experience in design and operation of high-temperature reactors
- Expansion of nuclear engineering application in the field of industrial high-temperature technologies.

EUROPEAN POSITION IN HTR-TN

D. Hittner, Framatome ANP, France

Paper will be handed out separately

Session 2

Fuel and Fuel Cycle

KEY DIFFERENCES IN THE FABRICATION OF U.S. AND GERMAN TRISO-COATED PARTICLE FUEL, AND THEIR IMPLICATIONS ON FUEL PERFORMANCE

D.A. Petti, J. Buongiorno, J. T. Maki, G. K. Miller
Idaho National Engineering and Environmental Laboratory
P.O. Box 1625, Idaho Falls, ID, USA 83415-3860
and

R. R. Hobbins
Consultant
Wilson, WY, USA 83014

ABSTRACT

Historically, the irradiation performance of TRISO-coated gas reactor particle fuel in Germany has been superior to that in the U.S. German fuel generally has displayed gas release values during irradiation three orders of magnitude lower than U.S. fuel. Thus, we have critically examined the TRISO-coated fuel fabrication processes in the U.S. and Germany and the associated irradiation database with a goal of understanding why the German fuel behaves acceptably, why the U.S. fuel has not faired as well, and what process/production parameters impart the reliable performance to this fuel form. The postirradiation examination results are also reviewed to identify failure mechanisms that may be the cause of the poorer U.S. irradiation performance. This comparison will help determine the roles that particle fuel process/product attributes and irradiation conditions (burnup, fast neutron fluence, temperature, degree of acceleration) have on the behavior of the fuel during irradiation and provide a more quantitative linkage between acceptable processing parameters, as-fabricated fuel properties and subsequent in-reactor performance.

1. Introduction

High temperature gas reactor technology is achieving a renaissance around the world. Without a conventional containment, this technology relies on high quality production and performance of coated particle fuel. The behavior of this fuel over the past three decades has been mixed. The Germans have demonstrated high quality production of TRISO-coated fuel and excellent irradiation and safety test behavior under reactor relevant conditions. By contrast, for nominally the same fuel under very similar service conditions, the U.S. fuel has been much less satisfactory. Our goal is to critically compare the German and U.S. fuel fabrication processes and the corresponding irradiation databases to identify the technical reasons for the differences in in-reactor behavior and to identify those specific fuel attributes and/or fabrication process conditions that impart superior in-reactor performance to TRISO-coated particle fuel.

2. Fabrication Processes

A review of the fabrication processes used in Germany and the U.S. to make coated particle fuel indicates that the scale of fuel fabrication and development efforts in the last 25 years were quite different. [1] German fabrication of modern TRISO fuel was industrial/production scale incorporating improvements from fuel production for the German AVR and THTR reactors. Only ~ 100 defects were found in 3.3 million particles produced. The U.S. program, for post Fort St. Vrain fuel production, was a mixture of lab scale and larger scale fabrication. The initial defect levels varied greatly and were much greater than those produced in Germany. Table 1 compares each of the steps in the fabrication of German and U.S. TRISO-coated fuel. The U.S. fabrication is based on the fabrication of fuel for the New Production Reactor program in the early 1990s. Many of the steps used to make this fuel were unique to the program and are not considered part of the traditional U.S. fabrication effort.

Table 1. Comparison of U.S. and German TRISO-coated Particle Fuel Fabrication

		U S. NPR	German
KERNEL FABRICATION			
KERNEL MATERIAL		HEU-UCO	LEU-UO2
GEL-PRECIPITATION		Internal	External
BROTH COMPOSITION		Aqueous solution of uranyl nitrate, carbon-black, Tamol, urea, HMTA	Aqueous solution of uranyl nitrate, polyvinyl alcohol and other non-specified additives
DROPLET FORMATION		Vibrating nozzle	Vibrating nozzle
GELATION MEDIUM		Trichloroethylene	Ammonia gas and ammonia solution
WASHING		Ammonia solution and clean water	Ammonia solution and isopropanol
DRYING		Air at 60°C	80°C
CALCINATION		Ar at 350°C	Air at 300°C
REDUCTION		H2 at 1600°C	Not applicable
SINTERING		CO at 1800°C	H2 at 1600-1700°C
COATING			
COATING PROCESS		Discontinuous	Continuous
BUFFER	Gas Composition	$Ar-C_2H_2$	$Ar-C_2H_2$
	Coating Temp.	1300°C	1250°C
	Coating Rate	Not available	6-10 µm/min
SEAL	Gas Composition	$Ar-C_3H_6$	Not applicable
	Coating Temp.	1200°C	Not applicable
IPYC	Gas Composition	$Ar-C_2H_2-C_3H_6$	$Ar-C_2H_2-C_3H_6$
	Coating Temp.	1230°C	1300°C
	Coating Conc. & Rate	Low/<4 µm/min	Higher/4-6 µm/min
SIC	Gas Composition	$H_2-CH_3SiCl_3$	$Ar-H_2-CH_3SiCl_3$
	Coating Temp.	1650°C	1500°C
	Coating Rate	0.2-0.4 µm/min	0.2 µm/min
OPYC	Gas Composition	$Ar-C_2H_2-C_3H_6$	$Ar-C_2H_2-C_3H_6$
	Coating Temp.	>1300°C	1300°C
	Coating Conc. &Rate	Low/<4 µm/min	Higher/4-6 µm/min
SEAL	Gas Composition	$Ar-C_3H_6$	Not applicable
	Coating Temp.	1200°C	Not applicable
PPYC	Gas Composition	$Ar-C_2H_2$	Not applicable
	Coating Temp.	1300°C	Not applicable
	Coating Rate	Not available	Not applicable
SEAL	Gas Composition	$Ar-C_3H_6$	Not applicable
	Coating Temp.	1200°C	Not applicable
FUEL ELEMENT MANUFACTURE			
FUEL ELEMENT		Compact	Pebble
MATRIX MATERIALS		Petroleum pitch, graphite flour, graphite shim	Graphite powder
BINDERS		Octadecanol, polystyrene	Phenol, hexamethylene-tetramine
MATRIX STATE		Liquid	Powder
OVERCOATING		Not applicable	200 µm
PRE-PRESSING		Not applicable	25°C, 30 MPa
PRESSING		160°C, 6.9 MPa	25°C, 300-350 MPa
LATHING		N/A	Yes
CARBONIZATION		900°C in alumina powder	800-900°C in inert gas
LEACHING		HCl	N/A
HEAT TREATMENT		1650°C	1800-1950°C in vacuum

Both German and U.S. fuel fabrication processes consist of a number of similar steps. Kernels are made via a traditional sol-gel process, followed by washing, drying and calcining to produce UO_2 kernels in Germany and UCO kernels in the U.S. The major difference consists of a sintering step using CO in the U.S. process to ensure adequate C/O stoichiometry in the kernel. The coating processes for the buffer are similar, based on chemical vapor deposition from a mixture of Ar and acetylene in a coater between 1250 and 1300°C. A 5-micron seal coat is produced in the U.S. to seal the buffer; this step does not occur in the German process.

A major difference in the production of the TRISO coating is that all three layers are coated in a continuous manner in the German process, whereas in the U.S. process the fuel particles are unloaded after each coating layer to perform QC measurements. The inner pyrocarbon layer in both cases is deposited from a mixture of acetylene, propylene, and argon. The temperature in the U.S. process is somewhat lower than in German process and coating gas concentrations are different, resulting in a different coating rate, and producing a different microstructure and density for the IPyC. The impact of this difference in IPyC properties is discussed in more detail in Section 4. The SiC layer is deposited from a mixture of hydrogen and methyltrichlorosilane, at similar coating rates although the temperature for U.S. coating is about 150°C higher than that used in the German process The implication of this difference is discussed in Section 4. The OPyC layer is coated in a manner similar to the IPyC layer. In the U.S. NPR fuel, seal coats and protective pyrocarbon (PPyC) were added which are not standard in U.S. fabrication. Neither is used in the German process.

The fuel pebble in Germany includes graphite powder and organic binders to produce a powder matrix that is used to overcoat the particles and to create the fuel pebble. In the U.S., a liquid matrix composed of petroleum pitch, graphite flour and graphite shim mixed with organic binders is used to make the fuel compact. Both fuel forms are pressed and carbonized at high temperature (800-900°C). HCl is used to leach impurities from the U.S. compact. Ultra high purity systems and feedstock are used in the manufacture of pebbles in Germany to ensure adequate control of impurities. Both fuel forms undergo a final heat treatment with the U.S. compact heated at 1650°C and the German pebble at 1800 to 1950°C in vacuum.

3. Irradiation Performance

Numerous in-pile irradiation experiments have been conducted in both the U.S. and Europe as part of the U.S. and German TRISO-coated particle fuel development efforts.[1,2] These irradiations were conducted at a variety of burnups, temperatures, and fluences. The rate of accumulation of burnup and fast fluence (i.e., the degree of acceleration) in the irradiation relative to that expected in the reactor is also an important parameter. For most of these fuels, the time to reach goal burnup and fast fluence is ~ 1095 days (3 years) whereas in the irradiations the time to reach peak conditions were accelerated by factor of 2 to 9. A summary of salient features of the irradiations is found in Table 2.

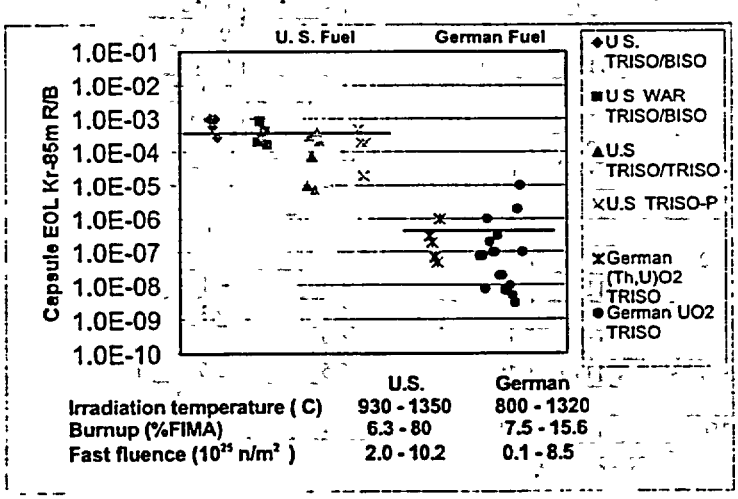

Figure 1. Comparison of end of life Kr-85m R/B from historic German and U.S. irradiations

Our detailed review indicates that the U.S. and German irradiation programs were implemented quite differently with very different results. The German program's focus

was on UO_2-TRISO fuel for AVR/THTR and all future designs such as HTR Modul, whereas the U.S. program examined many different variants (different coatings, different kernels) A plot in Figure 1 of the on-line fission gas release to birth ratios (R/B) from the Table 2 indicates that German fuel exhibits about a factor of 1000 less fission gas release under irradiation than U.S. fuel over a broad range of conditions (temperature, burnup, fluence).

Table 2. Summary of Particle Fuel Irradiation Experiments

Test/cell	Fuel forms	Irrad. time (d)/ Accel. Level	Peak temp. (°C)	Peak fissile/fertile burnup (%FIMA)	Peak fluence (10^{25} n/m^2)	EOL Kr-85m R/B (10^{-6})
U.S. Experiments						
F-30/1	$(Th,U)C_2$ ThC_2	269/4x	1100	15 0 / 3 0	8 0	8
F-30/2	$(Th,U)C_2$ ThC_2		1100	19 0 / 4.5	10 5	100
F-30/3	$(Th,U)C_2$ ThC_2		1120	20 0 / 5.0	11.5	10
F-30/4	$(Th,U)C_2$ ThC_2		1100	18 0 / 4.0	9.5	20
F-30/5	$(Th,U)C_2$ ThC_2		1200	12.0 / 1.5	12.0	20
HRB-4	UC_2 ThO_2	244/4.5x	1250	27.7 / 13.4	10.5	320
HRB-5	UC_2 ThO_2	107/10x	1250	15.7 / 4.3	4.7	100
HRB-6	$(Th,U)C_2$ ThO_2	183/6x	1100	26 6 / 9.3	7.9	270
OF-2/1	UCO UC_2 $(Th,U)O_2$ ThO_2	352/3x	1350	79.6 / 4.3	8.9	100
OF-2/2	UCO UC_2 $(Th,U)O_2$ ThO_2		1350	79.5 / 4.3	8.4	5
HRB-14	UCO UO_2 $(Th,U)O_2$ ThO_2	214/5x	1190	28.6 / 8.5	8.3	300
HRB-15B	UCO UC_2 $(Th,U)O_2$ UO_2 ThO_2	169/6 5x	915	26.7 / 6 0	6 6	5
R2-K13/2	UCO ThO_2	517/2x	1190	22.5 / 4.6	7 8	80
R2-K13/3	UCO ThO_2		985	22.1 / 4.5	7.4	8
HRB-15A	UCO UC_2 UO_2 ThO_2	174/6.3x	1150	29.0 / 6.4	6.5	380
HRB-16	UCO UC_2 UO_2 $(Th,U)O_2$ ThC_2 ThO_2	170/6.3x	1150	28.7 / 6.1	6.3	210
HRB-21	UCO ThO_2	105/10x	1300	22.0 / 2.2	3.5	200
NPR-1	UCO	170/6.3x	1240	79.0	3.8	300
NPR-2	UCO	172/6.3x	1030	79.0	3.8	60
NPR-1A	UCO	64/6.3x	1220	64.0	2.1	18
German Experiments						
HFR-P4/1	UO_2	351/3x	940	14.7	8.0	0 080
HFR-P4/2	UO_2		945	14 9	8 0	0.080
HFR-P4/3	UO_2		1075	14.0	8.0	0.008
SL-P1	UO_2	330/3x	794	11.3	6.8	1.200
HTR-K3/1	UO_2	359/3x	1200	7.5	4.0	0.200
HTR-K3/2	UO_2		920	10.0	5.8	0.100
HTR-K3/3	UO_2		920	10.6	5.9	0.100
HTR-K3/4	UO_2		1220	9.0	4.9	0.300
FRJ2-K13/1	UO_2	396/2.75x	1125	7.5	0.2	0 020
FRJ2-K13/2	UO_2		1150	8.0	0.2	0.020
FRJ2-K13/3	UO_2		1150	7 9	0 2	0.007
FRJ2-K13/4	UO_2		1120	7.6	0.2	0.007
FRJ2-K15/1	UO_2	533/2x	970	13.2	0.2	0 010
FRJ2-K15/2	UO_2		1150	14.6	0.2	0 005
FRJ2-K15/3	UO_2		990	13.9	0.1	0.003
FRJ2-P27/1	UO_2	232/4.7x	1080	7.6	1.4	1 600
FRJ2-P27/1	UO_2		1320	8.0	1.7	10 000
FRJ2-P27/1	UO_2		1130	7.6	1.3	0.120
R2-K12/1	$(Th,U)O_2$	308/3x	1100	11.1	5.6	0 300
R2-K12/2	$(Th,U)O_2$		1280	12.4	6.9	0 200
R2-K13/1	$(Th,U)O_2$	517/2x	1170	10.2	8.5	0 070
R2-K13/4	$(Th,U)O_2$		980	9.8	6.8	0.050
BR2-P25	$(Th,U)O_2$	350/3x	1070	15.6	8.1	1.000

Note: U.S. fluence is for E > 0.18 MeV and German fluence is for E > 0.10 MeV.

Furthermore, the results from the postirradiation examinations confirm the more extensive gas release data. German fuel is excellent. Out of ~ 340,000 particles tested there were no in-pile failures and only a few "damaged" particles due to experimental anomalies. Gas release was attributed only to as-manufactured defects and heavy metal contamination. By contrast, percent level failures of fuel and in many cases very high levels of failures of individual layers of the TRISO coated were observed following irradiation of U.S. fuel in most experiments (see Figure 2).

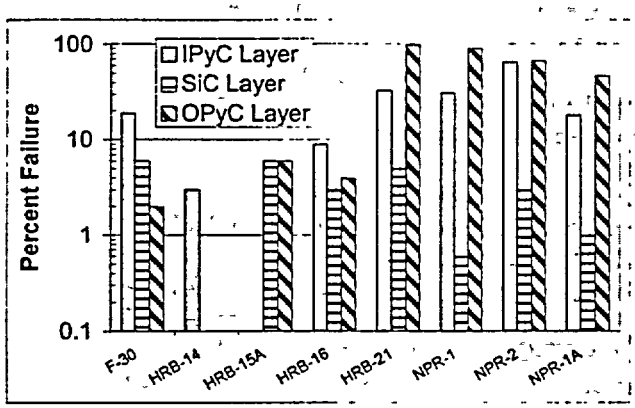

Figure 2. Failures observed during postirradiation examination of US coated particle fuel over the past 25 years.

Detailed review of the U.S. irradiation database indicates a number of different failure mechanisms of the individual layers of the TRISO coating contributed to the less than satisfactory U.S. fuel performance. Failures of the coating layers were attributed to: (a) pressure vessel failure, (b) kernel migration (amoeba effect), (c) fission product attack of the SiC layer, (d) irradiation induced IPyC cracking and/or debonding leading to cracking in the SiC layer, and (e) matrix-OPyC interaction and irradiation-induced OPyC failure. The PyC related mechanisms are strongly related to the anisotropy and porosity in the coatings. The anisotropy has a strong influence on the shrinkage and swelling behavior of the PyC layers under irradiation. The porosity of the layer has an impact on the strength of the interfacial bond between the SiC and PyC. Fission product attack of the SiC and kernel migration are thermally driven phenomena that are strongly influenced by the temperature gradient across the particle. The temperature gradient is a strong function of the packing fraction in the fuel and the degree of acceleration of the irradiation. A U.S. fuel compact has a higher packing fraction of particles (~ 50%) than German pebbles (~ 10%) and as shown in Table 2, the U.S. irradiations were accelerated 3 to 10 times real time compared to the 2 to 3 times acceleration for most of the German irradiations. Thus, some of the phenomena that were observed in US irradiations were attributed to the accelerated nature of the irradiation.

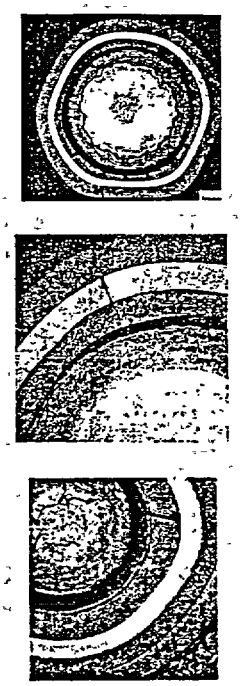

Figure 3. Irradiation induced cracking of inner PyC in F-30 irradiation (top two photographs) and NPR irradiation [4,5]

4. Impact on In-Reactor Performance

A comparison of the microstructures of the layers of the TRISO coatings in German and U.S. fuel and a detailed review of the fabrication processes has revealed many differences. There are three specific technical differences in the coating layers produced by the respective fabrication processes that have important impacts in terms of performance under irradiation and accident conditions: pyrocarbon anisotropy and density, IPyC/SiC interface structure, and SiC microstructure. Each has important implications on the behavior of the fuel under irradiation and safety testing.

4.1 Pyrocarbon anisotropy and density. The density and anisotropy of PyC is determined by the conditions in the coater. [3] German pyrocarbon is deposited at a higher coating gas concentration, which in turn results in a higher coating rate (~ 4-6 μm/minute). This pyrocarbon is very isotropic and thus survives irradiation quite well. However, the conditions lead somewhat greater porosity than in U.S. pyrocarbon. U.S. pyrocarbon has historically been coated at very low coating gas concentrations, which results in a lower coating rate (1-4 μm/minute), and leads not only to a very

dense and impermeable IPyC layer which is important to preventing attack of the kernel by the coating gas during deposition of the SiC layer but also to excessive anisotropy that can cause cracking of the PyC under irradiation. Postirradiation examination of many of the U.S. capsules indicate shrinkage cracks in the inner pyrocarbon layer which has been shown [6] to lead to stress concentrations in the SiC layer and subsequent failure of the layer. Photographs of such irradiation induced shrinkage cracks in the F-30 and NPR-1 irradiations are shown in Figure 3.

4.2 Nature of the IPyC/SiC interface. In the German process, each layer of the TRISO coating is deposited in the coater in a continuous fashion on one pass without interruption whereas in the U.S., the process is more batch-like with the particles being unloaded after each layer for QC measurements. This difference in the fabrication process of the TRISO coating layers and the difference in the porosity between the German and U.S. IPyC lead to differences in the nature of bond that exist between the layers. Photomicrographs of the IPyC/SiC interface in German and U.S. fuel are shown in Figure 4. This figure shows that the interface in German fuel is more tightly bonded because SiC is deposited into the more porous PyC. For the U.S. fuel, the denser IPyC and/or the unloading of fuel after each layer in the manufacturing process results in smoother, less strong bond. The TRISO coating of German fuel never exhibits debonding under irradiation whereas a review of the irradiation results indicates that the TRISO coating in U.S. fuel debonds quite frequently. The debonding is believed to be related to the strength of the IPyC/SiC interface. The debonding can lead to stress intensification in the SiC layer that may cause failure. [1]

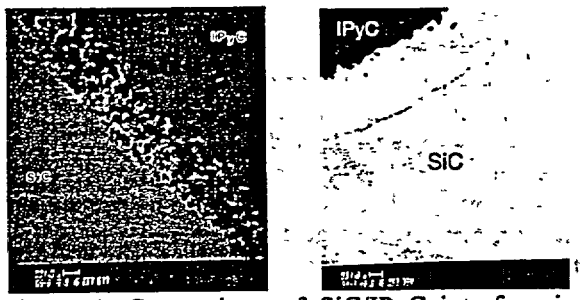

Figure 4. Comparison of SiC/IPyC interface in German (left) and US (right) fuel [7]

4.3 SiC microstructure. The microstructures of German and U.S. SiC are different. The German process results in small equiaxed grains whereas the U.S. process produces larger columnar thru-wall grained SiC. This difference in microstructure is believed to be primarily a function of temperature used during the SiC coating phase in the coaters, with the U.S. coater producing SiC at a higher temperature in some or all regions of the coater compared to the German process. A comparison of the microstructures is shown in Figure 5. These differences are believed to be important from a performance perspective because the smaller-grained German SiC with its higher tortuosity should in principle retain metallic fission products better than the large thru-wall columnar U.S. SiC. Data from the HRB-15A experiment suggests that Ag release is a function of the microstructure of the SiC. Figure 6 compares photomicrographs of two different types of SiC morphologies produced on U.S. UCO fuel. The fuel was irradiated to 26% FIMA and a peak fluence of 5.4 x 10^{25} n/m^2 at a temperature of ~

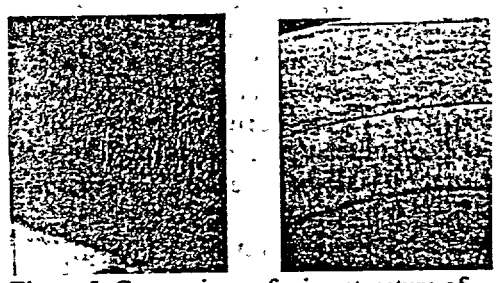
Figure 5. Comparison of microstructure of German (left) and US(right) produced SiC [7]

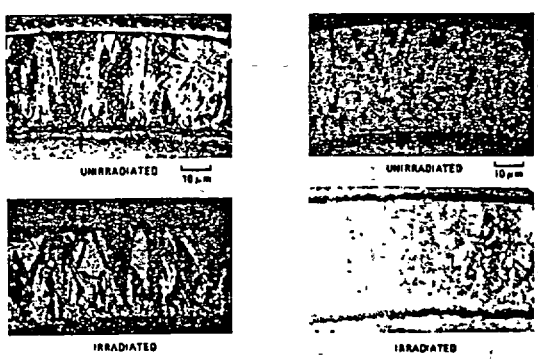

Figure 6. Photomicrographs of large thru-wall columnar SiC grains and smaller SiC grains produced in UCO fuel irradiated in US HRB-15A. Ag release from these two fuels were different [8]

1100°C. Approximately 90% of the Ag was released from the large columnar grained SiC whereas only ~ 30% was released in the smaller grained SiC microstructure. In addition, the effect of grain size size and morphology on Cs retention in SiC has been examined [9]. The diffusivity of cesium through columnar SiC was given as an order of magnitude greater than through laminar SiC. While clearly not conclusive, grain structure appears to be important to fission product retention Recently proposed experiments at MIT will attempt to answer this question more definitively. [9]

5. Summary and Conclusions

Our review has concluded that there have historically been differences in the quality of U.S. and German fuel as evidenced by results from many U.S. and German irradiations. These differences have in part been traced to technical differences in the microstructures of the PyC and SiC layers in the TRISO coating and the bonding of those layers, which in turn are related to differences in the fabrication processes used in Germany and the U.S. In addition, part of the difference in the performance of these fuels has been attributed to the different philosophies and approaches used to implement the irradiation and testing programs in the two countries. German fabrication was industrial/production scale supporting the German AVR and THTR reactors, with a focus on UO_2-TRISO fuel form. By contrast, post Fort St. Vrain the U.S. program was a mixture of lab scale and larger scale fabrication in which many different variants of TRISO coated particle fuel (different coatings, different kernels) were irradiated with apparently few lessons learned from one irradiation to the next and insufficient feedback to the fabrication process. The U.S. fuel was generally irradiated under very accelerated conditions, which may have overly stressed the fuel leading to a number of thermally activated failure mechanisms.

Acknowledgements

This work was supported through the INEEL Bechtel Corporate Funded R&D (CFRD) Program under DOE Idaho Operations Office Contract DE-AC07-99ID13727.

References

[1] D. A. Petti et al., "Key Differences in the Fabrication, Irradiation and Safety Testing of U.S. and German TRISO-Coated Particle Fuel and Their Implications on Fuel Performance," INEEL/EXT-01-xxx, forthcoming

[2] R. Contard and H. Nabielek, "Performance Evaluation of Modern HTR TRISO Fuels," HTA-IB-05/90, July 1990.

[3] D. Martin, "Irradiation Damage in Graphite due to Fast Neutrons in Fission and Fusion Systems, IAEA-TECDOC-1154, April 2000.

[4] G. K. Miller, D. A. Petti, D. J. Varacalle and J. T. Maki, "Consideration of the Effects on Fuel Particle Behavior from Shrinkage Cracks in the Inner Pyrocarbon Layer," *J. Nucl. Materials*, Vol. 295, 2001, p. 205-12.

[5] C. B. Scott and D. P. Harmon, "Postirradiation Examination of Capsule F-30," GA-A13208, April 1975.

[6] C. A. Baldwin et al., "The New Production Reactor Post Irradiation Examination Data Report for Capsules NPR-1, NPR-2 and NPR-1A," ORNL/M-2849, September 1993.

[7] J. Saurwein and L. Schilling, "Final Report-Testing of As-Manufactured NPR-PTF, German and U.S. Historical Fuel," General Atomics, No. 910647, September 30, 1993.

[8] J. W. Ketterer, M. J. Kania, R. E.Bullock, and I.K. Siman-tov, "Capsule HRB-15A Postirradiation Examination Report," GA-A16758, July 1984.

[9] B. F. Myers, "Selective Aspects of Transport in SiC," Presentation to Experts Meeting on MHTGR-HTR Fuel Performance under Accident Conditions," June 8-9, 1989.

[10] D. A. Petti et al., "Development of Improved Models and Designs of Coated-Particle Gas Reactor Fuels," International Nuclear Energy Research Initiative (INERI) Proposal for Collaborative Work with the French CEA, 2001.

HIGH TEMPERATURE REACTOR FUEL TECHNOLOGY PROGRAMME IN EUROPE

A. LANGUILLE, C. PERRAIS, M. PEREZ*, P. OBRY

*CEA Cadarache, Grenoble**

R. CONRAD

CEC/ JRC /IE Petten

P. GUILLERMIER

Framatome-ANP/ Lyon

H. NABIELEK, H. WERNER

FZJ/Juelich

D.HAAS, J. SOMERS, H. TOSCANO

JRC/ITU Karlsruhe

K. BAKKER

NRG/Petten

T. ABRAM

BNFL

ABSTRACT

In the frame of the European Network HTR-TN this paper presents the programme underway in the field of the HTR Fuel Technology which is mainly discussed in the relevant Task-Group 8 and also in the Share Cost Action (SCA) contracts HTR-F and HTR-F1 of the 5th Framework Programme. The major tasks covered concern a complete recovery of the past experience on fuel irradiation behaviour in Europe, qualification of HTR fuel by irradiating of fuel elements in the HFR reactor, understanding of fuel behaviour with the development of a fuel particle code and finally a recovery of fuel fabrication capability.

1. Introduction

The European Project for the Development of HTR Technology which is currently performed in the 5th Framework Programme concentrates on HTR-related key technologies and innovation potentials with the objective to consolidate advanced modular HTR technology. A common European approach to the renewal of HTR technology has been established through a work-shared programme within the European HTR Technology Network (HTR-TN), taking benefit of the considerable expertise existing within the European Community.

2. Background

The investigation of fundamental characteristics of HTR fuels has taken place since 40 years. The development of HTR's proceeded along two different directions, pebble bed design (Germany) and block-type design (USA, Japan) [Ref 1]. The same elementary fuel element was used, the coated fuel particle design. Coated particles are miniature fuel elements of the order of one millimetre diameter. The various designs of coated particles commonly used in the past are :

- the two-layer BISO particle where the kernel is coated with porous buffer and dense pyrocarbon (PyC) layers;

- the four-layer TRISO particle with a porous buffer layer and with a SiC layer between two high dense layers of PyC.
This reference TRISO particle is capable of complete retention of gaseous fission products and iodine and also provides the retention of metallic fission products under normal and off--normal conditions.
The high flexibility of HTR cores permit the use of different fuel types which can be fissile materials (U, Pu) or fertile materials (U, Th) or even minor actinides. These particles must be dispersed in a graphite matrix (or another matrix of a different nature for specific applications).
The design and safety of future HTR's are based on high quality fuel. There is an absolute need to be able to demonstrate the advantage of the first robust barrier offered by the fuel particle under high burn-up and accident conditions.

3. Global objectives of the fuel technology programme

A consortium of 7 contractors are participating in the HFR-F and HTR-F1 projects, CEA as co-ordinator and Framatome-ANP, NRG, FZJ, JRC-ITU, JRC-IE and BNFL. The HTR-F project has been approved under the contract N° FIKI-CT-2000-00099 [ref. 2] and HTR-F1 under the project N° FIKS-CT-2001-00150.
For the HTR-F and HTR-F1 projects, the global objective is focused on HTR fuel technology based on the TRISO coated fuel particle design. The different items covered are :
- A first task is to gather in a common data-base the available experience gained from various types of fuels tested in the past in European reactors;
- A second task is to perform in-pile and out-of-pile tests to qualify the fuel particle behaviour under irradiation;
- A third task which is performed in order to understand and predict the irradiation behaviour is to model the different phenomena occurring in the fuel in reactor;
- Finally a fourth task is to restore the fabrication capability in Europe with the challenge to reach a very high quality level.

4. Description of the programme

- Past experience retrieval.

Different types of fuels have been tested in various Material Testing Reactors since the 60's, the objective is to gather the results of these fuel testing programmes (conducted in various reactors in Europe such as HFR, SILOE, ...) in a common data base and to analyse these data for a better understanding of the fuel behaviour under irradiation. The main task is to collect past results available obtained in different reactors tests :
- Irradiation experiments performed in the HFR Petten in support of R&D for German modular HTR and US HTGR (HFR-K, HFR-B and HFR-P series);
- Irradiation experiments performed in the OSIRIS, SILOE reactors in support of CEA and collaborative CEA-GA programmes (CORAIL, GF,... series);
- Irradiation experiments performed in Great Britain (DRAGON fuel tests).
Beside this data base will be used also to store the new data of the HTR irradiation programme in progress. First specifications of this Fuel DB have been issued and the data-base server will be located at Petten with links with different European users.

- Fuel test qualification

The main objective of the EC projects is the qualification of the HTR fuel under irradiation with two incentives: first to recover capabilities of irradiation and examinations on fuel particles in HFR/Petten and secondly to start an experimental programme in order to qualify the HTR fuel at high burn-up.
Two main tasks are foreseen for the fuel qualification : the realisation of a first experiment HFR-EU1 on pebbles at high burn-up and the performance of heat tests in the KUFA equipment.

Performance of the HFR-EU1 experiment in HFR

The main objective of the HFR-EU1 irradiation test is the demonstration of the feasibility of high burn-up for the existing German and Chinese fuels with TRISO coated particles [Ref 3]. It will include in particular:

- the irradiation up to a burn-up of 20% FIMA (respectively 16% FIMA for Chinese fuel) to be achieved within 2 years;
- the evaluation of fuel performance at such ultra-high burn-up to explore the real limits of the existing CP;
- the extension of the existing data base for the EOL metallic fission product release and the demonstration of the ability of the LEU-TRISO CP for fission product retention at accident scenarios, e.g. post-irradiation heating beyond 1600°C.

The irradiation samples of the HFR-EU1 test will be five spherical fuel elements FE with 60mm outer diameter. Three spheres of German production are the type AVR GLE-4 (AVR reload 21-2) with 16.7% U_{235} enrichment and two spherical fuel elements of INET production (17.08 % U235 enrichment) [Ref 4].

The proposed irradiation facility of the HFR-EU1 test for testing spherical fuel elements simultaneously in two independent capsules, the FE are doubly contained in a sample holder, which is inserted into a rig, code-named REFA-172. This REFA-172 rig is a standard facility that can repeatedly be used. The GLE-4 and the INET fuel elements are located in two separate capsules, one superimposed on the other.

The HFR-EU1 test shall be conducted such that the surface temperatures of all fuel specimens be held constant at about 900 - 980 °C. The maximum burn-up target of the highest loaded FE will be 20% FIMA. Fast neutron fluence shall not exceed $6.5*10^{25}$ $n.m^{-2}$ (E>0.1MeV).

Non-destructive PIE of the above-mentioned five fuel elements and destructive PIE on one of the three German FE will be performed in NRG hot cells.

Heat-up experiments in KUFA facility

By means of heating tests simulating accident conditions, it is possible in hot cells laboratories to measure the release of the fission products (Cs, St, I,..) from compact and spherical fuel elements. These data enable the FP transport processes in the reactor core. FZJ has developed in the past a specific furnace called "cold finger test rig" (KUFA) in hot cell [Ref 5].

In the project HTR-F, the schedule for the reinstallation of the KUFA equipment is the following:

In a first step, the transfer of the equipment will be realised from Jülich/FZJ to Karlsruhe/JRC/ITU with the construction and licensing of the glove-box. In a second step, the cold testing of the equipment will be performed and the licensing of the α-containment will be prepared. In a last step, the installation of the equipment will be done and the licensing of the hot cell realised. The first measurement will be then performed.

Moreover 21 fuel elements irradiated in earlier HTR programmes will be transferred to ITU/Karlsruhe. Some of these fuel elements will be used to calibrate the installation. Three of the 21 pebbles will be tested in the HTR-F1 project in 2004. During the heating test, the content of noble gases and solid fission products in the cooling gas (He) will be established. This will supply an integral statement on the retention capability of the fuel elements under operating and accident conditions. The data obtained will provide understanding on the fuel behaviour, in particular results for code validation and will be used to make an effort to improve its performance.

Follow-up of the irradiation programme

In the frame of the HTR-TN project (TG8) a second experiment HFR-EU2 will be performed in HFR. The objective is to test 10 GA compacts in a dedicated sample holder that is irradiated in one leg of the so-called TRIO facility (TRIO6131). The compacts were fabricated at General Atomics with an improved compact fabrication process, each compact contains German reference coated particle (EUO 2358 – 2365 batches) enriched at 10.6 %U-235. The volume packing fraction is 35.5%. The irradiation conditions foreseen are : central compact temperature between 1100 °C and 1200 °C, maximum fast neutron fluence of $4.5x10^{25}$ $n.m^{-2}$ and a bur-up of 10 % FIMA

The two tests HFR-EU1 and HFR-EU2 will be conducted simultaneously in the reactor HFR, independently in different core positions but using the same SWEEP LOOP system.
PIE and heat-up tests will be performed respectively at NRG Petten and ITU Karslruhe.
Discussions are also engaged with JAERI to test Japanese annular compact elements in a similar device (TRIO leg) but not at the same time.

- Fuel modelling

In order to understand and to predict the irradiation and accident behaviour in different conditions a good modelling of the fuel particles is needed, it has been agreed to develop at the European level a common code taking into account the past experience.
A clear objective of such a code is to be flexible enough to calculate any type of fuel (U, Pu, Th,...) under steady-state and accidental conditions.
Fuel performance modellers with experience in irradiated fuels from different countries are collaborating to build this common European code for HTR fuels application. The first milestone is to provide a first version of the code end of 2003.
- In a first step collection of input data and selection of the best models will be performed.
Common input data will be agreed on the basis of the collection of data and models established in the HTR-F contract. The goal is to have a common data base (physical and mechanical properties on kernel and on coatings), which can be used by anybody in the HTR programme, in particular in code applications.
Each partner is bringing his specific knowledge in different areas (kernels, coatings, FP diffusion, ...) and a selection of the relevant models is made on a common agreement basis. This work is intended to be completed by end of 2002.
- In a second step the code will be applied to pre-calculate the HTR-EU1 irradiation test. The objectives of this application are first to have a correct idea of the behaviour of the pebbles at high burn-up (gas pressure, FP diffusion, particle failure probability,...) and secondly to provide a good basis for preparation of the PIE examinations of the irradiated pebbles.
- A third step which is the major work will be devoted to code qualification. For this purpose calculations will be performed on most interesting cases in particular past tests performed at higher burn-ups (i.e. HFR P4, FRJ2-K15, HFR-K3); for some of them heating tests have been realised or will be realised in this project. A comparison of experimental results could be done with calculated values.
These first test applications will provide a preliminary qualification of the European code end of 2004.

- Fuel manufacturing

The major objectives in the fuel fabrication studies are :
- To review the existing technologies for fabrication of kernels and coated particles;
- To select and to optimise reference fabrication process(es) for kernels and coatings;
- To study these processes at a laboratory scale in a first step;
- To fabricate and to characterise first batches of kernels and coated particles (uranium bearing particles).

In the first instance a general fuel particle specification is defined, which acts as guidelines and eventual goal for an industrial qualification. Initially, UO_2 LEU TRISO fuel is considered but, in a second stage, plutonium bearing fuel and innovative coatings will be studied.
The second task is to regain particle manufacturing knowledge for fabrication and coating of the kernels, with the aim of determining the key parameters for the construction of a modern fabrication plant.
- For kernel fabrication, based on past experience and new techniques, a review of potential fabrication processes has been made (dry route process, weak-acid ion-exchange resin WAR process, sol-gel process) developing different aspects of the fabrication (advantages, drawbacks, industrial scale feasibility). It is known the sol gel processes GSP (Gel Support Precipitation) and HMTA (Hexa-Methylene TetrAmine) are able to provide satisfactory kernels respecting the specifications. But only

the former has been used at industrial level, both by NUKEM and General Atomics. In more recent developments, the GSP route is being used to manufacture fuels for in Japan and China.
Preliminary fabrication tests are being performed at CEA/Cadarache and ITU/Karlsruhe on laboratory scale devices. Starting with non-active simulants these tests will continue with UO_2, with initial tests being made in 2002. Despite the large past experience key production parameters are not freely available and have to be ascertained anew. It is planned that in a second stage (HTR-F1) that kernels containing Pu i.e. $(U,Pu)O_2$ will be produced. The ultimate aim of these ivistagations is the recovery and a renewed realization of industrial production capability for HTR development in Europe.

- The fluidised bed technique is used for kernel coating. The kernels are batch-wise coated in fluidized bed furnace under an inert gas (usually argon) at high temperature (ranging from 1200°C up to 1900°C). First the porous buffer layer is deposited from C_2H_2, then the high dense inner and outer pyrocarbon layer is deposited from a mixture of C_2H_2 and C_3H_6, the layer SiC deposited from Methyl Chloro Silane (MTS) CH_3SiCl_3.
A device, used in the 1970's has been restored and renewed at CEA/Grenoble. Tests have started since mid 2001 on the buffer and I-PyC layers on simulant material (ZrO_2-Y_2O_3 material from TOSOH) and will be continued with SiC and O-PyC layers.
On innovative coatings (e.g. ZrC-TRISO), first a bibliographical review concerning these innovative coatings will be undertaken (comparison of the different state of the art ZrC coating processes, comparative behaviour under irradiation of ZrC and SiC). First thermo-dynamical studies and process development by simulant tests will be also performed.

The third task is the study of coated particle quality control methods. Tests are being made in support to the first manufacturing studies. Techniques considered in a first step are image analysis, laser light scattering and X-ray radiography for kernel shape and size and for layer thickness determination. These methods are being evaluated and compared with respect to the specification needs. The feasibility of other methods (both traditional and novel) will be reviewed in further steps of the programme.

5. Conclusion

The global working programme takes benefit of the international collaboration and it is being carried out over a period of four years within the the FP5 programme and will be continued, technical proposal is under preparation for the next step (6th Framework Programme) for continuing the development of fuel technology which will be needed by industry by the end of the decade for a large scope of HTRs applications. The future development of HTR technology has many aspects. Though earlier developments were eminently successful, innovations are possible in the kernel design and in the fabrication technologies. The understanding of the irradiation behaviour is also a key parameter in evaluating new designs and expected performance gains.

6. References

[1] Mc EACHERN D.W., MAKAROV V.M. and SUSLOV I.A. ; "The International GT-MHR Fuel Program " ; Intern. HTR Fuel Seminar, February 2001, Brussels, Belgium

[2] A. LANGUILLE, "Contract FIKI-CT-2000-00099", Shared Cost Action HTR-F, October 2000, "Contract FIKI-CT-2001-00150", Shared Cost Action HTR-F1, December 2001

[3] R. CONRAD, K. BAKKER, K. VERFONDERN, H. NABIELEK "Test specifications for the Irradiation experiment HFR-EU1" HTR-TN report HTR-F-01/07-D-2.1.1

[4] TANG C., ZHU J., QIU X., XU Z., ZHANG F. and NI X.. ; "Fabrication of the first loading fuel of 10 MW HTGCR" ; Intern. HTR Fuel Seminar, February 2001, Brussels, Belgium

[5] H. NICKEL, H. NABIELEK, G. POTT, A. W. MEHNER "Long Time Experience with the Development of HTR Fuel Elements in Germany" Intern. HTR Fuel Seminar, February 2001, Brussels, Belgium

Microspheres of UO_2, ThO_2 and PuO_2 for the High Temperature Reactor

EGBERT BRANDAU

BRACE GmbH

Taunusring 50

D-63755 Alzenau

ABSTRACT

The production of high temperature reactor fuel, so called pebble fuel, was done in the eighties by a special vibrational dropping process to obtain as sintered UO_2- or ThO_2-microspheres, so called "Kernels", with a diameter size of about 300 µm. These microspheres have been coated and embedded in carbon balls to get the pebble fuel. Since the early nineties BRACE is developing the processings of microspheres starting with sols and suspensions to produce Al_2O_3, ZrO_2, HfO_2 and Actinide oxide microspheres. Two main developments have been made: 1) the preparation of the feed solution (sol, suspension) and the solidification processing, and 2) the equipment, design, and electronic control have been completely changed.

A newly developed suspension process for actinide oxides and for metal oxides e.g. Al_2O_3, TiO_2, SiO_2, ZrO_2, HfO_2, CeO_2, ThO_2, UO_2, PuO_2 leads to cheaper production of as sintered microspheres.

The processing and the installations will be described and the experience of production will be shown.

1. Introduction

Up to the end of the eighties of last century, the so called "Kernels", microspheres with a diameter of about 300 µm as sintered out of ThO_2 and UO_2 have been produced by a special vibrational dropping process (Fig. 1, 3 and 2). After coating and embedding in carbon the pebble fuel balls with a diameter of 60 mm included 40.000 UO_2- or ThO_2-microspheres in the core.

The development has been made at the Nuclear Research Center Jülich and at the company Nukem GmbH has been stopped in the end of the eighties and the production line has been shut down.

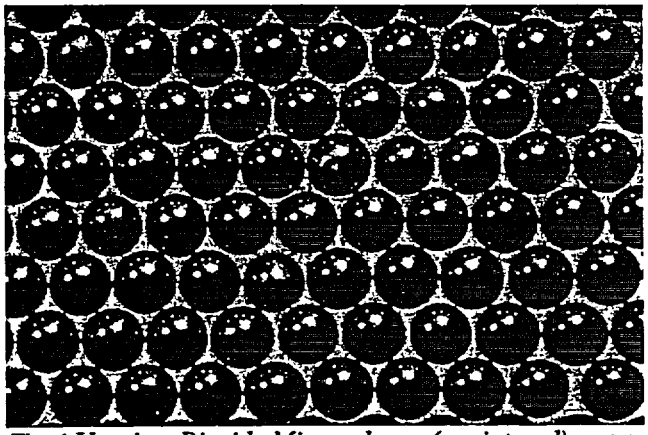

Fig. 1 Uranium Dioxide Microspheres (as sintered)

Since the early nineties BRACE is developing the processing of microspheres with a broad range of materials for applications in chemical, pharmaceutical, electronic, cosmetic and food industries. [1-8]

One of the developing areas is the production of microspheres out of metal oxides.

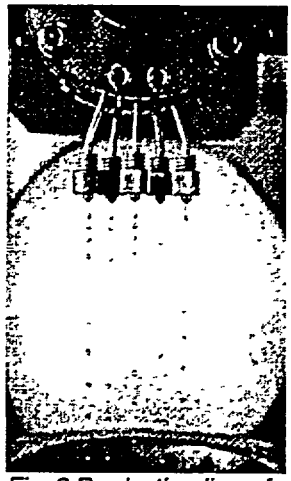

Fig. 2 Production line of "Kernels" (nozzlehead)

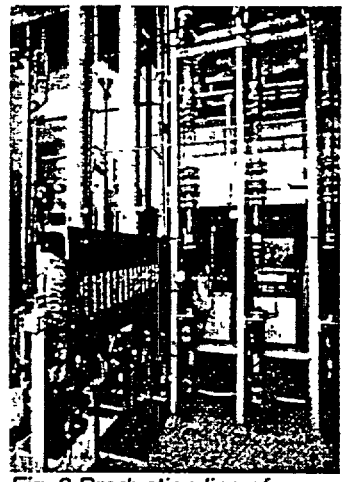

Fig. 3 Production line of "Kernels"

Different process are used:

1) The sol-gel process
2) Suspension process with a temporary binder
3) Mixed process: sol-gel and suspension.

With these three processes microspheres of nearly all metal oxides can be produced.

2. Theoretical background of the process

The patented BRACE-Microsphere Process is a drip casting process. A laminar liquid beam is generated through nozzles which are vibrated in the direction of the flow with an amplitude of some micrometers the flux breaks up in undercritical droplets which are stable. Due to the surface tension the droplets get a spherical shape (Fig. 5). The optimal frequency depends not only on the diameter of the nozzle, but also on the velocity of the flow and material's specific constants like Weber-, Reynolds- and Ohnsorge numbers (Fig. 4).

3. Sol-Gel Process

A number of metals can form hydroxide sols and can be used as starting material for the production of microspheres. Sols with low viscosity, such as Zirconium, Hafnium or Aluminium hydroxide stabilized with organic compounds like polyalcohols or with pore formers like urea, can easily be pressed through a nozzle system. Gelation in the gaseous phase is obtained by the reaction with ammonia. Solidification is continued by dropping the spheres in an aqueous solution of ammonia. This solidification can be tailored to the wanted properties of the microspheres by varying the reaction time and the concentration of ammonia in the precipitation bath.

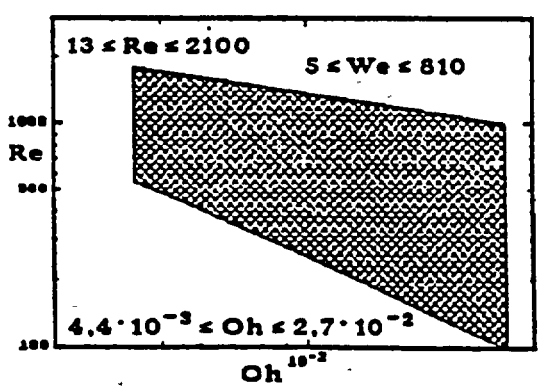

Fig. 4 Ohnsorge-diagram, outlined area marks allowed regions (Schmidt, P. and Richter, Th., University GH-Essen).

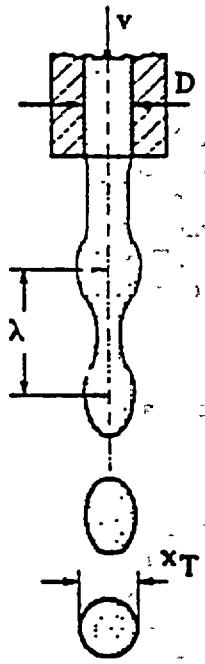

Fig. 5Formation of spherical droplets (Schmidt, P. and Richter, Th., University GH-Essen).

Not only sols can be used to obtain a fast and sufficient gelation during the short time of sphericity. Aqueous solutions of nitrates or carbonates are also excellent starting materials for the production of microspheres. The preneutralized solutions formed to spheres are also gelated in a gaseous reaction with ammonia. They are ultimately precipitated in an aqueous solution of ammonia. Even without chemical presolidification in the gaseous phase, the solidification is possible provided that the precipitation solution shows a low surface tension to avoid a deformation of the spheres.

In the case of Actinide metals the starting material can be a hydroxide sol or an aqueous solution preneutralized and with the addition of gelating aids like PVA, THF etc. For the preparation of ThO_2 and UO_2-microspheres ("Kernels") solutions of Thoriumnitrate and Uranylnitrate with PVA as gelating aids was used as starting solution. The gelating after moulding has to be exactly adjusted. A short presolidification with gaseous ammonia is the first sensitive step to obtain a solidified shell which has to be permeable for the following reaction in the Ammonia solution. The total solidified sphere has also to be porous to allow the diffusion of water and NH_4NO_3 during washing and drying of the spheres.

4. Suspension Process

The starting material for the suspension process is the powder of the metal oxide which will be formed to microspheres. The powder with a low grain size, preferably with d_{90}<3 µm is suspended in water. The Zetapotential has to be adjusted to get a stable suspension. Depending on the used temporary binder the pH-value has to be adjusted, too.

This suspension is then moulded with the vibrational dropping process of BRACE into microspheres. The solidification occurs by chemical reaction in an aqueous solution. After washing and drying the temporary binder is decomposed during a calcining step at about 500-600°C.

As temporary binder a broad range of organic compounds can be used. The most convenient compounds are Alginates. Materials like Agar-Agar, PVA, Polyethylene imine, Polyethersulfone, Gelatine ... can also be used.

The sodium or the ammonium salt of alginate is dissolved in water and added to the metal oxide suspension. The gelatine of the as moulded spheres can be done by bivalent (Me^{2+}), trivalent (Me^{3+}) metal ions e.g. Ca^{2+}, Ba^{2+}, Al^{3+}, and acids. Most salts of multivalent metal ions with alginate are insoluble in water.

This suspension process can be used to produce Actinide oxide microspheres without the use of Ammonia gas and Ammonia solutions.

The suspensions of ThO_2, UO_2 and PuO_2, other Actinide oxides, mixtures of this oxides or with additionally added metal oxides for the increasing sintering activity can be processed in a broad range and in one preparation step.

5. Mixed Process: sol-gel and suspension

To the sol or the solution of a metal hydroxide a suspension of the metal oxide can be added and this starting material is then moulded to microspheres. Mixed oxide microspheres can be produced if different metals are used in the sol/solution and the powder for the suspension. By this process mixed Actinide oxide microspheres are easily produced, e.g. ThO_2/UO_2-spheres or UO_2/PuO_2-spheres. Depending on the composition and concentration the gelation of the as moulded spheres is also obtained without the use of ammonia.

6. Subsequent Treatment of the Solidified Microspheres

Sol-Gel Process

The chemical reaction between metal salt solutions and ammonia produces ammonia salts (NH_4NO_3, NH_4Cl, $(NH_4)_2CO_3$, ...). These salts must be washed out before the particles are processed further, since otherwise the particles would be destroyed during heat treatment as these salts decompose. Washing of the spherical gel particles produced by the vibrational dropping process presents no difficulties, since the exchange rate (diffusion) between particles and surrounding liquid is fast. The removal of water from the gel particles using an alcohol that is miscible with water e.g. Isopropanol has higher efficiency and takes only a few minutes.

Suspension Process

In the case of the suspension process the washing process has only to remove the water, the small amounts of adhering metal salt of the solidification salt and the surplus of Na/NH_4-alginate.

Decomposing of Organics

After washing, the particles are dried at 100-180°C in air evaporating the washing fluid. The dried gel particles are then calcined in air (500°C to 600°C) in order to decompose the organic polymer. To improve the reproducibility of calcining products, it is useful to work under flowing air at a constant humidity in the range between 10 to 30 g of water per cubic meter of air. Depending on the composition of the precursor solution, residual carbon contents ranging from 10 to 50 ppm can be achieved.

Sintering

The following step of the microsphere production is the sintering in air or in the case of UO_2, PuO_2 in hydrogen to reach the high dense microspheres (96-99% of the theoretical density).

7. Production Units

The newly developed units for the production of ThO_2-, UO_2-, PuO_2- and mixed oxide microspheres provide the possibility to produce microspheres with a monomodal size distribution in a diameter range of 30-6000 microns. The ratio of dmax/dmin is close to 1,0.

The capacity of the unit begins with small lab scale quantities for example 0,5-1 l per hour of feed solution or suspension. Production units have a throughput of 100 to 1000 l per hour. Depending on the content of solids, expressed in percentage of metal oxide in the feed solution/suspension, the capacity of as sintered Actinide oxide spheres ranges from 20 to 700 kg per hour.

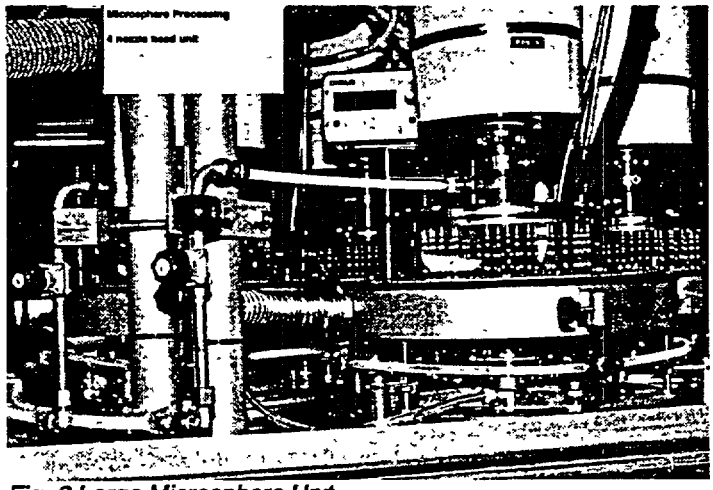

Fig. 6 Large Microsphere Unit

Figure 7 shows the principle of a production unit. The units operate at atmospheric pressure or slightly above and can be designed to be explosion proof and can be built in a glove box. All process

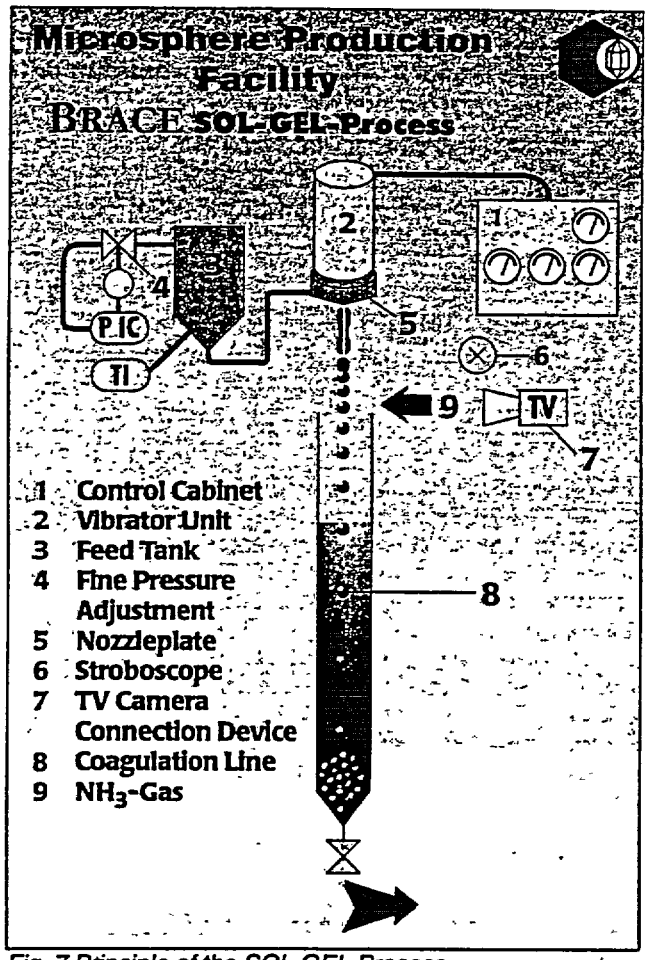

Fig. 7 Principle of the SOL-GEL Process

parameters are electronically measured and controlled. Remote control and modern control panels are a standard scope of supply.

The units have a minimum space requirement. The energy consumption is very low and they are noiseless during operation.

Figure 6 shows the moulding head of a bigger production unit.

With these installations manufacturing of monosized microspheres in a continuous production line is state of the art.

Figure 8 shows Uranium oxide microspheres as moulded, as dried as calcined and as sintered. The diameter shrinks from about 1 mm as moulded to 0,3 mm as sintered.

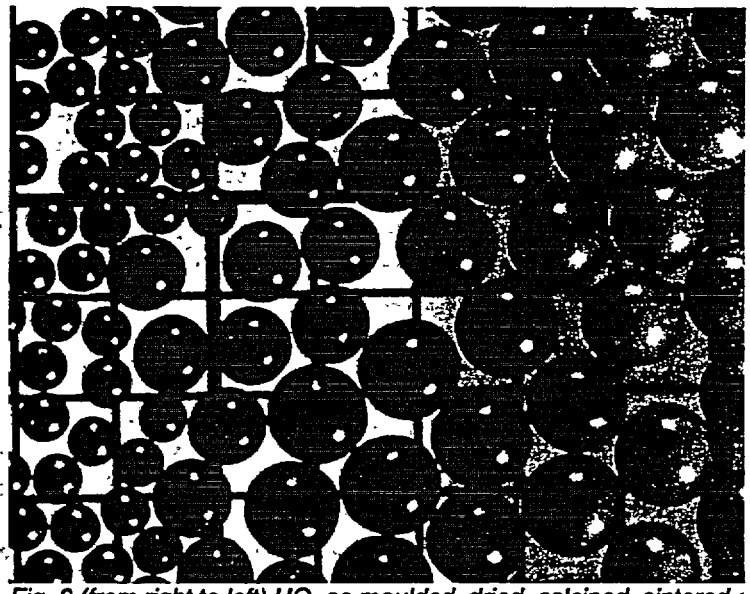

Fig. 8 (from right to left) UO_2 as moulded, dried, calcined, sintered

References:

[1] EP0556222
[2] EP0585264
[3] EP0687246
[4] DE4125133C2
[5] EP0597911
[6] EP0735940
[7] EP067221
[8] DE10046755.5

DEVELOPMENT OF AN INTEGRATED PERFORMANCE MODEL FOR TRISO-COATED GAS REACTOR PARTICLE FUEL

G. K. MILLER, D. A. PETTI, AND J. T. MAKI
Idaho National Engineering and Environmental Laboratory
P. O. Box 1625
Idaho Falls, Idaho, USA 83415

ABSTRACT

The success of gas reactors depends upon the safety and quality of the coated particle fuel. The understanding and evaluation of this fuel requires development of an integrated mechanistic fuel performance model that fully describes the mechanical and physico-chemical behavior of the fuel particle under irradiation. Such a model, called PARFUME (PARticle FUel ModEl), is being developed at the Idaho National Engineering and Environmental Laboratory. PARFUME is based on multi-dimensional finite element modeling of TRISO-coated gas reactor fuel. The goal is to represent all potential failure mechanisms and to incorporate the statistical nature of the fuel. The model is currently focused on carbide, oxide and oxycarbide uranium fuel kernels, while the coating layers are the classical IPyC/SiC/OPyC. This paper reviews the current status of the mechanical aspects of the model and presents results of calculations for irradiations from the New Production Modular High Temperature Gas Reactor program.

1. Introduction

The INEEL has begun development of an integrated mechanistic fuel performance model for TRISO-coated gas-reactor particle fuel termed PARFUME (PARticle FUel ModEl). Compared to light water reactor and liquid metal reactor fuel forms, the behavior of coated-particle is inherently more multidimensional. Moreover, modeling of fuel behavior is made more difficult because of the statistical variations in fuel physical dimensions and/or component properties, from particle to particle due to the nature of the fabrication process.

Our objective in developing PARFUME is to physically describe both the mechanical and physico-chemical behavior of the fuel particle under irradiation, with the proper dimensionality, and still capture the statistical nature of the fuel. The statistical variation of key properties of the particle associated with the production process requires Monte Carlo analysis of a very large number of particles to understand the aggregate behavior. Thus, state-of-the-art statistical techniques are being used to incorporate the results of the detailed multi-dimensional stress calculations and the fission product chemical interactions into PARFUME. Furthermore, we want to verify PARFUME using data from historical TRISO-coated particle irradiations so that the code can be used to design advanced coated-particle fuel with greater confidence for the gas reactor and other particle fuel applications (Pu and minor actinide burning, gas-cooled fast reactors).

2. Key Phenomena

Our mechanistic model for coated-particle fuel will consider both the structural and physico-chemical behavior of a particle-coated fuel system during irradiation. The following important phenomena will be included:

- Fission gas release from the kernel as a function of burnup, temperature and kernel type (oxide, carbide, oxycarbide);
- Anisotropic response of the pyrolytic carbon layers to irradiation (shrinkage, swelling, and creep that are functions of temperature, fluence, and orientation/direction in the carbon);
- Failure of the pyrolytic carbon and SiC layers based on the classic Weibull formulation for a brittle material either by traditional pressure vessel failure criteria or by mechanisms such as asphericity, layer debonding, or cracking;

- Fission product inventory generation as a function of burnup and enrichment of the particle;
- Chemical changes of the fuel kernel during irradiation (changes in carbon/oxygen, carbon/metal and/or oxygen/metal ratio depending on the kernel fuel type, production of CO/CO_2 gas) and its influence on fission product and/or kernel attack on the particle coatings;
- Kernel migration;
- Fission product diffusion, migration and segregation;
- Statistical variations of key properties of the particle associated with the production process, requiring Monte Carlo analysis of a very large number of particles to understand the aggregate behavior.

Due to space limitations, this paper will focus only on the structural aspects of the model.

3. Material Properties

A typical TRISO-coated particle is shown in Figure 1. Fission gas pressure builds up in the kernel and buffer regions, while the IPyC, SiC, and OPyC act as structural layers to retain this pressure. The basic behavior modeled in PARFUME is shown schematically in Figure 2. The IPyC and OPyC layers both shrink and creep during irradiation of the particle while the SiC exhibits only elastic response. A portion of the gas pressure is transmitted through the IPyC layer to the SiC. This pressure continually increases as irradiation of the particle progresses, thereby contributing to a tensile hoop stress in the SiC layer. Countering the effect of the pressure load is the shrinkage of the IPyC during irradiation, which pulls inward on the SiC. Likewise, shrinkage of the OPyC causes it to push inward on the SiC. Failure of the particle is expected to occur if the stress anywhere in the SiC layer reaches the fracture strength of the SiC. Failure of the SiC results in an instantaneous release of elastic energy that should be sufficient to cause simultaneous failure of the pyrocarbon layers.

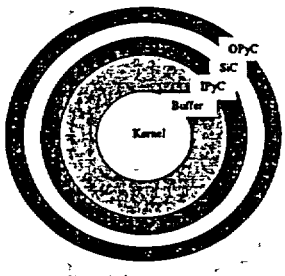

Figure 1. Typical TRISO-coated fuel particle geometry.

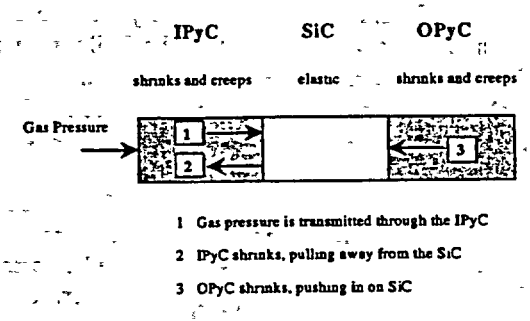

Figure 2. Behavior of coating layers in fuel particle.

Numerous material properties are needed to represent fuel particle behavior in the performance model. These include irradiation-induced strain rates to account for shrinkage (or swelling) of the pyrocarbon layers, creep coefficients to represent irradiation-induced creep in the pyrocarbon layers, and elastic properties to represent elastic behavior for the pyrocarbons and silicon carbide. The properties used in the model were obtained from data that was compiled in a report by the CEGA Corporation in July 1993. This data was based on a review and evaluation of material properties published in the literature to that date [1].

Irradiation-induced creep in the pyrocarbon layers is treated as secondary creep, i.e. the creep strain rate is proportional to the level of stress in the pyrocarbon. The creep coefficient increases significantly with increases in the irradiation temperature. Due to anisotropy in the swelling behavior of the pyrocarbon layers, the strains are different for the radial and tangential directions. The swelling strains are functions of four variables, i.e. fluence level, pyrocarbon density, degree of anisotropy (as measured by the Bacon Anisotropy Factor, BAF), and irradiation temperature. In the radial direction, the pyrocarbon generally shrinks at low fluences but swells at higher fluences. In the tangential direction, the pyrocarbon shrinks at all levels of fluence. The magnitude of the shrinkage increases as

BAF increases or as the irradiation temperature increases. The silicon carbide is a much stiffer material than the pyrocarbons, with a Young's modulus that is an order of magnitude larger.

4. Models

4.1 Structural

The ABAQUS program [2] is used in the performance model to perform finite element stress analysis on coated fuel particles. This program is capable of simulating the complex behavior of the coating layers, and can be used to evaluate multidimensional effects, such as shrinkage cracks in the IPyC, partial debonding between layers, and asphericity. We have shown [3] that radial shrinkage cracks in the IPyC could make a significant contribution to fuel particle failures, and such cracks have been observed in post-irradiation examinations. We have, therefore, devoted significant effort toward including this failure mechanism in PARFUME (in addition to the traditional pressure vessel failure associated with buildup of internal fission gas pressure).

ABAQUS models for both normal and cracked three-layer geometries are shown in Figure 3. These are axisymmetric models that allow for nonsymmetry in the plane of the model, thus enabling an evaluation of multidimensional effects on stress behavior of the coating layers. The model of the normal spherical particle has no cracks or defects in the layers of the particle. The IPyC and OPyC layers are assumed to remain fully bonded to the SiC layer throughout irradiation. This model is used to demonstrate behavior of a normal particle in expected reactor conditions, as well as to determine stresses in the various layers throughout irradiation. The model consists of quadrilateral axisymmetric elements, giving the effect of a full sphere. Only the three structural layers (i.e. the IPyC, SiC, and OPyC) of the particle are included in the model. The layer thicknesses for the IPyC, SiC, and OPyC are nominally set at 40, 35, and 43 μm, respectively, but these can be varied as desired. An internal pressure is applied in the analysis to simulate the buildup of fission gas pressure, and an external pressure is applied to represent either reactor or test conditions. Particles are analyzed in a viscoelastic time-integration analysis that progresses until the fluence reaches 3×10^{25} n/m^2, occurring at a time of 1.2×10^7 s in the analysis. These are representative conditions that can be varied as desired.

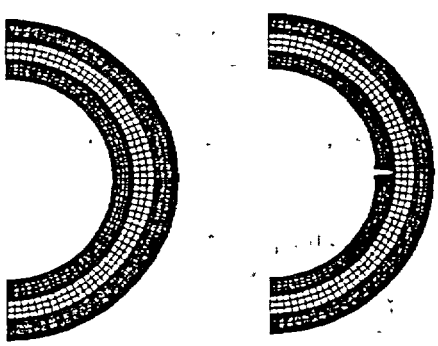

Figure 3. Finite element models for normal and cracked configurations.

The model for a cracked particle is identical to that of the normal particle except that it has a radial crack through the thickness of the IPyC layer. Such a crack is typical of those observed in post-irradiation examinations of the New Production Modular High Temperature Gas Reactor (NP-MHTGR) fuel particles. During irradiation, shrinkage of the initially intact IPyC layer induces a significant tensile stress in that layer. If the tensile strength of the IPyC layer is exceeded, then a radial crack develops in the IPyC layer. This crack is included in the model from the beginning of the solution since it is not feasible to initiate the crack later in the ABAQUS analysis. Because the shrinkage in the pyrocarbons dominates the particle behavior early during irradiation, large tensile stresses in the IPyC occur early. Therefore, the assumption of the presence of a crack at the beginning of the solution should be a reasonable approximation. The analysis does not include dynamic effects associated with a sudden failure of the IPyC, which could increase the magnitude of the stresses calculated.

Figure 4 plots the calculated tangential stress history for the SiC layer of a normal (uncracked) particle. As shown, the SiC remains in compression largely because of the shrinkage in the pyrocarbon layers (the IPyC pulls while the OPyC pushes on the SiC). Figure 4 also plots the maximum principal stress in the SiC layer near the crack tip of a particle with a cracked IPyC. In the

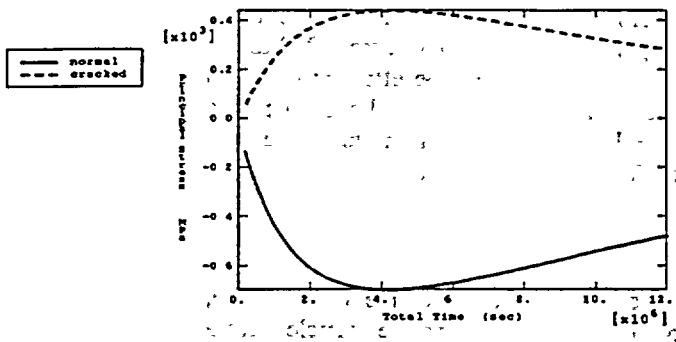

Figure 4. Time histories for stress in the SiC layer for normal and cracked particles.

particle analyzed, the crack leads to a calculated tensile stress in the SiC layer of about 440 MPa. It can be seen that a cracked IPyC greatly changes the stress condition in the SiC, which significantly increases the probability of SiC failure.

4.2 Statistical

We have also investigated the effect of statistical variations in fuel particle design parameters on the structural response of the fuel particle. In the case of a normal (uncracked) particle, statistical variations in design parameters are treated with simplified solutions built into the PARFUME code, rendering finite element analysis unnecessary. In the case of a cracked particle, however, finite element analyses are performed to capture the multidimensional behavior and thereby characterize the effects of variations in these parameters. Based on the results of analyses on cracked particles, there are a number of parameters that are important in describing the behavior of the cracked particle and thus merit a detailed statistical evaluation. These include the IPyC thickness, SiC thickness, OPyC thickness, the densities of the pyrocarbon layers, BAF of the pyrocarbon layers, irradiation temperature, particle diameter, and the creep coefficient for the pyrocarbon layers. For example, Figure 5 shows the maximum calculated stress in the SiC layer as a function of the irradiation temperature (when all other parameters are held constant). The stress decreases with temperature because the higher creep in the pyrocarbons at higher temperatures tends to relax stresses in the coating layers earlier during irradiation.

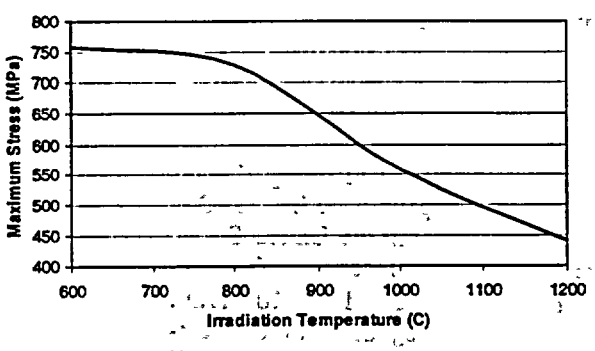

Figure 5. Calculated SiC stress as a function of irradiation temperature.

Initially, regression analyses were performed using the Design Expert program [4] to produce an algorithm that can be used to predict the stress level in the SiC layer of particles having a cracked IPyC. The program used response surface analysis to develop a sixth-order polynomial that statistically fit stress data to a high level of accuracy when variations in six parameters were considered. A full-factorial analysis required results from a total of 972 finite element analyses to successfully develop the algorithm. The problem with this statistical treatment is that it becomes impractical to consider further parametric variations or to redo the analysis if basic assumptions (such as the pyrocarbon shrinkage properties used) are changed. Therefore, an alternative method has been developed that greatly reduces the number of finite element analyses needed. In this approach, finite element analyses are performed on just enough cases to determine the effects of varying each parameter individually. We then analyze the same cases using a closed-form solution that solves for stresses in a normal (uncracked) TRISO fuel particle [5]. Finally, we perform statistical fits on the results of the analyses and draw a correlation between the stress in an uncracked particle with the stress in a cracked particle for the same parametric variations. In the PARFUME code, then, the stress in the SiC layer of a particle having a cracked IPyC is determined by first computing the stress for the same particle having an intact IPyC. This stress is then converted to a stress for a cracked particle by applying the correlations. With this approach, there is little effort involved in adding more parameters to the

statistical base, and there is no limit to the number of parameters that can be considered. The number of finite element analyses needed for statistical analysis of six parameters was reduced from 972 to 14. Thus, even if assumptions change or a new failure mechanism is introduced, the effort required to perform a new statistical analysis is easily manageable. The accuracy of this statistical approach was verified by comparing results with those obtained from the Design Expert algorithm. The two methods showed close agreement when used to calculate particle failure probabilities.

5. Approach for Determining the Particle Failure Probability

To treat the statistical variations in material properties and other parameters for the fuel particle, PARFUME uses Monte Carlo sampling on a batch of fuel particles in determining the particle failure probability. In these samplings, the code performs statistical variations on any number of parameters (such as IPyC, SiC, OPyC thicknesses, IPyC BAF, etc.) by applying Gaussian distributions to these parameters. When the code samples a particle, it first uses a closed form solution [5] to calculate the stress in the IPyC layer. Because of the brittle nature of pyrolytic carbon, the IPyC is expected to fail in a probabilistic manner according to the Weibull statistical theory [6]. As such, the calculated stress for the IPyC is compared to a Weibull strength for the IPyC to determine whether it cracks. This strength is obtained by sampling from a Weibull distribution having a mean strength σ_{mc} and a modulus m. The mean strength σ_{mc} is defined to be the stress level at which 63.2% of the IPyC layers would fail if all were stressed equally. It is derived from a volumetric integration of stresses in the IPyC, and is based on CEGA's data for the characteristic strength σ_0.

If it is determined that the IPyC layer of the particle cracks, then the statistical correlation equations described in Section 4.2 are used to calculate the stress in the SiC layer. As with the IPyC, the SiC layer is expected to fail according to a Weibull statistical distribution, having a mean strength σ_{mc} and a modulus m. The mean strength is derived from an integration of SiC stresses in the vicinity of the crack, and again is based on CEGA's data for the characteristic strength σ_0. If it is determined that the IPyC layer of the particle does <u>not</u> crack, then the code uses the closed form solution to calculate the SiC stress. In this case, the Weibull mean strength σ_{mc} is derived from an integration of the more uniform stresses of an uncracked particle.

6. Predictions for NPR Experiments

The current version of the PARFUME code has been used to analyze three irradiation experiments conducted as part of the NP-MHTGR program in the early 1990s. Fuel compacts were irradiated at the High Flux Isotope Reactor (HFIR) and the Advanced Test Reactor (ATR) in the United States. TRISO-coated particles containing high-enriched uranium were irradiated at temperatures between 750 and 1250 °C, burnups between 65 and 80% FIMA, and fluences between 2 and 3.8×10^{25} n/m^2. On-line fission gas release measurements indicated significant failures during irradiation. Post-irradiation examination (PIE) of individual fuel compacts revealed the presence of radial cracks in all layers of the TRISO coating. The irradiation conditions for the experiments are summarized in Table 1, while the levels of cracking measured during PIE are shown in Table 2. The particle dimensions, burnup, end-of-life fluence, irradiation temperature, and ^{235}U enrichment were set to appropriate values in the analysis for each experiment. Included in the results shown in Table 2 (column 5) are the percentage of particles predicted to have a cracked IPyC and the percentage of particles predicted to fail because of a cracked SiC. It is seen that PARFUME predicts that the IPyC layer cracks in 100% of the particles for every compact tested. In reality, the PIE revealed that the actual failure fractions were less than this, as shown in the table. Based on historical literature sources, it is believed that the creep coefficients currently used in the PARFUME code may be too low, which would allow the calculated shrinkage stresses to reach too high a value before creep relaxation takes effect. If the creep coefficients used in the analyses were amplified by a factor of 2, the number of failures in the IPyC and SiC decrease as shown in Table 2 (column 6). The higher creep gives significantly better correlation with the experimental results.

Table 1. Irradiation conditions for NPR experiments

Fuel Compact ID	Fast Fluence (10^{25} n/m^2)	Irradiation Temp. (°C)	Burnup (%FIMA)
NPR-2 A4	3.8	746	79
NPR-1 A5	3.8	987	79
NPR-1 A8	2.4	845	72
NPR-1A A9	1.9	1052	64

Table 2. Comparisons of ceramographic observations to PARFUME calculations for TRISO coated fissile fuel particles

IPyC Layer (a)					
Fuel Compact ID	Sample Size	% Failed	95% Conf. Interval (%)	Calc.	Calc. with 2× Creep
NPR-2 A4	83	65	54<p<76	100	99.6
NPR-1 A5	39	31	17<p<47	100	34
NPR-1 A8	53	6	2<p<16	100	94
NPR-1A A9	17	18	5<p<42	100	15
SiC Layer (a)					
	Sample Size	% Failed	95% Conf. Interval (%)	Calc.	Calc. With 2× Creep
NPR-2 A4	287	3	2<p<6	40.7	2.2
NPR-1 A5	178	0.6	0<p<3	16.1	0.2
NPR-1 A8	260	0	0<p<2	33.4	1.4
NPR-1A A9	83	1	0<p<5	10.8	0.04

a. Layer failure is considered as a through wall crack as measured by PIE.

7. Summary and Future Work

The INEEL has begun development of an integrated mechanistic fuel performance model for TRISO-coated gas reactor particle fuel named PARFUME (PARticle Fuel ModEl). The objective of PARFUME is to physically describe the behavior of the fuel particle under irradiation. Both the mechanical and physico-chemical behavior of the particle under irradiation are being considered. Statistical and modeling methods have been developed that enable prediction of the multi-dimensional behavior that is characteristic of TRISO-coated gas reactor fuel. These methods have been applied to particle failures caused by irradiation-induced shrinkage cracks in the IPyC layer. The model, with an adjustment in the creep properties for the PyC materials, makes predictions that are in reasonable agreement with the IPyC and SiC failures observed in the NP-MHTGR fuel irradiation experiments performed in the early 1990s. Future work in the code development includes:

- Completion of the fission product chemistry modules for the code
- Development of the fission product transport module
- Comparison of the code to other older gas reactor irradiations data
- Including the effects of asphericity and partial debonding between coating layers.

References

[1] CEGA Corporation, NP-MHTGR Material Models of Pyrocarbon and Pyrolytic Silicon Carbide, CEGA-002820, Rev. 1, July 1993.

[2] ABAQUS User's Manual, Version 5.8, Hibbitt, Karlsson, and Sorenson, Inc., 1988.

[3] G. K. Miller, D. A. Petti, D. J. Varacalle, J. T. Maki, Consideration of the Effects on Fuel Particle Behavior from Shrinkage Cracks in the Inner Pyrocarbon Layer, *J. Nucl. Mat.*, 295, 2001, p. 205.

4] P. Whitcomb et al., Design-Expert, Version 4.0, Stat-Ease Inc., 1993.

[5] G. K. Miller and R. G. Bennett, Analytical Solution for Stresses in TRISO-coated Particles, *J. Nucl. Mat.*, 206, 1993, p. 35.

[6] N. N. Nemeth et al., Ceramics Analysis and Reliability Evaluation of Structures (CARES) User's and Programmer's Manual, NASA Technical Paper 2916, 1989.

PROSPECTIVE STUDIES OF HTR FUEL CYCLES INVOLVING PLUTONIUM

B. BONIN and D. GRENECHE,

COGEMA, Direction de la Recherche et du Développement

F.CARRE, F. DAMIAN and J.Y. DORIATH,

CEA Direction de l'Energie Nucléaire

ABSTRACT

High Temperature Gas Cooled reactors (HTRs) are able to accommodate a wide variety of mixtures of fissile and fertile materials without any significant modification of the core design. This flexibility is due to an uncoupling between the parameters of cooling geometry, and the parameters which characterize neutronic optimisation (moderation ratio or heavy nuclide concentration and distribution).

Among other advantageous features, an HTR core has a better neutron economy than a LWR because there is much less parasitic capture in the moderator (capture cross section of graphite is 100 times less than the one of water) and in internal structures.

Moreover, thanks to the high resistance of the coated particles, HTR fuels are able to reach very high burn-ups, far beyond the possibilities offered by other fuels (except the special case of molten salt reactors).

These features make HTRs especially interesting for closing the nuclear fuel cycle and *stabilizing the plutonium inventory.*

A large number of fuel cycle studies are already available today, on 3 main categories of fuel cycles involving HTRs : i) High enriched uranium cycle, based on thorium utilization as a fertile material and HEU as a fissile material; ii) Low enriched uranium cycle, where only LEU is used (from 5% to 12%); iii) Plutonium cycle based on the utilization of plutonium only as a fissile material, with (or without) fertile materials.

Plutonium consumption at high burnups in HTRs has already been tested with encouraging results under the DRAGON project and at Peach Bottom. To maximize plutonium consumption, recent core studies have also been performed on plutonium HTR cores, with special emphasis on weapon-grade plutonium consumption. In the following, we complete the picture by a core study for a HTR burning reactor-grade plutonium. Limits in burnup due to core neutronics are investigated for this type of fuel.

With these limits in mind, we study in some detail the Pu cycle in the special case of a reactor fleet made of a mixture of LWRs and HTRs. It is reasonable to assume that if HTRs are to be deployed on an industrial scale, they will co-exist during a long period of time with already existing LWRs. The present paper investigates the symbiotic behaviour of LWRs producing plutonium, and of HTRs burning it.

1. Introduction

High Temperature, Gas-Cooled reactors (HTRs) have several fundamental features which distinguish them from other types of reactors, and provide significant operational advantages.

HTRs are able to accommodate a wide variety of mixtures of fuels without any significant modification of the core design. This flexibility is due to an uncoupling between the parameters of cooling geometry, and the parameters which characterize neutronic optimization (that is moderation ratio or heavy nuclide concentration and distribution). In fact, it is possible to modify the packing fraction of coated particles in the fuel within the graphite matrix without changing the dimensions of the fuel elements. Other physical reasons favour the much better adaptability of HTRs with regard to the fuel cycle in comparison with reactors using moderators in the liquid form, such as LWRs. An illustration of that is the void coefficient which limits the plutonium content of PWR MOX fuels and which is not a constraint for HTRs. It is to be noted also that an HTR core has a better neutron economy than a LWR because there is much less parasitic capture in the moderator (capture cross section of graphite is 100 times less than the one of water) and in internal structures.

Finally it must be noted that HTR fuels are able to reach very high burn-ups, which are far beyond the possibilities offered by other thermal reactors (except the particular case of molten salt reactors). This capability allows for essentially complete plutonium fission in a single burnup and minimizes the proliferation risk in the use of this fuel form.

2. - A classification of fuel cycles in HTRs

Numerous studies have been carried out in the past to assess and compare merits and drawbacks of all solutions which may be considered in HTRs, and which depend on:

- the type of fissile material (U233, U235, Plutonium) or fertile material (Th232, U238) with various enrichments,
- utilization conditions in the reactor: moderation ratio, frequency of reloads, fraction of the core replaced at each cycle, distribution of fertile and fissile materials among various categories of particles, etc.
- fissile material recycling strategy

A large number of results are available today [1], and these can be summarized by considering 3 main categories of fuel cycles :

1) High Enriched Uranium (HEU) cycle based on thorium utilization as a fertile material, and high enriched uranium (typically 93 %) as a fissile material

2) Low Enriched Uranium (LEU) cycle where only enriched uranium is used (from 5 % to 12 %)

3) Plutonium cycle based on the utilization of plutonium only as a fissile material, with (or without) fertile materials.

For completeness, it is to be noted that a kind of "hybrid" cycle called MEU (involving a mixture of medium enriched uranium (20%) with thorium) has also been considered. In the following, we shall discuss in more detail each of the three categories mentioned above.

2.1 – The HEU + Th cycle

Thorium, being the fertile material utilized in this cycle, generates U233, which is by far the best fissile isotope for thermal spectrum reactors. Furthermore, there are probably more thorium resources than uranium resources, and its utilization as a fertile isotope in reactors has been extensively studied, particularly for HTRs.

For these reasons, the HEU cycle was considered as the reference cycle at the very beginning of HTR development in both USA and Germany. As a result, 4 HTR prototype power reactors having operated in the past (AVR and THTR in Germany, Peach Bottom and Fort Saint Vrain in USA) were first loaded with fuel containing thorium in various forms such as carbides, oxides, and single thorium particles or mixtures with uranium.

The main advantage of this cycle is a small uranium consumption. Another advantage, which was not underlined in the past but which may become an important argument, is the significant reduction of minor actinides production if U233 is recycled in reactors. This would occur in reactors operated with Th-U233 cycles.

On the other hand, the competitiveness of an HEU cycle is questionable today, all the more so because there is a large uncertainty on thorium costs, since the market for this material is very limited. The main technical hurdle for the development of the HEU cycle comes from U233 recycling. The difficulty arises from the significant energetic γ emission of some daughter products of U232 (7 year period), which comes with U233. This harmful emission essentially requires a remote fabrication process of U233 fuels. Technically this operation is certainly feasible with modern technologies, but significant R&D effort would be necessary to industrialize it and to ensure its profitability.

2.2 – The LEU cycle

The LEU cycle uses uranium with a minimum enrichment of 5 to 6 %, which is more than the highest enrichments usually utilized in other current thermal reactors such as LWRs (for HTR's, the uranium enrichment for LEU cycles usually ranges from 5 % to 15 %). This is due to a rather diluted and homogeneous uranium distribution in HTR fuels which favours U238 resonance captures (self shielding effect is reduced). This greater neutron absorption must be compensated for by a higher enrichment. On the other hand, this apparent enrichment penalty goes with a higher conversion ratio (typically 0.7 to 0.8 or even more if needed), which compensates the higher uranium consumption due to initial enrichment, because of a greater "in situ" formation of fissile isotopes (plutonium). It also provides for a more uniform reactivity behaviour of the core life.

The LEU cycle was studied during the 60's and 70's in USA and Germany as well as in England and in France. Some LEU fuels were loaded in the European experimental reactor DRAGON. Furthermore, Germany decided in the 80's to select this fuel for their future projects. Japan has also selected this fuel as well for their HTTR experimental reactor, which is in operation today.

2.3 Plutonium fuel cycles with or without thorium

From a physics standpoint, the interest of plutonium use in HTRs comes from flexible features already discussed above. It is known that plutonium isotopes have very large capture resonances near the thermal range of the neutron spectrum. This is the reason why plutonium reactivity and evolution as function of time heavily depends upon its initial concentration and distribution in the fuel (because of self-shielding effect mentioned above). In that respect, a HTR provides a large margin to the designer for optimising fuel cycle characteristics.

The idea to use plutonium as the only fissile material but still with thorium as a fertile material was considered very early in the 60's within the framework of the DRAGON project. GA took up the studies in 1968 in a program with Edison Electric Institute. This program was carried out up to the manufacturing of a test fuel element and its irradiation in the Peach Bottom HTR.

To maximize plutonium consumption, more recent studies have been performed on plutonium HTR cores with no fertile material at all. This solution has been particularly considered in the framework of weapon-grade plutonium consumption. For the reasons already discussed above, only HTRs offer such a possibility (a part from fast neutron reactors for which it seems theoretically feasible to design core containing only plutonium).

As far as net plutonium consumption is concerned, performances claimed for this type of fuel cycle are remarkable. For example, if we refer to joint studies between GA and MINATOM on what they call the "PC-MHR" (Plutonium Consumption – Modular Helium Reactor), plutonium consumption reaches 90 kg/TW(e)hr[1]. As a guide, an EPR (European Pressurized Reactor) loaded with 100% MOX fuel could theoretically consume 65 kg/TW(e)hr. One can also compare with a Fast Neutron Reactor operating on "under-breeding" mode which could achieve a theoretical consumption of 80 kg/TW(e)hr, provided that advanced fuel containing 45% of plutonium are developed (see French "CAPRA" program).

From this short overview, we can draw the following main conclusions:

In spite of its potential advantages, the HEU cycle appears to be handicapped because of proliferation concerns. However it should be worthwhile to carry out further studies in order to better assess its potential benefits with regard to other questions, such as minor actinide generation, which took much more importance in recent years.

The LEU cycle benefits from the largest experience but needs an uranium enrichment beyond 5% which is the upper limit for most of fuel cycle facilities in many countries. It would be necessary to modify these facilities or to build new plants (particularly for enrichment), knowing that in any case, new fuel fabrication plants are needed to manufacture HTR fuels.

---

[1] It is easy to verify this figure by using a 50 % efficiency of the plant, and elementary fission energy release of 210 MeV. In fact, the net plutonium consumption reaches about 100 kg/TWhe due to the the formation of americium and curium from the plutonium by neutron capture.

Thorium use is not specific to HTRs even though they are better adapted than other reactors to take advantages of thorium properties. Recycling of U233 however would require more industrial experience.

For plutonium consumption, HTRs are, without doubt one of the best types of reactors. Only fast neutron reactors may compete in this domain, but at the cost of as much, or more, development as HTRs. Taking into account the acquired background on HTR fuels, it seems that there is no technological hurdle to achieve expected performances of plutonium consumption. However, 20 years ago, the context was not the same and in particular, questions such as plutonium consumption or long-term waste management were not so acute. Therefore, it is worthwhile to reconsider this option in light of these new challenges.

3. Burning reactor-grade plutonium in HTRs. A fuel cycle scenario.

3.1 Assumptions

In this paper, we studied the fuel cycle for a plausible scenario describing the progressive introduction of Pu-burning HTRs in a fleet initially composed of LWRs.

We did not try to treat the subject exhaustively. Indeed, we restricted ourselves to the assumption that the HTRs are exclusive Pu burners, and that the Pu comes from the LWRs.

Fuel cycle studies in steady state regime are of limited interest, because time constants for the introduction of new nuclear reactors are always very long. For the long-term future, the introduction of fast neutron reactors might possibly come into the game before a steady state regime for any existing reactor fleet can be established. For the sake of plausibility, the scenario in this paper has thus been studied in transient regime, and cover only the mid-term future.

We are interested mainly in the plutonium balance, because Pu is an important energetic resource, and because it is the major contributor of the radiotoxic fuel inventory.

Hypotheses underlying the scenario under study are as follows :

-The studied scenario is deemed to be realistic for the next 50 years. However, in order to gain some insight into the asymptotic behavior of the reactor fleet, the studied time window has been extended to 100 years, between 2000 and 2100.

-The total electric power produced by the reactor fleet is kept constant during this period.

-We start with a realistic initial inventory in 2025, supposed to be representative of the french situation at that time, namely 400 tons.

-We assume a gradual replacement of existing LWRs by Pu-burning HTRs. The rate of replacement is 2.1 % per year, between years 2025 and 2035. At that time, the reactor fleet is stabilized, and 21.25 % of the total installed electric power is produced by HTRs (Fig. 1).

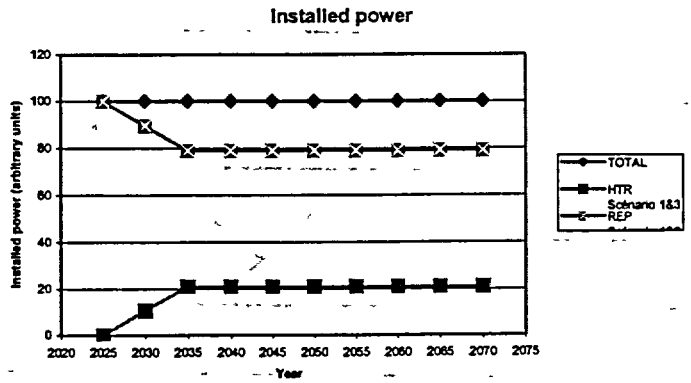

Fig. 1: Composition of the reactor fleet, vs time

-We assume that MOX fuel is used in 42% of the LWR fleet during the early years of the period under study (until 2025). After that date, we assume that the LWRs become exclusive UOX burners (stop of MOXing in LWRs in year 2025). However, all the UOX fuel burnt in the LWRs is still processed to produce the Pu fuel needed for HTRs.

-The burnup of the UOX fuel in LWRs is assumed to be 55 GW.d/t, with a fuel renewed by fifth every year. This corresponds to a net production of plutonium of 25 kg/TWhe.

-Since the high burnup achievable in HTRs does not encourage multiple recycling, we assume a one-through cycle of Pu in HTRs.

-We assume a net consumption of plutonium in HTRs of 100 kg/TWhe. The Pu burnup achievable in a thermal HTR has been assumed to be 500 GW.d/t. As will be justified in section 4, this is probably a rather conservative value.

3.2 Results of the fuel cycle study in this scenario

Stabilization of Pu inventory is achieved around year 2030. This Pu inventory has two components : in and out of the reactors. The plutonium inventory out of the reactors is plotted vs time in fig. 2. The mass of Pu discharged from the HTRs grows linearly with time, while the Pu mass still available for HTR fuel fabrication decreases linearly after year 2040.

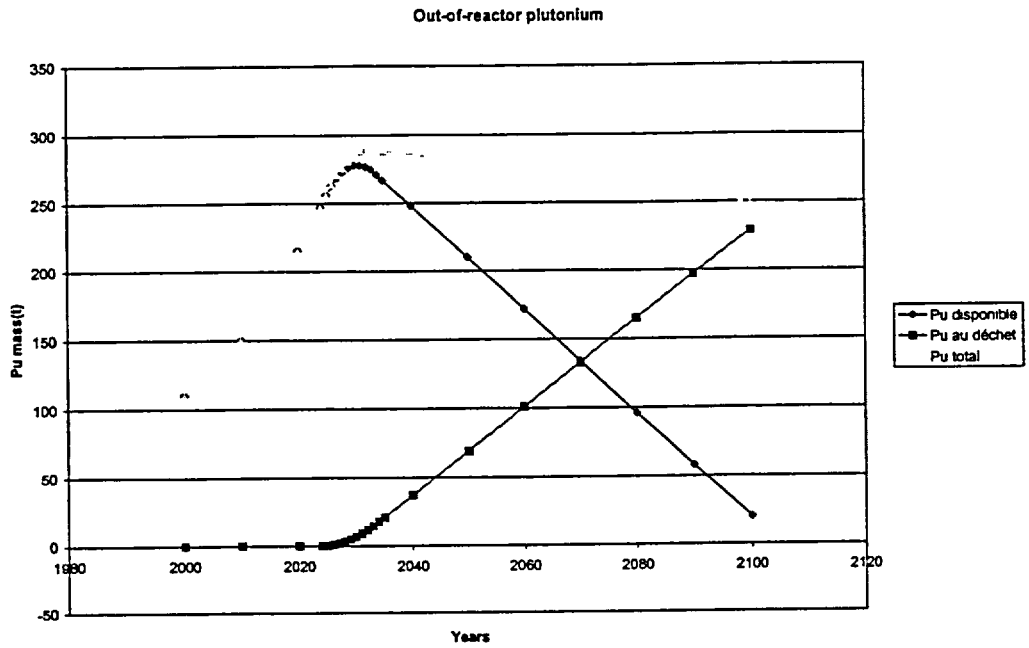

Fig 2: Evolution of the out-of-reactor Pu inventory for a fleet producing 400 Twhe/year

It can be seen that the plutonium mass available for HTR fuel fabrication almost vanishes around year 2100. We reach here the limits of a realistic scenario, since other types of reactors might possibly enter into the fleet long before this date.

The scenario under study is contemporary of the scenario of introduction of advanced fuels like CORAIL and APA in LWRs, whose goal is precisely to enhance the Pu consumption in LWRs. It is thus possible to compare these options with the symbiotic scenario LWR+HTR. The total Pu inventory versus time is plotted in Fig. 3 for all these options.

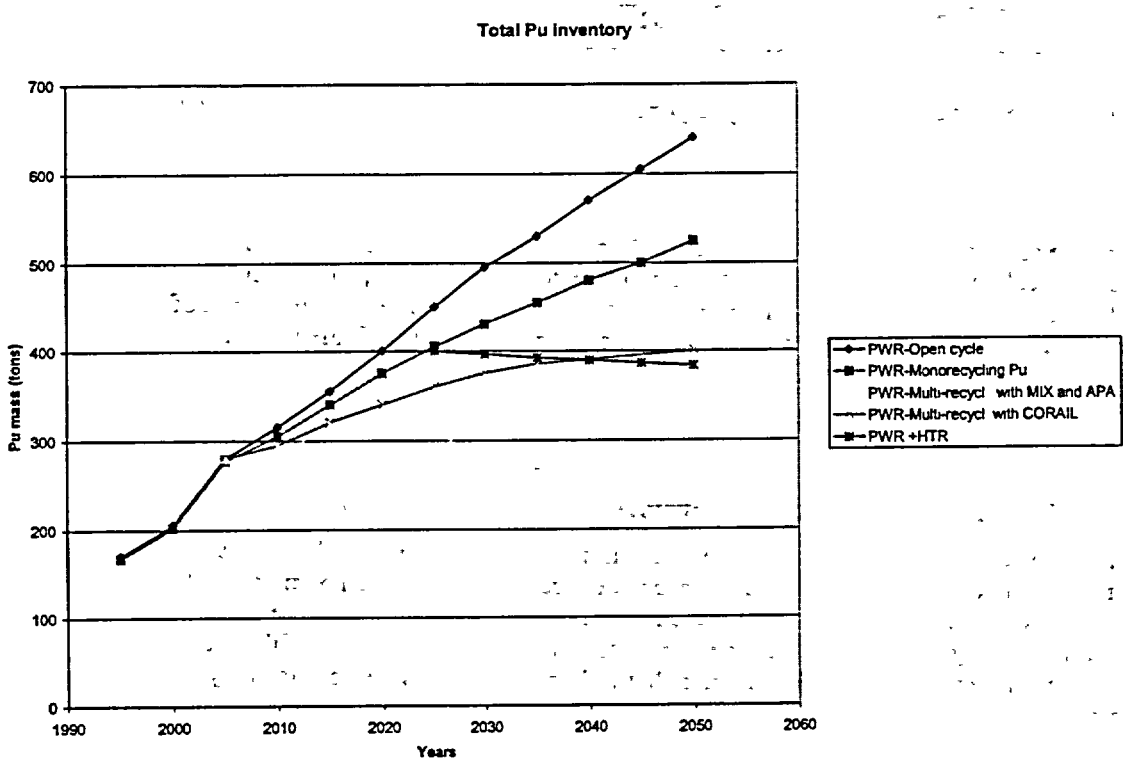

Fig. 3 Total plutonium inventory for a reactor fleet producing 400 Twhe/year

It can be seen here that for Pu burning, HTRs compare favorably to LWRs, even if LWRs use multirecycling with the most advanced fuels. The stabilization of Pu inventory is possible with LWRs only if advanced fuels are used and with multirecycling. A mixed fleet of LWRs and HTRs easily achieves the same result with standard fuel (for LWRs) and without multirecycling. However, the comparison between the various options is not straightforward, and needs a few comments. One should note that the isotopic composition of the Pu left as "waste" by the LWR + HTR symbiotic fleet is so degraded that the proliferation risk becomes negligible (Table 1).

Isotopic composition of the discharged plutonium	PWR/UOX 55 GWd/t	HTR/ Pu 575 GWd/t
Pu 238	3	10
Pu 239	58	8
Pu 240	27	23
Pu 241	4	24
Pu 242	8	35
% Pu fissile	62	32

Table 1. The plutonium isotopic composition of the fuel for a MOX 1 and for a typical spent HTR fuel.

Moreover, whereas the advanced fuel discharged from LWRs may need some further conditioning, the Pu discharged from HTRs is conditioned under the form of coated microspheres, which can be considered already as a suitable waste form for interim storage or for final disposal (the production of 1 TWhe by fission of 1st –generation plutonium results in the production of 12 kg of americium and curium).

4. Core studies for a Pu-burning HTR. Maximum Pu burnup achievable in a HTR

A key assumption in the above fuel cycle studies is the Pu burnup achievable in HTRs. The burnup limitation can come from two main causes : the resistance under irradiation of the fuel particles, and the neutronic behaviour of the core. The fuel particle themeselves do not seem to be a severe limitation, since burnups as high as 750 GW.d/t have been achieved without degradation of the fuel particles in previous experiments [2]. This encouraging –but isolated- result must be confirmed by future experiments.

In order to assess the feasibility of HTRs with an "all plutonium" core, preliminary core studies at CEA [3,4,5] were carried out in the special case of the Gas Turbine Modular Helium-cooled Reactor (GT-MHR) 600 MWth General Atomics concept. The annular core geometry of the GT-MHR (fig. 4) was selected to maximize the power density and still permit passive core heat removal while maintaining reasonable fuel temperatures during accident conditions.

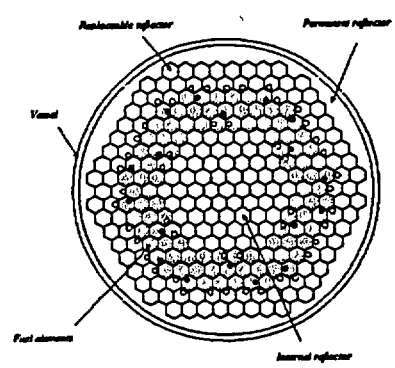

Figure 4 : GT-MHR 600 MWth Core

4.1 Categories of Pu fuels investigated

The Pu composition corresponding to the scenario studied in sect. 3 is of course the first-generation Pu coming from the spent LWR UOX fuel (Pu1), but we thought it would be worthwhile to perform core calculations for other Pu compositions as well (Table 2). MOX burning in LWRs generates a second generation of plutonium (Pu2) that has also been considered in the present core study. Plutonium coming from the dismantling of nuclear warheads has also been studied (WPu).

Cycle name	Plutonium origin	Pu_f/Pu_t
Pu1	PWR* 3,7 % (U5/U) 42 GWj/t - 1/4	66,2 %
Pu2	Second generation MOX-EPR 60 GWj/t	50,15 %
WPu	Weapons grade	94,6 %

*PWR, EPR : Pressurized Water Reactor and European Pressurized Reactor

Table 2 : Plutonium isotopic compositions

4. 2 Computer codes and methodology for core calculation

For the following calculations, the French reactor physics code system SAPHYR developed at CEA has been used. It is composed of several codes: *APOLLO2* (transport), *CRONOS2* (diffusion-transport), *FLICA4* (3D thermal hydraulics)..., which are interconnected.

4. 3 Plutonium fuel cycle characteristics

Fuel element analyses: reactivity margin and burnable poison impact

Figure 5 shows the evolution of infinite multiplication coefficient for Pu1. On the one hand, it should be stressed that compared to a similar fuel depletion without erbium (Pu1–701 kg), the fuel with poison presents an initial reactivity reduction of around 9000 pcm which almost disappears towards 600 GWd/t, corresponding to the loss of 90 % of ^{167}Er. The cycle lengths are however comparable. This important feature of the burnable poison equivalent to that observed with ^{10}B allows adjusting the initial reactivity of the different fuel cycle without changing the cycle lengths. On the other hand, the increase of the plutonium loaded in the fuel element leads to a spectrum hardening that induces a decrease of the reactivity margin at the beginning of cycle (increase of the resonance capture). Then, it is possible to adjust the initial reactivity by adjusting the plutonium loaded into the core. Nevertheless, we should not forget that the presence of the erbium in fuel elements may play an important part in the core behaviour with regard to the negative reactivity feedback especially with highly enriched plutonium.

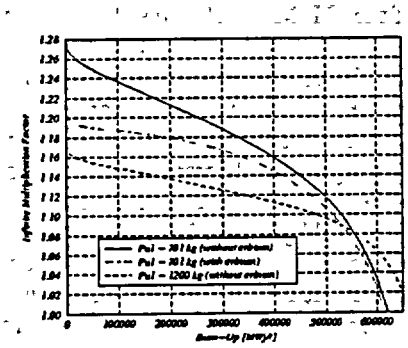

Figure 5 : k_{inf} in evolution

Fuel element temperature coefficient (infinite medium)

The results presented hereafter (Table 3) gather the average temperature coefficient (Doppler and moderator coefficient) between a cold state ($T_{fuel} = T_{moderator} = 20$ °C) and an arbitrary nominal state ($T_{fuel} = 900$ °C / $T_{moderator} = 500$ °C). The calculations have been performed for various types of fuel in order to evaluate both isotopic and core loading effects on these reactivity balance.

Burnup [GWj/t]	WPu - 701 kg with Er	Pu1 - 701 kg without Er	Pu1 - 1200 kg without Er	Pu1 - 1800 kg without Er	Pu2 - 1200 kg without Er
Doppler coefficient					
0	- 1,33	- 2,76	- 3,49	- 3,70	- 3,99
var	- 1,09 (700 GWj/t)	- 0,98 (625 GWj/t)	- 0,92 (650 GWj/t)	- 1,14 (650 GWj/t)	- 1,61 (550 GWj/t)
Moderator temperature coefficient					
0	- 5,33	- 2,29	- 1,91	- 1,46	- 1,83
var	+ 8,60 (700 GWj/t)	+ 8,15 (625 GWj/t)	+ 4,47 (650 GWj/t)	+ 1,74 (650 GWj/t)	+ 4,02 (550 GWj/t)

Table 3 : Fuel element temperature coefficient

Finally, whatever the plutonium loaded into the core or the plutonium quality are, the main tendency derived from these calculations is a decrease of the moderator temperature coefficient in evolution which can lead to a positive value at the end of life of the fuel element. This behaviour is due essentially to the neutron spectrum shift in evolution (strong increase of the thermal flux).
Altogether, these calculated temperature coefficients show the viability of the "all plutonium cores", for the three types of Pu composition and for the burnups mentioned above.

Residual decay heat

For various types of fuel, Figure 6 shows detailed evolution of the stored energy during a Loss of Coolant accident. This energy comes from the core decay heat of the GT-MHR-600 MWth calculated after a reactor shutdown occurring at the end of cycle. The calculation shows some differences depending on the plutonium composition. More important, the calculated values are significantly higher than for a typical "all uranium" core. The result will be an increase of the maximum temperature reached by the fuel in the course of the accident. No detailed thermal calculation has been undertaken so far but our first guess is that this temperature increase is still acceptable for a Pu fuel element.

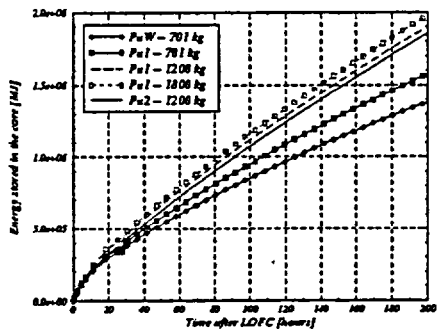

Figure 6 : Core decay heat after a reactor shutdown

5. Conclusion

Core studies with a wide range of plutonium isotopic compositions prove the capability of HTRs to use the plutonium as fuel with no major hurdle from the safety standpoint. For each plutonium composition, limits on the possible applications of long fuel cycle lengths have been assessed. Long cycles and high burnups are possible if fluences of about 12 n/kb (a factor 2 more than the common requirements) are technologically feasible. Nevertheless, more detailed core neutronic analysis are necessary to assess the reactivity control aspects, to define the appropriate fuel management and to answer the issues related to power distribution, which are especially important in the case of the plutonium use.

The present study confirms that a symbiotic reactor fleet involving LWRs and Pu1-burning HTRs would be a very effective way to master the plutonium inventory while providing energy in safe and economical conditions.

However, it must be stressed that even though a rather large experience has already been gained in HTR fuels, significant R&D effort would be still be necessary to perfect and qualify a high performance plutonium fuel on an industrial scale for this type of reactors.

REFERENCES

[1] International Atomic Energy Agency, International Nuclear Fuel Cycle Evaluation (INFCE), Vienna (1980)

[2] U. Hansen, ***"Plutonium in high temperature reactors"*** Dragon Project Report 899 (1974)

[3] X. Raepsaet, F. Damian, R. Lenain, and M. Lecomte, ***"Fuel cycle related-parametric study considering long-lived actinide production, decay heat and fuel cycle performances"*** - AIEA Technical Comittee Meetings- Beijin - (November 98)

[4] X. Raepsaet, F. Damian and M. Lecomte, ***"Fuel cycle performances in High Temperature Reactor"***, International Conference on Future Nuclear System - Global'99 (Vol.1)

[5] A.I. Kiryushin, N.G. Kodochigov, N.G. Kouzavkov, N.N. Ponomarev-Stepnoi E.S. Gloushkov, V.N. Grebennik, ***"Project of the GT-MHR high-temperature helium reactor with gas turbine"*** - Nuclear Engineering and Design 173, 119-129 (1997)

EXAMINATION OF THE POTENTIAL FOR DIVERSION OR CLANDESTINE DUAL USE OF A PEBBLE-BED REACTOR TO PRODUCE PLUTONIUM

A. M. OUGOUAG, W. K. TERRY, and H. D. GOUGAR
Idaho National Engineering and Environmental Laboratory
P. O. Box 1625, Idaho Falls, ID 83415-3885 – United States

ABSTRACT

This paper explores the susceptibility of Pebble-Bed Reactors (PBRs) to be used overtly or covertly for the production of plutonium for nuclear weapons. The basic assumption made for the consideration of overt production is that a country would purchase a PBR with the ostensible motive of producing electric power; then, after the power plant was built, the country would divert the facility entirely to the production of weapons material. It is assumed that the country would then have to manufacture production pebbles from natural uranium. The basic assumption made for covert production is that the country would obtain and use a PBR for power production, but that it would clandestinely feed plutonium production pebbles through the reactor in such small numbers that the perturbation on power plant operation would be very difficult to detect. This paper shows the potential rate of plutonium production under such constraints. It is demonstrated that the PBR is a very poor choice for either form of proliferation-intent use.

1. Introduction

The Pebble Bed Reactor (PBR) concept is receiving emphatic renewed interest. For example, an international consortium [1] is intent on developing and deploying such a reactor in the near future, with the ultimate goal of international commercialization and deployment of large numbers in developing countries and elsewhere. This optimistic business assessment stems from the numerous inherently and passively safe features of the reactor concept. Furthermore, modular design allows high technology fabrication to be shifted to centralized locations with deployment in low technology markets. The possible (and in some fuel cycle patterns, necessary) recirculation of the fuel pebbles and the online de-fueling and refueling of these reactors raise questions about their potential use as production facilities for weapons materials. However, these features also allow the reactors to operate with very little excess reactivity. In a previous study [2], it was demonstrated that the dual use of a PBR (simultaneous production of power and weapons materials) would be detected easily and promptly in the case where the production pebbles are designed to resemble the legitimate fuel pebbles closely. In this paper, additional scenarios are considered. These include more sophisticated cases of covert dual use with illicit production pebbles introduced into the core, overt diversion of the facility for weapons materials production, and construction of an even more suitable replacement facility using equipment removed from the original reactor. The principal assumptions of the study are presented in the next section. Then the scenarios considered are outlined. They are followed by a description of the various models and methods used. The subsequent section presents model results. The conclusion section summarizes the principal findings of this study.

2. Technological and Safeguards Context Assumptions

In this study, it assumed that a country purchases a PBR presumably for the legitimate purpose of producing energy (electricity and/or process heat, etc.). The purchasing country is assumed not to possess front-end fuel cycle capabilities or technology. Thus, it could not produce enriched fuel to supplement fuel that it acquires from an external supplier. It is assumed that the reactor owners and all possible reactor fuel suppliers subscribe to an established safeguards regime in which no new fuel is supplied until previous batches of spent fuel are returned or accounted for and safeguarded, as appropriate. Under these conditions, the illicit dual use of the facility would require the manufacture of production pebbles by the reactor owner, their illicit introduction into the reactor, and their retrieval

and extraction from the reactor fuel cycle prior to their detection by safeguard related systems. The principal controlling mechanism is the requirement that fresh fuel supplies be subjected to the concomitant return of corresponding batches of already used fuel. This requirement is based on the knowledge that the fuel utilization and the refueling patterns of a PBR used efficiently for power production are very highly and reliably predictable [3]. The fuel requirements for continued efficient operation can reliably and precisely be correlated to the power production at the facility. Thus, any significant departure from the known legitimate efficient utilization patterns would raise suspicions. The fuel vendor(s) and international safeguard organizations will know the fuel management plan that corresponds to the legitimate intended use of the reactor. Any change in fuel utilization will require satisfactory explanation.

3. Dual Use and Diversion Scenarios

Three principal scenarios have been identified in this study. These are (i) the covert dual use of the facility, (ii) the overt diversion of the facility as built, and (iii) the construction of an alternate facility using equipment diverted from the original facility ("cannibalization").

Covert Dual Use. In the first scenario, a small number of production pebbles are covertly introduced into the reactor to produce weapons materials while the reactor is still producing power. The goal of the reactor owner would be to produce weapons material at the maximum rate possible at which the effects on the legitimate fuel cycle use would be undetectable. In this scenario, the reactor owner expects to continue receiving replacement fresh fuel from the supplier. The maximum-dissimulation case of this first scenario was considered in a previous study [2]. In that study, it was assumed that illicit fuel pebbles were manufactured by the reactor owner and used as production targets in the reactor. Those illicit pebbles were assumed identical to legitimate fuel pebbles in all respects except uranium enrichment. Thus, they included the same physical features and compositions, save for the replacement of enriched uranium with natural uranium. In that earlier study, it was shown that this scenario was very impractical for the production of weapons materials and that it resulted in very early detection because of shortfalls in power production and an unjustified increase in fresh fuel needs. In that early study, the production pebbles were "optimized" to resemble the legitimate ones as much as possible. In this paper, a variant of the first scenario is considered in which the illicit pebbles are optimized to minimize the perturbation on the multiplication factor that they cause (and thus minimize their impact on neutron economy).

Overt Facility Diversion. The second scenario assumes that the reactor owner forgoes the reliance on an external fresh fuel supplier and operates the facility solely with indigenous natural uranium pebbles. In this scenario, all the reactor physical characteristics are retained, except for the use of an alternate fuel. The fuel is optimized to attempt to minimize the reactor critical size. It is shown in this paper that the original reactor cannot achieve criticality under these conditions and hence that the overt complete diversion of the facility is a physical impossibility without the connivance of a fuel supplier.

Facility Cannibalization. The third scenario examines the extreme and highly unlikely hypothesis of the "cannibalization" of the original reactor to construct a replacement facility capable of criticality. This scenario assumes that only specialized hardware and components are transferred from the original facility and used in the construction of the new one. In this scenario, it is necessary for a completely new reactor building and pressure vessel to be constructed. In this scenario, as in the previous one, no more regular fuel pebbles would be available, and the reactor owners would have to supply their own natural uranium-based fuel.

This study shows that a PBR fueled only by natural uranium pebbles would be large enough to be detectable by reconnaissance satellites. It also shows that adding natural-uranium production pebbles to the regular fuel pebble flow stream at undetectable rates would not only lead to slow production of weapons material but would also produce plutonium of very marginal quality. If higher quality plutonium is sought, the time to accumulation of sufficient materials for practical weapons use is shown to be extremely large, and not compatible with the speedy production of even a modest arsenal.

4. Methodology and Computational Models

There exist many ways by which covert production of weapons materials could be detected; here, it is assumed that a decrease in fuel utilization of more than 5% (or a commensurate increase in fuel requirements) would cause suspicion. Similarly, a discrepancy between energy production and fuel consumption or fuel requirements would raise suspicion. Furthermore, a departure of discharged fuel pebble isotopics from the nominal values that correspond to optimal plant operation would also be reasons for suspicion, because the isotopic distribution in an optimally operated PBR, a consequence of the asymptotic loading pattern, is likely unique and accurately predictable. The models developed in this study, as in the preceding one, rely on these measures to demonstrate that the PBR is not a good choice for production of weapons materials. The models developed in these studies are conservative. That is, they are devised so that their predictions are consistently more pessimistic than reality. For example, the quantity of concern [4] is taken as the lower range of a mass of weapons-grade Pu-239 that could conceivably be fashioned into a weapon regardless of the actual quality expected from the mode of production. This would assume a very sophisticated design and access to advanced technologies. Thus, in this study, about 5 kg of Pu-239 is the quantity of concern, regardless of the presence of additional Pu isotopes. Finally, it is noteworthy that the information presented in this paper contains a large number of approximations. It follows that the results, as presented, imply a certain degree of uncertainty. However, the orders of magnitude, the trends and the conclusions of the study are to be regarded as correct. The constraints on the various scenarios to weapons-material production were explored by constructing numerical models for analysis by the Monte Carlo code MCNP [5] and the new PBR fuel-cycle analysis code PEBBED [3]. These models are described in turn below.

Pebble Design Optimization Model. The objective of the production process is to transmute U-238 into Pu-239. The production pebble design is assumed to comprise a natural uranium metal sphere surrounded by a graphite shell for moderation. In this paper, these illicit production pebbles are optimized to minimize the impact from their introduction into a PBR using legitimate pebbles. An infinite lattice of these pebbles is modeled, assuming a body-centered cubic arrangement. The packing fraction for this arrangement is 0.67, which is larger than the normally observed values in the vicinity of 61% [6]. The latter value corresponds to a random arrangement, which cannot be modeled in MCNP. Other MCNP models using the body-centered cubic lattice structure [7] have adjusted the packing fraction by reducing the pebble radius, so that the pebbles do not actually touch. In an infinite lattice, this approach introduces no error, but if the array of reduced-radius pebbles were truncated into a finite region, streaming errors would be introduced. In order to have the same pebble arrangement in infinite and finite reactors, in this paper, the pebbles were allowed to be full size, and the larger packing fraction was accepted. This approximation causes the effective multiplication factor k_{eff} to be larger than it would be in reality, so it is a conservative approximation.

The production pebble is composed of a natural uranium metal sphere within a graphite shell. The uranium sphere was allowed to be either solid or hollow. Two different pebble radii were considered: the base case radius was 3.0 cm, and the radius in the other case was 2.0 cm. The inner void radius and the fuel-graphite interface radius were varied parametrically. As shown in the Results section, it was found that for either pebble radius and for any void radius the maximum value of k_∞ occurs for essentially the same value of the ratio of uranium volume to graphite volume.

MCNP Models for Reactor Diversion and Cannibalization. The second MCNP model is a finite cylinder with the same lattice arrangement as that used in optimizing the pebble design and with the pebble design selected to have the optimal uranium-to-graphite volume ratio. The core is surrounded by a graphite reflector 1 m thick, and there is an open space 1 m high between the top of the core and the bottom of the upper reflector. Some PBR studies [8] with MCNP have defined an "exclusion zone" [9] at the core periphery to eliminate partial pebbles, but no exclusion zone is defined here. The radius and height of the core were varied to seek a practical critical configuration. It is emphasized that these models specify the same fresh pebble composition throughout the core, and they take no

account of the various partially burned states of the pebbles. Thus, the actual reactor would need to be even larger than the size determined by these MCNP models.

PEBBED Models for Reactor Dual Use, Diversion and Cannibalization. To assess the practicality of clandestine use of the PBR, in which covert production of weapons materials is carried out simultaneously with production of electricity, the optimally moderated weapons-production pebbles found in the first part of the study were added to the regular pebbles in a PEBBED model. PEBBED computes the asymptotic steady-state distribution of burnup, pebble composition, and neutron flux, so this model does not suffer the drawback of uniform composition that was inherent in the MCNP model. PEBBED follows the production and depletion of nuclides specified by the user. In this study, U-235, U-238, the Xe and Sm fission-product chains, and the plutonium isotopes were included among these nuclides. For various proportions of regular and production pebbles, the consequences to the fuel cycle were found. The assessment of the facility cannibalization scenario was also conducted using the PEBBED code. In this instance, the code was used to find the minimum size of a reactor with a square-cylindrical core that uses the optimized natural uranium pebbles with a packing fraction of 61%, running with the OTTO ("once through then out") cycle.

5. Results

The model results for the pebble design optimization study are shown in Figure 1 for pebbles 3 cm in overall radius. The figure shows the variation of k_∞ with the uranium-graphite ratio for several values of void radius of the fuel sphere. For each value of the inner void radius, k_∞ attains some maximum value as the volume ratio varies. Figure 1 also shows how this maximum value of k_∞ varies with the inner void radius. The greatest maximum value is seen to occur when the void radius is zero – i.e., when the fuel sphere is solid. The same conclusions are reached for pebbles of 2 cm overall radius. The uranium-to-graphite volume ratio at which k_∞ is greatest for each value of the void radius was compiled for both pebble sizes considered. Although some scatter in the values for this ratio was found, it is attributed at least in part to statistical effects from MCNP modeling. Since the departure from the average value of this ratio is small, it seems appropriate to assume that the fuel-to-moderator ratio at which the highest value of of k_∞ occurs is the same value, regardless of the details of the pebble design. This means that the most successful production of Pu-239 would be achieved by using a pebble with this volume ratio, which we take to be 0.00564, the average of all the values found. This corresponds to a solid uranium inner sphere radius of 0.533 cm, or only 17% of the radius of the pebble.

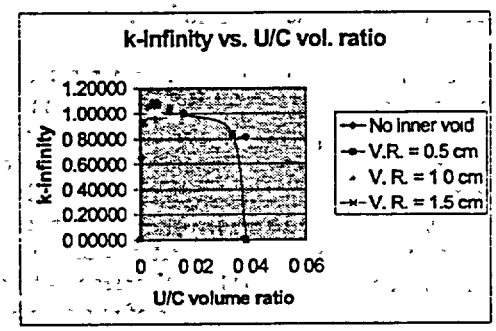

Figure 1. k_∞ vs. U/C Volume Ratio

For the various finite-reactor MCNP models, investigations were performed only for pebbles of 3-cm overall radius, optimized for maximum k_{eff}. As determined above, the fuel zone sphere is solid and the fuel-graphite interface radius is the optimally moderated value of 0.533 cm. Criticality searches were performed for two basic reactor configurations. The first one is based on a core diameter of 3 m, which is similar in scale to proposed PBR designs, and thus corresponds to the facility diversion scenario. In this search, the core radius is kept constant, but the core height is varied. Figure 2 shows the variation of k_{eff} with core height in this search. It is clear that

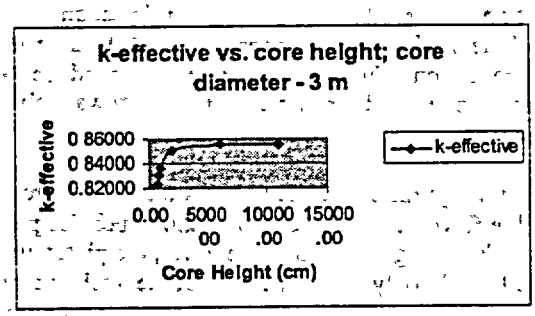

Figure 2. Criticality Search for a 3-m Diameter Core

the reactor can never become critical in this configuration. A PEBBED analysis of this scenario is redundant and was not attempted.

A second search was performed using MCNP models. This search assumed a "square cylindrical" core – i.e., the core height is equal to the core diameter. For an unreflected reactor, this is approximately the configuration that gives the minimum critical volume [10]. Since the dimensions are not constrained to those of the original reactor design, this search corresponds to the cannibalization scenario. Figure 3 shows the variation of k_{eff} with core volume. The figure shows that the reactor becomes critical when the core volume is 450 m^3, which corresponds to height and diameter of 8.3 m. This is a very large core for a PBR, requiring 2.7 million pebbles, an order of magnitude more than in a typical PBR power plant design. Furthermore, the critical volume predicted by this model applies only to the condition with all fresh fuel, and to the artificially exaggerated packing fraction in the body-centered cubic lattice. A practical production reactor would have to be even larger.

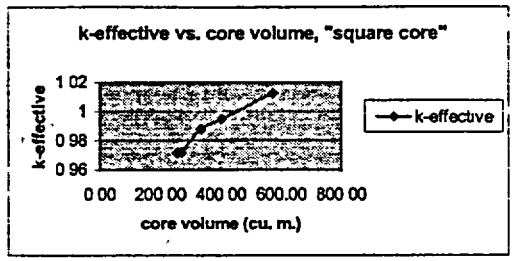

Figure3. k_{eff} for Square-Cylindrical Core Reactor

The PEBBED analysis of the cannibalization scenario reactor, completely fueled with optimized production pebbles, showed that a square-cylinder core, 11.1 m in diameter and height, operated on the OTTO cycle, could produce high-purity Pu-239 fast enough to manufacture the mass of concern (5 kg of Pu-239) in two years. This reactor also assumes a 1-m thick reflector on every side with a gap between the top reflector and the core. This configuration clearly results in an extremely large PBR; its volume is 2.39 times as large as that of the 8.3-m reactor identified in the MCNP analysis, and about 27 times as large as that of a practical PBR power plant. Such a reactor would be easily detected by satellite surveillance systems [11]. Numerous other technological challenges for the construction of such a reactor and further drawbacks of this choice of a reactor for weapons materials production exist. They are discussed elsewhere [12].

Production pebbles of the optimized design (i.e., natural uranium spheres 0.533 cm in radius within graphite shells 3 cm in external radius) were introduced into the PEBBED model of the fuel cycles of two realistic PBR designs. These designs are representative of two reactors that have been proposed for the generation of electric power: the HTR Modul 200 design and the Eskom PBMR design. PEBBED is capable of applying different recirculation schemes to different pebble types. In this study, the "driver" legitimate fuel pebbles were recirculated an average of 10 times, but the illicit production pebbles were removed after their first pass through the reactor for optimal plutonium isotopics. Introducing natural uranium into the core reduces the core reactivity. Thus, in order to maintain criticality the legitimate fuel pebble injection rate could be increased and/or their discharge burnup could be reduced. In this study, the fuel pebble injection rate was increased by 5%, an upper limit for the reduction, above which suspicion and detection would be immediate. The number of passes in a fuel pebble's life was held constant at 10, leading to a reduction in average discharge burnup. Then the production pebble injection rate was found that would restore criticality to the core. In this way, the increased demand for increased reactivity was split between lower burnup at discharge and increased injection rate.

For the PBMR, the average discharge burnup was found to decrease from 80.6 to 75.7 MWd/kg, and the production pebble flow rate was found to be 2.674 pebbles per hour. This production rate would take five years to produce 5 kg of Pu-239. However, the plutonium would be of very poor quality for weapons: the Pu-239 would only constitute 78% of the total plutonium. This low quality is due to the relatively slow passage of the production pebbles through the core. Furthermore, the decrease in legitimate pebble burnup and the increased fuel utilization would result in detection in the presence of a reasonable safeguards system. It is noteworthy that in this scenario the pebble flow rate cannot be increased in order to improve isotopics, as that would negate the assumption of *covert* dual use. For the Modul-200, the plutonium quality is similar and the production rate is even slower.

6. Conclusions

It has been shown that the dual use of a PBR to produce energy and clandestinely produce plutonium for a weapon is impractical and slow, and the plutonium yielded would be of very poor quality. It has also been shown that a PBR designed to produce weapons-quality Pu-239 using natural uranium fuel is achievable in principle. However, it would have to be very large, and it could not be entirely built by adapting a PBR initially designed for energy production using regular enriched fuel or by reusing its specialized hardware components in a new facility. The production rate of Pu-239 would be very low and incompatible with the goal of accumulating an arsenal. Such a large reactor would be remotely detectable by satellites.

It must be noted that the study ignored many issues of paramount importance to the safety and practicality of the various scenarios (dual use/cannibalization). For example, the design of the pebbles is likely to be improper for the retention of fission products and generated gases. Ensuing releases could cause health and safety concerns and would most likely make the facility easier to detect. The study could also be used for the identification of safeguard steps and procedures and for the identification of sensitive equipment. Such an extended study should be conducted.

7. Acknowledgement

Work supported by the U.S. Department of Energy, Assistant Secretary for Environmental Management, under DOE Idaho Operations Office Contract DE-AC07-99ID13727.

8. References

1. Nichols, D. R., "Status of the Pebble Bed Modular Reactor," Nuclear Energy, 2000, 39, No.4, Aug., 231-236.
2. Ougouag A. M., and H. D. Gougar, "Preliminary Assessment of the Ease of Detection of Attempts at Dual Use of a Pebble-Bed Reactor," Trans. ANS 85, 115-117, 2001.
3. Terry, W. K., H. D. Gougar, and A. M. Ougouag, "Direct Deterministic Method for Neutronics Analysis and Computation of Asymptotic Burnup Distribution in a Recirculating Pebble-Bed Reactor," Annals of Nuclear Energy 29 (2002) 1345–1364.
4. Mark, J. C., T. Taylor, E. Eyster, W. Maraman, and J. Wechsler, "Can Terrorists Build Nuclear Weapons?" pp. 55-65, in **Preventing Nuclear Terrorism**, Paul Leventhal and Yonah Alexander, Editors, Lexington Books, 1987.
5. Briesmeister, J. F., Ed., "MCNP – A General Monte Carlo N-Particle Transport Code – Version 4B," LA-12625-M (March 1997).
6. Benenati, R. F. ; and C. B. Brosilow, "Void Fraction Distribution in Beds of Spheres," A.I.Ch.E. Journal 8, No. 3, 1962, pp. 359-361.
7. Karriem, Z., C. Stoker, and F. Reitsma, "MCNP Modelling of HTGR Pebble-Type Fuel," paper NG-VIII/04 in proceedings of "Advanced Monte Carlo for Radiation Physics, particle Transport Simulation, and Applications (Monte Carlo 2000)," Lisbon, Portugal, October 23-26, 2000, sponsored by OECD/NEA and ANS.
8. Lebenhaft, J. R., and M. J. Driscoll, "MCNP4B Analysis of the HTR-10 Startup Core," Transactions of the American Nuclear Society, Vol. 84, 2001, pp. 214-215.
9. Murata, I., and A. Takahashi, "Analysis of Critical Assembly Experiments by Continuous Energy Monte Carlo Method with Statistical Geometry Model," Technology Reports of the Osaka University, 48(2304), April 1998, pp. 19-31.
10. Lamarsh, J. R., **Nuclear Reactor Theory**, p. 310, Addison-Wesley, 1972.
11. Zhang, H., "Civil Remote-Sensing Satellites and a Fissile Materials Cutoff Treaty: Some Case Studies on Verifying Nonproduction," JNMM, Vol. XXX, No. 2, pp. 20-28, Fall 2001.
12. Ougouag, A. M., W. K. Terry, and H. D. Gougar, to be submitted to Nuclear Engineering and Design.

DEEP BURN TRANSMUTATION OF NUCLEAR WASTE

CARMELO RODRIGUEZ, ALAN BAXTER, DONALD MCEACHERN
General Atomics, P.O. Box 85608, San Diego, California 92186-USA
FRANCESCO VENNERI
Los Alamos National Laboratory, Los Alamos NM 87545-USA
and General Atomics
DAVID WILLIAMS
Oak Ridge National Laboratory, P.O. Box 2008 Oak Ridge, TN 37831, USA

ABSTRACT

Helium-cooled, graphite-moderated reactors with ceramic-coated fuel particles offer unique advantages for the destruction of transuranic materials discharged in Light Water Reactor spent fuel. This is accomplished by fission, and capture-followed-by-fission processes. Three major features make it practical: (1) ceramic-coated particles accommodate high levels of burnup in one pass, thus reducing the need for repeated reprocessing; (2) graphite moderation produces valuable opportunities for thermal and epithermal neutrons to interact with fissionable and non-fissionable materials respectively; and (3) ceramic-coated particle kernel sizes can be adjusted to control the rate of such interactions. In the transmutation scheme proposed here, virtually complete destruction of weapons-usable materials, and 95% destruction of all transuranic waste is achieved. Higher levels of destruction are possible by repeated reprocessing and recycling, but there is little incentive to do so since each reprocessing step generates new secondary waste. After transmutation, the impervious ceramic-coated fuel particles provide an ideal residual waste form.

1. Introduction

To meet world power demands, the use and acceptance of nuclear power must continue to grow as a safe, reliable, and economical source of energy. A reason for concern in the U.S. is the fact that, at the rate waste is produced by the existing fleet of nuclear reactors, new repository capacity equal to the statutory capacity of the yet-to-open Yucca Mountain Geologic Waste Repository would be needed about every 20-30 years. Therefore, the ability to expand, or even maintain the nuclear power capacity in the U.S. may soon be limited, unless either additional disposal capacity is made available, or the volume, proliferation risk, and toxicity dose of the waste are significantly reduced. Based on this motivation, methods to reduce nuclear waste volume and toxicity have been proposed. However, while the potential advantages of such nuclear waste mitigation concepts are compelling, critics have argued that these methods would generate significant amounts of new waste, new opportunities for plutonium diversion would be created, deployment times would be long, and costs would be very high. In this paper, we propose a new option that addresses these objections. It is based on the use of modular helium-cooled reactor technologies.

2. The Deep Burn Concept

The concept described here, called Deep Burn transmutation, is based on the use of thermalized neutrons and high burnup fuel forms in modular helium reactor systems (MHRs). These reactors have annular graphite-moderated cores, and are designed to be passively safe at power levels up to 600 MW, such that there is no fuel failure or fission product release under any loss of coolant flow or pressure accident. They can also operate safely at very high temperatures resulting in electric power produced at close to 50% efficiency.

An essential feature of the deep burn transmutation concept is the use of ceramic-coated fuel particles (TRISO particles) that are strong and highly resistant to irradiation, thereby allowing very extensive destruction levels in one pass (figure 1). The ceramic coatings are also durable, and impervious to moisture for long times. Extrapolated corrosion test results by U.S. national laboratories indicate that the incremental waste exposure in the repository due to corrosion of the ceramic coatings is expected to be negligible for hundreds of thousands of years (figure 2). Thus, the discharge from the transmutation process provides a robust and attractive residual waste form. In addition, the MHR's fixed moderator (graphite), and neutronically transparent coolant (helium), provide inherent safety features and neutronics advantages for the destruction of nuclear waste that cannot be replicated in other design.

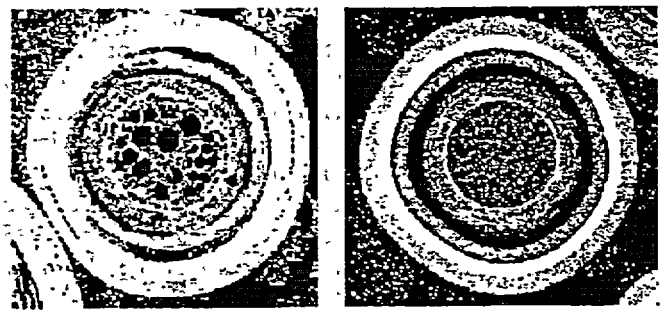

Pu Oxide
747,000 MWdays/tonne
>95% Pu-239, and
>65% all Pu transmuted

Th-Pu Oxide
183,000 MW-days/tonne
>95% Pu-239 Transmuted

Figure 1. Irradiated TRISO Particles

Another essential feature is that many more collisions are required to thermalize neutrons in an MHR than in water reactors. This produces valuable opportunities for epithermal neutrons to interact with non-fissionable materials. Specifically, since non-fissionable materials exhibit large neutron-capture resonances in the epithermal region (figure 3), they have a good chance to capture neutrons and become fissionable.

Yet another feature is that the size of the ceramic-coated particle kernels can be adjusted to create self-shielding so that fissionable materials, such as Pu-239, interact more readily with thermal neutrons, whereas non-fissionable minor actinides interact more readily with epithermal resonant neutrons. This produces enough neutrons to destroy fissionable materials by direct fission, and non-fissionable minor actinides by a capture-followed-by-fission process. Minor actinides behave as fertile fuel, helping maintain nuclear stability.

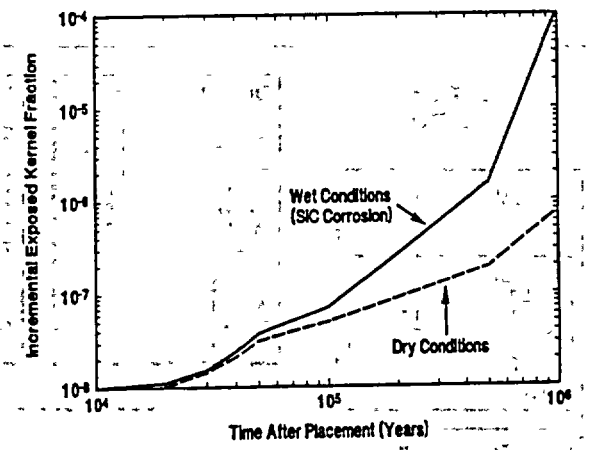

Figure 2. Durable Particle Integrity

3. The Process

The Deep Burn process starts with the separation of uranium and fission products from the LWR spent fuel. Plutonium and neptunium are then separated from the rest of the transuranic elements, and used to make TRISO Driver Fuel (DF), with kernels sized large to maximize the use of thermal neutrons. This maximizes fission and production of next-generation neutrons. The rest of the minor actinides are packaged in TRISO particles as Transmutation Fuel (TF), with kernels sized small to maximize the efficacy of epithermal resonant neutrons. This produces

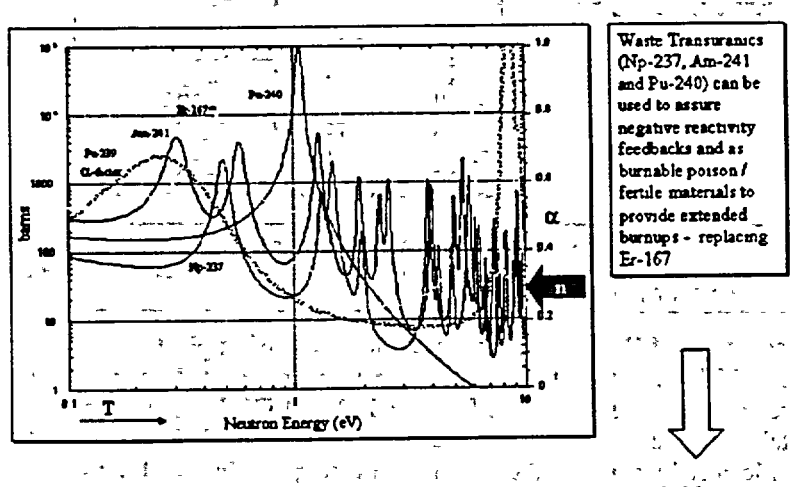

Figure 3: Capture cross-sections of selected minor actinides

transmutation into fissionable elements, which then it is followed by fission. We have selected block type fuel in an annular core configuration. The use of block fuel is important because the blocks stay exactly where they are placed until they are picked up. This makes the core configuration more predictable, allowing more control of flux distributions, better fuel utilization, and more predictable performance. It also reduces the opportunity for diversion, increasing proliferation resistance. One third of the Drivel Fuel (DF) is replaced with fresh DF at the end of each refueling cycle. It was originally proposed that each of these cycles would last a year. However, more recent calculations suggest that the refueling cycles may be as long as two years. The spent DF from the reactor is then reprocessed to remove fission products, mixed with the rest of the minor actinides left from the initial separation, fabricated into fresh Transmutation Fuel (TF), and reloaded in the reactor. In this reprocessing step, there is very little plutonium-239 handling since it is largely burned in the three preceding refueling cycles. At the end of each refueling cycle, one third of the TF (having been irradiated for three cycles) is replaced with fresh TF. The discharged TF may then be further irradiated (without reprocessing or refabrication) in an accelerator-driven subcritical MHR, or disposed of in a Geologic Repository.
This process has been evaluated using montecarlo and deterministic calculations combined with burnup calculations. The results show that virtually complete destruction of weapons-usable materials, and roughly 95% destruction of all transuranic waste is achieved (figure 4). Higher levels of destruction are possible by repeated reprocessing and recycling, but there is little incentive to do so as each reprocessing step generates new secondary waste.

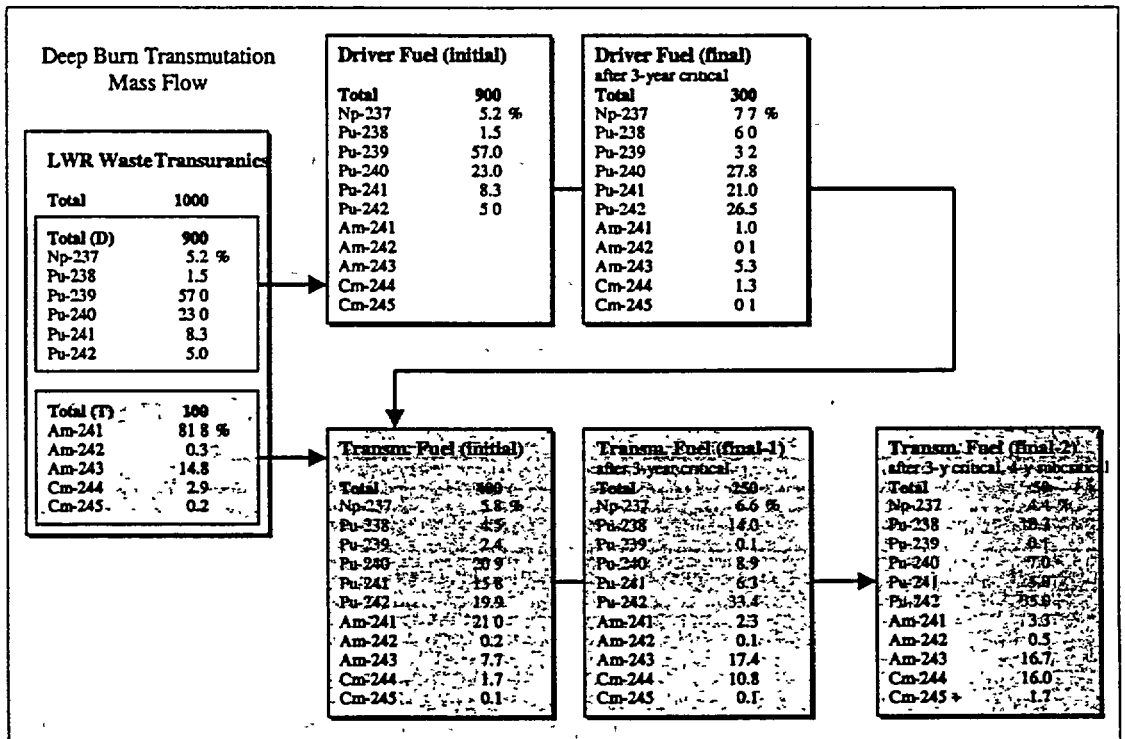

Figure 4 From LWR Waste to Final Waste after Deep Burn Transmutation: mass flow results from the Deep Burn Transmuter studies. The mass flow of the wastetransuranics is followed through the Driver andTransmuation Fuel stages, the critical (MHRbT) and subcritical (MHA-bT) irradiation periods.

The economics of Deep Burn have been analyzed using plant and fuel fabrication cost estimates from previous MHR reactor studies, particularly those related to plutonium burning. Separations and reprocessing costs were obtained from the DOE "ATW Roadmap" report of 1999. There are significant uncertainties about the cost of fabricating minor actinide fuel, and the cost of fabricating plutonium fuel is significantly higher than the cost of fabricating uranium fuel. However, despite this, it is interesting to note that the MHR Deep Burn feature leads to the production of much more electricity for a given amount of fabricated fuel, which leads to a fuel cost per kWh no much higher than the uranium fuel cost. More specifically, the total estimated cost is 3 ¢/kWh for plant amortization and Operations &

Maintenance, and 0.9 ¢/kWh for fuel and separations, for a total of 3.9 ¢/kWh. These costs include the cost of an accelerator for the subcritical part of the process, and suggest that the Deep Burn concept has the potential to be economically viable, particularly if it is carried through the completion of the critical phase only, or if the government is willing to pay for the separation step.

From the proliferation risk standpoint, Deep Burn requires no multiple or repeated reprocessing. There is the initial separation step where LWR fuel is processed to remove Uranium and fission products. However, fissionable actinide isotopes are not individually isolated in this step: Whole Plutonium is extracted simultaneously with whole Neptunium, and radioactive fission products could be left in the fuel to deter diversion at this stage. Later in the process, there is another intermediate reprocessing step, but it takes place at a point when there are essentially no Pu-239 or weapons grade elements. The whole process may be characterized as "separate and burn". There is no continuous or repeated reprocessing of weapons-grade material. This significant anti-proliferation advantage is made possible by the Deep Burn feature of the MHR design.

From the toxicity standpoint, Deep Burn and the isolation provided by the corrosion-resistant ceramic-coated particles lowers the ingested toxicity risk in a repository below that of natural uranium from the start (figure 5).

4. The Fuel

TRISO Fuel particles are an ideal form of fuel for transmutation (and other missions) because they can accommodate deep levels of transmutation (Deep Burn), make useful use of epithermal neutrons, and can be adjusted in size to preferentially expose minor actinides to epithermal neutrons and fissionable materials to thermal neutrons. These features are in addition to their ability to sustain high temperatures, which allows production of electricity at high efficiencies and unmatched safety.

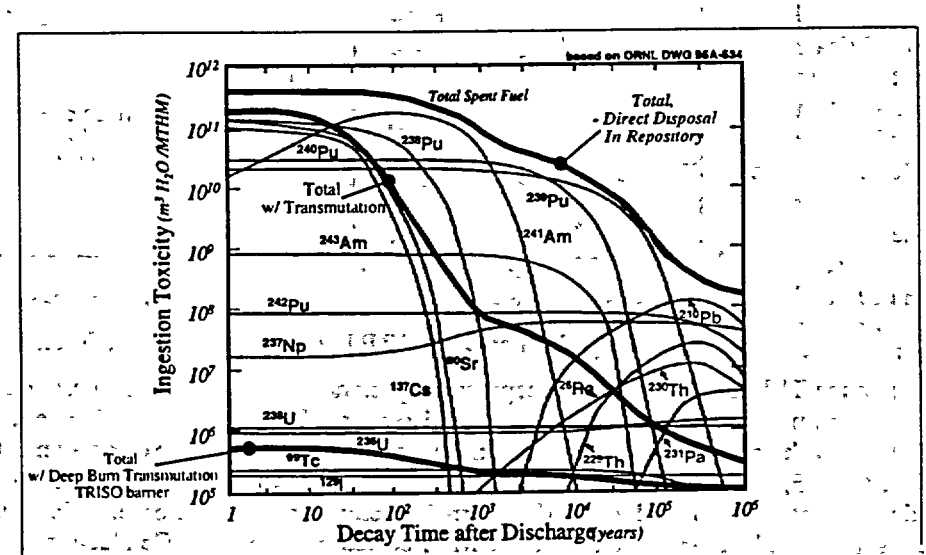

Figure 5. Toxicity in Repository after Deep Burn is Lower than that of Natural Uranium

There are two kinds of sizes of particle kernels envisioned for transmutation: A large DF kernel and a smaller TF kernel.

To achieve Deep Burn design and performance requirements, the DF should be in a form to provide initial self shielding of some of the fissionable material. This self-shielding will reduce beginning of life excess reactivity and allow power to be maintained throughout the planned fuel lifetime, and requires a large, dense kernel.

The neutrons from the fissioning of DF are used to convert the initially largely non-fissile isotopes into fissionable isotopes and then to fission them. At the same time the non-fissile nuclides in the TF have resonance capture cross sections at neutron energies slightly higher than the neutron energy characteristic of the operating moderator temperature. Capture in the TF provides a negative temperature coefficient throughout the cycle. The capture of neutrons in the non-fissionable actinide nuclei therefore performs the useful function of converting the non-fissile nuclei into fissionable nuclei (this is in contrast to the use of burnable poisons, such as erbium, to provide negative temperature coefficient where the neutrons captured do not further the transmutation function). The new fissionable

nuclei can then be fissioned, thus destroying long-lived transuranics. It is important that all of the material in the nuclei in the TF be available to the neutrons, i. e., no self-shielding. This is accomplished with a small diameter kernel, or a diluted or low-density kernel.

Developing fuel for high burnup and high fast neutron fluences containing undiluted fissile material (as required by the driver fuel) has been carried out with highly-enriched uranium as part of the Fort St. Vrain Nuclear Generating Station and subsequent commercial work in the U. S. The FTE-13 test in Peach Bottom demonstrated that TRISO-coated undiluted plutonium fuels could be irradiated successfully to high burnup. The behavior of high burnup fuels during core heat-up events has been studied at GA and KFA Jülich and the effect of burnup is included in the Goodin-Nabielek model applicable to uranium fuels. The ranges of burnup and fast neutron fluence covered by previous tests are compared to the requirements for the Driver and Transmutation Fuel in figure 6. The next step in the development of Driver and Transmutation fuels is to build on this technology to meet the projected fuel requirements. Oak Ridge National Laboratory (ORNL), with GA, will develop processes and equipment to fabricate DF and TF test samples for irradiation, accident simulation, and other testing. ORNL has extensive prior experience developing coated particle fuels, as part of the HTGR and Thorium Recycle programs, and relevant experience fabricating TRU targets containing neptunium, plutonium, americium, and curium as part of their on-going program for production of transuranic isotopes. The process development and test program will begin with uranium fuels contained in hoods, progress to glovebox containment for the development of the DF, and culminate with the development of the remote-handled TF in shielded cells. Irradiations are planned to be done in US thermal reactors, post-irradiation examinations in the ORNL hot cells, and accident simulations in the ORNL coated particle Core Conduction Cool down Facility. The uranium facility is currently under design and the DF and TF facilities are in the planning stages. Alternates to conventional TRISO coatings are included in the program. Tests of the performance of the TF in the repository are also an important part of the fuel development program.

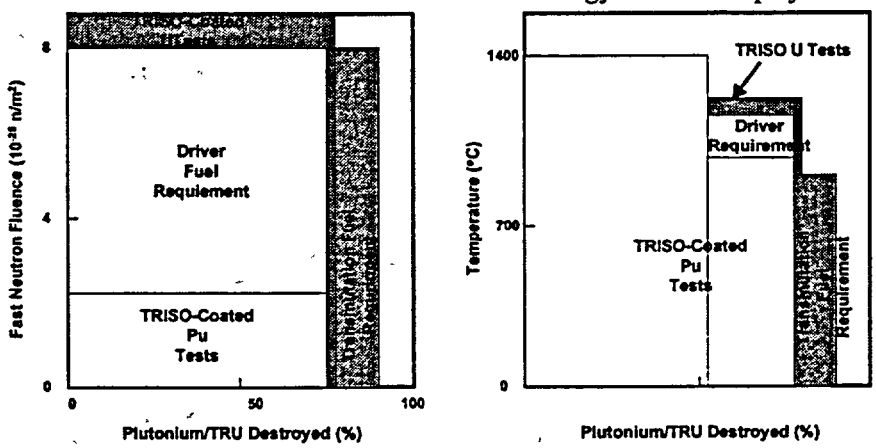

Figure 6.Comparison of DF and TF Requirements with the Irradiation Database

Development plans include meeting as-manufactured quality for glovebox and shielded-cell fabrication, high temperature processing of americium and curium, achieving in-service performance at high burnup and high fluence, and determining the limiting accident temperatures for DF and TF.

5. Conclusions

Deep Burn Transmutation allows the virtually complete destruction of weapons-usable materials, and roughly 95% destruction of all transuranic waste. Higher levels of destruction are possible by repeated reprocessing and recycling, but there is little incentive to do so as each additional reprocessing step will generate new secondary waste, which may eventually exceed the incremental destruction level achieved.

The Deep Burn concept would allow reductions in the volume of high level nuclear waste, and in toxicity and proliferation risk, safely, and in a potentially economic manner. Deep Burn MHR systems could be available for deployment in the near term to make a positive contribution to the solution to the waste problem. In addition to the deep burn transmutation capabilities, the MHR can, of course, burn uranium fuel or thorium in a high conversion ratio mode. This could lead to nuclear power scenarios that do not involve plutonium production and processing, and still maintain long-term sustainability.

Session 3

Physics and Neutronics

ANALYSIS OF THE EUROPEAN RESULTS ON THE HTTR's CORE PHYSICS BENCHMARKS

X. RAEPSAET and F. DAMIAN
CEN Saclay 91191 Gif-sur-Yvette CEDEX, France

U.A. OHLIG and H.J. BROCKMANN
FZJ Research Centre Jülich, 52425 Jülich, Germany

J.B.M. DE HAAS and E.M. WALLERBOSS
Nuclear Research Group, 1755ZG Petten, and Interfaculty Reactor Institute, 2629JB Delft, The Netherlands

ABSTRACT

Within the frame of the European contract HTR-N1, calculations are performed on the benchmark problems of the HTTR's start-up core physics experiments initially proposed by the IAEA in a Co-ordinated Research Programme. Three European partners, the FZJ in Germany, NRG and IRI in the Netherlands, and CEA in France, have joined this work package with the aim to validate their calculational methods. Pre-test and post-test calculational results are compared with each other and with the experiment. Parts of the discrepancies between experiment and pre-test predictions are analysed and tackled by different methods and models. In the case of the Monte Carlo code TRIPOLI4, used by CEA, the discrepancy between measurement and calculation at 18 fuel columns loading is reduced to $\Delta k/k \sim 0.85$ %, when considering the revised data of the HTTR benchmark. In the case of the diffusion codes, the discrepancy is reduced to: $\Delta k/k \sim 0.8$ % (FZJ) and 2.7 or 1.8 % (CEA).

1. Introduction

In the frame of the European contract HTR-N1 a work package is devoted to the validation of codes and the improvement of methods as far as the HTR modelling is concerned. Three partners are involved in this work package: FZJ in Germany, NRG and IRI in the Netherlands, and CEA in France. The HTTR's start-up core physics experiments are a good opportunity for the European partners to validate their calculational tools and methods. This paper provides an analysis of the pre-test and post-test calculations, performed in Europe on the benchmark problems of the HTTR's start-up core physics experiments: the number of fuel columns necessary to achieve the first criticality and the excess reactivity for 18, 24, and 30 fuel columns in the core, described in detail in [1].

2. Computational methods and nuclear data

The nuclear data libraries used by all partners are based on the JEF2.2 evaluation. Two Monte Carlo codes are used to model the HTTR: the KENO code at IRI, associated with a multigroup approximation (172 grps), provided by the SCALE4 code system, and the TRIPOLI4 code at CEA using pointwise cross sections everywhere in the core except in the fuel rod region where multigroup cross sections (172 grps) are generated by the transport code system APOLLO2 in order to treat the double heterogeneity of the coated fuel particles (CFP). The 1d or 2d transport / 3d diffusion code systems: WIMS/PANTHER, SCALE4/BOLD VENTURE, APOLLO2/CRONOS2, and TOTMOS-DORT/CITATION are used at NRG, IRI, CEA, and FZJ, respectively. The double heterogeneity of the CFPs and the self-shielding in the resonance region are taken into account in all cell calculations. In the FZJ cell calculations, a white boundary condition with no extra leakage term is used whereas in all other cell calculations a critical B^2_{crit}-search has been performed.

In the preliminary calculations the increased neutron streaming in the coolant channels and in the large holes of the core and the reflector is considered in the FZJ and NRG calculations. Later on, this enhanced neutron streaming is also taken into account in the post-test core calculations of CEA. The effect of the heterogeneous distribution of the burnable poison (BP) in the axial direction is evaluated at NRG and FZJ, afterwards also in the post-test diffusion calculations of CEA.

3. Preliminary calculational results

Calculations [2,3,4] performed with the different code systems are presented on Table 1 together with the experimental results. The higher k_{eff}-values obtained by BOLD VENTURE and CRONOS2 are explained by the fact that the streaming effect is not considered and that the fuel blocks are homogenised. The latter is also right for the CITATION calculation, however this effect is counter-balanced by the absence of neutron leakage consideration in the cell calculations.

The relatively good agreement for the thin annular core assembly between both MC codes disappears in the fully loaded core. One reason can be that the P_1 approximation describing the interaction between neutrons and graphite has a higher impact on the neutron leakage at fully loaded core with its harder neutron spectrum than in the thin annular core configuration.

Table 1 : Preliminary core calculations together with the experimental results

	CITATION	PANTHER	B. VENT.	KENO	TRIPOLI	CRONOS	EXPER.
	Diffusion 4 groups	Diffusion 2 groups	Diffusion 13 groups	M. Carlo 172 gr	M. Carlo 172 gr & pointwise	Diffusion 8 groups	
	3D triang.	3D hexag.	RZ	3D	3D	3D hexag.	
	1 reg/block	7 reg/block	6 rings			1 reg/block	
	finite diff.	finite elem.	finite diff.			finite elem.	
	6 mesh/bl.	7 mesh/bl.				24 mesh/bl	
30 col.	**1.1607** •	**1.1595**	***1.1885*** #•	**1.1600** ***±0.0005***	***1.1463*** • ***±0.0009***	**1.1698** •	**1.1363 ±** ***(> 3.6 %)***
18 col.	**1.0254** •			**1.0240** ***±0.0005***	***1.0171*** • ***±0.0009***	**1.0580** •	**≲1.0**

• *CR insertion considered $\Delta k = 0.004$* # *corrected for the BP effect from the KENO calculations*

4. Discussion of the preliminary results

The HTTR got critical with 19 fuel columns with an excess reactivity of 1.5%. All preliminary calculations underestimated the number of fuel columns needed for the first criticality (diffusion calculations: 9, 16 fuel columns; Monte Carlo calculation: 17 fuel columns). As can be seen on Table 1, the discrepancy between the calculations and the experiment at least ranges from $\Delta k = 0.017$ to 0.058 at 18 fuel columns loading, and from $\Delta k = 0.01$ to 0.052 at full core.

It is noteworthy that the observed discrepancies decrease with increasing number of fuel columns in the core. Due to the large experimental error at 30 fuel columns loading, the differences between the calculations and the experiment are within the error interval, whereas at the thin annular core assembly the discrepancies are significant. A reason for the latter circumstance can be the consideration of another than the actual boron impurity in the dummy fuel blocks and of helium instead of residual air in the graphite pores. Indeed, the impurity of one dummy fuel block has been re-measured by JAERI and revised data [5] have been recommended for the recalculation of the first criticality (HTTR-FC2).

Moreover, in the course of the studies the following reasons for the above mentioned discrepancies have been identified:

- the neglect of the detailed structure of the HTTR fuel block together with a non adequate modelling of the fuel and BP unit cells,

- the use of few group homogenized cross sections in the whole core diffusion calculation without neutron leakage in the transport calculations,
- a non-adequate treatment of the axial self-shielding in the BP rods,
- an underestimation of the neutron streaming.

Therefore, the HTTR-FC2 benchmark has been a good opportunity to implement the new enhanced methods coming from the analyses of all post-test studies.

5. New calculational results

CITATION results

The discrepancy between measurement and the pre-test FZJ diffusion calculation amounts to $\Delta k = 0.0287$ at the first criticality (e.g. 19 fuel columns in the core) for a 4 group diffusion calculation without leakage feedback. At 30 fuel columns in the core the difference is with $\Delta k = 0.0261$ of the same order. Parts of the discrepancies between measurement and former calculations are tackled by considering: the exact asymmetric position of the B_4C-rods in the HTTR fuel block in the core diffusion calculation, together with an improved modelling of the unit cells, the use of many group constants or of few broad group constants including detailed leakage information from the diffusion calculation of the whole core in order to describe the core/reflector coupling accurately, the treatment of the axial self-shielding of the B_4C-rods by a 2-d discrete ordinates cell calculation, and the consideration of an enhanced neutron streaming, brought about by an adaptation of the diffusion constants to results of Monte Carlo calculations.

When applying these improvements [6] and taking the revised data of the HTTR, the first criticality is recalculated for 18 fuel columns, in case of fuel loading from the core periphery. The number of fuel columns, necessary to achieve the first criticality, increases by about 2 fuel columns compared to the former results, and the discrepancy between measurement and diffusion calculation is reduced from $\Delta k = 0.0287$ to $\Delta k = 0.0111$ at 19 fuel columns in the core.

The effective multiplication constants obtained in the pre-test and post-test calculations are given in Fig. 1 together with the experimental results. When summing up all post-test studies, the analysis yields the following effects at 18/19 fuel columns in the core compared to the pre-test results:

- when considering the detailed structure of the HTTR fuel block in the whole core calculation the multiplication factor decreases by about $\Delta k \approx 0.043$,
- the description of the detailed energy-dependence of the neutron flux adequately by a fine energy group structure increases the k_{eff}-value by about $\Delta k \approx 0.035$,
- when considering the axial heterogeneity of the BP by 2-d cell calculations, k_{eff} of the whole core calculation increases by about $\Delta k \approx 0.0068$,
- when treating the neutron streaming effect by modified diffusion constants on the basis of the Japanese Monte Carlo results, k_{eff} is reduced by about $\Delta k \approx 0.0075$,
- and when taking into account the revised HTTR benchmark data, the multiplication factor is reduced by about $\Delta k \approx 0.009$.

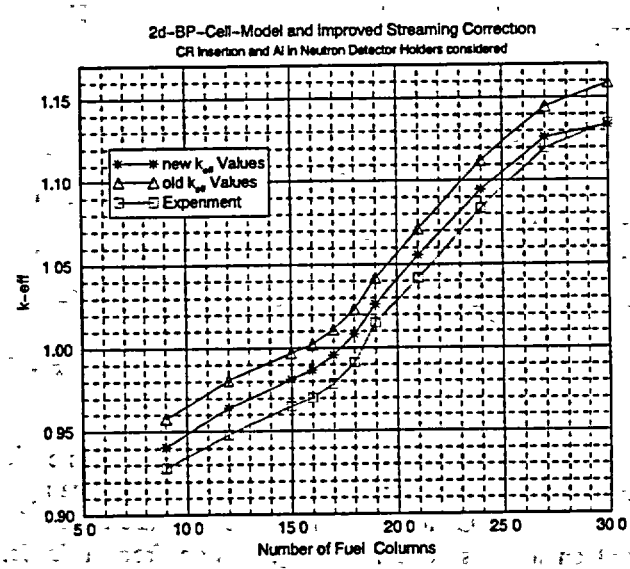

Fig.1: New and Old k_{eff}-Values of the Diffusion Calculations in Comparison with the Experiment

TRIPOLI4 and CRONOS2 results

Considering the new available data (HTTR-FC2), new Monte Carlo calculations have been performed with TRIPOLI4 for the 18, 19 and 30 columns configurations. The 18 columns case has been treated by taking into account or not the presence of the control rods slightly inserted in the upper part of the reflector ($\Delta k \sim 0.003$).

As far as the diffusion calculations are concerned, new developments carried out in APOLLO2 and CRONOS2 allow in future to take into account :

- the exact position of the BP in the fuel block by using new finite element mesh in the core model
- the streaming effect by generating anisotropic diffusion coefficients from the previous 2D-P_{ij} calculations

The use of the HTTR-FC2 data associated with a complete description of the axial heterogeneity of the BP has led to new core diffusion calculation results. This has been done for six different energy structures (2, 4, 6, 8, 13 and 20 groups) in CRONOS2 without observing a main trend. Furthermore, the Benoist method used for the treatment of the neutron streaming might not be applicable in the large channels of the control rod graphite blocks (18 columns) and underestimates this effect. Therefore, two other analytical models (Benoist) have been tested on a control rod block alone and validated by MC calculation. This led to better results on the whole core.

The final results are partially gathered in the Figures below. Fig. 2 illustrates, with 8 energy groups, the impact of the different model assumptions on the reactivity as a function of the number of fuel columns. Fig. 3 shows a streaming effect ranging from 2.25 % in the 18 columns core configuration to 1.8 % in the full core configuration. These results highlight also the importance of the used leakage model for evaluating the neutron streaming in the control rods graphite blocks. Indeed, the first model gave some values varying from 1.8 % to 1.5 %.

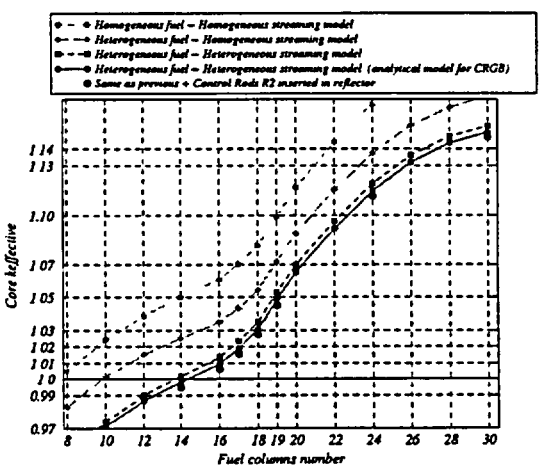

Fig 2. k_{eff}-values obtained by different core models

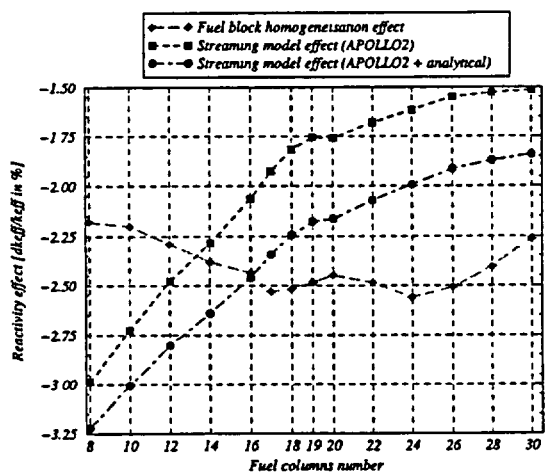

Fig 3. Neutron streaming and fuel block homogenisation effect

It is noticeable that the number of fuel columns needed to achieve criticality increases by about 7 or 8 in comparison with the former results (Table 1). At first criticality, a discrepancy remains between the diffusion and the Monte Carlo calculations (0.9 % < $\Delta k/k$ < 1.7 %). This underscores the limits of a method based on a cross section homogenisation from a fundamental mode calculation (infinite medium) that is barely pertinent for the 18 columns core configuration. The actual environment (reflector blocks) should be considered and should take place instead of the white boundary condition in the 2D APOLLO-2 transport calculations, before homogenising and collapsing locally the cross sections inside the fuel elements.

6. Final results and conclusion

All final results are given in Table 1. In the case of the Monte Carlo code TRIPOLI4, the discrepancy between measurement and calculation at 18 fuel columns in the core is reduced to $\Delta k/k \sim 0.85$ %, when considering the revised data of the HTTR benchmark. As to the diffusion codes, this discrepancy is now reduced to $\Delta k/k \sim 0.8$ % (FZJ) and ~ 2.75 (1.78) % (CEA), when taking into account the improved treatments and the revised data.

Table 2 : The new core calculations together with the experimental results

	CITATION	TRIPOLI	CRONOS	EXPERIMENT
	Diffusion 26 groups	M. Carlo 172 gr & pointwise	Diffusion 8 groups (4 groups)	
	3D triangular	3D	3D hexagonal	
	3 reg./block		3 reg/block	
	finite difference		finite element	
	24 meshes/block		24 meshes/block	
30 col.	**1.1336** [1]	**1.13833** [2] ***±0.00090***	**1.1451 (1.1362)** [2]	**1.1363 ± (> *3.6 %*)**
24 col.	**1.0944** [1]	-	**1.1096 (1.1000)** [2]	**1.0834 ± (> *2 %*)**
19 col.	**1.0263** [1]	**1.02692** [2] ***±0.00043***	**1.0432 (1.0351)** [2]	**1.0152 ± ?**
18 col.	**1.0080** [1]	**1.00855** [2] ***±0.00090***	**1.0275 (1.0178)** [2]	**≲1.0**

[1] *CR inserted considered $\Delta k = 0\ 004$ and detector impact included $\Delta k = 0.002$*
[2] *detector impact included $\Delta k = 0.002$*

Coorporation.

All calculational results obtained for the fully loaded core configuration agree well with each other and with the experiment, moreover when taking into account the experimental uncertainties. Furthermore, it is seen that there is an excellent agreement between the diffusion CITATION and Monte Carlo TRIPOLI4 results. Altogether it turns out that the following procedures seem to be necessary for a better approach to the experimental results:

- detailed heterogeneity of the BP- and fuel-region in the whole core calculation,
- use of fine group constants in the whole core (FZJ) diffusion calculation or consideration of the actual environment of the fuel blocks in the (CEA) transport cell calculations in order to describe the core/reflector coupling accurately,
- consideration of the axially heterogeneous distribution of the BP by 2d cell calculations (FZJ) or by 3d diffusion calculations (CEA and NRG),
- treatment of the enhanced neutron streaming whether by an adaptation of the diffusion constants to Monte Carlo calculations (FZJ) or by a leakage model combined with an analytical model (CEA).

7. References

[1] N.Nojiri et al.,priv. comm., Japan, January, 1998

[2] K.Yamashita et al., IAEA Benchmark Calculation Results of the HTTR's Start-up Core Physics Tests (JAERI-memo-11-030), 1.RCM of IAEA CRP-5, Vienna, Austria, August 24-28, 1998

[3] 2nd Research Coordinated Meeting of IAEA CRP-5 "Evaluation of High Temperature Gas-cooled Reactors", Beijing, China, October 18-22, 1999

[4] W. Bernnat, Faschinger, J. Kuijper, X. Raepsaet, J.Turner and W.von Lensa, HTR-N Annual Technical Progress Report (HTR-N-01/09-P-0.0.3), November, 2001

[5] N.Fujimoto, Data for re-calculation of HTTR-FC, priv. comm., November, 2000

[6] 3rd Research Coordinated Meeting of IAEA CRP-5 "Evaluation of HTGR Performance", Oarai, Japan, March 12-16, 2001

International Coorperation

INVESTIGATION OF CRITICALITY PARAMETERS OF HIGH-TEMPERATURE REACTORS AT THE KURCHATOV INSTITUTE'S ASTRA CRITICAL FACILITY

N.E. KUKHARKIN, E.S. GLUSHKOV, G.V. KOMPANIETS, ~~V.A. LOBYNTSEV~~, D.N. POLYAKOV, O.N. SMIRNOV

Institute of Nuclear Reactors

RRC Kurchatov Institute, Kurchatov sq. 1, 123182, Moscow, Russia

ABSTRACT

The basic parameters of critical assemblies created at the ASTRA critical facility of the RRC Kurchatov Institute for simulation of high-temperature reactors are given in the paper. Capability to simulate different HTGR reactors at the ASTRA critical facility is presented. Brief description of the experiments simulating the PBMR reactor being developed in Republic of South Africa is given. Spherical graphite elements with the outer diameter of 6 cm containing about 2.4 g of uranium with the enrichment of about 21 % are used as fuel elements at the facility. Fuel particles (kernels) made of uranium dioxide with the diameter of about 500 micrometers, having four-layer coating are evenly distributed in the graphite matrix in the central part (5 cm in diameter) of each spherical fuel element. Graphite blocks are used as moderator in reflectors. Up to 46000 spherical elements were loaded in the core in the most recent experiments. Anticipatory computations of critical parameters of the assemblies performed at the RRC KI for the substantiation of criticality safety of the experiments are described in the paper. The calculations were performed with the Russian MCU program complex, which uses Monte-Carlo method. The MCU code was modified for calculations of the double heterogeneity of the HTGR fuel. Kernels of coated fuel particles were not smeared with graphite matrix of fuel elements, and their heterogeneous structure was directly taken into account in the calculations. Results of the implemented experiments are intended for validation of calculational codes used in HTGR designing and justification of neutronics of HTGRs under development.

1. Description of the ASTRA Critical Facility

The ASTRA critical facility at the Kurchatov Institute is intended for experimental investigation of neutron - physical characteristics of HTGR reactors. At the moment the ASTRA critical assembly represents graphite block masonry in the form of a cylinder with internal cavity to form a core. The outer diameter is 380 cm, equivalent inner diameter is 181 cm, height is 460 cm and thickness of the bottom reflector that is also made of graphite blocks is 40 cm (Fig. 1). The central cavity is filled with spherical elements. The set of spherical elements available at the facility includes 2500 absorbing elements (AE), about 15000 graphite elements (GE), and about 50000 fuel elements (FE). Additional graphite blocks available at the facility can be used for mounting of an internal reflector and/or top reflector. All the graphite blocks are made of reactor-grade graphite (the impurity concentration in terms of boron equivalent is about 1.1 ppm wt.) and have the cross section of 25x25 cm and height of 60 or 40 cm. The average density of the graphite mass is about 1.65 g/cm^3.

Spherical fuel elements with the diameter of 6 cm represent a graphite matrix in the central part of which the fuel particles with multilayer coatings (diameter of this central part is 5 cm) are evenly distributed. The density of the fuel element graphite matrix is 1.85 g/cm^3. A fuel particle represents a kernel made of uranium dioxide with the diameter of about 500 μm with four layers of coatings applied to it. Layer 1 (buffer) is made of pyrocarbon (PyC) with the graphite density of 1.1 g/cm^3, the thickness of this layer is 90 μm. Layer 2 (dense layer) is made of pyrocarbon (PyC) with the graphite density of 1.8 g/cm^3, its thickness is 70 μm. Layer 3 is made of silicon carbide (SiC) with the density of 3.2 g/cm^3, the thickness of the layer is 60 μm. Layer 4 is made of pyrocarbon (PyC) with the graphite density of 1.8 g/cm^3 and its thickness is 60μm.

The central fueled zone (5 cm in diameter) of each spherical fuel element contains 2.4g of uranium of the following isotopic composition (wt. %): U-234 - 0.15, U-235- 20.66, U-236 - 0.09, U-238 - 79.10.

A spherical absorbing element with the outer diameter of 6 cm represents a graphite matrix, in central part of which the tiny particles made of boron carbide with the average diameter of about 60 micrometers are evenly distributed. The diameter of this central part is 4 cm. The total mass of natural boron in one absorbing element is 0.1 g. The isotopic composition of the natural boron (at. %) is: B-10 - 19.8, B-11 - 80.2. The density of graphite matrix of the absorbing element is 1.75 g/cm^3.
A spherical graphite element is made of reactor-grade graphite. The outer diameter of the spherical graphite element is 6 cm. The graphite density is 1.68 g/cm^3.
Up to 24 control rods can be used at the ASTRA critical facility. Each absorbing control rod represents a cluster consisting of 15 steel pipes. The outer diameter of the pipe is 12.5 mm and wall thickness is 1.2 mm. The pipes are filled with natural boron carbide with the density of 1.53 g/cm^3. The centres of the pipes are uniformly located on a circle with the diameter of 76 mm. Material of the pipes is stainless steel. The control rod consists of two parts along the height, and the total height of absorber is about 380 cm. The manual control rod has a different design. It represents an aluminium pipe without any additional absorber. All control rods are placed in the central channels (11.4 cm in diameter) of specified side reflector graphite blocks (Fig. 1).

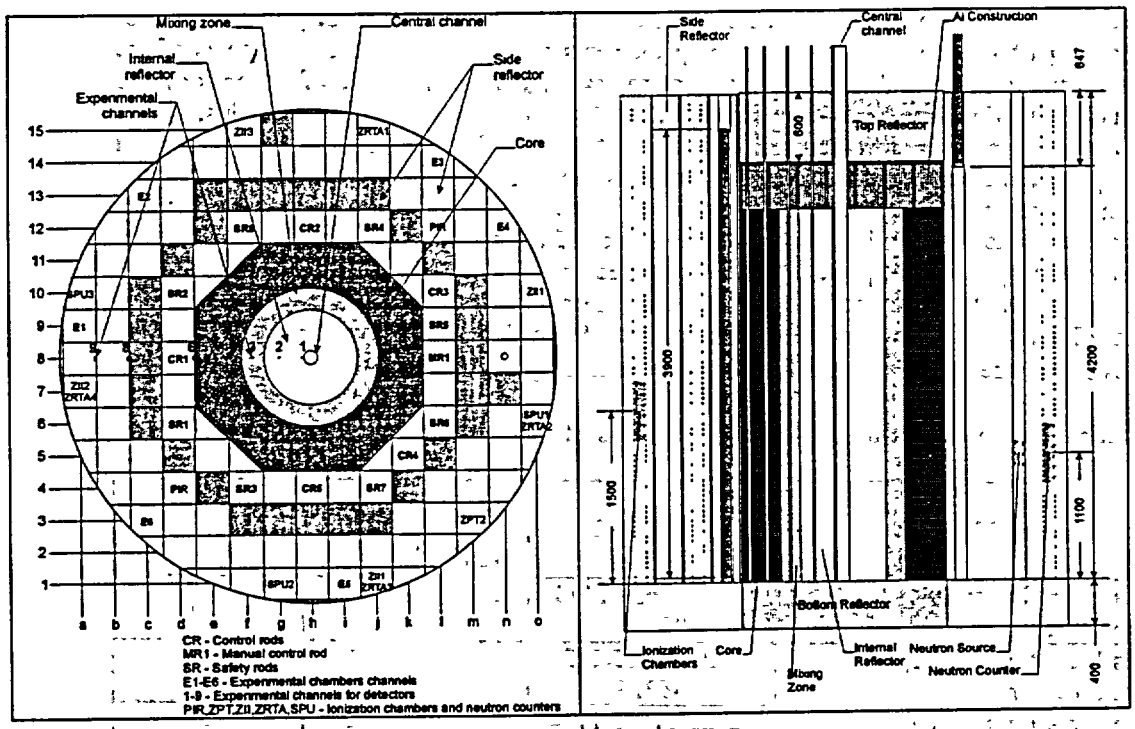

Fig. 1. Cross section and axial section of a critical assembly.

2. Configurations of the Critical Assemblies

A lot of experiments on investigation of high-temperature reactors have been performed at the ASTRA critical facility [1]. The cavity inside the reflector described above (graphite block masonry) represented squares, octagons, and circles of different dimensions without an internal reflector. Some examples of the previously investigated core configurations are given in Table 1.

Table 1. Examples of the Core Configurations at the ASTRA Facility

Configuration	Cross Section	Core Height, m (Total Number of FE)	Spherical Element Ratio in the Core
1	Octagon Øeff=1.8 m	1.76 (23600)	FE/AE=100/5
2	Circle Ø =0.938 m	3.02 (11300)	FE/AE=100/0

3	Circle ∅ =0.938 m	3.8 (14050)	FE/AE=100/1
4	Circle ∅ =0.938 m, density of polythene in the core 10.6 kg/m^3	3.2 (11920)	FE/AE=100/1
5	Square 1*1 m	2.27 (12330)	FE/AE=100/0
6	Square 1*1 m	2.91 (12790)	FE/GE=4/1

The recent experiments carried out at the ASTRA critical facility were intended for simulation of the PBMR high-temperature modular reactor with annular core being developed in South Africa [2,3]. The works were performed under the contract with the ESKOM company. In these experiments the core represented a pebble bed consisting of three radial zones (see Fig. 1). In the central part of the core the graphite spherical elements forming the internal graphite reflector were placed. Around the internal reflector, a so-called mixing zone representing a mixture of spherical fuel elements, graphite elements and absorbing elements was formed. Between the mixing zone and the side graphite reflector a zone consisting of fuel elements and absorbing elements was created. One of the goals of the experiments carried out at the ASTRA facility was to investigate the influence of dimensions and composition of the mixing zone on the reactor neutronics. All zones were equal in core heights.
Three series of experiments were carried out at the ASTRA facility. Each of the series is characterized by its own type of critical assembly. These types of the assemblies were created one after another and they differ in dimensions and composition of the radial zones. Within each series of the experiments different configurations of critical assemblies were created. They differ from each other by the core height (reactivity margin) and the presence of the top reflector.
Critical parameters of the basic configurations of the assemblies simulating the PBMR reactor are given in Table 2. Critical states of the assemblies were attained with control rods. Measurements of the critical states of the assemblies were performed with the accuracy of 0.0005βeff.

Table 2. Critical Parameters of the Basic Configurations of the Assemblies Simulating the PBMR Reactor

#	Assembly Type	FE/PE/GE Total	H, (cm)	K eff	Reactivity Margin ρ/β_{eff}
1	Series 1, configuration 1, no top reflector	27477/9659/1448 38584	268.9	1.000	0.10
2	Series 1, configuration 2, no top reflector	32929/11553/1734 46216	320.8	1.000	3.7
3	Series 1, configuration 3, top reflector	32929/11553/1734 46216	320.8	1.000	5.8
4	Series 2, configuration 1, no top reflector	27144/9545/1434 38123	267.3	1.000	0.09
5	Series 2, configuration 2, no top reflector	27477/9659/1448 38584	270.3	1.000	0.39
6	Series 3, configuration 1, no top reflector	25308/8884/1334 35526	247.6	1.000	0.09
7	Series 3, configuration 3, no top reflector	27477/9659/1448 38584	268.7	1.000	2.48

Total – Total number of spherical elements in the assembly,
H – Average height of the pebble bed,
K eff – Multiplication factor,
ρ – Reactivity margin with all control rods withdrawn.

Different configurations for simulation of the annular core at the ASTRA critical facility can be proposed under the GT-MHR international project (Russia, USA, France, Japan). The internal and side reflectors can be assembled of graphite blocks, and the annular core can be made up of spherical fuel elements or actual prismatic assemblies with fuel compacts as they are fabricated. One variant of such configurations is shown in Fig. 2. It should be emphasized that the design of the control rod system at the ASTRA critical facility allows placing control rods not only in the side reflector, but also in the core and/or internal reflector. The equipment available at the critical facility allows performing measurements of the following characteristics: criticality parameters, worth of control rods (and plotting of their calibration curves), distributions (profiles) of neutron fluxes (reaction rates) along the radius and height of assemblies simulating HTGR, etc. It is possible to investigate methods of power density distribution profiling over the core volume, influence of synchronous insertion of a group of control rods on power density distribution, etc.

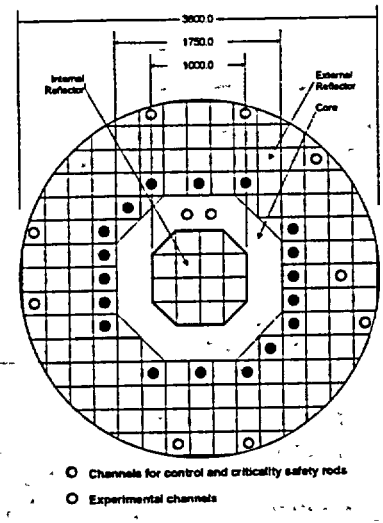

Fig. 2 Variant of cross section of a critical assembly simulating the GT-MHR reactor.

3. Anticipatory Computations of the Critical Assemblies

The anticipatory computations with the goal of substantiation of criticality safety of the experiments implemented at the ASTRA facility have been generally performed with the MCU program complex [4,5]. This code is intended for solution of critical problems of neutron transport with the Monte-Carlo method. The continuous energy range from 20 MeV up to 10^{-5} eV and combinatorial geometry modules allowing computations of real three-dimensional configurations of critical systems are used in the MCU code. In the thermal energy region the Monte-Carlo method uses the S (a, b) scattering model or the free gas model.

The MCU uses an original system of nuclear data libraries. This system includes: ABBN library (26 groups), LIPAR library of resonance parameters in the resolved resonance region, VESTA library of thermal cross sections based on phonon data from the ENDF. In cell computations the TEPCON library can be used instead of the VESTA library. The TEPCON library represents a multigroup library of data for thermal neutrons for energies below 1eV at different temperatures.

Scientists at the RRC Kurchatov Institute developed a special approach on the basis of the Monte-Carlo method for calculation of systems with tiny fuel particles [6]. So, in the calculations of the ASTRA critical assemblies the fuel kernels were not homogenized with the graphite matrix of spherical fuel elements, and the heterogeneous structure of fuel kernels was directly taken into account in the calculations. Two procedures (two systems) are considered for neutrons. The first procedure is used for neutron migration in a fuel zone and the second one is used for neutron migration in a kernel only. The heterogeneous distribution of poison particles (B_4C) in spherical absorbing elements is similarly taken into account.

A stochastic pebble bed was modeled with a regular three-dimensional lattice of spheres of 6 cm in diameter. This lattice (Fig. 3) is characterized by a set of packing factors – spherical element spacing in the layer, and the distance between the layers. Each cell represents the rectangular parallelepiped with square cross section (in the XY plane). In all eight corners of a parallelepiped the centers of spheres are located, and 1/8 part of each sphere belongs to this cell. A centrally located sphere wholly belongs to the cell. FE, AE, or GE can be placed in the center of the cell, and FE, GE – in the corners.

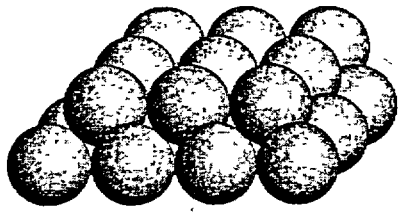

Fig. 3 Model of a pebble bed.

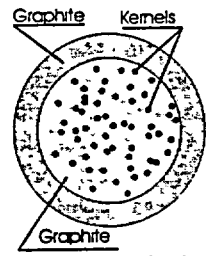

Fig. 4. Model of a fuel element.

The computations predicted critical states of the assemblies with the accuracy of about 0.5 %. Further, on the basis of the refined benchmark models of the investigated configurations of critical assemblies (including detailed description of their structure, dimensions, and compositions), the work on validation of computational methods and codes used in HTGR designing is planned.

4. Conclusion

The experimental investigations performed at the ASTRA facility demonstrate the following:

- For the designing of new HTGR reactors, it is very important to perform experimental modeling of the reactor, and results of the experiments should be used for validation of calculational codes used in HTGR designing and HTGR criticality safety analysis.
- The cost of experimental investigations at the ASTRA critical facility, in view of the available materials, equipment, and licensed personnel, is relatively low.
- Works with critical assemblies are safe, there is no radiation release or other environmental impacts.
- Computational methods used in support of experimental investigations (substantiation of criticality safety of experiments, prediction of results of the experiments, etc.) are acceptable for analysis of neutron - physical characteristics of HTGR under development.

5. References

[1] S.V. Bakulin,V.P. Garin, Y.S. Glushkov and others, Study of HTGR Nuclear Safety at the GROG and ASTRA Facilities, Proceedings of the Fifth International Conference on Nuclear Criticality Safety, Albuquerque, NM, USA, September 17-21, 1995, v1, pp 6-18...6-24.

[2] New nuclear generation – in our lifetime, Nuclear News, October 2001

[3] http://www.pebble-bed.co.za

[4] L.P. Abagian, N.I. Alekseev, V.I. Bryzgalov and others, MCU Monte-Carlo code for Nuclear Reactor Calculations. Verifications, RRC Kurchatov Institute, Preprint IAE-5751/5, 1994.

[5] L.P. Abagian, N.I. Alekseev, V.I. Bryzgalov and others, The MCU-RFFI/A Code with DLC/MCUDAT-1.0 Nuclear Data Library, Applicant and Developer: RRC Kurchatov Institute, Certificate Number PC # 61 of 10.17.96, Russian Federal Agency for Supervision of Nuclear and Radiation Safety, Moscow, 1996.

[6] M.I. Gurevich, V.I. Bryzgalov " The Nutrons Flux Density Calculation by Monte-Carlo Code for the Double Heterogeneity Fuel". Proceedings of the International Conference on Reactor Physics and Reactor Computations, Tel-Aviv, January 23-26, 1994,p.p. 190-196.

DESIGN OF SPHERICAL AND 'HOLLOW' BURNABLE PARTICLES FOR UO_2 FUELS IN HIGH TEMPERATURE REACTORS

J.L. KLOOSTERMAN, H. VAN DAM, AND T.H.J.J VAN DER HAGEN

Interfaculty Reactor Institute
Delft University of Technology
Mekelweg 15, NL 2629 JB Delft
The Netherlands
E-mail: J.L.Kloosterman@iri.tudelft.nl

ABSTRACT

Burnup calculations have been performed on a standard HTR fuel pebble (R=3 cm) containing 9 grams of 8% enriched uranium and burnable particles made of B_4C highly enriched in B-10. The radius of the burnable particles and the number of particles per fuel pebble have been varied to find the flattest reactivity-to-time curve. It was found that for a target k_∞ of 1.1, a reactivity swing as low as 2.4% can be obtained when each fuel pebble contains about 1300 burnable particles with a radius of 70 μm. For other values of the target k_∞ even lower values can be obtained. For 'hollow' burnable particles that consist of a graphite kernel with a radius of 300 μm covered with a burnable poison layer of 30 μm, the reactivity swing is only 2%. In general, the modification of the geometry of burnable particles is an effective means to tailor the reactivity curve of HTRs.

1. Introduction

During the operation of a nuclear reactor, the reactivity effect of fuel burnup must be compensated by some means of long-term reactivity control, especially when the reactor operates with batch-wise fuel loads. An elegant way for such a control is the use of burnable poison in the fuel elements to balance the reactivity loss caused by fuel burnup and fission product poisoning by the reactivity gain due to the disappearance of the burnable poison.

The possibility of continuous fuel loading is a very nice feature of pebble-bed type High Temperature Reactors (HTRs) that enables one to reach a high fuel burnup. However, it is also likely to increase the manufacturing and operational costs of such a reactor. Besides the fact that fuel-loading machinery is complex and sensitive to malfunctioning, high-skilled operators are needed to guarantee long-term operation without interruption, which inherently limits the application of this reactor type to (co) generation of heat and electricity in well-developed countries.

A batch-wise fuel load scheme in HTRs combined with burnable poison has some attractive properties not offered by the continuous loading scheme. The use of the burnable poison diminishes the role of the active reactivity control mechanisms, which paves the way for long-term unattended reactor operation. This makes the HTR technology applicable to ship propulsion and to (co) generation of heat and electricity for all kind of purposes in remote areas.

In this paper, we consider poisoning of the fuel in a heterogeneous way by mixing burnable particles in the fuel elements. The reason for this is given in chapter 2 of this paper. The burnable particles themselves contain B_4C made of boron highly enriched in the isotope B-10. As a fuel we used 8% enriched UO_2 particles embedded in a graphite pebble with diameter of 5 cm surrounded with a graphite layer with thickness of 0.5 cm. This fuel is very similar to that adopted by the PBMR [1,2]. The initial uranium mass per pebble was 9 gram. The core power density was 3 $W.cm^{-3}$, and assumed constant during the burnup. The temperature was 900 K in all calculations

2. Theory

For absorbing nuclides homogeneously distributed in the core, the macroscopic neutron absorption cross section Σ_a is an exponentially decaying function of time t:

$$\Sigma_a(t) = \sigma_a N(t) = \sigma_a N_0 \exp(-\sigma_a \Phi_0 t). \tag{2.1}$$

Here, σ_a is the microscopic absorption cross section of the absorbing nuclide (e.g. B-10), N_0 its initial atomic density, and Φ_0 the neutron flux density.

For a small particle that absorbs all impinging neutrons, a so-called black particle, the effective absorption cross section is equal to its geometrical cross section [3]. This means that the neutron absorption rate depends on the geometry and size of the burnable particle, but not on its actual composition. For a spherical particle, the effective absorption cross section is a quadratic function of time:

$$\Sigma_a(t) = N_p \pi R_0^2 \left(1 - \frac{\Phi_0 t}{4NR_0}\right)^2. \tag{2.2}$$

Here, N_p is the density of the burnable particles, R_0 the initial radius of the particle, and N the atomic density of the absorbing nuclide in the particle. Although Eq. (2.2) does not contain the microscopic absorption cross section σ_a of the absorbing nuclide, it is implicitly assumed that its value is such high that the burnable particle can be considered as 'black'. Equations (2.1) and (2.2) clearly illustrate that lumping the burnable absorber into particles enables one to tailor the time-dependence of the neutron absorption rate by the absorber. The purpose of this paper is to find the optimum radius of a burnable particle containing B_4C made of highly enriched boron.

3 Calculational scheme

From the SCALE code system [4], we used the BONAMI-S code for the resonance treatment in the unresolved energy region, the NITAWL-II code for the resonance treatment in the resolved energy region, and the XSDRNPM-S code for the cell-weighting calculations. The actual burnup calculations were performed by the ORIGEN-S fuel depletion code. All codes were coupled to each other via PERL scripts and via own-made FORTRAN programs. All nuclear data used are based on the JEF-2.2 nuclear data library.

In all calculations, a macro cell was modeled containing one burnable particle made of B_4C surrounded with a smeared fuel layer. The latter contains all nuclides present in a standard fuel pebble, i.e. the nuclides from the TRISO coated fuel particles (including fission products and actinides), the carbon from the graphite matrix in between the fuel particles, and the carbon from the 0.5 cm thick outer layer.

Because the SCALE code system cannot handle explicitly the double heterogeneity of the fuel, the cell-weighting procedure had to be split up in two parts. First, the homogenized resonance-shielded and cell-weighted cross sections of the fuel layer were calculated in a micro-cell calculation with the unit cell made up of a TRISO coated fuel particle with a nuclide composition characteristic for the actual burnup time step surrounded with an equivalent amount of graphite. Secondly, a macro-cell calculation was done to calculate the neutron flux density in the burnable particle, and to calculate the fission power density in the smeared fuel layer.

Besides the resonance-shielded cell-weighted cross sections to be used in the macro-cell calculation, also the resonance-shielded *zone*-averaged cross sections were calculated, and passed to the burnup data library. Burnup calculations were done for each fuel layer and for each layer of the burnable particle using the nuclide cross sections updated at each burnup time step. The whole sequence of micro-cell calculations, macro-cell calculations, and burnup calculations for the fuel layers and the burnable particle layers are repeated 10 times to calculate the $k\infty$ and the composition of each layer as a function of burnup. Furthermore, at each burnup time step, the temperature reactivity coefficient was calculated.

4 Results for spherical burnable particles

This section presents the results for the spherical burnable particles made of B_4C. For a specific composition of the burnable particle and the fuel pebble, there remain only two parameters to be varied: the radius of the burnable particle and the number of burnable particles per fuel pebble. The latter number is presented in a more abstract way by the ratio of the volume of one fuel pebble, and the volume of all burnable particles in that pebble.

There are two output parameters of major interest: the *initial* k_∞ and the *reactivity swing* Δk. Because the definition of these parameters is not unambiguous, we will clarify their definition. The *initial* k_∞ is the value of the k_∞ curve directly after saturation of all short-lived fission products like Xe and Sm. In practice, the value of the k_∞ after 10 days of burnup is used for this. The reactivity swing is defined as the variation of the k_∞ between 10 days of burnup and the burnup value for which the k_∞ of the reference curve (without a burnable particle) crosses the *initial* k_∞. This makes sense as one would like to achieve a reactivity curve as flat as possible. Fig 1 illustrates the parameters defined above.

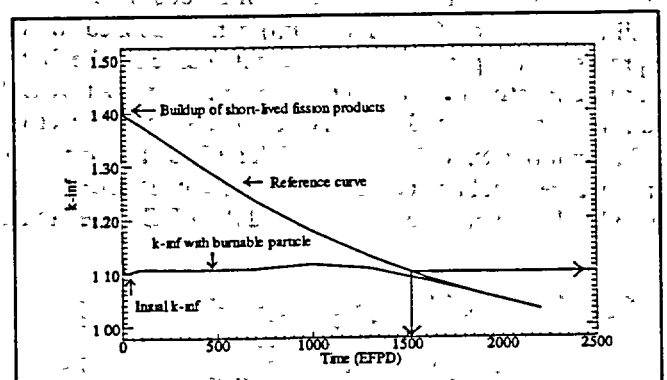

Fig 1. Illustration of the parameters used to characterize the fuel with burnable particles. The reactivity swing is the variation of the k_∞ between 10 EFPD and 1520 EFPD, where the reference curve crosses the initial k_∞ of 1.1.

Figures 2 and 3 show the initial k_∞ and the reactivity swing of the fuel for radii of the burnable particle varying from 10 to 200 μm and for the fuel volume ratio varying from 10,000 to 200,000. Figure 2 shows that the initial k_∞ increases when either the fuel volume ratio or the burnable particle radius increases. The latter can be understood from the theory in section 2: for a fixed volume of the burnable poison (constant fuel volume fraction), the larger the radius of the burnable particle, the more heterogeneously distributed the burnable poison, and the smaller the effective absorption cross-section. On the other hand, the reactivity swing shows a 'valley' ranging from the upper-left corner to the lower-right corner. The optimization procedure would be first to find the range of 'coordinates' (burnable particle radius and the fuel volume ratio) that fulfills the requirement on the initial k_∞ (this could be, for example, that in order to have a critical reactor, the initial k_∞ must be 1.1). Secondly, from the coordinates found, one should extract that pair that gives the lowest reactivity swing. The result is visualized in Fig. 4.

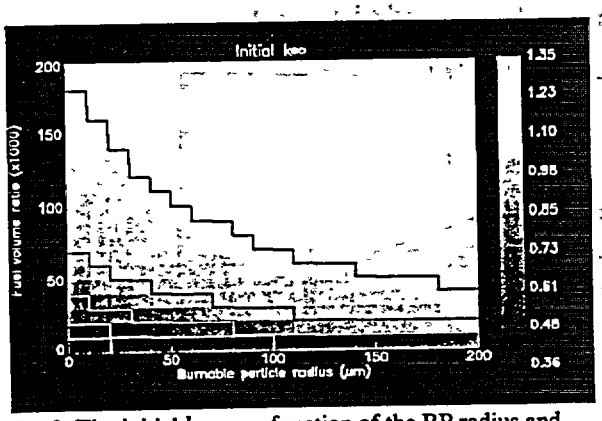

Fig 2. The initial k_∞ as a function of the BP radius and the fuel volume ratio.

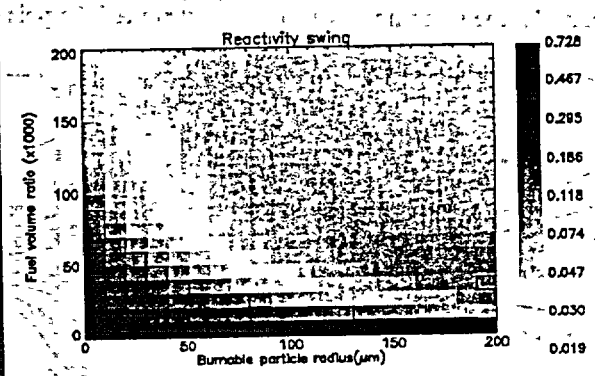

Fig 3. The reactivity swing as a function of the BP radius and the fuel volume ratio.

Figure 4 shows the absolute difference of the initial k_∞ and the target value (arbitrarily chosen to be 1.1) multiplied with the reactivity swing. The 'valley' in the plot shows the combinations of the BP radius and the fuel volume ratio that gives an initial k_∞ close to 1.1 and a reactivity swing as small as possible. Two combinations are most favorable: a BP radius of 70 µm with a VF ratio of 60,000, (reactivity swing of 2.4%) and a BP radius of 90 µm with a VF ratio of 50,000 (reactivity swing of 1.9%). However, a broad range of BP radii (say between 60 and 100 µm) can be applied, which relaxes the requirements in the manufacturing process of the particles. The reactivity curve for the first-mentioned fuel is shown in Fig 1, while the temperature reactivity coefficient is shown in Fig 5. At BOL the influence of the poison on the neutron spectrum is quite large and the UTC is more strongly negative. However, the burnup averaged UTC values differ not too much (≈1 pcm/K). With a UTC of -8 pcm/K and a reactivity swing of 2.4%, the temperature of the core would vary 300 K during the lifetime of the fuel. After about 2000 EFPD, virtually all boron has been burnt (<0.1% left), and the UTC is the same for both curves.

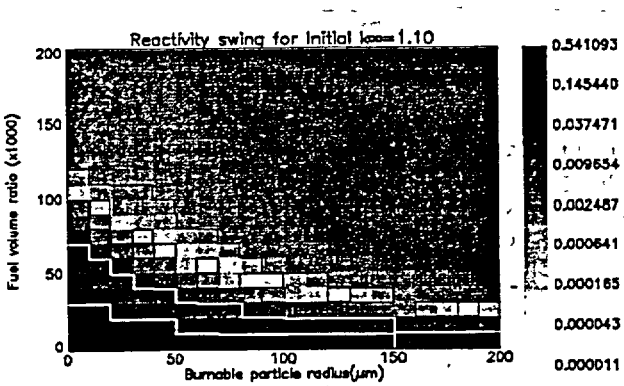

Fig 4. Result of the optimization procedure. The light 'valley' shows the range of parameters that gives the smallest reactivity swing at a target k_∞ of 1.10.

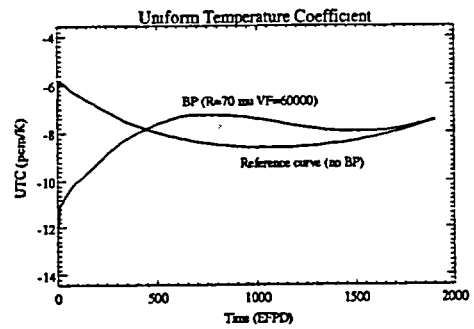

Fig 5. The UTC as a function of burnup for the fuel with a BP radius of 70 µm and a fuel volume ratio of 60,000 compared with the reference fuel. The average values are -7.6 pcm/K (reference curve) and -8.7 pcm/K.

Figures 6 and 7 show the relationship between the BP radius and the reactivity swing at the one hand, and between the fuel volume ratio and the reactivity swing at the other. Figure 6 shows that the larger the fuel volume ratio, the less influence the poison has on the reactivity. In Fig 7, the initial amount of poison is the same in all curves, and the effect of lumping the burnable poison into particles is clearly seen. The smaller the particle, the more homogeneously distributed the poison, and the lower the initial k_∞.

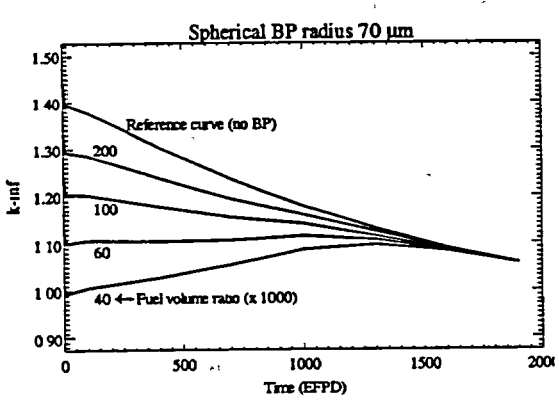

Fig 6. The k_∞ as a function of burnup with the fuel volume ratio as a parameter.

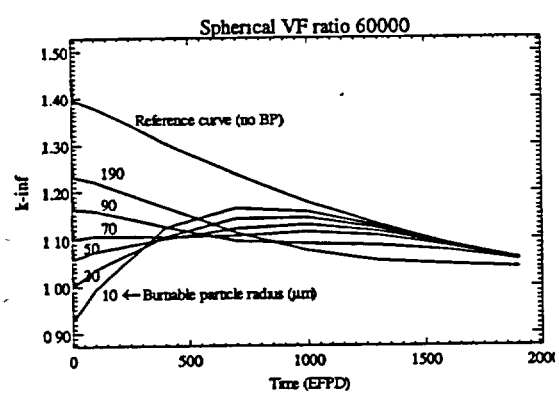

Fig 7. The k_∞ as a function of burnup with the burnable particle radius as a parameter.

5 Results for hollow burnable particles

Similar results can be obtained by using 'hollow' particles. These particles contain a graphite kernel with a radius of 300 μm covered with a thin layer of B_4C fully enriched in B-10. The results of the optimization procedure are shown in Fig 8. The best result at an initial k_∞ of 1.1 is obtained for a burnable poison layer with a thickness of 50 μm and a fuel volume ratio of 40,000. Then the reactivity swing is 5.8%. However, for a burnable poison layer of 30 μm and a fuel volume ratio of 50,000, the reactivity swing is 2% only at an initial k_∞ of 1.08. Some freedom in the choice of the target k_∞ can therefore lead to lower values for the reactivity swing. Calculations with a graphite kernel with radius of 500 μm give similar results.

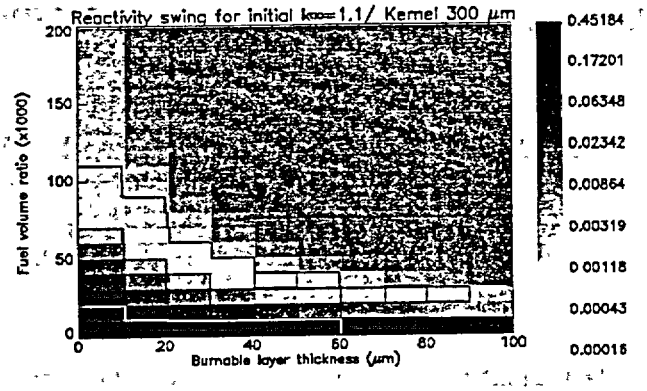

Fig 8. Result of the optimization procedure for a 'hollow' particle made of a graphite kernel (R=300 μm) covered with a B_4C layer with thickness between 10 and 100 μm.

6 Conclusions

With burnable particles mixed in the fuel of an HTR, it is possible to control the excess reactivity present at BOL. For 8% enriched UO_2 fuel, mixing 1300 spherical particles made of B_4C with radius of 70 μm through the fuel of a standard HTR fuel pebble (with radius of 3 cm), the reactivity swing is 2.4% at a constant k_∞ of 1.1. Using burnable particles with a radius of 90 μm, the reactivity swing drops to a value below 2%. This means that, with no active reactivity control mechanisms (e.g. no shim rods) and a uniform temperature coefficient of -8 pcm/K, the temperature of the core would vary between 250 and 300 K during the lifetime of the fuel. ?

The application of 'hollow' burnable particles, which consist of a non-poisonous graphite kernel covered with a B_4C burnable poison layer, gives similar results. Particles with a kernel radius of 300 μm and a burnable poison layer of 30 μm give a reactivity swing of 2% at an initial k_∞ of 1.08, while the reactivity swing is almost 6% for an initial k_∞ of 1.1. This example shows that some freedom in the selection of the target k_∞ may lead to even lower values of the reactivity swing. In general, we can conclude that modifying the geometry of burnable particles is an effective means to tailor the reactivity-to-time curve of HTRs. Further research will focus on the application of other burnable absorbers like Er and Gd, and other fuel types like PuO_2 fuel.

Acknowledgements

The authors wish to acknowledge the European Commission for co-funding this work under project number FIKI-CT-2000-00020 ("High Temperature Reactor Physics and Fuel Cycle Studies (HTR-N)").

References

1. J. H. Gittus, "The ESKOM Pebble-Bed Modular Reactor", *Nuclear Energy*, 38, pp. 215 (1999).
2. D. R. Nicholls, "The ESKOM Pebble-Bed Modular Reactor", *Nuclear Energy*, 39, pp. 231 (2000).
3. H. Van Dam, "Long-term Control of Excess Reactivity by Burnable Particles", *Annals of Nuclear Energy*, 27, pp. 733 (2000).
4. SCALE 4.2, Modular Code System for Performing Standardized Computer Analyses for Licensing Evaluations, Oak Ridge National Laboratory, Oak Ridge, Tennessee (1994)

MATRIX FORMULATION OF PEBBLE CIRCULATION IN THE PEBBED CODE

H. D. GOUGAR, W. K. TERRY, and A. M. OUGOUAG
Idaho National Engineering and Environmental Laboratory
Nuclear Engineering Design and Research Department
MS-3885, P. O. Box 1625
Idaho Falls, IDAHO 83415-3885

ABSTRACT

The PEBBED technique provides a foundation for equilibrium fuel cycle analysis and optimization in pebble-bed cores in which the fuel elements are continuously flowing and, if desired, recirculating. In addition to the modern analysis techniques used in or being developed for the code, PEBBED incorporates a novel nuclide-mixing algorithm that allows for sophisticated recirculation patterns using a matrix generated from basic core parameters. Derived from a simple partitioning of the pebble flow, the elements of the recirculation matrix are used to compute the spatially averaged density of each nuclide at the entry plane from the nuclide densities of pebbles emerging from the discharge conus. The order of the recirculation matrix is a function of the flexibility and sophistication of the fuel handling mechanism. This formulation for coupling pebble flow and neutronics enables core design and fuel cycle optimization to be performed by the manipulation of a few key core parameters. The formulation is amenable to modern optimization techniques.

Introduction

The PEBBED [1] code is a new tool for analyzing the asymptotic fuel cycle in recirculating pebble-bed reactors. Equations for neutron flux and nuclide distribution in a pebble-bed core are solved self-consistently by an iterative scheme, and the algorithm is shown to converge quickly to a solution unique to the pebble flow pattern. The neutronics solver currently relies on a standard finite difference technique, but more advanced solution methods are planned. The burnup solver uses a semi-analytical method that guarantees convergence with accuracy. A key step in the algorithm is the computation of the entry-plane density of each nuclide of interest in each axial flow channel. These values depend upon the pebble loading and recirculation policy and the burnup accrued by pebbles on successive passes through the core. The current iterate of the flux is used to compute the exit-plane nuclide density in a pebble after one pass through the core in each channel, based on the density of that nuclide in a fresh pebble. Pebbles are then distributed according to the recirculation scheme to generate the entry-plane density in each channel on the next pass. This is repeated until the pebbles exceed the discharge burnup. The exit-plane values are then averaged according to the recirculation scheme in order to produce the actual entry-plane nuclide densities. The entry-plane nuclide flow rate is derived in the next section.

The homogenized entry plane nuclide density of a given nuclide for each flow channel, expressed here as the vector $\bar{N}$, is computed as a weighted average of the contributions from pebbles of various types and trajectories. The symbol ${}^{m}\bar{N}^{p}$ refers to the number density vector (the elements of which correspond to the flow channels) of that nuclide in a pebble of type p that has passed through the core m times. A *recirculation matrix* **R** stores the weight of each contribution so that

$$\bar{N} = \mathbf{R}\,{}^{m}\bar{N}^{p} \quad . \tag{1}$$

It is shown in this paper that the values of the elements of R are dependent upon basic core parameters and thus can be computed manually or generated using a suitable optimization algorithm.

Theory

The flow rate of a given nuclide in pebble flow channel i is composed of contributions from pebbles of different types (p) and different prior histories. For a core with P pebble types each undergoing an average of M_p passes before discharge, the flow rate (atoms per second) of that nuclide at the entry plane of channel i is the sum of of the flow rates of the nuclide in pebbles of all types and pass histories at this location, expressed as

$$\dot{n}_i = \sum_{p=1}^{P}\sum_{m=1}^{M_p} {}^m\hat{N}_i^p f_i \cdot \alpha_i^p \cdot {}^m\alpha_i^p \quad , \qquad (2)$$

where

α_i^p	is the fraction of channel i flow that consists of type p pebbles,
${}^m\alpha_i^p$	is the fraction of type p pebbles in channel i flow that are on their m^{th} PASS,
${}^m\hat{N}_i^p$	is the number density of the nuclide of interest within pebbles of type p, entering channel i, starting their m^{th} pass, and
f_i	is the volumetric flow rate of pebbles through channel i.

One can show that the channel-averaged nuclide density at the entry plane of channel i is given by

$$N_i = \sum_{p=1}^{P}\left\{ {}^1\hat{N}_i^p \cdot {}^1\alpha_i^p \cdot \alpha_i^p + \sum_{m=1}^{M_{max}-1}\sum_{j=1}^{J} {}^m\hat{N}_j^p \cdot \left[\frac{\alpha_j \cdot \alpha_j^p \cdot {}^m\alpha_j^p \cdot {}^m\alpha_{ij}^p}{\alpha_i}\right]\right\} \quad , \qquad (3)$$

where

α_i	is the fraction of pebble flow that passes through channel i,
${}^m\alpha_{ij}^p$	is the fraction of type p pebbles in flow channel j, and on pass m, that are transferred to channel i, following this m^{th} pass,
${}^m\hat{N}_j^p$	is the number density of the nuclide of interest within pebbles of type p, exiting channel j, after completing their m^{th} pass, and
f_j	is the flow rate of pebbles through channel j.

The values are shown here to be functions of the flow properties of the core and the fuel loading mechanism. Three models are discussed: the HTR Modul 200 [2], the PBMR [3], and an alternative PBMR cycle.

The HTR Modul 200 (Figure 1a) possesses a single loading tube and a single discharge tube. The channel coefficients α_i are determined by the channel boundaries and the radial flow distribution. There is only one pebble type (P = 1), thus $\alpha_j^p = 1$. The pebbles emerging from the bottom are randomly dropped back onto the bed, so the so-called *transfer* coefficient ${}^m\alpha_{ij}^p = \alpha_i$ for all i, j, p, and m. The random recirculation also implies that the burnup classes are equally represented in each zone, i.e. ${}^m\alpha_j^p = (M_{max})^{-1}$. The recirculation matrix for a core with J flow channels is then given by

$$\mathbf{R} = \frac{1}{M_{max}}\begin{bmatrix} \alpha_1 & \alpha_2 & \cdots & \alpha_J \\ \alpha_1 & \alpha_2 & \cdots & \alpha_J \\ \vdots & \vdots & \ddots & \vdots \\ \alpha_1 & \alpha_2 & \cdots & \alpha_J \end{bmatrix} . \qquad (4)$$

The value of M_{max} is fixed by the core power, geometry, heavy metal content of pebbles, and discharge burnup. Hence the recirculation matrix elements are also entirely determined by these quantities and the partition of the core flow. The fuel handling mechanism in this design cannot be used to vary the asymptotic core nuclide distribution.

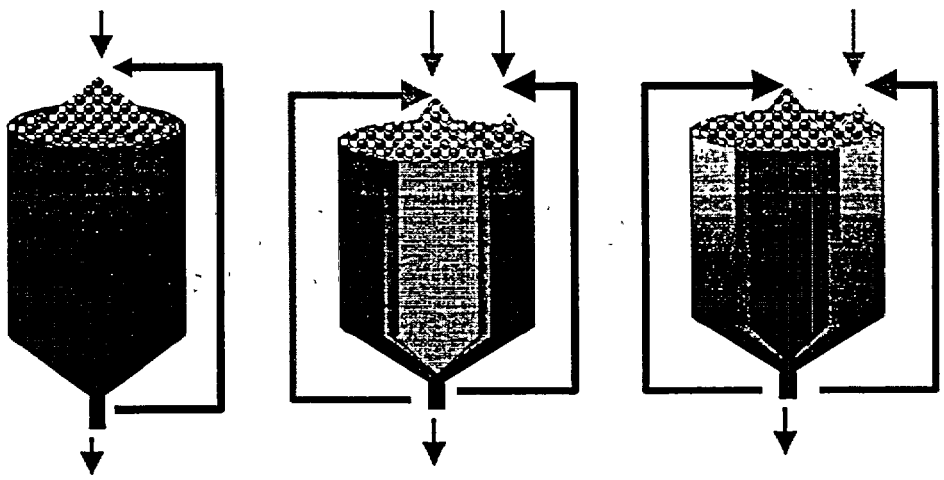

(a) HTR Modul 200 (b) PBMR with Graphite Inner Reflector (c) PBMR with OUT-IN Fuel Cycle

Figure 1. Modular Pebble-Bed Cores with Different Fuel Cycles

The Pebble-Bed Modular Reactor (PBMR) design under consideration by the South African utility Eskom uses two pebble types (graphite and fuel) flowing in separate regions of the core (Figure 1b). The graphite pebbles are dropped onto the bed via a central loading tube. The fuel pebbles are loaded by a number of loading tubes evenly spaced near the core periphery. There is no barrier between the two regions, so there is a zone between them in which the pebble types are mixed. The asymptotic core consists of a central reflector region composed entirely of graphite and a surrounding annulus of fuel pebbles. The size of the graphite region is regulated by the relative flow rates in the central and peripheral loading tubes. Many models of the PBMR core feature five concentric flow zones with roughly equivalent flow rates[4]. The volume of the graphite reflector is about 25% of the pebble bed volume. Thus the innermost channel is composed of only graphite, the second channel contains roughly equal portions of fuel and graphite pebbles, and the outer three channels consist only of the fueled type. The radial placement and discharge of pebbles is not burnup (pass) dependent, so the burnup classes are equally represented in all channels. Though slightly more complicated than the HTR Modul 200, the partition coefficients are again simple functions of core flow properties, power, and discharge burnup. The recirculation matrix (R) can be expressed as two submatrices; one each for fuel (f) and graphite (g):

$$\mathbf{R}^f = \frac{1}{M_{\max}\alpha^f}\begin{bmatrix} 0 & 0 & 0 & 0 & 0 \\ 0 & .25\alpha_2 & .5\alpha_3 & .5\alpha_4 & .5\alpha_5 \\ 0 & .5\alpha_2 & \alpha_3 & \alpha_4 & \alpha_5 \\ 0 & .5\alpha_2 & \alpha_3 & \alpha_4 & \alpha_5 \\ 0 & .5\alpha_2 & \alpha_3 & \alpha_4 & \alpha_5 \end{bmatrix}, \quad \mathbf{R}^g = \frac{1}{M_{\max}\left(1-\alpha^f\right)}\begin{bmatrix} 0 & .5\alpha_2 & 0 & 0 & 0 \\ .5\alpha_1 & .25\alpha_2 & 0 & 0 & 0 \\ 0 & 0 & 0 & 0 & 0 \\ 0 & .0 & 0 & 0 & 0 \\ 0 & 0 & 0 & 0 & 0 \end{bmatrix}. \quad (5)$$

The coefficient α^f refers to the fraction of total core flow consisting of fuel pebbles. This value is a simple function of the relative flow rates through the central and peripheral loading tubes and thus offers a degree of freedom in core design not available in the HTR Modul 200. By "tuning" the tube flow rates, one alters the sizes of the central reflector and active core annulus.

The fuel loading mechanism of the PBMR also allows for another type of two-region core. An "OUT-IN" cycle [5] is possible in which fresh fuel pebbles are loaded via the peripheral tubes but no graphite pebbles are used (Figure 1c). The fuel circulates in the outer region until an intermediate burnup threshold is exceeded. This occurs after a specified number of passes M_T, after which the pebbles are then loaded via the central tube. At equilibrium, the central region then consists of highly depleted elements while the annulus is composed of relatively fresh elements. Like the HTR Modul, there is only one pebble type ($\alpha_j^p = 1$), but the transfer coefficients vary with the pass number m. To conserve pebble flow, only a fraction α_T of the pebbles completing pass M_T are diverted to the inner region; the remainder are circulated once more and diverted on the following pass. Defining α_j^o as the fraction of flow in channel j that is in the outer region, one can derive the following expressions for the transfer coefficients:

$$ {}^m\alpha_{ij} = \frac{\alpha_i^o \alpha_i}{\sum_{\text{all } i} \alpha_i^o \alpha_i} \qquad m < M_T \tag{6a}$$

$$ {}^m\alpha_{ij} = \alpha_T \alpha_j^o \frac{(1-\alpha_i^o)\alpha_i}{1-\sum_{\text{all } i} \alpha_i^o \alpha_i} + (1-\alpha_T)\alpha_j^o \frac{\alpha_i^o \alpha_i}{\sum_{\text{all } i} \alpha_i^o \alpha_i} + (1-\alpha_j^o)\frac{(1-\alpha_i^o)\alpha_i}{1-\sum_{\text{all } i} \alpha_i^o \alpha_i} \qquad m = M_T \tag{6b}$$

$$ {}^m\alpha_{ij} = \frac{(1-\alpha_j^o)\alpha_i}{1-\sum_{\text{all } i} \alpha_i^o \alpha_i} \qquad m > M_T \tag{6c}$$

Furthermore, conservation of flow also fixes the values of the fraction of outer flow transferred (α_T) and the transfer pass number M_T according to

$$ \alpha_T = 1 + M_T - \frac{F \sum_{\text{all } j} \alpha_j^o \alpha_j}{{}^1F}, \qquad M_T = INT\left(\frac{F \sum_{\text{all } j} \alpha_j^o \alpha_j}{{}^1F}\right), \tag{7}$$

in which F is the total core pebble flow and ${}^1F$ is the total fresh fuel injection rate.

Obtaining *pass* coefficients ${}^m\alpha_j^p$ is less straightforward. The burnup-dependence of this recirculation scheme means that the burnup classes are not equally represented in each channel. Here, flow conservation is exploited to obtain a system of algebraic equations that represents the flow balance of all the channels. The flow of pebbles commencing their m^{th} pass in channel i consists of contributions from pebbles having completed m-1 passes in all channels. This fact yields m-1 equations for each channel i and pebble type p of the form

$$ \alpha_i \cdot \alpha_i^p \cdot {}^m\alpha_i^p = \sum_{j=1}^{J} \alpha_j \cdot \alpha_j^p \cdot {}^{m-1}\alpha_j^p \, {}^{m-1}\alpha_{ij}^p \tag{8}$$

The final equation required to determine the system completely is a direct consequence of flow conservation; i.e., the pass partition coefficients must sum to unity. Since all channels are coupled, the

solution to this system involves inverting a matrix of order M_p*J, the product of the number of channels and the total number of passes traversed by each pebble type p.

The values of α_j^o are computed in the same manner as the type coefficients in the previous example, They are a function of the size of the inner region and thus can be "tuned" by adjusting the relative flow rates in the loading tubes. Tuning the size of the inner region in this way also changes the value of the intermediate threshold burnup above which the fuel is transferred from the outer to the inner channel. Although computing the coefficients in a burnup-dependent recirculation scheme such as this is rather more complicated than in the other core types, all of the coefficients can be easily computed from the basic core parameters of power, fuel content in the pebbles, discharge burnup, flow velocity, core height and radius, and loading tube flow rates.

Results

Figure 2 illustrates the results of PEBBED calculations for the nominal PBMR (with graphite pebbles) and the same core with the OUT-IN fuel cycle described above. No attempt was made to optimize either core for a particular characteristic. Rather, the flow rate of the OUT-IN core was adjusted so that the high-burnup inner region was the same size as the graphite reflector region in the PBMR. This sets the transfer burnup threshold at about 62 MWD/kg_{hm} which is attained during the tenth pass through the core. Each pebble then circulates four times in the inner region.

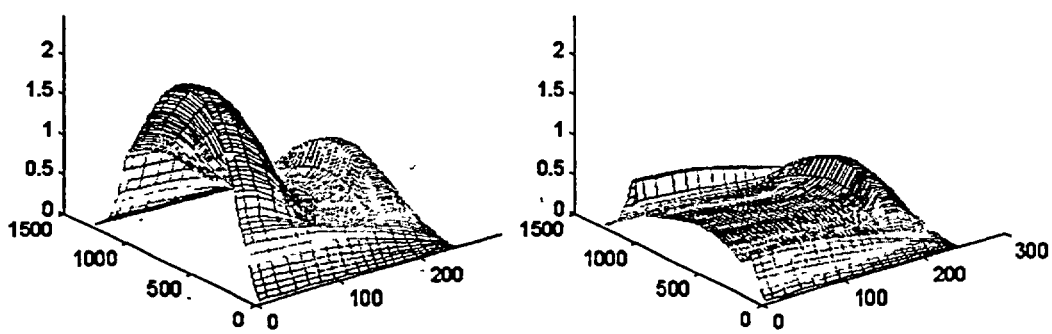

Figure 2. Thermal Flux in Nominal PBMR (left) and PBMR with OUT-IN Cycle (the origin corresponds to the top and center of the pebble bed)

The thermal flux peak in the graphite inner reflector clearly distinguishes the two cases. For the nominal PBMR, the peak fission power density is computed to be 5.57 W/cm^3. For the OUT-IN core, the peak fission power density is computed to be 4.78 W/cm^3. The lower peak power density was achieved at the expense of neutron economy. Compared to the nominal PBMR fuel enrichment of 8%, the OUT-IN core required an fresh pebble enrichment of 10% to maintain criticality.

Although an advanced optimization algorithm has yet to be added to the code, PEBBED has been used for some simple applications. In a study described elsewhere in these proceedings[6], the code was used to assess some of the proliferation characteristics of a pebble bed reactor. The ability to model and track pebbles of different types and trajectories was also exploited to develop a fuel testing and qualification plan for PBMR fuel at the INEEL[7]. Small quantities of fuel pebbles were restricted to specific flow channels to determine the extreme conditions and operating envelope of the fuel. Figure 3 shows the accumulated burnup and fluence for average pebble and for pebbles restricted to channels 3 and 5 (all fuel).

Conclusions and Further Work

The matrix formulation for coupling nuclide flow to neutronics in the PEBBED code provides an efficient method for accurately modeling all types of pebble bed cores and for performing advanced core design and fuel management. This work reveals how generalized flow coefficients are derived from basic core parameters so that different pebble types and trajectories can be modeled with ease. With this tool, advanced techniques such as genetic algorithms can be applied to perform rapid, accurate, and comprehensive scoping studies and core optimization.

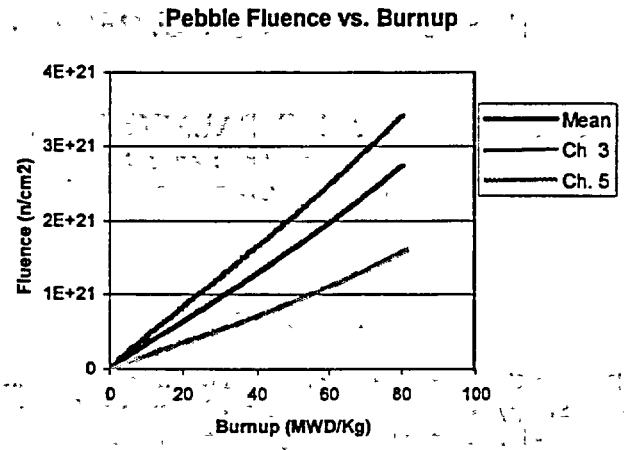

Figure 3. Fast Fluence vs. Burnup for PBMR Fuel

Currently, the code assumes that pebble flow is strictly axial. For an accurate model of the discharge conus region, the pebble flow grid must be decoupled from the diffusion grid and generalized to two or three dimensions. This is not anticipated to invalidate the matrix approach. Future work will also include the development of a three-dimensional nodal diffusion solver and the matrix formulation will be expanded to allow for azimuthal variation in pebble placement. Advanced cross-section generation and thermal feedback parameterization must also be incorporated to capture spectral and thermal effects. All of these improvements are part of the work scope of PEBBED development.

Acknowledgement

Work supported by the U.S. Department of Energy, Assistant Secretary for Environmental Management, under DOE Idaho Operations Office Contract DE-AC07-99ID13727.

References

[1] W.K. Terry, H. D. Gougar, and A. M. Ougouag, "Deterministic Method for Fuel Cycle Analysis in Pebble Bed Reactors", Transactions of the American Nuclear Society Winter Meeting, Washington, DC, November 2000.

[2] H. Frewer, W. Keller, and R. Pruschek, "The Modular High Temperature Reactor", Nuclear Science and Engineering: 90, pages 411-426, 1985.

[3] D. Nicholls, "The Pebble-bed Modular Reactor," *Nuclear News*, American Nuclear Society, Lagrange Park, IL, Vol. 44, Number 10, September 2001.

[4] J. de Haas, J. Kuijper, and J. Oppe, "PBMR: Evaluation of the Equilibrium Core Enrichment", 3rd Meeting of the IAEA CRP-5, Oarai, Japan, March 2001.

[5] W. Gießer, H. Jung, and L. Massimo, "Fuel Management Methods for Pebble-bed Reactors and their Applications to the AVR", Atomkernenergie, Vol. 14. No. 10, pp. 43-46, 1969.

[6] A. M. Ougouag, W. K. Terry, and H. D. Gougar, "Examination of the Potential for Diversion or Clandestine Dual use of a Pebble-Bed Reactor to Produce Plutonium," Proceedings of the HTR 2002 – 1st International Topical Meeting, Petten, Netherlands, April 22-24, 2002.

[7] W. K. Terry, Editor, "Modular Pebble-Bed Reactor Project – FY2001 Annual Report", INEEL/EXT-2001-1623, Idaho National Engineering and Environmental Laboratory, December 2001.

PHYSICS STUDIES FOR A PARTICLE-BED GAS COOLED FAST REACTOR CORE DESIGN

T. A. TAIWO, M. FATONE, G. PALMIOTTI, and R. N. HILL
Reactor Analysis and Engineering Division
Argonne National Laboratory, Argonne, IL 60439, USA

ABSTRACT

A Particle-Bed Gas-Cooled Fast Reactor (PB-GCFR) proposed and funded under the U.S. Department of Energy Nuclear Energy Research Initiative (USDOE NERI) Program is discussed, along with the preliminary physics results that have been obtained for a reference compact core (~50 W/cc) based on the pebble-bed system. Parametric studies are performed using homogeneous-cell and full-core physics models to investigate the impact of different fuel forms, pebble matrix material, temperature, fuel packing fraction, and core reflector material and dimension on the PB-GCFR design. One goal of this study is to assess the potential for a long-lived 300 MWt core design with a high conversion ratio that could sustain a cycle length of 15 to 30 years. The results of this study indicated that new fuel forms have to be considered in order to achieve a compact core design because the standard pebble-bed design has a significant material porosity that limits the core fuel volume fraction.

1. Introduction

The USDOE-sponsored NERI project on a Particle-Bed Gas-Cooled Fast Reactor (PB-GCFR) design will study different fuel forms and type, in order to meet the Generation-IV-systems goals of improved safety, enhanced proliferation resistance, nuclear waste minimization, and reduced system cost. The key innovation of this project is the application of a fast neutron spectrum environment to enhance both the passive safety and transmutation characteristics of the advanced particle-bed and pebble-bed reactor designs. The core design would meet the future needs of the nuclear industry, by being passively safe with reduced need for engineered safety systems. One of the major issues arising from previous gas-cooled fast reactor designs is the poor heat removal property of the helium coolant at low pressure. This issue was previously addressed by the use of highly reliable redundant coolant circulators. Passive-safety-in-the-design is however a major goal of this project. The ability to remove decay heat through conduction pathways, mainly, for station blackout and depressurization conditions and the capacity to tolerate failure to scram without reaching core disruption will be the focus of the design. The PB-GCFR design is supported by a long-life core concept that is refueled infrequently and hence reduces the potential for fuel diversion. The application of a fast neutron spectrum environment makes this design feasible since it permits compact core designs and fuel burnup characteristics that reduce the burnup reactivity control requirements. A low burnup reactivity swing also implies a low control rod worth requirement, which aids passive safety. The high neutron fluence inherent in the fast spectrum design coupled with the high operating temperature (for high efficiency) however provides challenges that have to be resolved. This would necessitate the investigation of materials that can withstand the high temperature and flux environments of the system.

As a basis for quantifying the performance trade-off associated with long lifetime cores, a reference compact fast-spectrum core based on the pebble-bed system is being developed. This core is designed for a power rating of ~300 MWt (about 50 W/cc) and has no blanket zone, in order to make it unattractive for proliferation. Also for proliferation reasons, it is assumed that the fuel type would be based on the transuranics (TRU) component of spent nuclear fuel that has been extracted by a separation process. The rational in this scenario, is that by making use of the transuranics (Pu, Np,

Am, Cm, and higher actinides), the heavy metal in the spent fuel could be consumed and become unavailable in a repository that could be construed as a plutonium mine. For comparison purposes, however, cores using reactor-grade and weapons-grade plutonium, as well as enriched uranium, were also evaluated.

2. Fuel Pebble Design and Dimensions

The pebble fuel type typically consists of a spherical container (pebble) made of matrix material that contains a central zone of coated or particulate fuel dispersed in the matrix material. Since the graphite used as matrix material in the PBMR design [1] would not be appropriate for the fast concept, because of its strong neutron moderating properties, alternative matrix materials were used in this study. The requirements for high operating temperatures that give a high thermal efficiency (45-50%) necessitated the use of refractory metals and high melting point materials having favorable fast neutron properties (e.g., low absorption cross section). Matrix materials that have been considered in this study include vanadium (V), titanium (Ti), titanium-nitride (TiN) enriched to 99.9% in N-15, and zirconium carbide (ZrC).

Physics studies have been performed for two different particulate fuel designs. The first design uses coated fuel particles dispersed in a matrix. This design has a central fuel kernel and two coating layers typical of one of the fuel types employed in gas-cooled thermal systems. The first layer, called the buffer, is made of low-density graphite, and performs two vital functions. This layer protects the outer layer against fission product recoil bombardment effects. It also provides a free volume through its internal porosity and, by irradiation-induced shrinkage, permits kernel swelling and minimizes fission gas pressure. The outer layer is made of SiC. This layer functions as the pressure vessel and acts as barrier for solid fission product diffusion. Calculations presented in this paper were done with a fuel kernel diameter of 800 μm, a buffer thickness of 30 μm and a SiC layer thickness of 70 μm. These low layer thicknesses were used to get a higher fuel kernel volume fraction in the particle, compared to PBMR designs. For this case, the fuel volume fraction in a given particle is ~0.5. Optimization of the coated particle dimensions will depend on fuel performance and would be investigated later in the project. The other design is for a fuel particle with same matrix and coating material (or uncoated). This design permits a core fuel volume fraction of up to ~30% which ensures a sustained critical mode operation for a 15-30 years fuel irradiation cycle. Currently we have used potentially compatible fuel and matrix forms for this fuel type, e.g., carbide fuel in a zirconium carbide matrix and nitride fuel in a titanium nitride matrix. Additional fuels material work is however required to ensure that these are feasible fuel-matrix forms in the irradiation and temperature fields of the PB-GCFR.

The pebble employed in this study has an outer radius of 6 cm. A dispersion fuel zone diameter of 5.5 cm was used in the study (compare to 5 cm for PBMR), in order to increase the fuel loading in the pebble. The pebbles are packed into a cylindrical core and are assumed to occupy 61% of the volume. Helium gas flows through the pebble-bed to remove the heat generated by the fission process. The helium coolant, being neutronically benign (i.e., low neutron absorption), does not adversely affect the fraction of neutrons available for converting fertile nuclides to fissile nuclides. Thus, reactivity losses can be effectively compensated by the inclusion of fertile material, which tends to reduce the enrichment and excess reactivity requirements of long-lived systems.

The requirement of a long life design necessitates a fuel converter core in which sufficient fissile material is charged and produced for the duration of the long cycle, in order to reduce the cycle excess reactivity requirements. A uranium-transuranics (U-TRU) based fissile fuel system was considered in the current study. Depleted or natural uranium fertile constituent is also employed. In this fuel form, the fertile U-238 is converted to fissile material that is used to sustain the long life core. Additionally, for comparison, uranium-plutonium (U-Pu) fuel was also considered with the Pu being reactor-grade or weapons-grade. Because of the fast spectrum, it is anticipated that the discharge isotopic vector would be similar to the charge vector, and so the irradiated fuel could be reprocessed to recover the TRU that could additionally be used in other fuel irradiation cycles, hence sustaining the nuclear fuel cycle.

The fuel forms considered in this study included mixed transuranics (TRU) and uranium oxide [(U,TRU)O1.7], carbide [(U,TRU)C, UC, TRUC, PuC] and nitride [(U,TRU)N, (U,Pu)N] fuels, with different TRU isotopics (LWR-discharge and weapons-grade). The weapons-grade constituents and carbide or nitride fuel forms were employed to boost the core neutron multiplication factor (k-eff). Previous work has shown that carbide fuels offer significant economic and doubling time advantages over oxide fuel, as a result of its better neutron economy.[2] The carbide fuel also has a superior thermal conductivity than oxide fuel and hence allows operation at a higher linear power. The fuel also has a significant economic advantage over nitride fuel because of its better neutron economy. The behavior of carbides under fast neutron fluence can be problematic, however. Nitride fuels have several advantages such as heavy metal density (larger than oxides) and a better thermal conductivity. However, there is only a limited knowledge about their properties, in particular regarding their stability at high temperatures. Moreover the production of the radioactive isotope C-14 (unless enrichment in N-15 is performed) is another negative feature. The advantages of oxide fuel are that they are very well known and have a good tolerance to radiation and fission, and also a good capacity for relatively high burnup and temperature.

3.0 Reactor Physics Analysis Methodology

The reactor physics calculations reported here have been done with the ERANOS (European Reactor Analysis and Operation System) code [3]. In this study, the ECCO module is used for generating 33-broad group cross-section data for actual material composition and temperature. The multigroup cross-section library contained in the ECCO code is based on the JEF2.2 nuclear data library. The 33-group cross sections are used in a finite-difference transport and diffusion theory module (BISTRO) for core calculations.

The current model for the coated fuel particles in a matrix assumes that the fuel pebble can be homogenized into a single region. Previous calculations performed for the thermal PBMR and GT-MHR systems suggest that a rigorous and explicit treatment of the double heterogeneity be performed to get an accurate multiplication factor (k-inf) for each of the systems. Those calculations indicated that simply homogenizing pebble regions results in an underprediction of the k-inf by as much as 8-14%. These mispredictions arise because the smeared models inadequately represent the resonance self-shielding of the fuel kernel, and result in higher resonance cross sections (primarily U-238) compared to explicit models. From physics considerations, it is expected that such simple homogenization models should be able to adequately treat the double heterogeneity effect in the fast system that is of interest in this project. This is because the resonance region's (4 to 9000 eV) contribution to the k-inf is small in such systems. Preliminary evaluation of this effect seems to confirm this trend. However it is additionally planned to perform a more rigorous investigation of this issue in the future using an MCNP model as reference. Small differences in the k-inf are however expected.

4. Results of Unit Pebble and Whole-Core Parametric Studies

Preliminary calculations have been performed to provide an indication of the impact of pebble packing fraction on the multiplication factor (k-inf). This issue is considered important because in the thermal PBMR system, the k-inf does not vary linearly with fuel particle packing fraction in the nominal range. Two core depletion cases using pebble packing fractions of 0.70 and 0.61, respectively, have been performed for the PB-GCFR design. Typically observed values for the packing fraction of fuel pebbles in a pebble-bed reactor are about 0.60-0.65. A decrease in the pebble packing fraction from 0.7 to 0.61 results in a decrease of 2%Δk in the multiplication factor of the initial state. Additional calculations utilizing lower pebble packing fractions similarly show monotonically lower multiplication factors. Parametric studies on material temperature indicated that the PB-GCFR would have a negative temperature coefficient. Material temperatures of 800 and 1000 K were used in the study. The temperature value of 1000 K is used to represent the average fuel and matrix temperature being proposed for the PBMR (~1040 K for fuel and ~970 K for graphite).

The impact of power density on the core physics performance was also evaluated. Passive safety is usually enhanced by low power density, since a large surface area is available for heat removal. The low power density of the PBMR core is one of its advantages in achieving a passively safe system. However, the anticipated "exotic" materials and high heavy-metal loading required for fast-spectrum designs necessitate a reduced core volume. A reduced core volume would also give economic benefits, provided it does not adversely impact the system pumping requirements and the passive safety in design that could result in the need for expensive backup/redundant systems. For these reasons, the targeted power density of the PB-GCRF is about 50 W/cc, which would be about one order of magnitude greater than that in thermal gas cooled-systems and a factor of two lower than that for thermal LWRs. For an ortho-cylindrical core and total power of 300 MWt this power density implies an active core height and diameter of ~2 meters. If system-cooling costs/penalties become prohibitive, this power density would be reduced. As would be expected however, for a given irradiation time, a higher power density implies a higher flux level and material depletion (burnup). This results in a lower k-inf value at the end of irradiation, compared to a lower power density case that gives a longer cycle length at a sustained critical core operation. Additionally, a low power density results in a large core size (which reduces the core neutron leakage), a high total material loading, and a flat reactivity letdown with burnup. The system cost which increases with core size could limit the core size. The trade-off of rated power density on system passive safety, feasibility of a long-lived core, and system cost, is yet to be evaluated.

A detailed evaluation of fuel and structural materials applicable to the higher temperature and irradiation fields expected in the PB-GCFR design has not been completed. However, parametric studies have been done to investigate the impacts of fuel, matrix and reflector materials on the potential for obtaining a sustainable critical core for a long life design. The results have provided indications that titanium is desirable as matrix material because of its low absorption of neutrons. The lower melting temperature of titanium, compared to TiN and ZrC might negate this advantage however. The performance behaviors with vanadium and zirconium-carbide as matrix materials are fairly similar. Application of TiN-15 results in the highest matrix absorption; when compared to Ti, TiN-15 has a higher material density. The desirable fuel material is [TRU,U]N because it results in the highest multiplication factor and gives a slightly better conversion ratio than carbide fuel. Enrichment considerations might however make carbide fuel the preferred choice. The application of both enriched uranium and weapons grade constituents of the fuel has been discarded in our current outlook, because of the potential proliferation issues that could arise by the use of these fuel forms and because they generally result in a higher reactivity swing than TRU fuel. Reflector studies indicated that for the same reflector thickness, graphite reflector competes favorably with beryllium and beryllium-oxide, nickel, and stainless steel (SS-316). Additionally it appears that graphite is also acceptable because the resulting core-average neutron spectrum is still a fast spectrum (median energy greater than 125 KeV). Graphite however has the disadvantage that it results in undesirable power peaking at the core reflector interface, and has a negative impact on the conversion ratio when compared to SS-316 and other reflector materials.

The preliminary assessment of a PB-GCFR core indicated that the goal of a long-life core (with conversion ratio greater than one) requires a fuel volume fraction larger than employed in present High Temperature Reactor (HTR) designs. The original coated fuel particle in pebble design used in this study results in a core fuel volume fraction of 15%. Preliminary investigations indicated that a higher core fuel volume fraction (~30%) or core size (power density less than 25 W/cc) is required to get the desired sustainable design with a high conversion factor. Achieving a high fuel volume fraction would require a redesign of the coated fuel particles, as it implies that the low-density carbon buffer and SiC zones be replaced with fuel to get the higher fuel volume fraction. Calculations made under this assumption, using [TRU,U]N in TiN-15 matrix or [TRU,U]C in ZrC matrix, indicated that a high conversion ratio (greater than 1.2) can be obtained with low reactivity losses over the 15 to 30 years of irradiation with a capacity factor of 0.91 (see Fig. 1). These finding therefore suggest that the developments of materials in layers, or possibly in compacts, must trend toward a minimization of their volume without losing their ability for high temperature confinement.

5. Conclusions and Future Work

Calculations in support of a reference compact fast-spectrum core based on the pebble-bed design have been performed in this work. These calculations were done with the ERANOS code models that have undergone moderate verification and therefore, additional verification is planned. Parametric studies were done to investigate the impacts of fuel-pebble packing fraction, fuel material form and temperature on the potential for obtaining a sustainable critical core for a long-lived design. Different fuel matrix and reflector materials were also investigated. The results have provided indications that titanium is desirable as matrix material, though it might be discarded because of its relatively low melting point. The desirable fuel material is nitride fuel enriched in N-15 to almost 100%. Enrichment considerations might however make carbide fuel the preferred choice. Reflector studies indicated that for the same reflector thickness, graphite reflector competes favorably with beryllium and beryllium-oxide, nickel, and stainless steel, although other considerations (conversion ratio) might preclude its use. By employing a core fuel volume of about 30%, it is possible to obtain a neutronically sustainable long life core with a core life of 15 to 30 years and operating at a power density of 50 W/cc.

6. References

[1] "Review of the Pebble Bed Modular Reactor (PBMR) Plant", in Current Status and Future Development of Modular High Temperature Gas-Cooled Reactor Technology, IAEA-TECDOC 2000-08-21 (Electronic Version), IAEA 2000.

[2] S. A. Capersson, et al., "Economic and Nuclear Performance Characteristics of 500-MWe Oxide, Carbide and Nitride LMFBRs," ANS Topical Meeting Advanced Rectors: Physics, Design and Economics, September 8-11, 1974.

[3] G. Palmiotti, et al., "New Method Developments and Rationalization of Tools for LMFBR Design in the Frame of the European Collaboration," Proc. Int. Conf. Fast Reactors and Related Fuel Cycles, Kyoto, Japan, October 28-November 1, 1991.

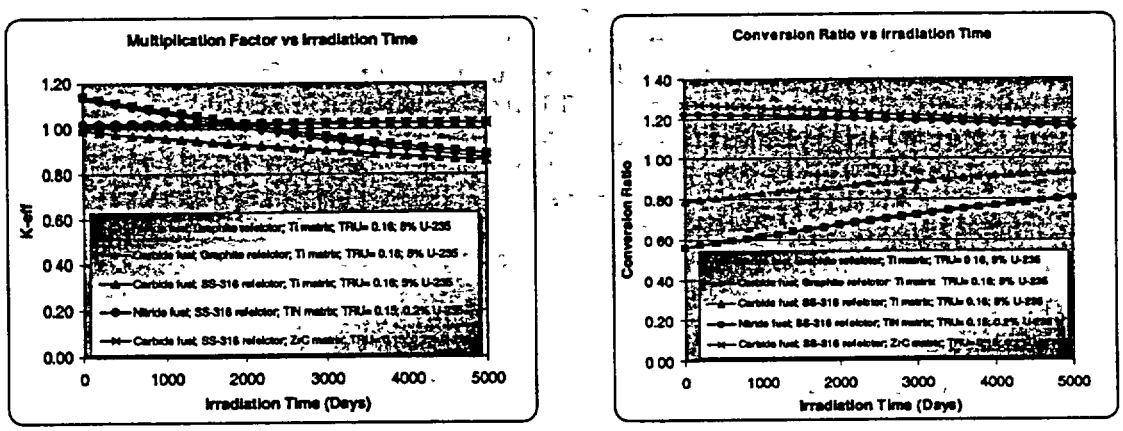

Fig 1. Multiplication factor and conversion ratio as function of irradiation time for PB-GCFR designs.

MODELS FOR NEUTRONICS CALCULATIONS FOR HTR PEBBLE BED MODULAR REACTORS

W. Bernnat and W. Feltes, University of Stuttgart, Germany

Paper will be handed out separately

AN EVALUATION OF THE CONTROL ROD MODELLING APPROACH USED IN VSOP BY COMPARING ITS RESULTS TO THE EXPERIMENTS PERFORMED IN THE ASTRA CRITICAL FACILITY

F. REITSMA, D. NAIDOO and Z. KARRIEM
Radiation and Reactor Theory
NECSA, Pelindaba, PO BOX 582, 0001 PRETORIA, South Africa

ABSTRACT

The modelling of strong absorber regions in diffusion theory is a well-known problem and many methods have been developed to accommodate the transport effects in diffusion theory. In this work the method of equivalent cross sections is evaluated for the ASTRA critical facility at the Russian Research Centre – Kurchatov Institute in Moscow. The measured reactivity worths of the control rods situated in the side reflector, are compared with the calculated values making use of equivalent diffusion parameters in VSOP. Favourable results were obtained for the control rods positioned within the first ring of reflector blocks with larger errors obtained for control rods positioned further from the core. Furthermore, the use of an equivalent boron concentration to represent the absorber regions was also investigated and shown to be useful if applied correctly and with care. However, the practical difficulties and restrictions imposed by the two approaches make the investigation of an alternative method, which should remove these shortcomings, attractive.

1. Introduction

Experiments performed in the ASTRA facility at the Russian Research Centre – Kurchatov Institute in Moscow [1] have specifically been defined to simulate the characteristics of the Pebble Bed Modular Reactor (PBMR) design. The most important of these is the presence of the central column or inner reflector region that contains only graphite spheres. This increases the neutron leakage into the side reflector with the benefit of increased reactivity worth of the control rods that are situated within the side reflector. A detailed description of the facility is included in Section 2.

The deficiencies of diffusion theory to model highly absorbing regions are well known and a lot of work has been performed to calculate the so-called equivalent diffusion parameters. In the PBMR design and also in the ASTRA critical facility, the positioning of these highly absorbing regions in the side reflector, where the leakage out of the core adds a directional dependence to the flux, further complicates the problem. Despite these problems, reasonable results have been reported using the Method of Equivalence Cross Sections [2, 3] that is based on the principle of combining transport and diffusion methods to calculate adjusted diffusion coefficients.

VSOP (Very Superior Old Programs) [4,5] is used as the main design tool for the PBMR core and makes use of the finite difference diffusion code CITATION as its flux solver. The validation of the code and specifically its accuracy in control and shutdown margin calculations are of particular interest. The use of ASTRA as a tool for code validation, but also in particular to evaluate the control rod modelling approach, is therefore valuable. In this work the control rod models used in VSOP calculations at PBMR Pty Ltd are evaluated by comparing the calculated control rod worth to the measurements made on the ASTRA facility. In some cases geometrical approximations are quantified by comparisons with MCNP [6] calculations.

A short description of the ASTRA models employed and the required approximations are given in Section 3. The detail of the control rod models used and some of the difficulties are discussed in Section 4, with the control rod worth comparison with results included in Section 5. This is followed by the conclusions and future work.

2. The ASTRA critical facility

The ASTRA facility represents an upright graphite cylinder (the side reflector) with an octagon shaped core. Figure 1 shows a schematic view of the critical assembly cross-section as well as the longitudinal section. The outer reflector diameter is 380 cm while the core equivalent diameter is 181 cm. The core contains fuel, graphite and absorber spheres, all having a 6 cm diameter. The core is divided into three zones. The inner reflector zone, filled only with graphite spheres, has an outer diameter of 72.5 cm and is surrounded by the mixing zone with a thickness of 16.5 cm. The fuel only zone surrounds the mixing zone.

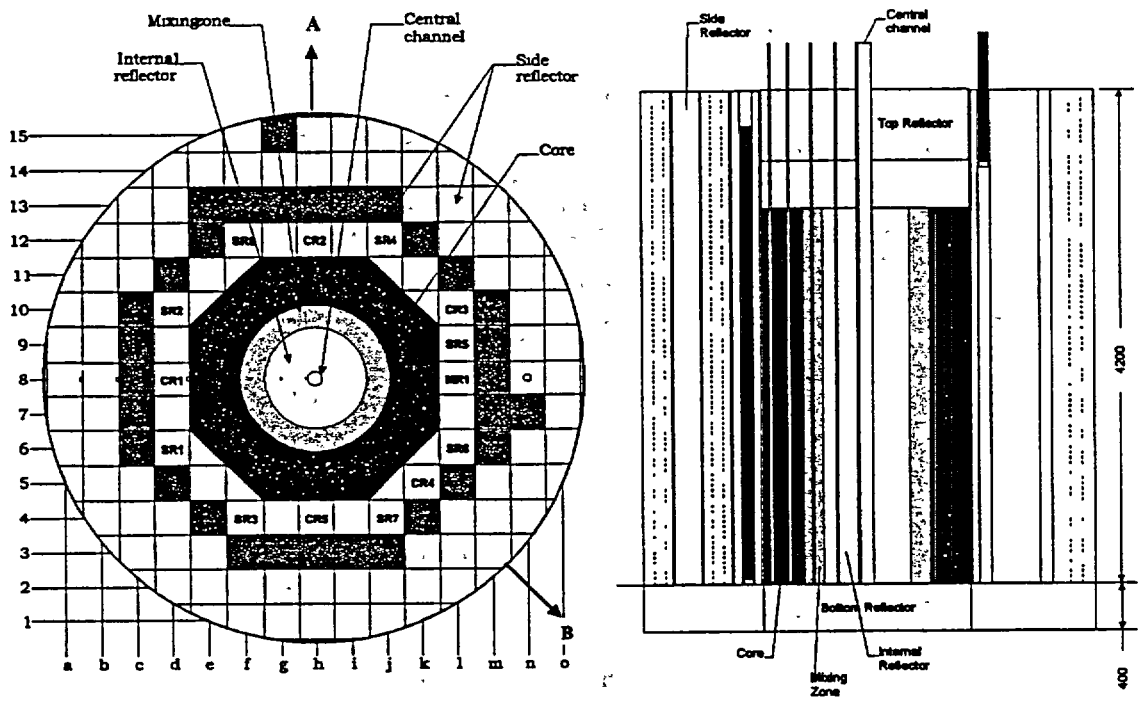

Figure 1 Radial and axial representation of the ASTRA critical facility

The fuel design is similar to that of the PBMR with UO2 fuel kernels that are encased in carbon and silicon based coatings. These fuel particles are uniformly distributed in a graphite matrix. The main difference is that the fuel spheres contains 2.44 g of uranium that is about 21% enriched in comparison to the 9 g uranium of about 8% enrichment considered in the PBMR design. In an effort to simulate the PBMR spectrum in ASTRA, absorber spheres, which contain 0.1 g of boron in the form of uniformly distributed 60 μm boron-carbide particles, were added in the ratio 5 : 95 to regions containing fuel.

The mixing zone contains a mixture of fuel, absorber and graphite spheres in the ratio 47.5 : 2.5 : 50. The fuel only zone contains only fuel and absorber spheres in the ratio 47.5 : 2.5. A random mixture was obtained by mixing the appropriate quantities beforehand, and then loading it by hand in the appropriate region. A packing ratio of 0.625 was measured and assumed throughout. The shutdown rods (SR) and control rods (CR) are positioned in the side reflector as shown.

3. ASTRA core models

ASTRA facility calculational models were created for MCNP and VSOP. The MCNP model contains as much geometrical detail as possible. This includes the holes in the side reflector and the detailed control rod design. In the core the different pebbles were also modelled in detail, for example, the coated particles with its three coatings are modelled explicitly. Details of the fuel model in MCNP and the ASTRA initial criticality MCNP results can be found in reference [7].

A cylindrical coordinate system was selected for the VSOP ASTRA model with the result that a cylindrical core, with an equivalent outer diameter of 181 cm, was defined to approximate the octagonal outer boundary of the core region. The effect of the approximation was quantified with the use of two MCNP calculations (a homogenised core representation without any control and which conserve masses were used) where the geometrical effect on k-eff was shown to be relatively small (~100 pcm). However, the cylindrical core approximation also leads to a further complication in the positioning of the control rods. The rods can no longer be positioned at their physical positions, but were placed such that the distance from the control to the core-edge was preserved. It has not been verified if the geometrical effect would be similar for cases where the rods are inserted.

4. Method of Equivalent Cross Sections and the control rod model

Diffusion methods are generally not valid inside or in the vicinity of regions of strong absorbers. To overcome these problems combined transport-diffusion methods have been developed. One of these, the Method of Equivalent Cross Sections (MECS), has been applied with success in some HTR applications [2,3]. The principle is to model the absorber and its environment in transport theory (S-N) and then extract cross sections and diffusion parameters from the transport solution that will represent the absorber region accurately in subsequent 3-D diffusion calculations. In this paper MECS was applied to the ASTRA control rods and the obtained equivalent diffusion parameters evaluated in full-core VSOP reactivity calculations.

The steps followed in MECS and in this work can be summarised as follow:

- perform a 1-D cylindrical unit cell transport calculation for a heterogeneous control rod model (fine-group, fine spatial discretization, S-8/P-3)
- calculate the few-group equivalent macroscopic cross sections and equivalent diffusion constants
- perform the 3-D ASTRA core calculations in VSOP in six groups making use of the equivalent macroscopic parameters in the absorber region.

The following characteristics of MECS and their practical implications are of importance in support of the arguments presented in this paper:

- the volume of the absorber region in the transport and diffusion calculation must be conserved
- equivalence is assumed between transport and diffusion theory at some point outside the absorber region surface
- the equivalent parameters are dependent on the diffusion code solution method
- the practical implication that the diffusion mesh size of the absorber region and its immediate neighbours are prescribed, and also, that these meshes may not be subdivided (no additional inner mesh points allowed).

These cause difficulties in practical applications as will be discussed as part of the results in Section 5.

Lets now consider the ASTRA control rods and the associated 1-D cell calculation. The control rods (CR) in the ASTRA critical facility are situated in the side reflector inside the axial channels (with a diameter of 11.4 cm) in the graphite blocks with positions as indicated in Figure 1. All these rods have the same configuration, consisting of 15 steel tubes, filled with natural boron carbide, arranged in a circle as shown in Figure 2a. Since a 1-D transport super-cell calculation is used as part of the process to determine equivalent diffusion parameters, the control rod was approximated as an annulus of boron carbide that is surrounded by steel (see Figure 2b). The midpoint of the absorber annulus was positioned at the 76 mm diameter and all material masses were conserved. In auxiliary MCNP calculations the validity of the smeared 1-D approximation of the ASTRA control assembly (the 15 absorber rods smeared into a ring) was evaluated. The approximate model over-predicted the total control rod worth of CR5 by 0.05$ (2%). Although this can be considered small, the 1-D ring model can be adjusted to reproduce the reference. This was left for future work.

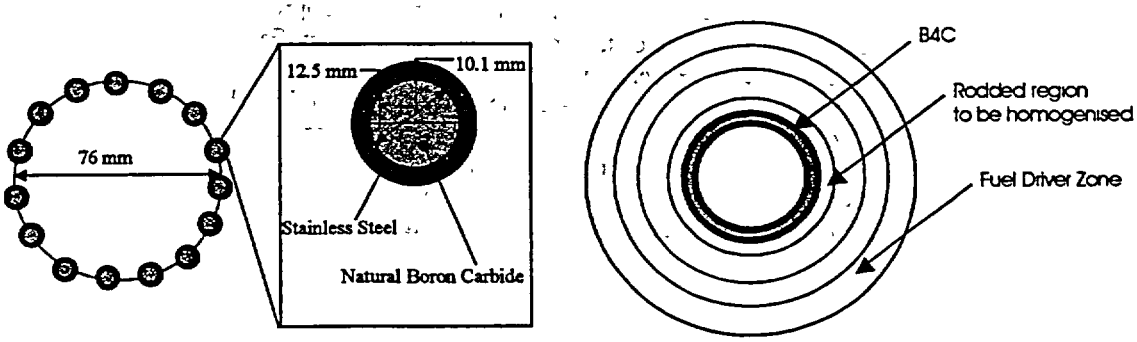

a b

Figure 2 Control rod configuration (a) and equivalent model used in the cell calculation (b)

The rest of the cylindrical super-cell was defined to represent the environment surrounding the control rod (void and graphite reflector block) with a fuel driver zone defined as the outer region. The area to be "homogenised" is defined as the rodded region and is selected to correspond with the volume of the mesh in the CITATION model where the equivalent diffusion parameters will be applied. In practice a mesh size of about 11.4 cm was used that is similar to the diameter of the channel accommodating the control rods. In order to satisfy the assumed equivalence between transport and diffusion theory at some point outside the absorber region surface, the sizes of the neighbouring meshes were found to be at least 6.4 cm.

The total distance of the three meshes (absorber region and two neighbours) is thus in the order of 24 cm. In the radial direction these three meshes are defined for the total angular space and therefore prevent the accurate modelling of any other control rods that are at a different distance from the core and who's meshes overlap that of the first control rod. This limits the usability of MECS for the ASTRA facility.

5. Results and discussion

The control rod worths were calculated by performing k-eff calculations in VSOP for the cases with control totally inserted and totally extracted. The convergence in CITATION was set to be 1pcm in k-eff and 0.0001 for the flux. In all cases the reactivity for each control rod is given in dollars where the experimentally measured β of 0.0072 [8] was assumed.

In Table 1 the reactivity worth of individual control rods are given for both the measured and the VSOP calculation making use of MECS. In each case the shortest distance from the core edge to the centre of the control rod or equivalent rod region is also given.

Table 1 Reactivity worth of individual control rods represented by MECS

CR and block position	Distance from core (cm)	Measured [$]	VSOP [$] (MECS)	% difference
CR5 h4	12.5	-2.53	-2.40	-5.2%
CR2 h12	12.5	-2.55	-2.39	-6.2%
CR1 d8	13.0	-2.46	-2.33	-5.2%
CR4 k5	17.7	-1.95	-1.95	0.2%
CR2 h13	37.5	-0.88	-0.75	-15.2%
CR2 h14	62.5	-0.22	-0.20	-11.2%
CR2 h15	87.5	-0.03	-0.022	-26.7%

The calculated results compare favourably with the measured values for the control rods positioned in the closest reflector positions (results above the line). For the three rods positioned closest to the core, the reactivity worths are all under-predicted and lie within a small band (0.6%) around –5.7%. For CR4, positioned an additional 5cm away from the core, the predicted worth falls within the quoted experimental uncertainty of ± 2.5% [8]. When the results for increasing distances are considered (results below the line), the differences are generally larger and increased significantly to -26.7% as the control is moved to the outermost rod position. At larger distances from the core the error made by diffusion theory is expected to increase. Note that in the last case (h15) the absorber region was positioned so close to the VSOP outer boundary that the mesh size, prescribed by MECS could not be satisfied. The discrepancy seen in the result of CR4 / k5 can also possibly be attributed to the presence of the two shutdown rod positions in close proximity to the control rod and the approximation used to account for the streaming effects in these two void areas. This will be investigated further in future.

Although the results with MECS are very promising it should be noted that for each core-to-control distance, a separate model with radial diffusion meshes corresponding to the distances of concern, was used. As explained in Section 4, this presents a dilemma if multi-rod reactivity worth calculations are to be performed, since the diffusion meshes required to accurately represent the individual control rods will overlap. In most HTR designs and also in the current PBMR design, all the control and shutdown system positions can be accommodated within a single set of radial meshes so that MECS is applicable.

Since the manual input option is used to introduce the equivalent cross sections in VSOP, the stepping out of the control rods can only be performed with the help of restart calculations (one required for each control rod step). This adds a practical difficulty in using MECS for incremental control rod VSOP calculations. Therefore, the equivalent cross sections are often replaced by an Equivalent Boron Concentration (EBC) smeared throughout the control rod region. In this case the rod movement can be defined in a single VSOP run and no restarts are required. The EBC is obtained by adjusting the absorber region boron concentration in the diffusion calculation until the control rod worth obtained from MECS is conserved. Although this approach will always conserve the MECS case's reactivity worth (by definition), it does not conserve the flux distribution and reaction rates in the absorber region. Also the EBC for each assembly position should, in principle, be calculated separately, especially if they are positioned at varying distances from the core. This is illustrated below.

A single EBC was determined to conserve the experimentally obtained worth of CR2 in position h12. The control rod was then moved away from the core to positions h13, h14 and h15. In the VSOP model the same EBC was then used to represent the rod when moved to the other positions further from the core edge, as indicated in Table 2. The calculated VSOP results are compared to measurements.

Table 2 Reactivity worth of CR5 at different positions represented by a single EBC.

Block position (see Figure 1)	Distance from core (cm)	Measured [$]	VSOP [$] Boron equivalent	% difference
h13	37.5	-0.88	-0.77	-12.1 %
h14	62.5	-0.22	-0.19	-14.1 %
h15	87.5	-0.03	-0.008	-72.5 %

It is immediately apparent that the calculated boron concentration can not be applied to other control regions. A similar effect was seen when control rod CR4 was moved from position k5 to l4. A possible reason is that the diffusion error increases for increased distances from the core. Also, the calculated boron concentration corrects the diffusion calculation for transport and self-shielding effects. These can be expected to be different for each control position, especially when positioned further away from the core. The use of a single set of EBC for control rods of the same design and at equal distances from the core, should however be acceptable.

As a last example, the combined reactivity worth of several combinations of rods inserted in ASTRA was compared with the measured result. In this case the EBC for each control rod was determined and

applied in the VSOP calculations. The differences shown in Table 3 are therefore due to the combined control rod effects, also called the interference effects. The results obtained are satisfactory and we conclude that the EBC method can be used to represent the reactivity effects of control rods, provided that an EBC is calculated for each "type" of control rod (in the sense of design or placement in the core).

Table 3 Reactivity worth of combination of control rods each represented by its equivalent boron concentration

Control Rod Combination	Measured [$]	VSOP [$] Boron equivalent	% difference
CR1 + CR5	-5.16	-5.12	-0.9%
CR2 + CR5	-5.57	-5.53	-0.7%
CR4 + CR5	-4.31	-4.34	0.8%
CR1 + CR2 + CR5	-8.42	-8.43	0.1%
CR1 + CR4 + CR5	-7.15	-7.31	2.2%
CR2 + CR4 + CR5	-7.57	-7.76	2.5%

6. Conclusions and future work

The Method of Equivalent Cross Sections (MECS) applied for a single control rod positioned close to the core yields acceptable results (within 6.2%). This compares favourably with the typical errors reported in literature [3]. In this reference a 5% difference in absorber reactivities was reported for MECS applied to a realistic HTR design. A core with a diameter of 280 cm and control rods positioned about 15cm from the core was considered. Since the ASTRA facility is smaller (diameter of 181 cm) the slightly larger errors could be expected.

The MECS has the restriction that only a single inner mesh point in the absorber diffusion mesh can be specified. This restriction prevents the accurate modelling of the combined effects of ASTRA control rods, positioned at different core-to-control distances. This is due to the overlap in the individual control rod radial meshes. Although the method can theoretically be extended to allow more inner mesh points, this adds difficulties to the analytic expressions used in the determination of appropriate diffusion constants.

The use of Equivalent boron Concentration (EBC) was shown to be a valuable practical tool in calculating control rod worths, provided that the reference rod worth is known. This can be calculated by MECS (for individual rods) or by any other reference calculation (for example MCNP). It performed well when the control rod interferences or combinations of control rod movements were studied. Since the method does not conserve reaction rates or the flux distribution, it should be used with care.

In the current PBMR design, where all control and shutdown channels are equidistant from the core, both the MECS and EBC should be valuable tools in estimating the rod worths. The restrictions of MECS, although they do not present an immediate problem, may influence the diffusion model negatively when mesh refinement may be required by external factors or if the equal distance approach may be discarded in future designs.

Since the control rods are positioned in cylindrical channels in the side reflector the neutron flux has some gradient in these regions. This will lead to effects of asymmetry that were not taken into account. These effects should be quantified and the possibility to investigate new methods, based on MECS, could perhaps be of value. Finally, the availability of MCNP to perform benchmark calculations must be seen as an essential part of any control rod worth evaluation.

7. Acknowledgement

The authors would like to thank PBMR Pty Ltd for their financial support and permission to publish this work.

8. References

[1] V. P. Garin et al, "Stage A-1.1.1 Technical Description of the ASTRA Facility and the Conclusion from the Evaluation of Possibility to Carry out Experiments on it", PBMR internal report, RRC KI, Moscow, 1999.

[2] W. Scherer and H.J. Neef, "Determination of Equivalent Cross sections for Representation of Control Rod Regions in Diffusion Calculations", Jül 1311, 1976.

[3] V. Fen, M. Lebedev, V. Sarytchev and W. Scherer "Modelling of Neutron Absorbers in High Temperature Reactors by Combined Transport-Diffusion Methods", Jül 2573, 1992.

[4] E. Teuchert *et al.*, "V.S.O.P. ('94) Computer Code System for Reactor Physics and Fuel Cycle Simulation, Input Manual and Comments," Jül 2897, 1994.

[5] W. R Joubert, "PBMR VSOP: Verification of Differences Relative to VSOP ('94)" PBMR internal report 8814-325 Rev 1, 2001.

[6] Judith F. Briesmeister, Editor, "MCNP™ – A General Monte Carlo N-Particle Transport Code, Los Alamos National Laboratory", Report LA-12625-M, Version 4B2 (March 1997).

[7] Z. Karriem, C.C.Stoker and F. Reitsma. "MCNP Modelling of HTGR Pebble-Type Fuel", Proceedings of MC2000 conference, Portugal, October 2000.

[8] V.P. Garin, E.S. Glushkov, V.E. Demin, A.A. Zimin, G.V. Kompaniets, N.E. Kukharkin, V.A. Lobyntsev, P.V. Mikhailov, S.G. Nedorezov, V.I. Nosov, D.N. Poliakov, N.N. Ponomarev-Stepnoi, R. P. Petrushenko, E.N. Samarin, B.S. Stepennov and E.I. Chuniaev, "Stage A-1.2.3. Investigation of Critical Parameters with Varying Height of the Pebble Bed, Worth of Control Rods depending on their Position in the Side Reflector, and Differential Reactivity of the Control Rod depending on the Depth of its Insertion, with Calculational Analysis of Results obtained." PBMR Internal Report, RRC KI, Moscow, 2000.

CREATION OF THE EQUILIBRIUM CORE PBMR ORIGEN-S CROSS SECTION LIBRARY

C.C. STOKER, F. REITSMA and Z. KARRIEM
Radiation and Reactor Theory
NECSA, Pelindaba, PO Box 582, Pretoria, 0001, South Africa

ABSTRACT

As part of the design calculations for the Pebble Bed Modular Reactor (PBMR), fuel inventories, neutron and gamma sources and decay heat needs to be determined for the fuel spheres. Using the SCALE4.4 code system, a PBMR specific cross section library was created for the ORIGEN-S depletion calculations, assuming a 10-pass refueling system for the PBMR. In this paper the rationale for the creation of the PBMR library is evaluated in terms of the spectrum dependence due to burn-up. The ORIGEN-S PBMR library was further evaluated comparing the results for different parameters calculated with the reactor analysis diffusion code VSOP and the Monte Carlo code MCNP4C.

1. Introduction

The Pebble Bed Modular Reactor (PBMR) design applies a continuous reloading scheme where unloaded fuel spheres, which have not reached the target burn-up, are returned to the top of the core. For a so-called 10-pass equilibrium core this implies that the fuel spheres will circulate ten times, on average, through the core. In practice it means that fuel spheres at different burn-up surround any single fuel sphere. As part of the PBMR design calculations the fuel sphere inventories, neutron and gamma sources and decay heat needs to be determined as a function of burn-up. In order to solve the burn-up equations, spectrum averaged neutron interaction cross sections are required. However, due to the changes in the isotope concentrations with burn-up, the neutron spectrum, and thus the spectrum averaged cross sections, becomes burn-up dependent. Therefore, when creating a cross section library, the spectrum dependence due to burn-up needs to be determined.

The depletion and decay calculations for the PBMR design are performed using the ORIGEN-S module of the SCALE4.4 [1] code system. The reliability of the ORIGEN-S results depends mainly on the appropriateness of the neutron cross section library used for the calculations.

In Section 2 the rationale for the creation of the PBMR library is evaluated in terms of the spectrum dependence due to burn-up. Based on these conclusions a PBMR specific ORIGEN-S library has been created for a 1 dimensional PBMR model described in Section 3. The PBMR library was evaluated comparing the one energy group ORIGEN-S neutron interaction cross sections with the cross sections obtained from the reactor analysis diffusion code VSOP [2,3] and the Monte Carlo code MCNP4C [4,5]. In Section 4 comparisons are provided for the ORIGEN-S and VSOP depletion calculations. Section 5 contains the conclusions.

2. PBMR Library Generation Rationale

Within the traditional PWR fuel assembly reload methodology the ORIGEN-S cross section libraries are often created with the assumption that the neutron spectrum within the fuel assembly is dominated by the burn-up of the fuel assembly itself and that the specific burn-up of the surrounding assemblies are less important. However, with the small PBMR fuel spheres (assemblies) and the graphite moderation environment, the PWR approach might not be valid. While evaluating the PBMR 10-pass continuous reloading scheme, it became evident that the flux spectrum within a fuel sphere was mostly

determined by the burn-up of the surrounding spheres, while the burn-up of the fuel sphere itself only had a secondary effect on the spectrum.

In the 10-pass PBMR continuous reloading scheme a fuel sphere will on average reach its target burn-up (80 GWD/TU) after ten circulations. The average burn-up for the upper layer of fuel spheres is about 41 GWD/TU, ranging from zero up to about 74 GWD/TU burn-up. The average burn-up of the bottom fuel layer is about 49 GWD/TU. Thus, a fuel sphere burning over its life from zero up to 80 GWD/TU will always be surrounded by fuel spheres being at an average burn-up between 41 GWD/TU and 49 GWD/TU.

For the evaluation of the cross section spectrum dependence due to burn-up, a spherical reactor model was constructed consisting of a single fuel sphere in the center, surrounded by a 1 m fuel driver zone and a 1 m graphite reflector. Using the flux spectrum within the central fuel sphere, ORIGEN-S cross section libraries has been generated for the following cases:

REF The central fuel sphere and the driver fuel zone at equilibrium (45 GWD/TU) burn-up
A-1 The central fuel sphere at 0 GWD/TU surrounded by fuel spheres at 45 GWD/TU burn-up
A-2 The central fuel sphere at 80 GWD/TU surrounded by fuel spheres at 45 GWD/TU burn-up
B-1 The central fuel sphere at 45 GWD/TU surrounded by fuel spheres at 0 GWD/TU burn-up
B-2 The central fuel sphere at 45 GWD/TU surrounded by fuel spheres at 80 GWD/TU burn-up

All the SCALE calculations were performed in 238 energy groups using the 238-GROUP ENDF/B-V library from the SCALE system. All the isotopes treated explicitly in the VSOP calculation, and available in the SCALE 238-Group library, were specified. Additional fission product isotopes (with negligibly small atom densities) were also specified for the central fuel sphere to enable an update of the ORIGEN-S cross sections for these isotopes. These fission product isotopes were specified due to its importance with regard to the burn-up measurements. Using the 238 energy group flux spectrum, calculated for the central fuel sphere in the spherical reactor model, the isotopic cross sections were collapsed to the ORIGEN-S 3 energy group structure. The ORIGEN-S cross section library was then updated by replacing the original ORIGEN-S cross sections with the 3 group cross sections for all the isotopes specified in the single fuel sphere. The ORIGEN-S cross sections (the updated and not updated) were then collapsed to one energy group using the 3 group spectrum in the single fuel sphere.

Using the different ORIGEN-S libraries created for the central fuel sphere, the burn-up was performed for 874 days, irradiating at a thermal flux (<0.5 eV) of 6.3×10^{13} $n.cm^{-2}.s^{-1}$. However, for these relative comparisons the exact flux used for the ORIGEN-S burn-up calculation is not important. The activities and masses obtained for the reference ORIGEN-S library are tabulated in Table 1 for a selection of isotopes. The percentage differences with respect to the reference case (REF) are provided for the different ORIGEN-S libraries.

The percentage differences in Table 1 clearly shows that the results for cases A-1 and A-2 are much closer to the REF case than cases B-1 and B-2. Also, when burning cases B-1 and B-2 to the REF target burn-up, the differences have decreased but were still large in comparison with cases A-1 and A-2. Thus, it can be concluded that the burn-up of the surrounding spheres on the spectrum within the specific sphere is much more important than the burn-up of the sphere itself.

The reason for the spectrum within a fuel sphere to be mainly dependent on the burn-up of the surrounding fuel spheres is due to the large scattering to absorption ratio in graphite and that the UO_2 micro-kernels are relatively far apart (packing ratio 0.015). The scattering mean free path for thermal neutrons in carbon is about 2.6 cm, while the absorption mean free path is about 31 m. This implies that neutrons originating from fuel spheres relatively far from a specific fuel sphere, can also contribute to the spectrum within the fuel sphere.

Table 1 ORIGEN-S results for 874 days burn-up (thermal flux 6.3 x 10^{13} n.cm^{-2}.s^{-1})

Library Case	A-1	A-2	REF	B-1	B-2
Central Fuel Burn-up (GWD/TU)	0	80	45	45	45
Driver Fuel Burn-up (GWD/TU)	45	45	45	0	80
Activities	%	%	Bq	%	%
Sr-90	0.0	0.0	6.4 x 10^{10}	1.2	-1.8
Nb-97	0.0	-0.4	9.8 x 10^{11}	3.4	-6.8
Ag-110m	1.2	-1.3	2.5 x 10^{9}	11	-21
I-131	0.0	0.0	6.2 x 10^{11}	3.6	-7.7
I-132	0.0	0.0	9.1 x 10^{11}	4.1	-7.4
I-133	0.0	-0.3	1.3 x 10^{12}	3.5	-7.3
Cs-134	1.8	-1.8	1.1 x 10^{11}	6.3	-12
Cs-137	0.0	0.0	8.8 x 10^{10}	2.5	-4.4
Ba-137m	0.0	0.0	8.3 x 10^{10}	2.7	-4.7
Ce-143	0.0	-0.4	9.4 x 10^{11}	3.2	-6.3
TOTAL	0.3	0.0	1.1 x 10^{14}	3.8	-6.6
Mass	%	%	gram	%	%
U-235	0.6	-0.6	0.158	-0.6	1.3
U-238	0.1	0.1	7.82	-0.3	0.6
Pu-239	-1.0	0.0	0.0502	4.4	-10
Pu-241	0.4	-0.4	0.0246	6.9	-13
Heavy metal	0.0	0.0	8.22	-0.1	0.4
Burn-up	%	%	GWD/TU	%	%
	0.04	-0.1	80.06	2.5	-4.6

Similarly, ORIGEN-S cross section libraries have been created for the central fuel sphere (equilibrium burn-up) surrounded, respectively, by spheres at 41 GWD/TU (average upper layer burn-up) and spheres at 49 GWD/TU (average bottom layer burn-up). The ORIGEN-S activities and masses calculated for these two libraries compares within 1 %.

In conclusion, the use of a single ORIGEN-S cross section library, generated for the 10-pass PBMR design at equilibrium burn-up conditions, should be acceptable for most practical applications.

3. PBMR ORIGEN-S Library

Based on the conclusion in Section 2, an equilibrium core PBMR ORIGEN-S cross section library has been created with a 1-dimensional cylindrical PBMR reactor model. Table 2 provides a summary of the model. All fuel spheres were at equilibrium core burn-up (~45 GWD/TU) with the isotopic atom densities provided in Reference [3].

Table 2 PBMR cylindrical model used in SCALE

Region	Radius (cm)	Material
Central column	87.5	100% graphite spheres
Mixed region	112.5	50% graphite & 50% fuel spheres
Fuel region	175.0	100% fuel spheres
Reflector	275.0	Graphite (1.7 g.cm^{-3})

In reference [6] it is stated that the SCALE Dancoff factor calculation for tiny fuel kernels dispersed in graphite with a large number of equivalent unit cells per mean free path is questionable. The Dancoff factors derived from reference [6] for the PBMR fuel compares well with the VSOP Dancoff factors. A summary of the Dancoff factors are tabulated in Table 3.

Table 3 Dancoff factors for fuel spheres

Origin	Infinite system of microspheres	Infinite system of fuel spheres
SCALE	0.882	same as microspheres
VSOP	0.512	0.405
Reference [6]	~ 0.52	~ 0.42

A PBMR ORIGEN-S library has been created for both the SCALE and VSOP Dancoff factors, called D_{SCALE} and D_{VSOP}. In Table 4 the ORIGEN-S fuel zone microscopic cross sections are tabulated together with the VSOP and MCNP calculated values. The VSOP and MCNP values were obtained for 3-dimensional PBMR models.

Table 4 Microscopic fuel zone cross sections calculated with SCALE, MCNP and VSOP

REACTION	SCALE (D_{SCALE})	SCALE (D_{VSOP})	MCNP*	VSOP
	1173K	1173K	1200K	~1100K
U-235 (n,g) U-236	22.7	22.3	20.9	22.3
U-235 (n,fission)	109.0	106.8	105.2	105.5
U-238 (n,g) U-239	2.63	3.47	3.45	3.45
U-238 (n,fission)	2.46e-2	2.54e-2	2.73e-2	2.35e-2
Pu-239 (n,g) Pu-240	267.8	262.1	262.9	264.2
Pu-239 (n,fission)	432.9	423.7	428.7	425.3
Pu-241 (n,g) Pu-242	145.6	142.6	128.3	126.8
Pu-241 (n,fission)	370.0	362.3	355.5	358.5

* Nominal relative error of 0.2%

Comparing the SCALE (D_{VSOP}), MCNP and VSOP cross sections for the fuel zone, the values are of the same order. The SCALE (D_{VSOP}) and VSOP values compare well, except for the Pu-241 capture cross section, which differs with 12%. Further evaluation for this difference falls outside the scope of this paper.

The SCALE cross sections calculated, respectively, for D_{SCALE} and D_{VSOP} compare reasonably well, except for the U-238 capture cross section that differs with 32%. This is as expected since the U-238 resonance shielding is dominant for low enriched uranium fuel. This is also the reason why resonance shielding in VSOP is only taken into account for the U-238 capture cross section.

Similarly the SCALE, VSOP and MCNP cross sections have been compared for the mixed fuel region. The cross section differences were of the same order as for the fuel region.

From the comparisons above, the neutron interaction cross sections in the PBMR ORIGEN-S library seems to compare favorably with VSOP and MCNP. In Section 4 the PBMR ORIGEN-S library, created with SCALE using the D_{VSOP} value, is evaluated for burn-up calculations.

4. ORIGEN-S Burn-up Comparisons with VSOP

The PBMR ORIGEN-S library, created with D_{VSOP}, was evaluated by comparing different ORIGEN-S burn-up results with VSOP. Parameters compared are burn-up and actinide masses. To determine the thermal flux below 0.5 eV, which is used as ORIGEN-S input, the flux spectra calculated with MCNP, SCALE (D_{VSOP}) and VSOP were at first compared for the VSOP energy group structure. These results are tabulated in Table 5.

Table 5 Fuel region flux spectra for the VSOP energy group structure

Energy	VSOP	SCALE (D_{VSOP})	MCNP*
10 MeV - 0.1 MeV	0.167	0.176	0.183
0.1 MeV - 29 eV	0.287	0.278	0.288
29 eV - 1.86 eV	0.070	0.070	0.072
1.86 eV - 0 eV	0.476	0.476	0.457

* Nominal relative error of 0.2%

The results in Table 5 show that the flux spectra calculated with VSOP, SCALE (D_{VSOP}) and MCNP compares reasonably well; specially the thermal flux fraction (<1.86 eV) for VSOP and SCALE. Based on this it should be reasonable to assume that the SCALE thermal flux fraction below 0.5 eV (namely 0.42) can be used for the ORIGEN-S burn-up calculations. Therefore, the ORIGEN-S depletion calculations have been performed specifying the ORIGEN-S thermal flux as 42% of the VSOP fuel region axially dependent total flux values.

The end-of-pass burn-up values calculated with ORIGEN-S and VSOP for the 10 passes, are tabulated in Table 6. In Table 7 the end-of-life masses calculated with VSOP and ORIGEN-S are tabulated for U-235, U-238, Pu-239 and Pu-241.

Table 6 End-of-pass fuel sphere burn-up (GWD/TU) calculated with ORIGEN-S and VSOP

Pass	ORIGEN-S	VSOP	Pass	ORIGEN-S	VSOP
1	10.7	10.9	6	54.8	55.0
2	21.0	21.2	7	61.8	62.0
3	30.5	30.7	8	68.2	68.4
4	39.3	39.5	9	74.3	74.4
5	47.3	47.6	10	80.0	80.1

Table 7 ORIGEN-S and VSOP actinide masses (g) after 874 days burn-up

Isotope	ORIGEN-S	VSOP	% Difference
U-235	0.133	0.119	11.8
U-238	7.90	7.92	-0.3
Pu-239	0.0413	0.0374	10.4
Pu-241	0.0195	0.0199	-2.0
Total	8.25	8.15	1.2 %

The burn-up values as tabulated for ORIGEN-S and VSOP in Table 6 correspond well. The actual mass differences (Table 7) between the ORIGEN-S and VSOP values are up to 10 %. However, since the actual fission product yields for the different fissionable isotopes generally do not differ too much, it can be expected that the ORIGEN-S and VSOP fission products should compare well within 10%.

5. Conclusions

In this paper the creation of the PBMR library was evaluated in terms of the spectrum dependence due to burn-up. The results clearly showed that the flux spectrum within a fuel sphere is dominated by the average spectrum of all fuel spheres around the sphere. In most cases the resulting error for not taking the spheres own burn-up into account in the spectrum calculation will be less than 1%.

Following on this, a single equilibrium PBMR ORIGEN-S cross section library has been created for a 1-dimensional cylindrical model, based on the VSOP PBMR model. The ORIGEN-S PBMR library was evaluated comparing cross sections, fluxes, fission product activities, actinide masses and burn-up with results obtained from VSOP and MCNP-4C.

Based on the results obtained, the equilibrium core PBMR ORIGEN-S cross section library can be used with confidence for the 10-pass PBMR fuel depletion calculations.

6. Acknowledgement

The authors would like to thank PBMR Pty Ltd for their financial support and permission to publish this work.

7. References

[1] SCALE4.4: RSICC - Modular Code System for Performing Criticality Safety Analyses for Licensing Evaluation, CCC-545 (2000).

[2] E. Teuchert et al, VSOP - Computer Code System for Reactor Physics and Fuel Cycle Simulation, Kernforschungsanlage Jülich, JUL-1649 (March 1994).

[3] F. Reitsma, Neutronic and Other Interface Data from VSOP as Interface for PBMR 268 MW 10-Pass ORIGEN-S Library Creation, PBMR 010518-324 Rev 1, October 2001.

[4] J.F Brismeister, MCNP-4C - A General Monte Carlo N-Particle Transport Code, Los Alamos National Laboratory, LA-13709, April 2000.

[5] Z. Karriem, The PBMR Core MCNP Model RPV1.0, PBMR 008274-34 Rev B, 2001.

[6] E. Bende et al, Analytical Calculation of the Average Dancoff Factor for a Fuel Kernel in a Pebble Bed High Temperature Reactor, Nuclear Science and Engineering 133, 147-162 (1999).

HTR CORE PHYSICS ANALYSIS AT NRG

J.C. KUIJPER, J.B.M. de HAAS and J. OPPE
Fuels, Actinides & Isotopes department
NRG, Westerduinweg 3, P.O. Box 25, NL-1755 ZG Petten, The Netherlands

ABSTRACT

Since a number of years NRG is developing the HTR reactor physics code system PANTHERMIX. In PANTHERMIX the 3-D steady-state and transient core physics code PANTHER has been interfaced with the HTR thermal hydraulics code THERMIX to enable core follow and transient analyses on both pebble bed and block type HTR systems. Recently the capabilities of PANTHERMIX have been extended with the possibility to simulate the flow of pebbles through the core cavity and the (re)loading of pebbles on top of the core.The PANTHERMIX code system is being applied for the benchmark exercises for the Chinese HTR-10 and Japanese HTTR first criticality, calculating the critical loading, control rod worth and the isothermal temperature coefficients at zero power conditions. Also core physics calculations have been performed on an early version the South African PBMR design. The reactor physics properties of the reactor at equilibrium core loading have been studied as well as a selected run-in scenario, starting form fresh fuel. The recently developed reload option of PANTHERMIX was used extensively in these analyses. The examples shown demonstrate the capabilities of PANTHERMIX for performing steady-state and transient HTR core physics analyses. However, additional validation, especially for transient analyses, remains desirable.

1. Introduction

Research, relevant to the design of high temperature gas-cooled reactors (HTR), is performed in the Netherlands at NRG Petten/Arnhem, JRC-IE Petten (previously JRC-IAM) and IRI–Delft University of Technology, Delft. A comprehensive overview of these experimental and computational research activities is presented in [1].

In this paper we will focus on the computational HTR reactor physics activities at NRG Petten, employing the HTR reactor physics code package PANTHERMIX, which is based on the well-known lattice code WIMS (versions 7 and 8), the 3-D steady-state and transient core physics code PANTHER and the HTR thermal hydraulics code THERMIX-DIREKT. In this paper examples will be shown of PANTHERMIX calculations on pebble-bed and hexagonal block type HTR systems, demonstrating the capabilities of the code system.

2. The PANTHERMIX code system

Since a number of years NRG is developing a HTR reactor physics code system PANTHERMIX [2,3,4], based on the well-known lattice code WIMS (versions 7 and 8) [5], the 3-D steady-state and transient core physics code PANTHER [6] and the HTR thermal hydraulics code THERMIX-DIREKT [7]. At NRG the PANTHER code has been interfaced with THERMIX-DIREKT to enable core follow and transient analyses on both pebble bed and block type HTR systems.

The PANTHER code calculates the 3-dimensional neutron flux and power distribution for a given temperature distribution whereas the THERMIX-DIREKT code, calculates (in steady-state or transient mode) the temperature and flow distribution for a given power distribution. THERMIX-DIREKT is an improved version of the THERMIX-KONVEK module of the VSOP code [8]. The combined code system is controlled from the PANTHER code, which calls THERMIX-DIREKT from within an iteration (steady-state) or time step (transient) calculation loop.

PANTHER approximates the 2-D R-Z geometrical structure employed in THERMIX-DIREKT by a 3-D Hex-Z model with small stacked hexagons or, alternatively, a X-Y-Z model of pillars of small rectangular blocks. This is done as follows. A radial mesh in the THERMIX-DIREKT geometry

specification can be associated with a set of radial hexagons (blocks) in the PANTHER geometry, of which the total area is equal to the area of the THERMIX-DIREKT radial mesh. The validity of this approach has been confirmed by intercomparison of calculations in the framework of an MHTGR benchmark exercise [9]. For radial meshes and hexagon (block) sets associated in this way the power distribution and temperature distribution information is transferred between the codes.

PANTHERMIX requires a nuclear database containing - presently - 2-group nuclear data (macroscopic cross sections) for all reactor materials, depending on irradiation, fuel temperature, xenon density, etc. The WIMS code was selected to generate these databases, in view of the presence of the special PROCOL module and also because of the possibility to perform burn-up calculations in a convenient way within the WIMS code system. As only 2-group nuclear constants are presently employed in PANTHERMIX, the fine spectrum effects have been accounted for in the generation of the nuclear database. Therefore, in addition to the usual unit cell calculations, one-dimensional radial and axial models of the (pebble-bed) HTR under study are employed in the fine (16-) group calculations in the database generation calculations prior to the collaps to 2 energy groups. The WIMS code system also provides the 6-group delayed neutron data (yields β_i), required for transient calculations by PANTHERMIX. In the near future the multigroup (up to 12 neutron energy groups) capabilities of the present version of PANTHER will be tested for HTR applications.

Several benchmark exercises have been carried out, together with FZ Jülich, on the PAP20 pebble-bed HTR [4], comparing PANTHERMIX with the FZ Jülich HTR code package VSOP, demonstrating the feasibility of the PANTHERMIX code combination for pebble-bed HTR applications. In Section 3 some examples of these calculations will be presented. Extensive static and dynamic calculations on HTR pebble type cores with PANTHERMIX have been reported elsewere [10,11,12].

Recently the capabilities of PANTHERMIX have been extended with the possibility to simulate the flow of pebbles through the core cavity and the (re)loading of pebbles on top of the core [13,14,15]. Besides a considerable extension to the modelling in PANTHER this also requires an extension of the procedure for the generation of the nuclear database. Now these cross sections must not only be dependent upon the local burnup (irradiation) and the local temperature but also, in case of the mixed pebbles in the core cavity, upon the local enrichment and the local heavy metal mass per unit height, the latter being representative of the local mixture of moderator and fuel pebbles. For each combination of enrichment and heavy metal mass per unit height, a burn-up sequence calculation with xenon- and temperature branchings is performed by means of the WIMS code. The resulting databases are combined into a single nuclear database with enrichment and heavy metal mass per unit height as extra dependencies, ready to be used in the PANTHERMIX calculations. It should be noted that also a run is included with 100% moderator pebbles, in order to accommodate mixtures with a high fraction of moderator pebbles. Examples of calculations employing these enhanced capabilities are presented in Section 5.

In the recent past the PANTHERMIX code system has been applied in studies on Pu-incineration in HTRs and transient behaviour of HTRs in combination with an energy conversion system. For this purpose the PANTHERMIX code system was coupled to an extended version of the RELAP5 mod 3.2 code system. An extensive description of these activitities has been presented elsewere [10,11,12,16,17,19,20].

3. PAP/ACACIA steady-state and transient analyses

PAP20 is a conceptual design of FZ Jülich for a small simplified pebble-bed reactor of 20 MW (thermal) where fresh fuel elements (the well-known 6 cm diameter pebbles) are added little by little (peu-à-peu) to maintain criticality during operation [18]. No fuel is removed during the life of the core. At end of life all fuel elements are unloaded in one step. The initial core height, in a cavity of 2.50 m diameter, is about 1 m, using pebbles containing 12 g heavy metal (in UO_2, enrichment 10.0 %) [4]. At the end of core life (about 18 years) the core height is about 4 m, when pebbles are added containing fuel at 19.75 % enrichment. In the benchmark exercise the initial critical core height H_c, at Cold Zero Power (CZP), Hot Zero Power (HZP) and Hot Full Power (HFP) conditions, as calculated by PANTHERMIX, SNAP (CZP and HZP only), MCNP (detailed 3-D point energy monte carlo; CZP only) and VSOP were intercompared. At CZP a good correspondence was found between the results of PANTHERMIX (H_c = 0.81 m), SNAP (0.822 m) and MCNP (0.82 m). At HZP and HFP conditions also a good correspondence was found between the PANTHERMIX (0.95 m; 1.125 m), SNAP (0.964 m; HZP only) and VSOP (0.94 m; 1.10 m) results [4]. Generally, at HFP a good

correspondence was found as well between the PANTHERMIX and VSOP results for other parameters, like the maximum power density and the coolant and fuel temperatures in the core [4]. Transient simulation calculations by PANTHERMIX for LOFI (Loss Of Flow) and LOCI (Loss Of Coolant) incidents have been carried out for the PAP20 reactor [4] and also for the INCOGEN/ACACIA, the Dutch design of a small, 40 MWth pebble bed HTR for cogeneration, based on the PAP20 [1,4,11,16,17,19,20]. In Figure 1 an example is given of the total reactor power (prompt + decay), max. fuel temperature and xenon reactivity as function of time for a LOFI and a LOCI incident for a fresh core (after 5 days burnup), initially at HFP and Xe equilibrium [11,17]. Also a distinction has been made between cases employing thermodynamical data for irradiated and unirradiated graphite, respectively. It should be noted that the calculations employing the thermodynamical data for irradiated graphite in the fuel yield higher fuel temperatures than the corresponding cases employing data for unirradiated graphite, due to the lower thermal conductivity of irradiated graphite. Some time after recriticality the power will reach its maximum and the xenon concentration will be in equilibrium with the fission power level. Then, the fission power will balance to compensate for the heat leakage of the reactor and the temperature distribution over the reactor will reach its equilibrium shape accordingly.

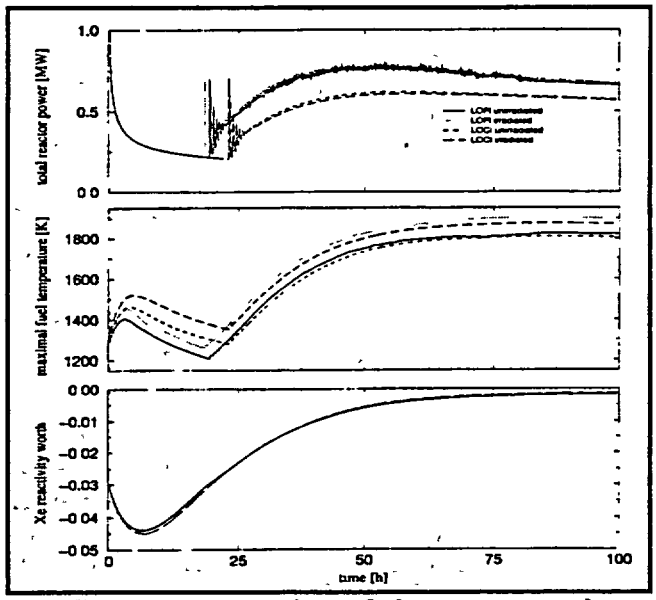

Fig. 1 Reactor power, maximum fuel temperature and xenon reactivity for the fresh core (5 days burnup) for the LOFI and LOCI incidents.

4. HTR-10 and HTTR benchmark exercises

The PANTHERMIX code system is being applied for the benchmark exercises for the Chinese HTR-10 and Japanese HTTR first criticality [21,22], calculating the critical loading, control rod worth and the isothermal temperature coefficients at zero power conditions. As an example in Table 1 a comparison is listed between calculations by several different codes and measurements of k_{eff} and the critical control rod insertion for the HTTR (Benchmark Phase 1) [4,23,24]. In these calculations without thermal hydraulics only the PANTHER part of PANTHERMIX has been used. A good correspondence is found between the PANTHER and KENO (monte carlo) results for the unrodded cases. The calculations of the – partially – rodded cases seem to require some improvement of the modelling in PANTHERMIX.

Table 1 HTTR Benchmark Phase 1

	KENO (IRI/NRG)	BOLD-VENTURE (IRI)	PANTHER (NRG)	Measured (JAERI)
k_{eff} simple core	1.1278 ± 0.0005	1.1592	1.1251	
k_{eff} fully loaded core				
- rods withdrawn	1.1584 ± 0.0005	1.1974	1.1595	
- rods inserted	0.6983 ± 0.0005		0.7510	0.685 ±0.010
critical insertion				
- above bottom core	170.5 cm		161.5 cm	178.9 cm

For the HTR-10 the initial critical height (at CZP conditions; T = 20 °C), as calculated by PANTHERMIX, was found to be 1.25 m, which corresponds quite well to the actually measured value of 1.23 m (at T = 27 °C) [23].

5. PBMR analyses

Also core physics calculations have been performed on an early version the South African PBMR design [25,26]. The reactor physics properties of the reactor at equilibrium core loading have been studied as well as a selected run-in scenario, starting from fresh fuel. The recently developed reload option of PANTHERMIX was used extensively in these analyses. In Figure 2 the results are presented of the determination of the critical equilibrium enrichment as function of the burnup time step between reloads. This equilibrium enrichment is determined as follows. At the end of each burnup time step the pebbles in the core cavity are shifted downwards and an amount of pebbles is unloaded at the botton equivalent to 4000 pebbles per day (2800 fuel + 1200 moderator). Unloaded fuel pebbles with a burnup less than 80,000 MWd/t are reloaded at the top of the core, together with fresh fuel and moderator pebbles, so that in total again 2800 fuel pebbles and 1200 moderator pebbles are loaded at the beginning of the next burnup time step. A burnup calculation is then performed for the specified number of days. This procedure is repeated until k_{eff} at the end of the burnup time step is constant within 0.01 %. This is considered to be the equilibrium state and it is reached after about 10 passes of the fuel pebbles through the reactor (about 800 days). As the reactivity varies approximately linearly with enrichment, the value for equilibrium enrichment can be found by linear interpolation from the equilibrium k_{eff} values of the 8.5% and 7.5% enrichment cases. This scenario has been run threefold, one with time steps of 7.5 days (i.e. 30000 pebbles per time step), one with time steps of 3 days (i.e. 12000 pebbles per time step), and one with time steps of 1 day (i.e. 4000 pebbles per time step). Different values of equilibrium k_{eff}, and consequently different equilibrium enrichments have been obtained for different time step lengths. For each time step two k_{eff} values have been calculated, one at the beginning of the time step (k_{upper}) and one at the end of the time step (k_{lower}). Both values are used for determining the equilibrium enrichment. So two values, ε_{upper} and ε_{lower}, have been obtained for the equilibrium enrichment. Also the step-averaged reactivity is calculated as the mean value of the reactivities at the beginning and the end of the burnup time step. Extrapolation to zero time step yields the equilibrium enrichment of 7.63 % for the real continuous reload case. Also note the close agreement between the critical enrichment of 7.87 % found by the VSOP code for a burnup time step of 6.4 days [25] and the values calculated by PANTHERMIX from the mean values of the reactivity.

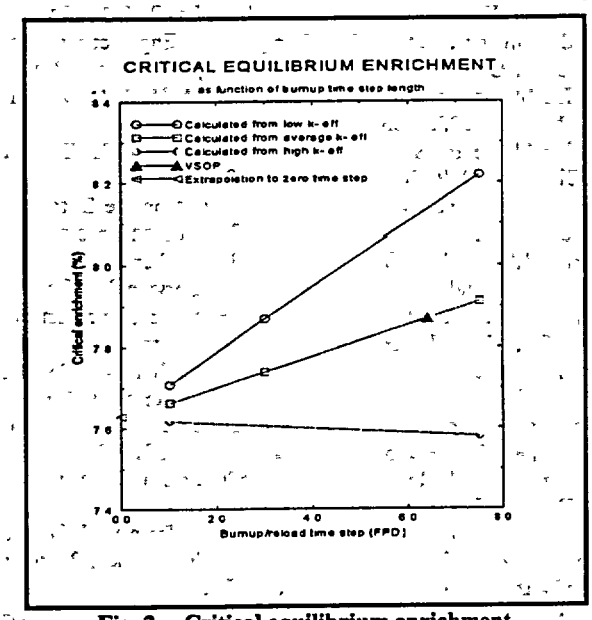

Fig. 2 Critical equilibrium enrichment.

6. Conclusions

An overview has been presented of the activities at NRG Petten concerning HTR core physics calculations, employing and developing the HTR reactor physics code package PANTHERMIX. The capabilities of PANTHERMIX have been demonstrated by performing a variety of steady-state, core follow and transient analyses on peble bed and hexagonal block type HTR systems. Additional validation of the code system, especially for transient analyses, remains desirable.

7. References

[1] J.C. Kuijper *et al.*, "Present status in the Netherlands of Research Relevant to High Temperature Gas-Cooled Reactor Design", paper presented at the OECD/NEA 2nd Information Exchange Meeting on Basic Studies in the Field of High Temperature Engineering, Paris, France, 10-12 October 2001. Also published as NRG report no. 20631/01.43344/P, NRG Petten, 3. October 2001.

[2] J. Oppe, J.B.M. de Haas and J.C. Kuijper, "PANTHERMIX – a PANTHER-THERMIX interaction", Report ECN-I—96-022, ECN Petten, May 1996.

[3] J. Oppe, J.B.M. de Haas and J.C. Kuijper, "PANTHERMIX (PANTHER-THERMIX) User Manual", Report ECN-I—98-019, ECN Petten, June 1998.

[4] J.C. Kuijper *et al.*, "Reactor Physics Calculations on the Dutch Small HTR Concept", IAEA Technical Committee Meeting on High Temperature Gas Cooled Reactor Development, Johannesburg, Republic of South Africa, IAEA-TECDOC-988, 13 - 15 November 1996.

[5] "WIMS8 User's Guide", ANSWERS Software Service, Winfrith, U.K.

[6] P.K. Hutt *et al.*, "The UK Core Performance Package", Nucl. Energy, 30, No. 5, 291, October 1991.

[7] S. Struth, "THERMIX-DIREKT: ein Rechenprogramm zur instationaeren, zweidimensionale Simulation thermohydraulischer Transienten", ISR-KFA Juelich, August 1994 (*private communication*).

[8] E. Teuchert, U. Hansen, K. A. Haas, "VSOP – Computer Code System for Reactor Physics and Fuel Cycle Simulation", Kernforschungsanlage Jülich, JÜL-1649, March 1994.

[9] H.Th. Klippel *et al.*, "Reactor physics calculations of HTR type configurations", Proc. ECN workshop on the role of modular HTRs in the Netherlands, Petten, the Netherlands, 30 November-1 December 1994, Report ECN-R—95-027, June 1995.

[10] E.E. Bende, "Plutonium burning in a Pebble-Bed Type High Temperature Nuclear Reactor", Ph.D thesis, Delft University of Technology, Delft, the Netherlands, Nuclear Research and Consultancy Group, Petten, the Netherlands, ISBN 90-9013168-X, 1999.

[11] E.C. Verkerk, "Dynamics of the Pebble-Bed Nuclear Reactor in the Direct Brayton Cycle", Ph.D thesis, Delft University of Technology, Delft, the Netherlands, Nuclear Research and Consultancy Group, Petten, the Netherlands, ISBN 90-9014203-7, 2000.

[12] A.I. van Heek, J.C. Kuijper, J. Oppe and J.B.M. de Haas, "Transient behaviour of Pebble Bed HTR at Different Power Levels", IAEA Technical Committee Meeting, Petten, November 1997.

[13] J. Oppe, "PANTHERMIX99 Reference Manual", NRG report no. 20708/01.39132/C, February 2001.

[14] J. Oppe *et al.*, "Modeling of continuous reload HTR systems by the PANTHERMIX code system", Proc. M&C 2001, Salt Lake City, USA, September 2001.

[15] E.C. Verkerk and J. Oppe, "Reproducing the VSOP pebble flow pattern in PANTHER calculation", NRG report 20429/01.40032/P, 19. March 2001.

[16] E.C. Verkerk and A.I. van Heek, "Transient Behaviour of Small HTR for Cogeneration", OECD NEA First Information Exchange Meeting on High Temperature Engineering, Paris, France, September 1999.

[17] E.C. Verkerk and A.I. van Heek, "Dynamics of a small direct cycle pebble bed HTR", Proc. IAEA Technical Committee Meeting on Gas Turbine Power Conversion Systems for Modular HTGRs, Palo Alto, 14 - 16 November 2000.

[18] E. Teuchert and K.A. Haas, "Features of safety and simplicity of advanced pebble bed HTRs", Proc. IAEA Technical Committee Meeting on the Development Status of Modular HTGRs and their Future Role, Petten, the Netherlands, 28 - 30 November 1994, Report ECN-R—95-026, September 1995.

[19] A.I. van Heek *et al.*, "Nuclear Cogeneration Based on HTR Technology", Proc. ENC '98, Nice, France, 25 - 28 October 1998.

[20] A.I. van Heek, "The Pebble Bed HTR, the Nuclear Option in the Netherlands", Paper presented at the Seminar of HTGR Applications and Development, Beijing, China, 19 - 21 March 2001.

[21] Y. Sun and X. Jing, "Benchmark Problem of the HTR-10 Initial Core Prepared for the IAEA Coordinated Research Program (CRP)", INET, Beijing, March 2000.

[22] M. Nakano *et al.*, "Benchmark Problems of Start-up Core Physics of High Temperature Engineering Test Reactor (HTTR)", JAERI-10-05, Japan, 1998.

[23] L. Brey *et al.*, "Evaluation of High Temperature Gas Cooled Reactor Performance Part I: Benchmark Analysis Related to Initial Testing of the HTTR and HTR-10", IAEA-TECDOC-TBD (CRP-5), December 2001.

[24] J.B.M. de Haas and E. Türkcan, "HTTR criticality, Physical Parameter Calculations and Experimental Results", Proc. ICENES 2000, Petten, the Netherlands, 24 – 28 September 2000, ISBN 90-805906-2-2.

[25] H.Th. Klippel *et al.*, "PBMR Burn-in core analysis", NRG report no. 20429/0038175/C (Rev. 1), January 2001 (*Confidential*).

[26] A.I. van Heek *et al.*, "Comparison of core calculations on the Pebble Bed Modular Reactor", NRG report no. 910516/01.41920, November 2001.

NEUTRONIC FEATURES OF THE GT-MHR REACTOR

N. KODOCHIGOV, YU. SUKHAREV, E. MAROVA
OKB Mechanical Engineering, Nizhny Novgorod, 15, Burnakovsky proezd, 603074, RUSSIA

N. PONOMAREV-STEPNOY, E. GLUSHKOV, P. FOMICHENKO
RRC Kurchatov Institute, Moscow, RUSSIA

ABSTRACT

The design of a Gas Turbine - Modular Helium Reactor (GT-MHR) of 600 MWt power is being developed in frames of "The Agreement between the Government of the United States of America and the Government of the Russian Federation on Scientific and Technical Cooperation in the Management of Plutonium That Has Been Withdrawn from Nuclear Military Programs" signed on July 24, 1998. The reactor concept is based on the deep burnup of initially loaded plutonium fuel in a single pass through the reactor and the subsequent disposal of the spent fuel without additional processing.

The present report describes the analysis of the basic features of the reactor core fueled by plutonium:

(1) The annular type core design is used to decrease fuel temperature in accidents without active heat removal.

(2) Unlike other alternatives for plutonium disposition, in the GT-MHR reactor no fertile materials like U-238, or Th-232 are used. Erbium is used as a burnable poison and means for ensuring the negative temperature coefficient of reactivity.

(3) Deep fuel burnup (640 MW d/kg on the average) leads to the significant accumulation of Pu-241 during irradiation of weapons grade Pu fuel. This fact determines the specific time dependence of the multiplication factor in the end of the fuel lifetime.

(4) Rather hard neutron spectrum in the annular-type active core, and the essentially thermal spectrum in the reflectors cause a peak in the power distribution near the core-reflector boundary. Fuel and burnable poison zoning are used to control power profile.

(5) The movement of control rods located in the side reflector noticeably deforms the power distribution in the core.

(6) The temperature coefficient of reactivity depends both on the temperature and burnup level. In the GT-MHR reactor with plutonium fuel the temperature reactivity coefficient has values close to zero for temperatures less than 400°C at the end of the partial fuel cycle.

(7) Deep fuel burnup, achievable through the use of fuel particles with multilayer coatings, and high efficiency of transforming the thermal energy into electricity allow the effective utilization of plutonium in the GT-MHR reactor.

1. Introduction

Large amounts of weapons grade plutonium (WGPu) have been currently accumulated in the world. These stockpiles of accumulated plutonium are potentially hazardous because of the possibility of proliferation with the subsequent manufacture and use of nuclear weapons. From this point of view, the problem of the plutonium disposition is urgent.

On the other hand, plutonium is an extremely valuable source of energy, so it has to be efficiently used. The idea of WGPu burning in nuclear power plants to ensure electricity production is the official Russian position [1]. WGPu burning in reactors is considered as a long-term problem connected with the modification of existing power plants as well as with the development of new reactor technologies.

Along with operating VVER-1000 and BN-600 reactors, the high temperature reactor with gas turbine GT-MHR [2] of 600 MWt power is considered in the Russian Federation as a candidate reactor for WGPu disposition. Its design is developed in frames of "The Agreement between the Government of the United States of America and the Government of the Russian Federation on Scientific and Technical Cooperation in the Management of Plutonium That Has Been Withdrawn from Nuclear Military Programs", signed on July 24, 1998.

The GT-MHR is being developed under the international cooperative program involving institutions of the Russian Federation Ministry of Atomic Energy, Russian Research Center "Kurchatov Institute", foreign companies and laboratories: General Atomics, ORNL, LANL (USA), Framatome ANP (France), Fuji Electric (Japan). The overall goals of the cooperative program are initially to develop the GT-MHR for the disposition of surplus weapons plutonium in Russia, and then to offer GT-MHR plants fueled by uranium to the international market for the electricity generation.

2. Conception of WGPu Use in the GT-MHR Reactor

The idea of WGPu disposition in the GT-MHR [3] is based on the high burnup of initially loaded Pu in one pass through the reactor core and the subsequent storage of spent fuel without processing in MPC in the final disposal facility.

Plutonium fuel in reactor is used in the form of fuel particles with multilayer coatings. Plutonium oxide spheres of 200 μm diameter are coated firstly by low-density pyrocarbon, then by high-density pyrocarbon and silicon carbide (TRISO coated particles). The outside diameter of particles is about 620 μm. The coated fuel particles are bonded together with carbonaceous matrix into rod-shaped compacts that are stacked in fuel holes of hexagonal-shaped nuclear-grade graphite blocks 0.8 m height and 0.36 m across flats size. The design of these fuel blocks is the same as proven in the Fort Saint Vrain (USA) demonstration plant. The standard fuel block contains about 20 million coated fuel particles; only 0.7 kg of Pu is loaded per 115 kg mass of graphite fuel block. The core fuel blocks have burnable absorber rods on the basis of natural erbium (Er_2O_3). The absorber performs two functions: compensation of reactivity margin during reactor operation between refuelings and ensuring the negative value of the temperature coefficient of reactivity. Erbium contains ~23 % of Er-167 which has a pronounced resonance (almost 10^4 barn) at the neutron energy about 0.5 eV, and blocks the neutron capture by Pu-239 at the decrease of temperature. Burnable absorber compacts and fuel compacts have the same design and dimensions.

The annular type reactor active core (Fig. 1) is composed of hexagonal graphite fuel blocks arranged in 102 columns, each 10 blocks high. Each fuel block has 202 channels for fuel compacts (15 fuel compacts per channel through its height), 108 channels for coolant and 14 channels for Er_2O_3 burnable poison compacts (15 poison compacts per channel through its height). These channels are arranged in the triangular lattice with 19 mm pitch. The channels for scram absorber rods of 130 mm diameter are arranged in 12 fuel columns of the first internal row of the core.

The channels for the RSS containing small B_4C absorber balls are placed in 18 fuel columns of the second and third internal rows of the core. The annular fuel assembly stack (core array) is surrounded by the inner, outer, upper and lower replaceable reflectors.

The replaceable reflector is built up from 163 columns, each 13 blocks high. There are 102 columns in the side replaceable reflector and 61 columns in the inner one. The upper and lower reflectors are arranged above and below of the fuel assembly stack, respectively. Blocks in 36 columns of the side reflector have channels for control rods.

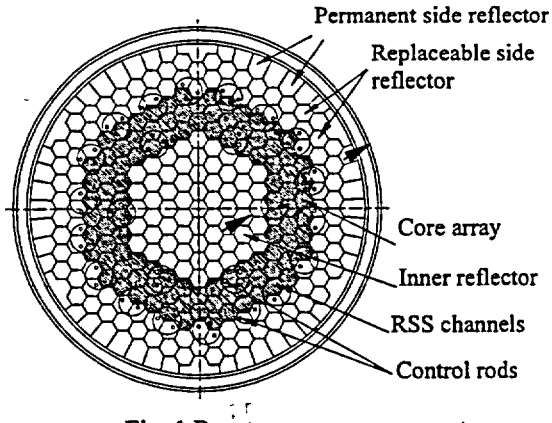

Fig. 1 Reactor core arrangement

The main core design parameters are presented in Table 1.

Table 1 Basic design parameters of the reactor plant [4]

Performance	Value
Full thermal reactor power, MWt	600
Inlet helium temperature, °C	490
Outlet helium temperature, °C	850
Core geometric parameters:	
- equivalent core diameter, inner/outer, m	2.96/4.84
- core height, m	8.00
Average core specific power, MW/m^3	6.50
Number of fuel blocks	1020
Prismatic fuel block geometrical parameters:	
- height, m	0.80
- size across the flats, m	0.36
- number of fuel compacts per fuel block (in core average)	2862
Fuel temperature limit, °C	≤ 1600
Number of reactivity control rods:	
- in core	12
- in side reflector	36
Number of reserve shutdown system channels	18
Allocated operative reactivity margin on control rods, % Δk/k	5.0
Xe- decay at transient from 100 % to 15 % of full power, % Δk/k	2.0

3. Neutronic features of the GT-MHR

The GT-MHR reactor is characterized by the following specific features:

(1) Use of the coated fuel particles in fuel blocks, that ensures for the GT-MHR reactor additional effective barriers to the release of radioactivity to the environment in contrast to other types of reactors. This fuel block structure results in the double heterogeneity of the fuel location in the core, which must be accounted for in the calculation of the neutronic characteristics.

(2) Use of the pure Pu fuel without fertile materials such as U-238 or Th-232, that results in the deep fuel burnup, and need to use burnable poison.

(3) High working temperatures in the core, that can result in positive temperature effect of reactivity at the use of Pu fuel without fertile materials.

(4) Use of erbium as burnable absorber in the reactor core to guarantee the negative value of the temperature reactivity coefficient and to minimize the reactivity change during burnup.

(5) Use of the annular-type active core design to prevent fuel damage in accidents even with the failure of helium circulation, that results in the non-symmetric radial power distribution.

(6) Location of operational control rods outside of the active core in the side reflectors.

(7) Long core axial size vs. its diameter (H/D≈1.5), that results in the noticeable non-uniformity of the axial power distribution.

All these neutronics features of the GT-MHR reactor have an essential influence on the basic reactor parameters and were accounted for the reactor design.

Neutronic analysis was carried out in the 3-D diffusion approximation by the JAR code [5]. Neutron cross-sections were prepared for different physical zones of the GT-MHR reactor by the WIMS-D/4 code [6].

Some illustrations for these neutronic features are presented below.

The double heterogeneity of fuel arrangement in fuel blocks with Pu has a weak effect on the neutronic characteristics.

The multiplication coefficient in the reactor with plutonium fuel depends only slightly on the fuel particle parameters. The fuel composition in the GT-MHR is 'weakly heterogeneous' in comparison, for example, with HTGRs with low-enriched uranium fuel, where the variation of the fuel kernel diameter from 200 to 500 μm results in the variation of multiplication coefficient more than 3 %.

The variation of the multiplication coefficient vs. time is shown in Figure 2.

The decrease of K_{mf} during burnup has a flatter character (see curve 1) that is caused by the Pu-241 accumulation. Difference of K_{eff} in reactor with and without burnable poison (curves 3 and 2) shows the incomplete burnup of Er isotopes compared to Pu isotopes. This causes the sharp decrease of the multiplication coefficient at the end of fuel life. This incomplete burnup of Er leads to the loss of about 150 EFPDs in the fuel lifetime. The last fact is unfavorable from the viewpoint of fuel cycle economics, but presence of Er is necessary for the reactor fueled by pure Pu to ensure the negative temperature reactivity coefficient.

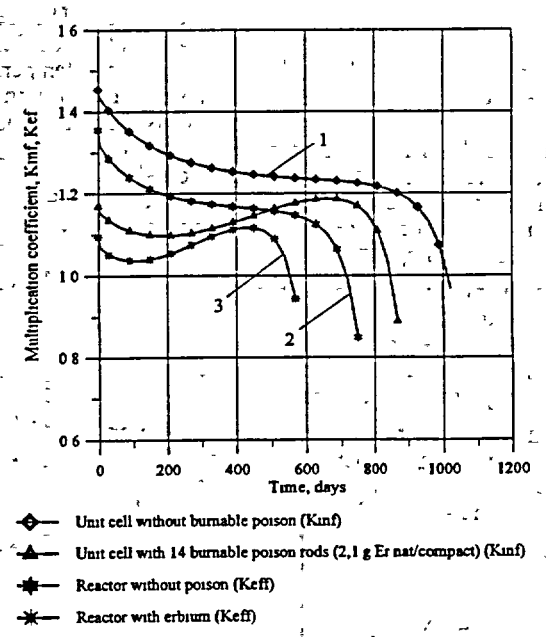

Fig. 2 K_{mf}, K_{eff} dependence vs time

There is an essential non-uniformity in the power distribution at the core and internal reflector boundary for the annular-type core with Pu fuel. This fact is caused by accumulation of thermal neutrons in the reflectors, combined with a rather hard neutron spectrum in the active core and its relatively small thickness. The leakage of neutrons from the active core is significant.

Figure 3 shows the power distribution in some chosen radial direction (see Figure 1) obtained from reactor calculation in the fine-mesh approximation with all control rods withdrawn. The maximum value of peaking factor reaches ~2.4 at the internal reflector / core boundary in

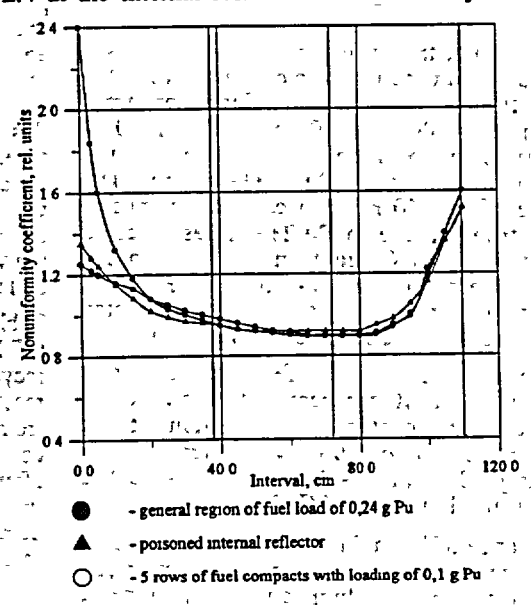

Fig. 3 Radial power distribution

the case without fuel and poison zoning. By reducing the Pu loading in five rows of fuel compacts adjacent to the internal reflector to 0.1 g Pu / compact (instead of 0.24 g Pu / compact in the rest of the core), the peaking factor can be reduced to 1.25. Practically the same result can be achieved by the "poisoning" of the internal reflector adjacent to the core boundary by uniform placing of the additional boron rods in the section of graphite blocks. The peaking factor reaches ~ 1.35 in this option.

At the actual position of the control rods in the outside reflector, the peaking factor reaches 1.6 at the core / internal reflector boundary, and can be additionally reduced by the fuel and erbium poison zoning along the core radius.

To illustrate the effect of the core temperature on reactivity, the energy dependence of the neutron cross sections for main isotopes in the core is shown in Figure 4. The thermal neutron flux has

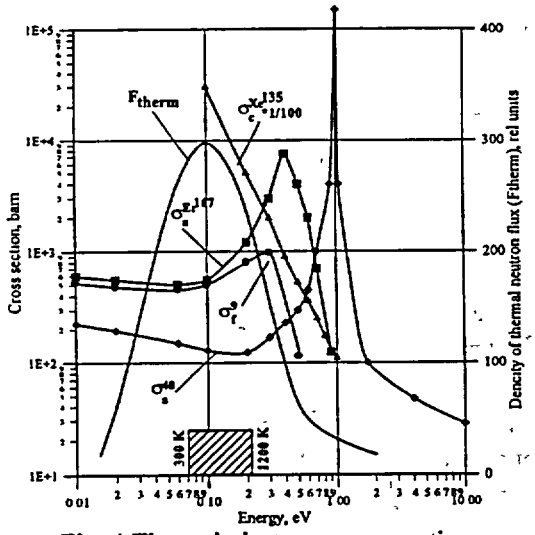

Fig. 4 The main isotopes cross section

its maximum at the energy of 0.1 eV. As shown in Figure 4, with the increase of temperature, the Pu-239 fission cross section increases from 450 barn at T=300 K to 800 barn at T=1200 K. This causes the positive reactivity temperature coefficient in a pure Pu fueled core. The influence of Pu-240 resonance, which competes with neutron capture in Pu-239, takes place at high temperatures (more than 1000 K). In the poisoned reactor (with Xe-135), the effect of multiplication coefficient increase is aggravated by the decrease in the Xe-135 cross section.

To compensate for these effects in the reactor core with WGPu, it is necessary to use a poison with increasing capture cross section at the energy range above 0.08 eV. Natural erbium containing 23 % of Er-167, which has such a feature, is used in the GT-MHR reactor.

The presence of Er in the required amounts leads to the hardening of the neutron spectrum, additional parasitic neutron capture, and increase in the fissile materials consumption.

The dependence of the reactivity temperature coefficient (both of fuel and moderator) on the temperature for the reactor poisoned by Xe at the beginning and the end of equilibrium burnup cycle is shown in Figure 5.

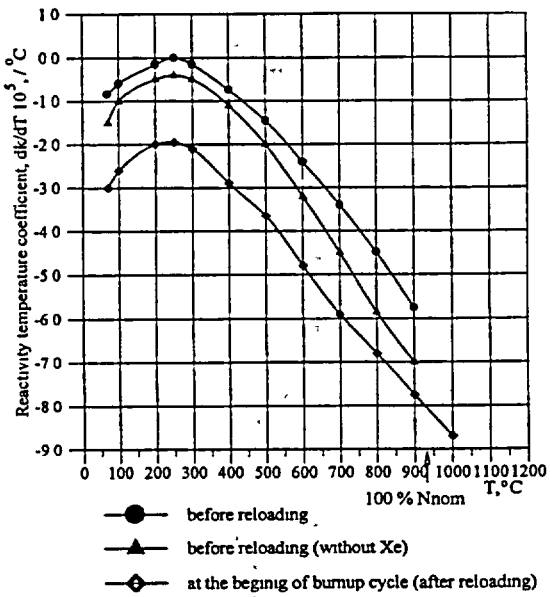

Fig. 5 Reactivity temperature coefficient

The reactivity temperature coefficient for the state after refueling is obviously negative, but for the state before reloading there is the temperature range (below 400 °C) where the reactivity temperature coefficient is close to zero. In the reactor without Xe poisoning the reactivity temperature coefficient is negative in the whole temperature range.

Because of the high burnup and absence of new plutonium accumulation, the GT-MHR consumes about 90 % of initially charged Pu-239 or approximately 270 kg of WGPu per year in one reactor module. A single GT-MHR plant consisting of four reactor modules can achieve this level of Pu-239 destruction for 50 metric tones of WGPu in 46 years of operation with concurrent electricity generation of 42 GWe-yr at the 0.8 capacity factor. In this evaluation it is assumed that the GT-MHR has 3 refuelings per the whole fuel cycle, fuel lifetime is 750 EFPDs, and the average burnup is 640 MW·d/kg.

Table 2 illustrates the advantages of the GT-MHR for the WGPu disposition (without fuel recycling) in comparison with other types of reactors. Plutonium of the spent fuel discharged from the GT-MHR after one pass through the core contains about 30 wt% of Pu-239 and about 30 wt% of Pu-240 that makes such spent fuel unattractive for the reprocessing both for commercial or military use, and, thus, effectively resolves the proliferation issue.

Table 2 Comparison of Pu disposition in reactors of different type (without fuel recycling)

Reactor characteristic	GT-MHR	VVER-1000 (with loading of MOX in 1/3 core)	Fast sodium reactor BN-800
Thermal power, GW	0.6	3.0	2.1
Net efficiency, %	48	33	38
Annual WGPu consumption, t	0.27	0.27 [7]	1.65
Electricity generation at disposition of 50 t WGPu, GWe·yr	42	47	19
Level of Pu-239 burning, %	90	63	17

4. Conclusions

The fundamentals of the WGPu disposition in the GT-MHR, as a high temperature gas cooled reactor, are the following:

(1) Efficient plutonium burning in one pass through reactor core, and concurrent electricity generation.

(2) Use of WGPu in the form of coated fuel particles with multi-layer ceramic coatings, resulting in the high burnup (640 MW·d/kg on average through the core), and eliminating the need for the processing of the spent fuel before its final disposal in the form of whole fuel elements. This is the more effective option of WGPu utilization than vitrification or any other option of WGPu disposition in reactors without fuel recycling.

The physical characteristics of the GT-MHR reactor with WGPu (high fuel burnup, essential non-uniformity of power distribution in the annular core, complicated dependence of the temperature reactivity coefficient versus isotope content) require comprehensive calculational and experimental justification.

To qualify the design characteristics, it is expected to perform the experimental simulation of annular core configurations at the Russian critical facilities. The goals of these experiments are to study the power distribution and the possibility of its flattening, to investigate control rod worth in the side reflector and in the active core, to study the effect of rod position on core neutronic characteristics, etc. Benchmark calculations of the initial loading of the HTTR reactor (Japan) could contribute to the resolution of these problems, too.

For the verification of calculational methods of Pu fuel burnup in the reactor, it is necessary to carry out the benchmark calculations and experiments addressing the high burnup of Pu fuel compacts in reactor conditions close to actual ones in the GT-MHR reactor.

5. References

[1] N.N.Ponomarev-Stepnoy, Plutonium – Man-Made Fuel of the 21st Century, Proc. of Int. Conf. "Plutonium Futures – The Science", Santa Fe, New Mexico, USA, July 2000.

[2] A.I.Kiryushin, N.N.Ponomarev-Stepnoy et al., The Project of the GT-MHR High-Temperature Helium Reactor with Gas Turbine, Nuclear Engineering and Design, 173 (1997) p.119-129.

[3] A.I.Kiryushin, N.N.Ponomarev-Stepnoy et al., Burning of weapons-grade plutonium in the gas-turbine modular helium reactor, Col. "Questions of Atomic Science and Technique", series "Physics of Nuclear Reactors", Moscow, 1998.

[4] N.G.Kodochigov et.al., Analysis of different fuel cycles for GT-MHR, IAEA IWGGCR Meeting, June 27-29, 2000, Vienna, Austria.

[5] M.N.Zizin, L.K.Shishkov, L.N.Yaroslavtseva. "Bench-scale neutronic analysis of nuclear reactors", M. Atomizdat, 1980, p.9

[6] Askew J.R., et.al. A general description of the lattice code WIMS, JBWES, Oct.1966, p.564

[7] Joint U.S./Russian Plutonium Disposition Study. Prepared by the Joint U.S.-Russian Plutonium Disposition Steering Committee. U.S. Department of Energy, 2001, http://plutonium-erl.actx.edu/jointusrusspds.html

Session 4

Thermohydraulic Calculation

THREE-DIMENSIONAL NUMERICAL SIMULATION OF FLOW AND HEAT TRANSPORT IN A HIGH-TEMPERATURE REACTOR

S. BECKER and E. LAURIEN
Institute for Nuclear Technology and Energy Systems (IKE)
University of Stuttgart, Pfaffenwaldring 31,
D-70550 Stuttgart, Germany

ABSTRACT

In the PBMR with an annular core layout consisting of a central column of graphite pebbles and a surrounding ring of fuel pebbles three-dimensional effects may become important. Hence a new code system based on CFX-4 has been developed and verified by comparison with previous two-dimensional simulations of the HTR-MODUL. As an example of three-dimensional flow and heat transport the influence of an eccentric misplaced package of fuel pebbles in the central column is investigated. A significant influence on the temperature distribution and the maximum temperature is found.

1. Introduction

The correct simulation of flow and heat transport is of great importance for the next generation high temperature gas-cooled reactors (HTR) such as the "Pebble Bed Modular Reactor (PBMR)" [1]. This reactor is currently under development in South Africa on the basis of the HTR-Modul of Siemens/Interatom [2] but with increased thermal and electrical power. In the European High Temperature Reactor Network (HTR-TN) reactors with relatively high power will also be investigated.

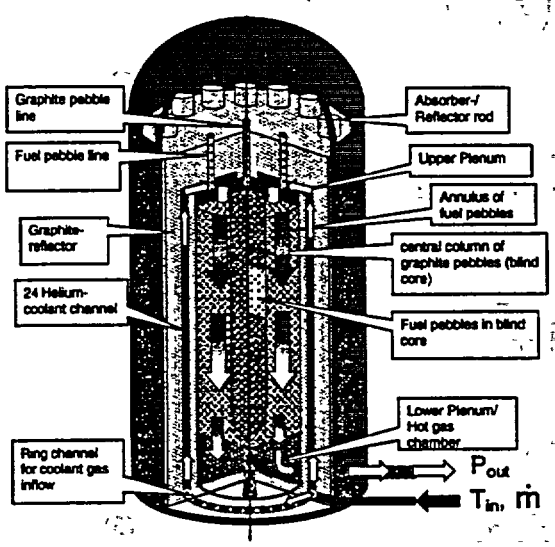

Fig. 1 : Sketch of a HTR with annular core

Higher thermal power than of the HTR-MODUL under the condition of limited maximum core temperature can be obtained by using an annular core consisting of a central column of graphite pebbles with a surrounding ring of fuel pebbles. However, three-dimensional effects of flow and heat transport may arise, e.g. by a package of eccentrically misplaced fuel pebbles in the central graphite column.

Currently only two-dimensional special purpose codes like THERMIX/KONVEK of Forschungszentrum Jülich are available for thermal analysis. Therefore it is necessary to develop three-dimensional (3D) tools.

In this work the already existing code CFX-4 for three-dimensional flow analysis from AEA Technology [3] has been employed. The necessary models for pebble beds and the corresponding flow and heat transport phenomena have been implemented.

The new code has been validated for several steady state and transient high-temperature experiments for Helium and Nitrogen flow in a pebble bed conducted at the SANA (Selbsttätige Abfuhr von Nachwärme) test rig of Forschungszentrum Jülich, Germany [4]. In the experiments the heat transport has been investigated for a simplified model of a

HTR-MODUL 3-4 hours after reactor shutdown. The simulations have shown good agreement to the experimental results for both gases [5].

In this paper preliminary 3D results of the new code for a simplified model of the South-African PBMR as of 2000 with 270 MW thermal power are discussed. Steady simulation results show the influence of a package of eccentrically misplaced fuel pebbles in the central column on the maximum temperature for (i) short time after injection and for (ii) an instant shortly before release of the fuel pebbles.

In order to demonstrate that the unsteady results of the new code agree with the two-dimensional simulation results of THERMIX/KONVEK unsteady 3D-simulations of the HTR-MODUL (HTR-200) have been performed. Results are presented for a loss-of-forced-coolant accident at nominal pressure and with fast depressurisation.

2. Mathematical Model

The flow and heat transport in a High-Temperature Reactor is simulated unsteadily by the Heterogeneous Model, consisting of two sets of equations for both media, the gas, eqs. (1)-(3), and the pebble bed together with the solid parts, eq. (5). The volume porosity φ is used to determine, whether a single phase gas flow (φ=1), flow and heat transport through the pebble bed ($0<\varphi<1$) or heat transport in the solid parts (φ=0) are simulated. The heat transport in the pebble bed and the solid parts of the reactor like the side reflector are described by a temperature equation. The interaction of both media, gas and pebble bed, is modelled by interaction terms for pressure drop B_j, eq. (4), and heat exchange $\dot{q}'''$.

The gas flow in the upper plenum, the coolant channels and the pebble bed are described by the three-dimensional spatially averaged conservation equations for flow through a porous medium as given below

$$\frac{\partial \varphi \rho}{\partial t} + \frac{\partial \varphi \rho u_i}{\partial x_i} = 0 \tag{1}$$

$$\left(\frac{\partial \varphi \rho u_j}{\partial t} + u_i \frac{\partial \rho \varphi u_j}{\partial x_i}\right) = B_j - \varphi \frac{\partial p}{\partial x_j} + \varphi \frac{\partial}{\partial x_i}\left(\mu\left(\frac{\partial u_i}{\partial x_j} + \frac{\partial u_j}{\partial x_i}\right)\right) + \varphi \rho g_j \tag{2}$$

$$\frac{\partial \varphi \rho h}{\partial t} + \varphi \frac{\partial \rho u_i h}{\partial x_i} = \varphi \frac{\partial}{\partial x_i}\left(\frac{\lambda}{c_p}\frac{\partial h}{\partial x_i}\right) + \dot{q}''' \tag{3}$$

with fluid density ρ, velocity u, static pressure p, viscosity μ, enthalpy $h=c_p*(T-T_{ref})$, heat conductivity λ, heat capacity c_p, volumetric exchange heat flux $\dot{q}''' = \alpha(T_{POR} - T)$ between pebbles and gas, the volume porosity φ and the additional body force B_j in j-direction due to additional flow resistance caused by the pebble bed, modelled by Ergun's law

$$B_j = -\frac{150\mu(1-\varphi)^2}{d_p^2\varphi^3}u_j - \frac{1.75\rho(1-\varphi)}{d_p\varphi^3}|u|\cdot u_j \tag{4}$$

with the diameter d_p=0.06m of the pebbles.

The pebble bed and the solid parts are described by the continuous porous medium approach and the heat transport is modelled by

$$(1-\varphi)(\rho c)_{por}\frac{\partial T_{Por}}{\partial t} - (1-\varphi)\lambda_{eff}\frac{\partial^2 T_{Por}}{\partial x_i^2} = \dot{q}_N''' - \dot{q}''' \tag{5}$$

with T_{Por} as the temperature of the pebble bed, the exchanged volumetric heat flux $\dot{q}'''$ between pebble bed and gas, the volumetric nuclear heat production $\dot{q}_N'''$ and the effective heat conductivity λ_{eff} of the porous medium including a model for radiation described by the correlation of Zehner and Schluender [6]. The variation of porosity near the walls is modelled by the correlation of Cheng and Hsu [7] resulting in a 50% higher maximum porosity than in the interior (φ_∞=0.4). The heat transfer from the porous medium to the fluid is described by a volumetric heat transfer coefficient α in accordance to

KTA-rule 3102.2. Thermal dispersion effects due to additional mixing of gas in the core is taken into account by a model of Bauer [8] by increasing λ.

3. Numerical Method

The set of equations given above is integrated in space and time by the finite-volume CFD-code CFX-4 for steady state and transient cases. The equations have been solved using the SIMPLEC-algorithm. The solid parts in the reactor model are described as conducting solids and are solved accordingly. All necessary models have been implemented by the USER-FORTRAN interface. The transient cases have been solved by a second-order accurate backward difference implicit time stepping method. The time step width was chosen to resolve the initially steep gradients of the decay heat curve.

4. Results

The three-dimensional reactor models of the HTR-MODUL (HTR-200) and the PBMR (PBMR-270) are shown in fig. 2 with the initially given power distribution. For the HTR-MODUL the power distribution was taken from THERMIX/KONVEK coming from neutronic Monte-Carlo-calculations with ORIGEN. For the PBMR an axisymmetric power distribution with given total thermal power was assumed to have a distribution similar to the HTR-MODUL but with no power production in the central column. To simulate the effect of misplaced fuel pebbles an eccentric power-generating section in form of a quarter cylinder with 1 m height as shown in fig. 2 right is used, resulting in a total power of 280 MW.

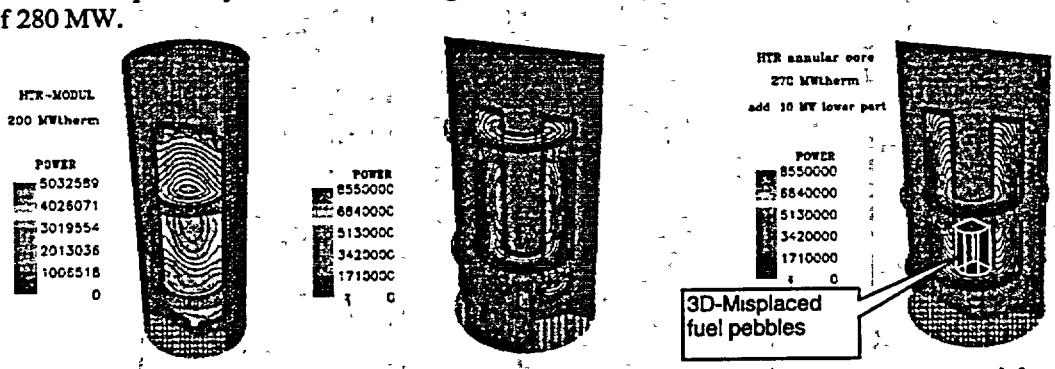

Fig. 2. Model of HTR-200 (left) and of the PBMR-270 (middle: nominal power, right: with additional fuel pebble package in the lower part of the core)

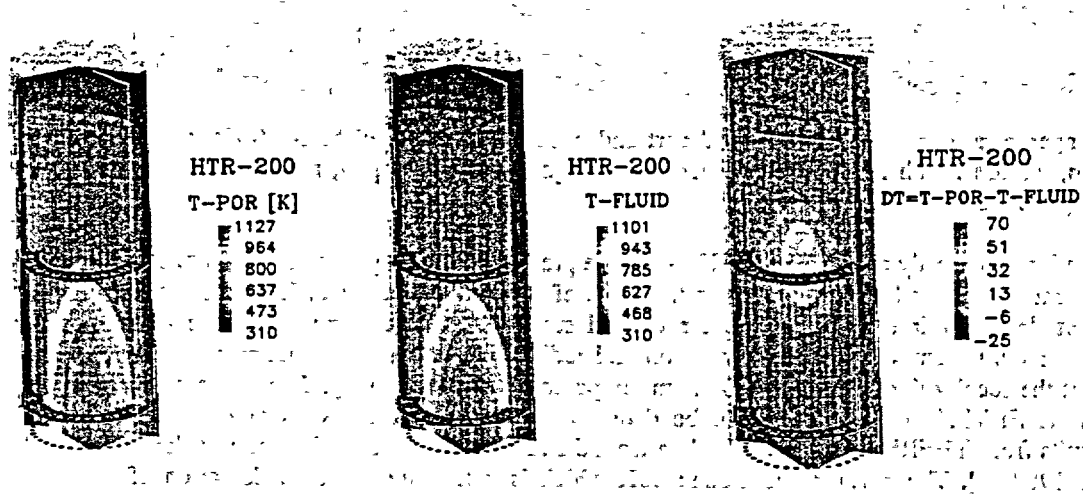

Fig. 3 : HTR-200 - Distribution of temperature in the solid part and pebble bed (left), fluid (middle) and the temperature difference between pebble bed and fluid (right)

First, the operational state of the reactor has been simulated as a basis for later transient accident simulations. The simulation results for the operational state of the HTR-MODUL with 200MW thermal power and a mass flux of 80 kg/s at 250°C is given in fig. 3 with the distribution of the temperature in the pebble bed (left), in the gas (middle) and the temperature difference $dT=T_{Por}-T$ (right). The pressure drop due to the core of 0.6 bar was in good agreement to documented data. The maximum temperature of 1130 K agrees well with 1139 K from THERMIX/KONVEK.

As an initial condition for the unsteady cases of the PBMR-270 a steady simulation with 126 kg/s inlet mass flux of Helium at 500°C was performed. The symmetric case at nominal power of 270 MW_{therm} is shown in fig. 4 left. A maximum temperature of around 1230K has been calculated. In case the misplaced fuel pebble package is located in the upper part of the core, which corresponds to an instant shortly after injection, we have calculated an increase in the maximum temperature of 20K compared to the standard operational case. The maximum temperature is almost not affected if the additional fuel pebbles are in the lower part of the reactor core, which corresponds to a later time shortly before the pebbles will be taken out of the reactor core.

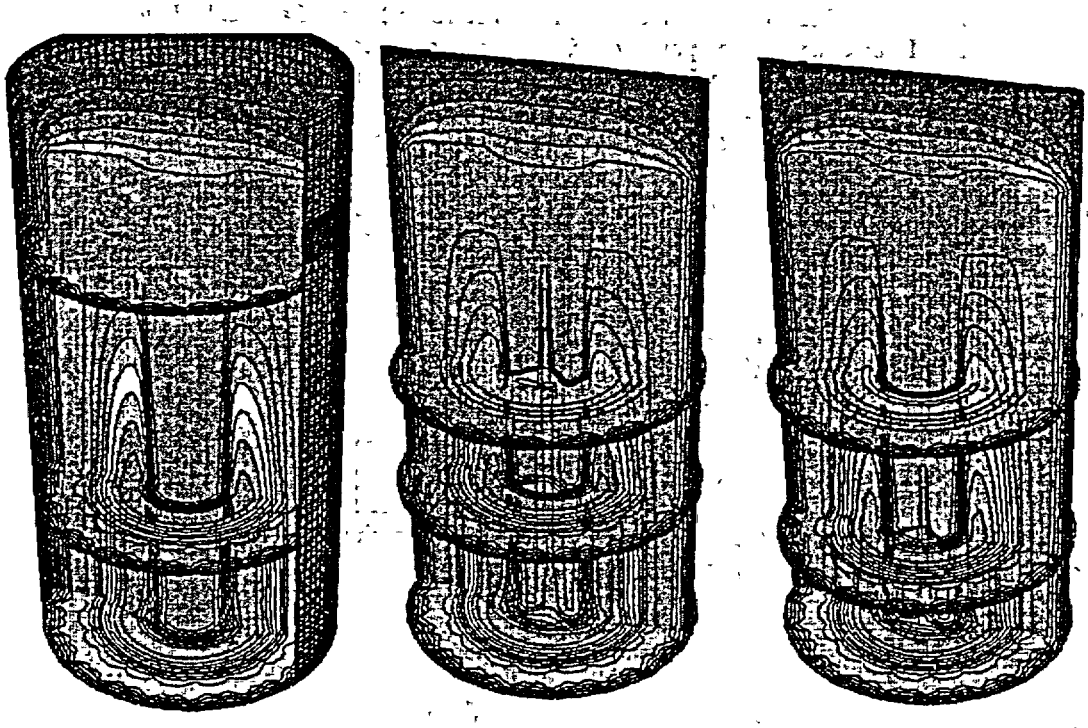

Fig. 4. Temperature distribution in the solid part and pebble bed of the PBMR-270 (left: nominal configuration, middle : with misplaced fuel pebble package in the upper part, right: misplaced fuel pebble package in the lower part)

Next, preliminary unsteady results for the HTR-200 are presented for the pressurised loss-of-forced-coolant-accident which has been simulated on the basis of the operational state. Here the reactor is suddenly shut down by inserting all control rods and stop of forced cooling. Heat can only be transferred by natural convection, heat conduction and radiation. The maximum temperature in the pebble bed at the locally fixed point of maximum temperature is shown in fig. 5 together with data achieved by THERMIX/KONVEK. As can be deducted from fig. 5 the results agree well with previous results from THERMIX/KONVEK taken from the reactor safety analysis report of the HTR-MODUL of 1988 [9]. The deviation is around 20K which is within the standard deviation of the results due to the accuracy of the models used.

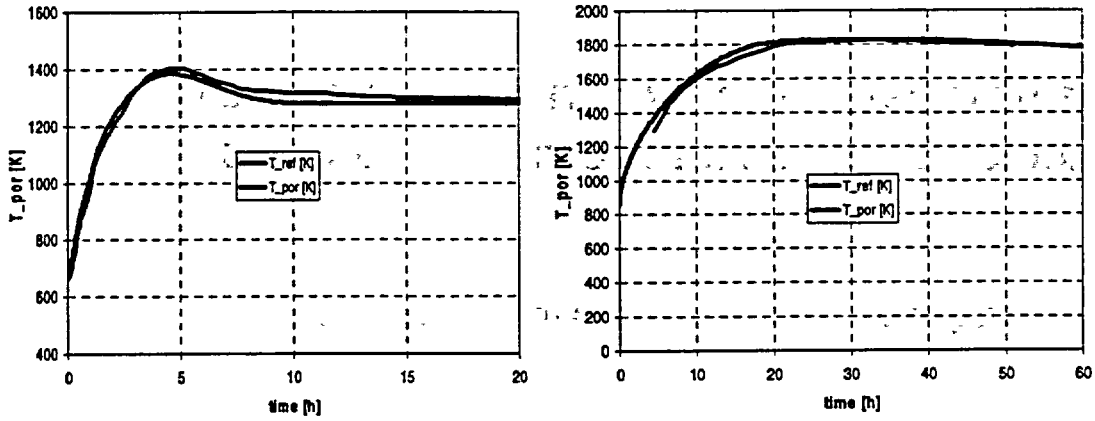

Fig. 5. Temperature in the pebble bed T_por at the point of maximum temperature of the HTR-MODUL for passive decay heat removal at nominal pressure (left) or with fast depressurisation to 1 bar (right) compared to previous results T_ref from [9] (reference data : black line; calculated data : grey/red)

5. Conclusions and Outlook

It has been shown that the CFD-code CFX-4 with our extensions predicts the three-dimensional heat transfer in modular HTRs well. The time-dependent temperatures in the reactor have been simulated accurately for the HTR-MODUL of Siemens/Interatom. These simulations are only possible on supercomputers. The preliminary steady simulations of three-dimensional effects for the PBMR have shown the influence of non-symmetric power distributions on the temperature distribution and the maximum temperature in the reactor.

Unsteady three-dimensional simulations are possible and will be performed for the PBMR.

References

[1] Reactor safety analysis report of the South-African Pebble-Bed Modular Reactor (PBMR), Rev. E, PBMR Ltd., Centurion, South-Africa, 2000

[2] Reutler, H. and Lohnert, G.H. : *Der modulare HTR - Ein neues Konzept für den Kugelhaufenreaktor*, Atomwirtschaft, Januar 1982, pp. 18-21

[3] User's manual to CFX-4 Version 4.4, AEA Technology, Harwell, UK, 2001

[4] Stöcker, B. : *Untersuchungen zur selbsttätigen Nachwärmeabfuhr bei Hochtemperaturreaktoren unter besonderer Berücksichtigung der Naturkonvektion*, Dissertation RWTH Aachen, Forschungszentrum Jülich, Jül-3504, 1998

[5] Becker, S. and Laurien, E. : *Numerical simulation of the convective heat transport in pebble beds at high temperatures*; Annual Meeting Nuclear Technology 2001, May 14-17, 2001, Dresden, Germany

[6] Zehner, P. and Schlünder, E.U. : *Wärmeleitfähigkeit von Schüttungen bei mäßigen Temperaturen*, Chemie-Ing.-Techn., 1970, pp. 933-941

[7] Cheng, P. and Hsu, C.T.: *Fully-developed, forced convective flow through an annular packed-sphere bed with wall effects*, Int. J. Heat Mass Transfer, Vol. 29, 1986, pp. 1843-1853

[8] Bauer, R.: *Effektive radiale Wärmeleitfähigkeit gasdurchströmter Schüttungen mit Partikeln unterschiedlicher Form und Größenverteilung*; Dissertation, Universität Karlsruhe, 1977

[9] Reactor safety analysis report of the HTR-MODUL, Siemens/Interatom, Germany, 1988

DECAY HEAT REMOVAL BY PASSIVE MEANS IN CASE OF A BLOCK TYPE HTR REACTOR CORE - CFD ANALYSIS

A. Woaye-Hune and S. Ehster, FRAMATOME-ANP, France

Paper will be handed out separately

THERMAL HYDRAULIC SIMULATIONS ON HIGH TEMPERATURE REACTORS

N.TAUVERON, M.ELMO, O.CIONI, T. CHATAING

Department of Thermal hydraulics and Physics
C.E.A., 17 rue des Martyrs, 38054 Grenoble - France

ABSTRACT

This paper describes two typical studies on thermal hydraulic problems on high temperature reactors. The first concerns the core heat transfer performance of a pebble bed core (which have some different characteristics from the PBMR design),the second deals with thermal stresses on the core outlet region of the GT-MHR concept. These simulations are performed with the TRIO_U/PRICELES code developed by the C.E.A.

1 Introduction

As a result of a screening review of candidate technologies, CEA has selected an innovative concept of high temperature gas cooled reactor with a fast neutron spectrum [1]. This long term objective partly builds on the current updating of High Temperature Reactor technologies that CEA carries out with European networks to support the development of Modular Helium cooled Reactors by Framatome-ANP and international partners. In this context the GT-MHR and the PBMR designs are under inverstigation. Thermal hydraulic performances are a key issue for the core design, the evaluation of the thermal stresses on the structures, the efficiency of decay heat removal systems and safety analysis. This paper presents two typical studies concerning the core heat transfer performance of a pebble bed core (which have some different characteristics from the PBMR design), and thermal stresses on the core outlet region of the GT-MHR concept.

The TRIO_U/PRICELES code and the CATHARE code used for these applications are both developed by CEA. The TRIO_U/PRICELES code [2] is a general 3D CFD code in which various statistical turbulence models (RANS) and Large Eddy Simulation models are implemented.The CATHARE code [3], developed in collaboration between CEA, EDF, IPSN and FRAMATOME, is the reference code in France for the PWR safety analysis, but it has also been used for other reactors applications.

2 Thermal Fluctuations in the Lower Plenum on the GT-MHR Design

2.1 Technical context : GT-MHR Core Outlet Flow

In the GT-MHR core design, the helium is flowing downwards through vertical columns at the exit of the hexagonal blocks (Fig. 1). The cylindrical structure of each column is perforated by holes which allows the helium to exit horizontally in a plenum limited by two horizontal plates. The helium is then flowing in the radial direction to the hot duct which connects the core vessel to the power conversion system vessel. These internal structures below the reactor core have an important mechanical function as they take part to the support of the core. The structures placed at the outlet of the core are submitted to a helium temperature of about 850°C. However, the cold helium coming from the cold duct at a temperature of 490°C is flowing under the lower plate of the previous plenum. The vertical columns

may also be affected by significant temperature gradients and temperature fluctuations which can led to thermal fatigue phenomena. As a consequence, the estimation of the thermal stresses induced by the temperature gradients on the vertical columns and the lower horizontal plate is required. This estimation is rather difficult because of the complex flow pattern in the plenum.

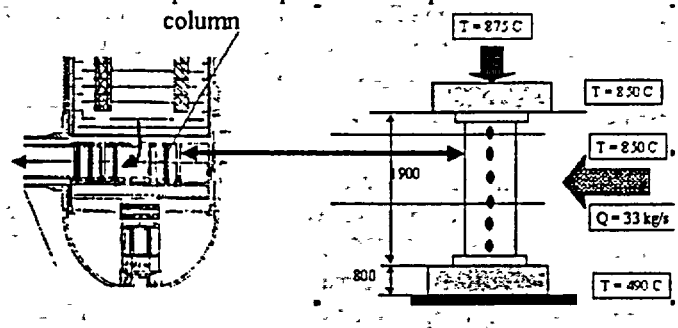

Figure 1: Modelling of the core outlet region

2.2 Requirement : global thermal hydraulic behaviour

The understanding of the core outlet flow requires a quantitative description of global thermal hydraulic behaviour. For the calculation of the nominal situation, the whole GT-MHR plant has been modeled with the CATHATE code, with the following characteristics. The core is modeled by two parallel 1D circuits. The turbine and the compressors are modeled in a first step without dynamical characteristics, but these developments are in progress. The recuperators, pre-cooler and inter-cooler are modeled by two parallel counter current 1D circuits, which can exchange heat through a wall. Pressure drop and heat transfer correlations are based on the geometrical and thermal hydraulic characteristics of the component. The various volumes and plena are modeled by a 0D approach. A nominal steady state situation at a power of 600 MW is presented (Fig. 2). The evolution of the pressure and temperature along the circuit is estimated. These results are in good agreement with reference data on the GT-MHR design.

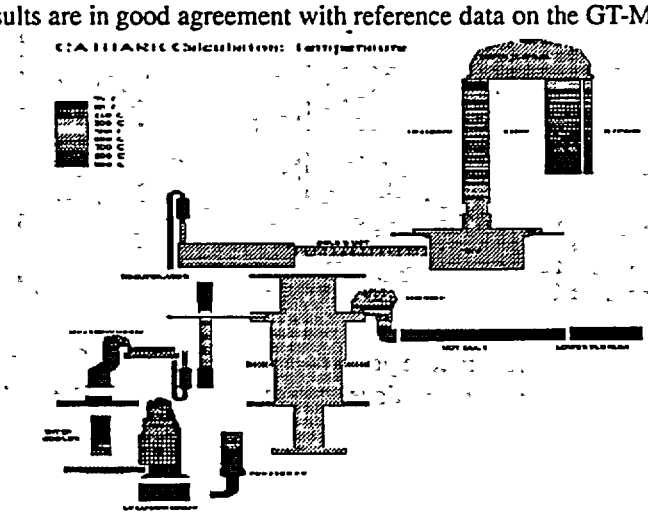

Figure 2: Global calculation of the GT-MHR using the CATHARE code (temperature field)

2.3 Conditions of the calculation

As a preliminary step, 3D computations of one isolated column were performed to evaluate the ability of the Large Eddy Simulation approach to calculate the local thermal hydraulic characteristics. Due to the huge simulation domain, a insufficiently resolved Large Eddy Simulation approach is used which can be characterised as " simulation of the system instabilities ". This approach has been widely validated for PWR applications. As the flow patterns are highly dependent on the transverse flow rate, a computation with a transverse flow rate is presented which corresponds to a location of the column near the outlet of the plenum.

The main physical characteristics of the computation which takes into account both the heat conduction in the solid and the heat and mass transport in the gas-phase are : a pressure of 7 Mpa, a column inlet flow rate of about 0.5 kg/s and a temperature of 875°C, a transverse flow rate of 33.5 kg/s and a temperature of 850°C, the downward face of the lower plate maintained at 490°C.

The present computation is using Boussinesq's approximation and the similarity of heat and momentum transfer (Prandtl modeling), non slip boundary conditions on walls, typical mesh size of about 10 mm what leads to about 1 million meshes (fluid and solid).

2.4 Main results

The computation results presented in (Fig. 3) show :

- a not expected motion of the transverse flow into the upper part of the column
- the jet through each opening of the column depend on the vertical and angular position of the opening
- the wake flow pattern of the transverse flow around the column, with typical von-Karman instabilities
- the hot helium penetrating in the plenum and mixing with the transverse flow.

These preliminary numerical results give a first evaluation of the temperature gradients and the temperature fluctuations on the structures of the lower plenum.

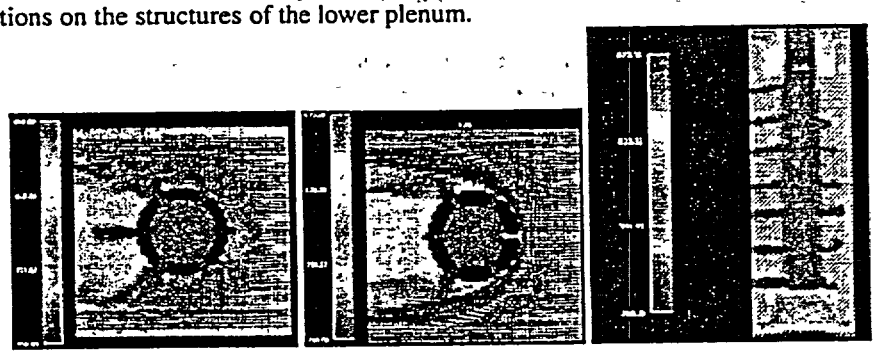

Figure 3: Computation of the GT-MHR core outlet region using the TRIO_U/PRICELES code (temperature field). The two first figures are horizontal sections of a column, the third is a vertical section

2.5 Future work on the subject

Further computations with the same spatial resolution are in progress using up to 7 columns to take into account more realistic transverse flow conditions. A cross-comparison between different turbulence codes is organised by the CEA on the subject in 2002.

3 Quasi-compressible flows model and application to the pebble bed modular reactor

In gas cooled reactor studies, the fluid is considered as a perfect gas but it cannot be considered as an incompressible fluid due to the large temperature variations. A low mach number model [4] is then used in order to take into account the density variations.
The quasi-compressible model is built as follows: the pressure is split into two parts $P(t;\overline{x}) = P_{th}(t) + P_h(t;\overline{x})$ with $P_h << P_{th}$: P_{th} is the thermodynamic pressure, only time-dependent and it is used in the perfect gas law to compute the density. The acoustic waves are then filtered out. P_h is the hydrodynamic part of the pressure and it is used in the momentum balance equations.

According to this splitting, the governing equations of the quasi-compressible model is written :

$$\begin{cases} \partial_t \rho \overline{u} - div\left(\mu\left(\overline{\overline{\nabla}}\overline{u} + \overline{\overline{\nabla}}\overline{u}^T\right) - \frac{2}{3}\mu div(\overline{u})\overline{\overline{I_d}}\right) + div(\rho\overline{u}\,\overline{u}) = \rho\overline{g} - \overline{\nabla}P_h \\ \rho C_p \partial_t T - div\left(\lambda\overline{\nabla}T\right) + \rho C_p \overline{u}\cdot\overline{\nabla}T = \frac{dP_{th}}{dt} \\ \partial_t \rho + div(\rho\overline{u}) = 0 \\ P_{th} = \rho R T \end{cases}$$

where $\overline{u}$, ρ, C_p, T, μ, λ are the velocity, the density, the calorific capacity, the temperature, the first viscosity and the conductivity of the gas respectively; $\overline{g}$ represents a constant gravity.
The thermodynamic pressure is determined by solving an ordinary differential equation. Moreover the viscosity is computed by the Sutherland's law while the conductivity is constant. In addition the Darcy and Forchheimer laws are used to model the porosity of the medium (Ergun equation).

The precedent models are introduced in the thermal-hydraulic code Trio_U/PRICELES. In this section, we present an application of these models to a pebble bed modular reactor. This approach was validated in a wide range of applications [5].

3.1 Problem description

The geometry of the reactor is cylindric (height $H = 8.49$ m ; radius $R = 1.75$ m). The reactor is a bed of spherical particles of diameter $D_p = 6$ cm : the indice of porosity of the bed is $\phi = 0.38$. In the core there are three zones of pebbles with different neutronical properties, generating different thermal power sources (P_1, P_2, P_3) :
1. the relectrice zone : inactive pebbles $R_1 = 0.77$ m, $P_1 = 0$ MW.m^{-3}
2. intermediate zone $R_2 = 1.1$ m, $P_2 = 2.3$ MW.m^{-3}
3. active zone $R_3 = 1.75$ m, $P_3 = 4.6$ MW.m^{-3}

The cooled gas is Helium under high pressure (70 bars) and high temperature (1000 K) :
$\mu = 4.54911 \times 10^{-5}$ kg.m^{-1}.s^{-1}; $\rho = 3.34362$ kg.m^{-3}; $\lambda = 0.351647$ W.m^{-1}.K^{-1}; $C_p = 5193$ J.kg^{-1}.K^{-1}

The gas runs across the pebble bed from the top with the inlet velocity $V_e = 5$ m.s^{-1} and inlet temperature $T_e = 809$ K.

Due to the symmetry of the reactor, only the quarter of the geometry is studied. A three dimensional structured mesh of about 26000 elements is used.

The figure 4 a) shows the computing domain with boundaries conditions and it also illustates the geometry.

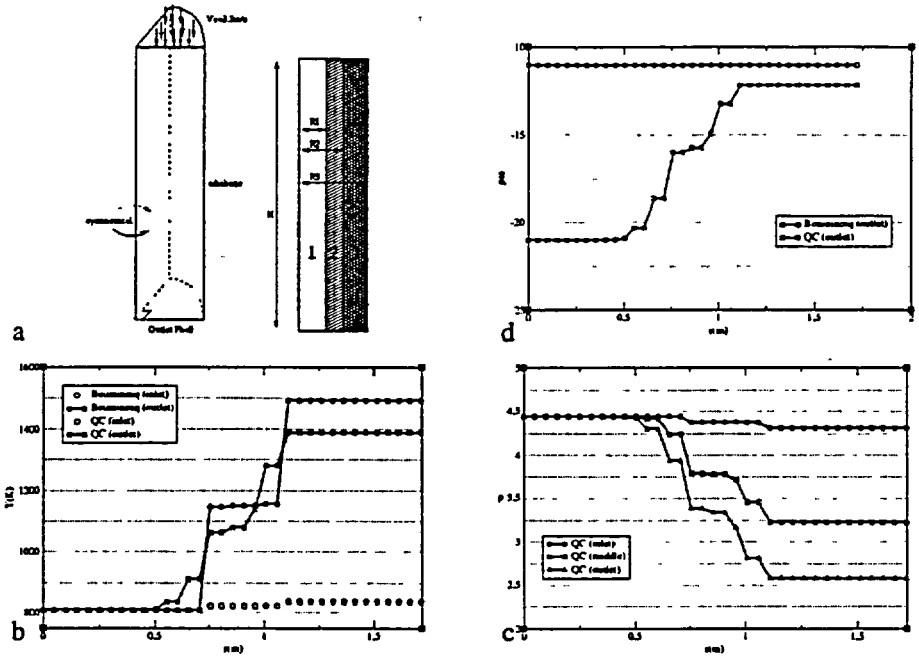

Figure 4: a) Computing domain and boundaries conditions; b) Temperature profiles in the inlet and outlet sections for Boussinesq and quasi-compressible calculations (qc); c) Density profiles in the inlet, middle and outlet sections (qc); d) Density weighted vertical velocity (qc).

3.2 Numerical results

In this paper, two calculations were performed: the first with Boussinesq's approximation, the second with quasi-compressible model.
The Fig. 4 b) shows the temperature profiles in the inlet and outlet sections for both Boussinesq and quasi-compressible calculations. It is seen that the maximum value is reached for the Boussinesq case. The Fig. 4 c) shows the density in the inlet, middle and outlet sections for the quasi-compressible calculation. The density shows a strong dependence on the temperature. The fluid becomes lighter as temperature increases. The Fig. 4 d) shows the density weighted vertical velocity for the quasi-compressible case. It can be observed how the dilatability affects the velocity field.

References

[1] CARRE, F., THOMAS, J.B., BOIDRON, M., "Significance of the Fuel Cycle Aspects in CEA Studies on Future Nuclear Systems", Proc.of GLOBAL 2001, Paris, France.

[2] BIEDER,U.,CALVIN,C.,EMONOT,P., "PRICELES : An object oriented code for industrial Large Eddy Simulations" Proc.of the 8th Annual conf. of the CFD Society of Canada, Montreal, June11-13, 2000.

[3] BESTION, D., BARRE, F., FAYDIDE, B., "Methodology, status and plans for development and assessment of Cathare code" OECD/CSNI, Annapolis, USA, November 5-8, 1999

[4] PAILLERE, H., VIOZAT, C., KUMBARO, A., TOUMI, I. Comparison of low Mach number models for natural convection problems, Heat and Mass Transfer 36, pp 567-573, 2000

[5] ELMO, M., CIONI, O. Validation et utilisation du module quasi-compressible du code TRIO_U/PRICELES, N. T. DEN/DTP/SMTH/LDTA/2002-019, 2002

STEADY-STATE AND ACCIDENT ANALYSES OF PBMR WITH THE COMPUTER CODE SPECTRA

MAREK M. STEMPNIEWICZ
NRG, An ECN KEMA Company,
Utrechtseweg 310, 6800 ET Arnhem, The Netherlands

ABSTRACT

The SPECTRA code is an accident analysis code developed at NRG. It is designed for thermal-hydraulic analyses of nuclear or conventional power plants. The code is capable of analysing the whole power plant, including reactor vessel, primary system, various control and safety systems, containment and reactor building. The aim of the work presented in this paper was to prepare a preliminary thermal-hydraulic model of PBMR for SPECTRA, and perform steady state and accident analyses. In order to assess SPECTRA capability to model the PBMR reactors, a model of the INCOGEN system has been prepared first. Steady state and accident scenarios were analyzed for INCOGEN configuration. Results were compared to the results obtained earlier with INAS and OCTOPUS/PANTHERMIX. A good agreement was obtained. Results of accident analyses with PBMR model showed qualitatively good results.

It is concluded that SPECTRA is a suitable tool for analyzing High Temperature Reactors, such as INCOGEN or for example PBMR (Pebble Bed Modular Reactor). Analyses of INCOGEN and PBMR systems showed that in all analyzed cases the fuel temperatures remained within the acceptable limits. Consequently there is no danger of release of radioactivity to the environment. It may be concluded that those are promising designs for future safe industrial reactors.

1. INTRODUCTION

The development of High Temperature Reactors (HTR) is taking place for more than thirty years now. The major developmental activities presently proceeding for introduction of HTR power systems are the 600 Gas Turbine - Modular Helium Reactor (GT-MHR), and the 268 MWth Pebble Bed Modular Reactor (PBMR). PBMR is currently planned to be built in the Republic of South Africa.

An HTR pre-feasibility study has been performed in the past in the Netherlands[1], using a 40 MWth base configuration, named INCOGEN. A number of analyses were performed for the INCOGEN configuration, including steady-state and accident scenarios performed with INAS and PANTHERMIX/OCTOPUS codes.

Nuclear Research and Consultancy Group (NRG) is participating in the PBMR project, performing design and safety analyses. The aim of the work presented in this paper was to prepare a preliminary thermal-hydraulic model of PBMR for the computer code SPECTRA[2], and perform steady state and accident analyses. In order to assess SPECTRA capability to model the PBMR reactors, a model of the INCOGEN system has been prepared first. Steady state and accident scenarios were analyzed for INCOGEN configuration. Results were compared to the results obtained earlier with INAS and OCTOPUS/PANTHERMIX.

The first part of this paper presents comparison of SPECTRA results obtained for INCOGEN, for steady state cases and two accidents: Loss of Coolant Accident (LOCA), and Loss of Flow Accident (LOFA) with the results of the INAS and OCTOPUS/PANTHERMIX codes. The second part presents results of steady state calculations as well as LOCA and LOFA cases obtained with the preliminary SPECTRA model of PBMR.

2. SPECTRA CODE AND IT'S APPLICABILITY FOR PBMR

The SPECTRA code is an accident analysis code developed at NRG, the Netherlands. SPECTRA (Sophisticated Plant Evaluation Code for Thermal-hydraulic Response Assessment)[2], is a computer program designed for thermal-hydraulic analyses of nuclear or conventional power plants. The code is capable of analysing the whole power plant, including reactor vessel, primary system, various control and safety systems, containment and reactor building. The models applied in the code were selected after an extensive literature review, as well as review of models available in other codes (CONTAIN, MAAP, MELCOR, RELAP, TRAC-BF1). The best available models were selected, which makes SPECTRA not only an accident analysis tool but also a library of physical models, well documented and tested, and easy to use.

In case of PBMR an important issue is the ability of a computer code to model multiple non-condensable gases, in particular helium. In contrast to codes like RELAP, TRAC, which are basically steam-water codes, SPECTRA has been built to allow presence of a mixture of multiple gases. SPECTRA contains a built-in library of fluid properties, consisting of the properties of water, steam, and non-condensable gases, such as H_2, He, N_2, O_2, CO_2. The gas properties are calculated using a large database, covering the range from 270 K to 2070 K, and from virtually 0 Pa to 10^7 Pa. If needed, properties of other gases may be easily implemented into the program. The solution scheme is general, and may theoretically accommodate any number of gases. Practical limit is imposed by the physical memory size of the computer designated to perform calculations.

A reactor kinetics model together with an isotope transformation model are present in the SPECTRA code. They are suitable for simple (point kinetics) analysis of reactivity transients. The isotope transformation model can deal with 200 isotopes; typically about 30-40 isotopes are tracked, including fuel chains, main poisons, such as Xe-135, Sm-149, and their precursors, as well as main decay heat producers.

3. INCOGEN Analyses - Comparison with INAS, OCTOPUS/PANTHERMIX

This section provides description of the steady state and accident analyses performed for the High Temperature Reactor (HTR), the conceptual design of INCOGEN. All data required to build the SPECTRA model of the INCOGEN reactor was obtained from reference [1]. The SPECTRA model of the INCOGEN reactor is shown in figure 1. The model consists of 8 Control Volumes (CV), 7 Junctions (JN), 9 Solid Heat Conductors (SC). The net enclosure thermal radiation model is used, with two enclosures: the reactor core (TR-101 - TR-105), and the gas inlet annulus (TR-202 - TR-204). The Reactor Kinetics model is used to calculate core power.

The following calculations were performed:

- Steady state analyses:
  - Steady state run with constant power (SS-CP),
  - Steady state run with reactor kinetics, reactivity control by continuous fuel addition (SS-RK-1).
  - Steady state run with reactor kinetics, reactivity control by temperature changes (SS-RK-2).
- Accident analyses:
  - Loss of Flow Accident (LOFA).
  - Loss of Coolant Accident (LOCA).

The first steady state calculation was performed using a constant reactor power. This was done just to obtain a good starting point for the subsequent analyses with the reactor kinetics model. The next two steady state analyses were performed using two different methods of reactivity control. First, the reactivity was controlled by a continuous fuel addition (SS-RK-1). Fuel addition rate was

controlled in order to keep the desired reactor power. In the next run (SS-RK-2) no fuel was added to the core. The reactivity loss due to slow fuel burn-up was compensated by a slow temperature decrease, which added reactivity due to negative reactivity coefficient. Results of these two runs are compared to the results of the INAS code (presented in reference [1]) in figures 2 and 3.

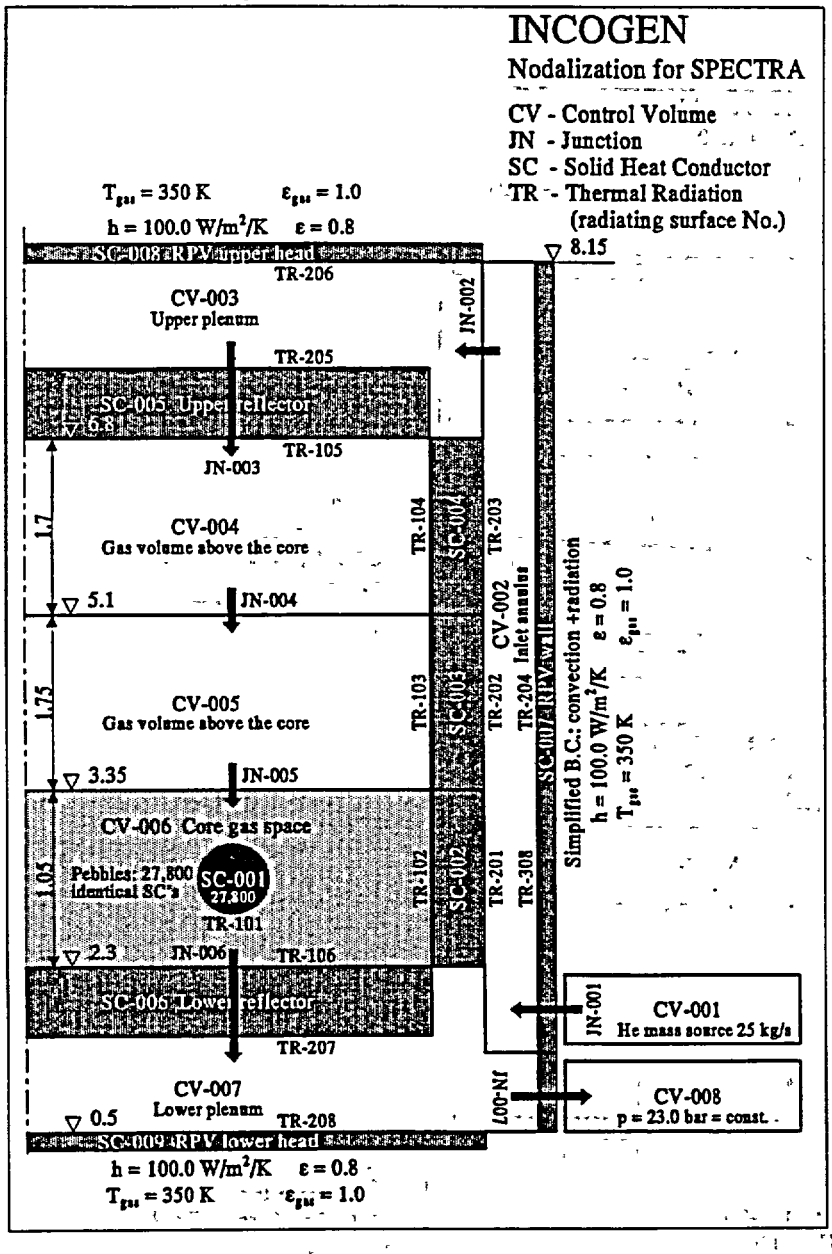

Figure 1
SPECTRA model of the INCOGEN reactor.

Figure 2 shows the fuel loading rate in case SS-RK-1. The SPECTRA calculated stable value of fuel loading rate is equal to about 10^{-8} [s^{-1}], a little more than 20 pebbles per day. The value obtained from the INAS code for the fresh core configuration is equal to 48 pebbles per day, more than twice more than the SPECTRA value. This discrepancy is caused by a non-uniform neutron flux distribution (no upper reflector), which cannot be taken into account with the point kinetics model. The neutron flux in the upper part of the core is nearly twice smaller than in the lower part of the core. The fresh pebbles, landing on the top of the core, therefore "see" only relatively small neutron flux and therefore their reactivity worth is significantly smaller than it would be if the neutron flux was uniform (as it is, by definition, in the point kinetics model). Consequently, more pebbles are needed to maintain criticality than it is predicted by the point kinetics model. In case

of PBMR reactor the neutron flux is much more uniform and the point kinetics provides more accurate results (see section 4).

Figure 3 shows core average temperature during the second day of the SS-RK-2 run. The temperature decreases steadily, with the rate of about 7.1 K per day. The value obtained from the INAS code is 7.8 K per day. The agreement between SPECTRA value and the value from INAS is in this case relatively good.

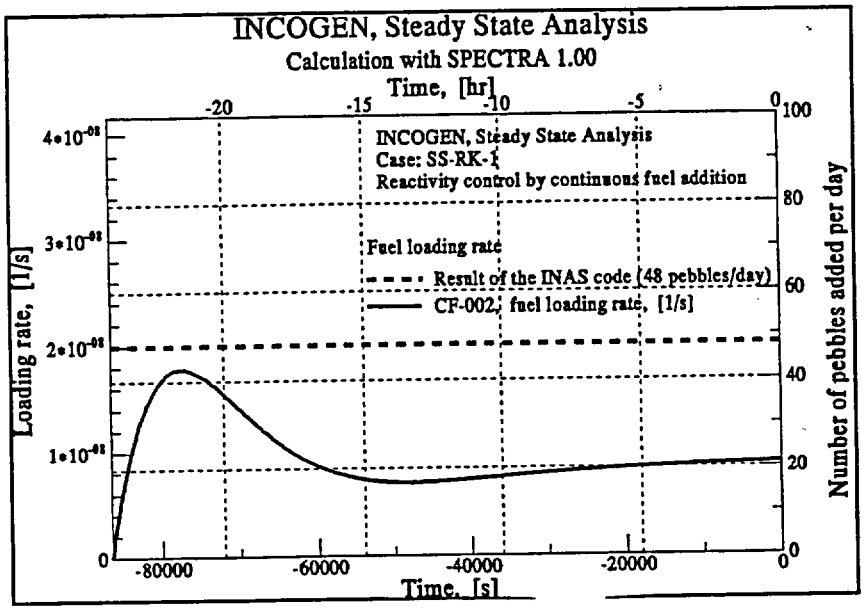

Figure 2
Fuel loading rate, INCOGEN, Case SS-RK-1, continuous fuel addition, comparison of SPECTRA and INAS results.

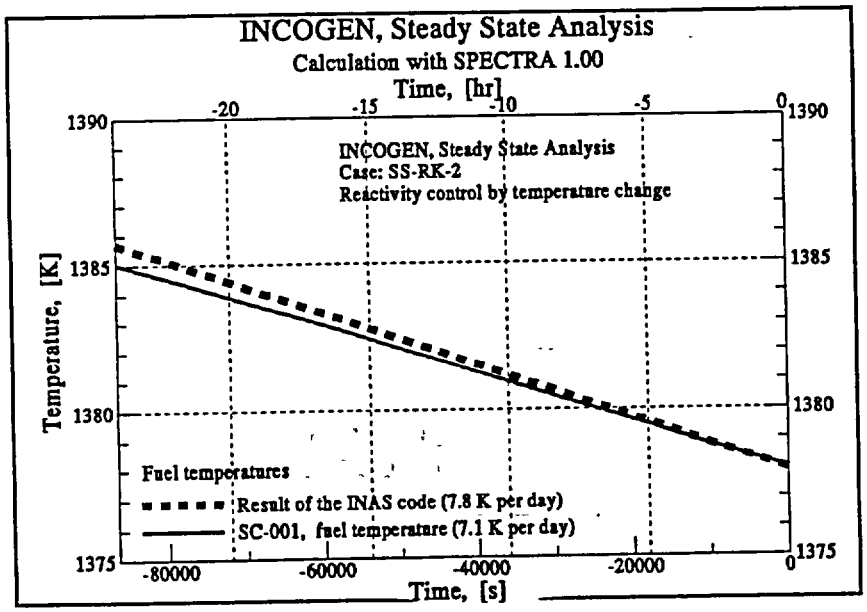

Figure 3
Core average temperature, INCOGEN, Case SS-RK-2, no fuel addition, comparison of SPECTRA and INAS results.

Results of accident analyses are shown in figures 4 - 9. The reactivity calculated for the LOFA case by the OCTOPUS/PANTHERMIX code and the SPECTRA code are compared in figures 4 and 5. Both result are in good agreement as to the depth and the duration of the "reactivity well". The reactivity behavior in OCTOPUS/PANTHERMIX show some irregularities around 500 min and 900 min (figure 4), the nature of which are not quite clear. Probably they are a consequence of some space dependent effects, that cannot be captured with point kinetics.

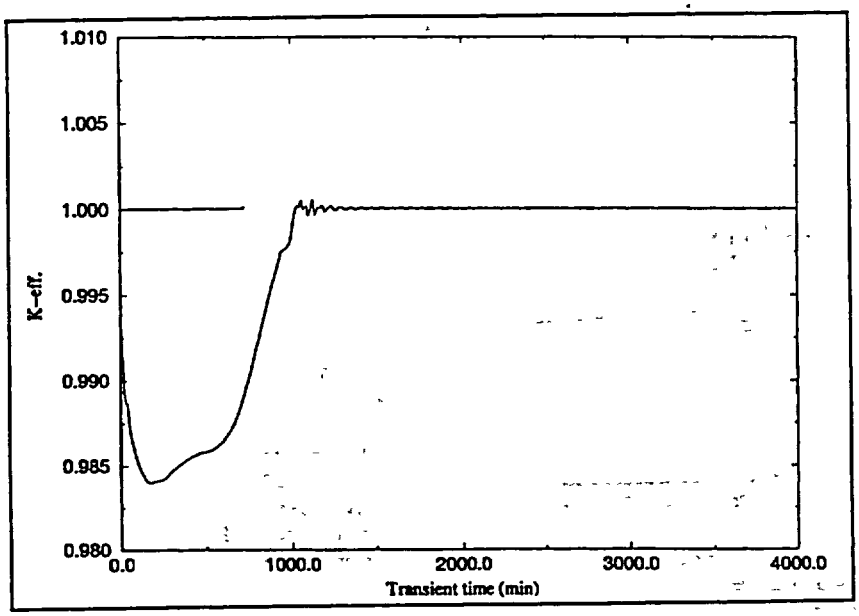

Figure 4
Total reactivity,
INCOGEN, Case: LOFA,
Loss of Flow Accident,
results of OCTOPUS/
/PANTHERMIX code
system (reproduced from
reference [1].

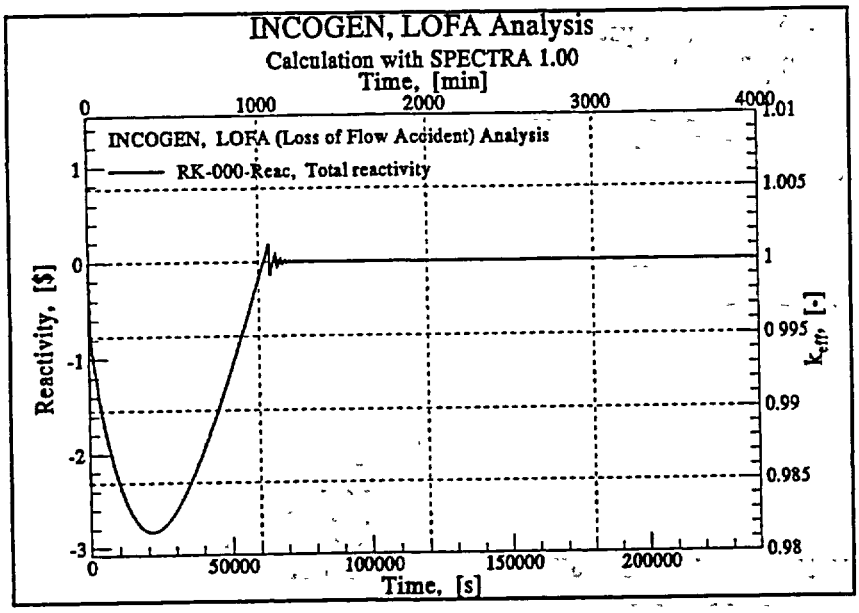

Figure 5
Total reactivity,
INCOGEN, Case: LOFA,
Loss of Flow Accident.
SPECTRA results.

Figures 6 and 7 show reactor power calculated for both LOFA and LOCA cases by OCTOPUS/PANTHERMIX and SPECTRA respectively. Generally the agreement is very good. In SPECTRA the power peaks occurring just after reaching criticality are higher, but the OCTOPUS/PANTHERMIX results indicate that the peaks might have been flattened by rare plot frequency. OCTOPUS/PANTHERMIX show somewhat oscillating long term reactor power for LOFA case. The nature of this oscillations are unclear. Possibly they are created by some numerical problems (for example explicit coupling between the codes which constitute the OCTOPUS/PANTHERMIX code system). These oscillations should be distinguished from the oscillations which occur just after reaching criticality, and are observed in all calculations. These are rather regular oscillations, with the time period close to 2000 s (half an hour). Those oscillations are physical and are caused by inertial effects in thermal-neutronic interactions.

In both LOCA and LOFA cases the calculated maximum fuel temperature remained within acceptable limits. In all calculations the fuel temperature did not exceed 1500°C.

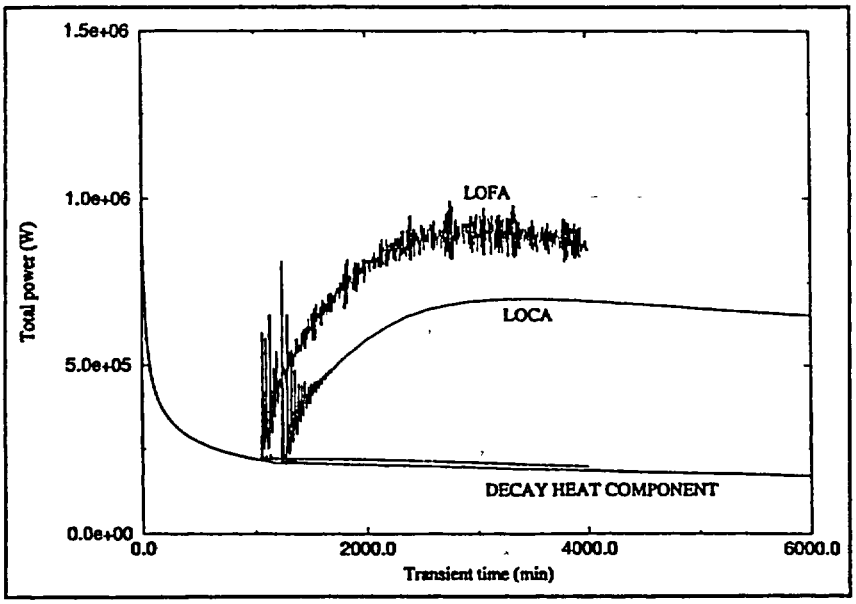

Figure 6
Reactor power, INCOGEN, Cases: LOFA and LOCA, results of OCTOPUS/ /PANTHERMIX code system (reproduced from reference [1]).

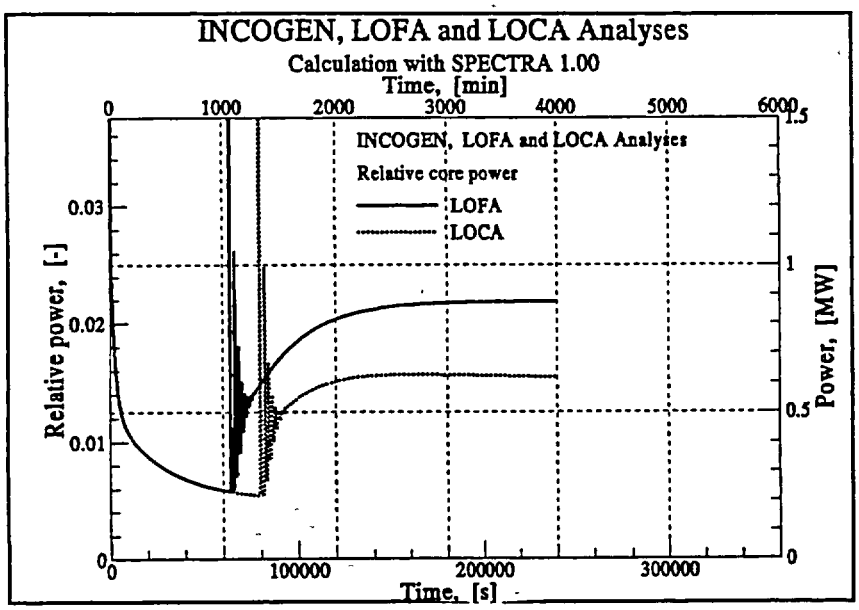

Figure 7
Reactor power, INCOGEN, Cases: LOFA and LOCA, SPECTRA results.

4. PBMR ANALYSES

SPECTRA model of PBMR[3] is shown in figures 8 and 9. The model includes the Reactor Unit (figure 8), the Power Conversion Unit (figure 9), the Confinement Building, as well as various safety systems and the environment. The model is considered to be preliminary. Some parts of the system were modelled in a simplified way because no sufficient data were available at NRG. In the future the model will be updated according to the most recent data and design drawings. This task will be performed within the cooperation between the South African PBMR and NRG.

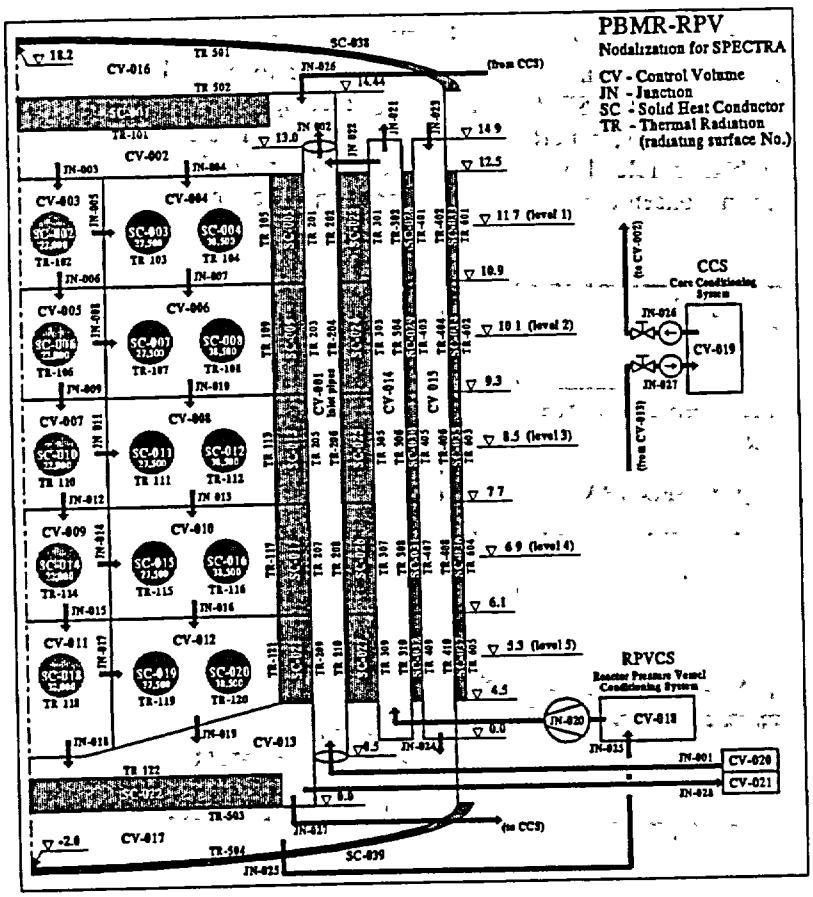

Figure 8
SPECTRA model of PBMR.
Nodalization of the Reactor Unit.

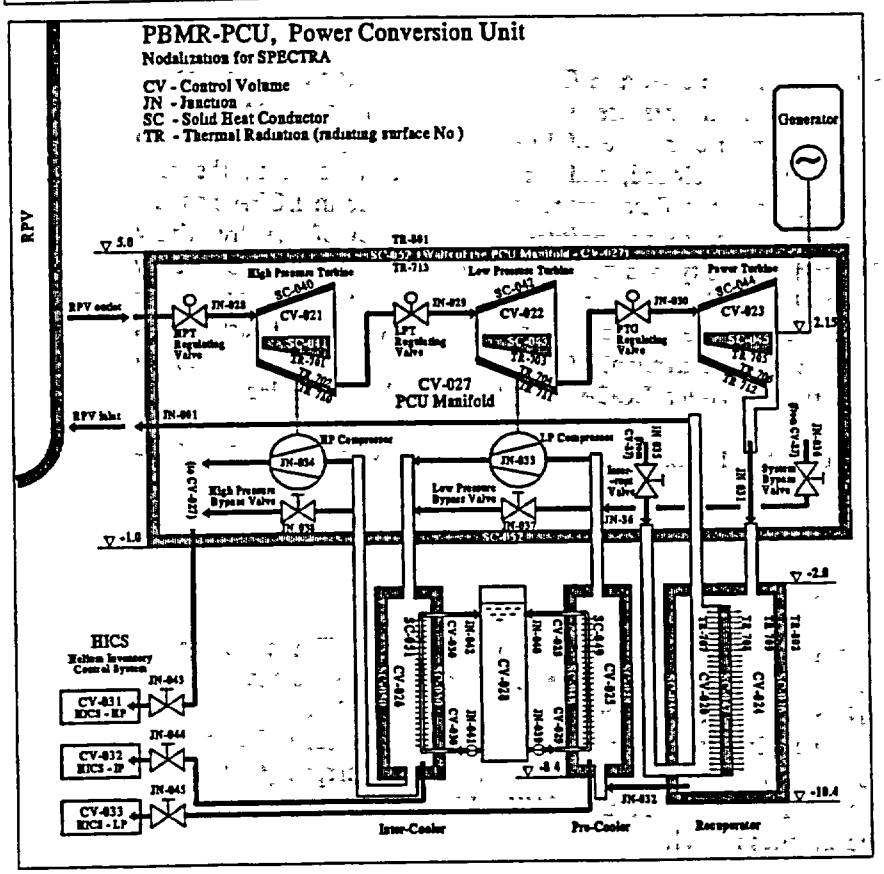

Figure 9
SPECTRA model
of PBMR.
Nodalization of the Power
Conversion Unit.

As in case of INCOGEN, steady state and accident analyses (LOCA and LOFA) were performed with the model. Steady state calculation was performed using continuous fuel reload to control reactivity. Resulting fuel reload rate is shown in figure 10. SPECTRA results are compared with the values obtained with PATHERMIX and VSOP codes, reported in [4]. The calculated reload rates are in good agreement. (The initially higher reload rate in SPECTRA was needed to overcome some small initial changes in Xenon concentration, resulting from imperfections in defining the initial conditions.)

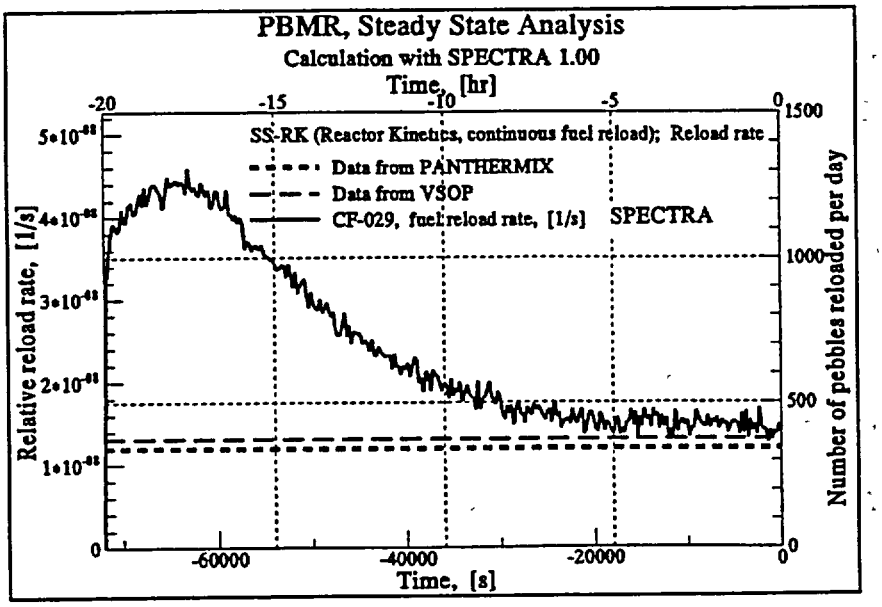

Figure 10
Fuel reload rate, PBMR, comparison of SPECTRA PANTHERMIX and VSOP results.

The results of the LOCA and LOFA analyses are shown in figures 11 and 12. The main difference between LOCA and LOFA cases is the system pressure during the major part of the transient (about 70 bar in case of LOFA and atmospheric in case of LOCA). In the high pressure case a relatively good natural circulation flow was developed, and some heat was removed by the pre-cooler and the inter-cooler. As a consequence the fluid temperature was lower in LOFA and the reactivity was higher (negative temperature reactivity coefficient). The depth of the "reactivity well" was smaller in case of LOFA, and criticality was reached faster (figure 11). After criticality was reached, the power stabilized at higher level in case of LOFA, since more power was removed by the pre- and the inter-cooler. In the accident scenarios it was assumed that pumps cooling the secondary side of the coolers were available (the only available active systems). If these pumps were unavailable the difference between LOCA and LOFA would be smaller.

In both LOCA and LOFA cases the calculated maximum fuel temperatures were below 1400°C - within acceptable limits.

5 SUMMARY AND CONCLUSIONS

Steady state operation and accident scenarios were analyzed with the SPECTRA code for the INCOGEN and the PBMR reactors. In case of INCOGEN the results of steady state analyses were compared to the results of the INAS code. A good agreement was obtained for the run with reactivity control by temperature changes. In case of reactivity control by continuous fuel addition a discrepancy was found in the fuel addition rate. It was found out that the discrepancy was caused by strongly nonuniform neutron flux distribution in the INCOGEN core, a phenomenon that cannot be represented with the point kinetics model.

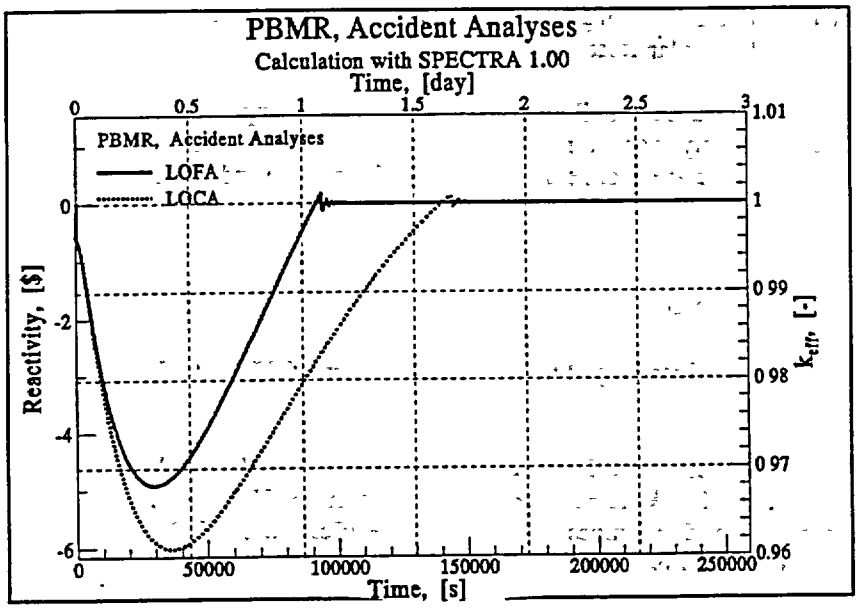

Figure 11
Total reactivity, PBMR
Cases LOFA and LOCA,
SPECTRA results

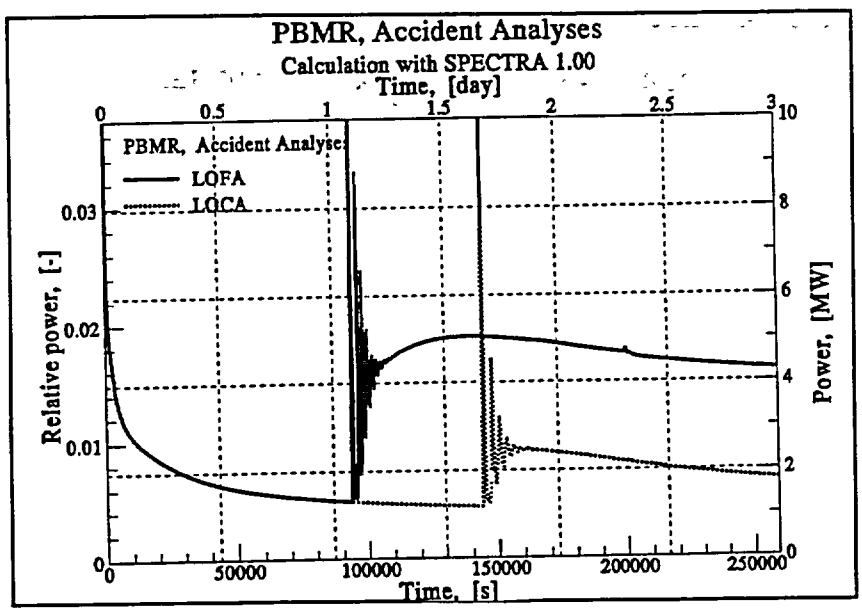

Figure 12
Reactor power, PBMR,
Cases: LOFA and LOCA,
SPECTRA results.

In case of PBMR the results of steady state analysis were compared to the results of the PANTHERMIX and VSOP codes. A good agreement was obtained. In PBMR the core is relatively uniform because of continuous fuel reload and mixing, and the point kinetics model gives satisfactory results.

Results of accident analyses with the INCOGEN model were compared with the results of OCTOPUS/PANTHERMIX code system. Generally a very good agreement was obtained. Results of accident analyses with PBMR model showed qualitatively qood results. Further improvement in the detail of modelling is needed to provide reliable results.

It is concluded that SPECTRA is a suitable tool for analyzing High Temperature Reactors, such as INCOGEN or for example PBMR (Pebble Bed Modular Reactor).

Analyses of INCOGEN and PBMR systems showed that in all analyzed cases the fuel temperatures remained within the acceptable limits. Consequently there is no danger of release of radioactivity to the environment. It may be concluded that those are promising designs for future safe industrial reactors.

References

[1] A.I. van Heek, et al., "INCOGEN Pre-Feasibilty Study", ECN report, PINK 1997, September 1997.

[2] M.M. Stempniewicz, "SPECTRA - Sophisticated Plant Evaluation Code for Thermal-hydraulic Response Assessment, Version 1.00; Volume 1: Program Description; Volume 2: User's Guide, Volume 3: Description of Subroutines; Volume 4: Verification", 26094-/99.52612/C, NRG report, Arnhem, October 1999.

[3] M.M. Stempniewicz, K. Spijker, "Development and Verification of SPECTRA Model of PBMR", NRG report, 20352/01.52091/C, Arnhem, February 2001.

[4] H.T. Klippel, et al., "PBMR Burn-in Core Analysis - PBMR Benchmark with PANTHER-MIX", NRG report 20429/00.38175/C (Rev. 1), Petten, December 2000.

DESIGN OF A PHYSICAL MODEL OF THE PBMR WITH THE AID OF FLOWNET

G.P. GREYVENSTEIN and P.G. ROUSSEAU
Department of Mechanical Engineering
Potchefstroom University for Christian Higher Education, Potchefstroom, 2531, South Africa

ABSTRACT

The design of a physical model of the PBMR with the aid of the code Flownet is discussed in this paper. The purpose of the physical model is to test the control strategies and operating procedures of the PBMR and also to demonstrate the accuracy of Flownet. Flownet is first used to do component matching and to determine the detail steady-state performance of the system. It is then demonstrated how the code was used to simulate the start-up procedure as well as a load following and a load rejection scenario. The study demonstrates how a micro model of the PBMR can be designed with the aid of a powerful simulation tool in a relatively short period of time and at low cost using commercially available turbochargers.

1. Introduction

The Pebble Bed Modular Reactor (PBMR) is a new type of high temperature gas nuclear power plant that is currently being developed by the South African utility ESKOM. The PBMR is based on closed cycle three-shaft recuperative Brayton cycle and it uses helium as the working fluid.

Although it is relatively easy to predict the steady-state performance of a plant such as the PBMR the prediction of the dynamic behaviour of the PBMR, which is required for the design of the control system, presents unique challenges. A great effort was therefore put into the development of a powerful new dynamic modelling tool, called Flownet.

One of the distinguishing features of the PBMR, which complicates the design of the control system, is the use of three separate shafts for the different compressor/turbine and turbine/generator pairs as opposed to one or two shafts used in other designs. In order to test the control strategies of the PBMR and also to demonstrate the accuracy of Flownet, it was decided to develop a micro model of the power conversion cycle of the PBMR. The model will use an electrical heater to emulate the nuclear reactor. Since the objective of the micro model is not to address specific issues related to the use of helium as the working fluid or to test the performance of individual components such as compressors, turbines or heat exchangers, it was decided to use nitrogen instead of helium as the working fluid. This makes it possible to use off-the-shelf single stage centrifugal compressors and turbines instead of more expensive multi-stage centrifugal or axial flow machines. It should be stressed that the micro model is not a scale model of the prototype plant but a system that will have the same characteristics and degrees of freedom and therefore also the same control topology as the prototype plant.

In this paper the design of the micro model with the aid of Flownet will be discussed. Emphasis will be placed on modelling of transient phenomena such as start-up, power control and load rejection.

2. The PBMR power conversion cycle and comparison with the micro model

A schematic layout of the PBMR power conversion cycle is shown in Figure 1. Starting at 1, helium at a relatively low pressure and temperature is compressed by a low-pressure compressor (LPC) to an intermediate pressure (2) after which it is cooled in an intercooler to state 3. A high-pressure compressor (HPC) then compresses the helium to state 4. From 5 to 6 the helium is preheated in the recuperator before entering the reactor, which heats the helium to state 8. After the reactor the hot high-pressure helium is expanded in a high-pressure turbine (HPT) to state 9 after which it is further expanded in a low-pressure turbine (LPT) to state 11. The high-pressure turbine drives the high-pressure compressor while the low-pressure turbine is drives the low-pressure compressor. After the

low pressure turbine the helium is further expanded in the power turbine to pressure 13. From 13 to 14 the still hot helium is cooled in the recuperator after which it is further cooled in the pre-cooler to state 1. This completes the cycle. The heat rejected from 13 to 14 is equal to the heat transferred to the helium from 5 to 6.

The output of the plant can be controlled by changing the helium inventory of the system or by opening and closing of the bypass valve (BPV). Changing of the helium inventory is a relatively slow process and is used for load following while the faster bypass control is used for load rejection.

Although the design of the micro model closely resembles that of the PBMR plant it is important to highlight the following differences:

(i) The micro model will use nitrogen instead of helium as the working fluid. This will not subtract from the objective of the model which is not to address specific issues related to the use of helium a the working fluid but to develop a system that will have the same overall characteristics as that of the prototype plant.

(ii) The micro model will use cheap off-the-shelve single stage centrifugal compressors and turbines rather than axial flow machines. The performance characteristics of centrifugal machines closely resembles that of axial flow machines and it will therefore suffice for the purpose of this project.

(iii) In the micro model the nuclear reactor will be emulated by an electrical resistance heater, which will, like the pebble bed reactor, have a large thermal capacity.

(iv) The generator will be emulated by a load compressor connected to a power dissipation loop consisting of a flow control valve and a heat exchanger as shown in Figure 2. Variations in load can be affected by increasing or decreasing the pressure level in the load rejection loop.

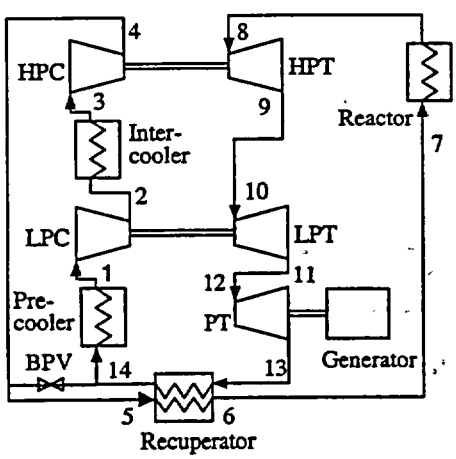

Fig 1. Schematic layout of the PBMR recuperative Brayton cycle.

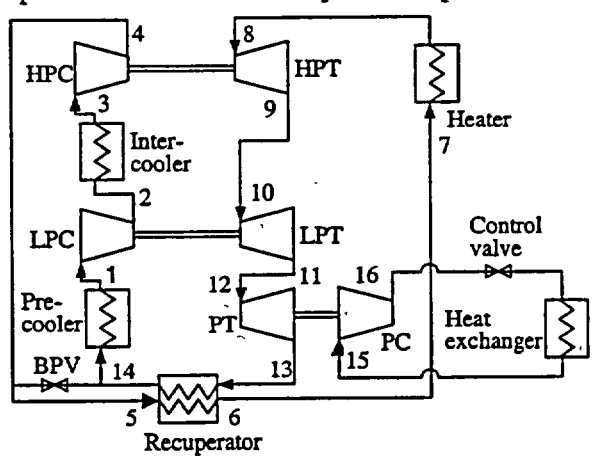

Fig 2. Layout of the micro model cycle.

3. First-order cycle analysis

The first step in the design of the micro model was to do a first-order cycle analysis to determine a suitable operating point for the system. Figures 3 and 4 show the result of this analysis with the following assumptions: compressor efficiency = 75 percent, turbine efficiency = 72 percent, precooler and intercooler outlet temperature = 26 °C, heater outlet temperature 700 °C, turbocharger mechanical efficiency = 98 percent, pipe pressure loss = 2 percent of inlet absolute pressure and heat exchanger pressure loss = 10 percent of inlet absolute pressure.

As can be seen from Figure 3 the cycle efficiency increases with recuperator efficiency over the whole range of pressure ratios. At a recuperator efficiency of 1.0 the cycle efficiency decreases with pressure ratio while it shows an optimum at recuperator efficiencies of smaller than 0.95. Figure 4 shows that the specific work increases with pressure ratio irrespective of the recuperator efficiency.

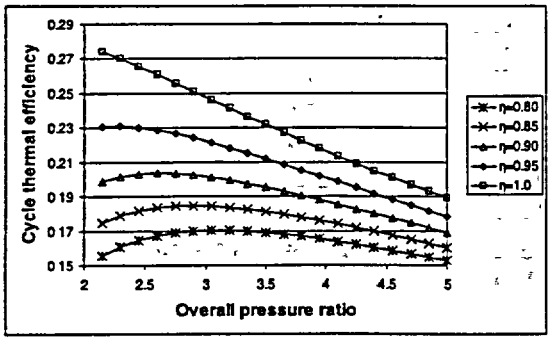

Fig 3. Thermal efficiency as function of recuperator efficiency and overall pressure ratio.

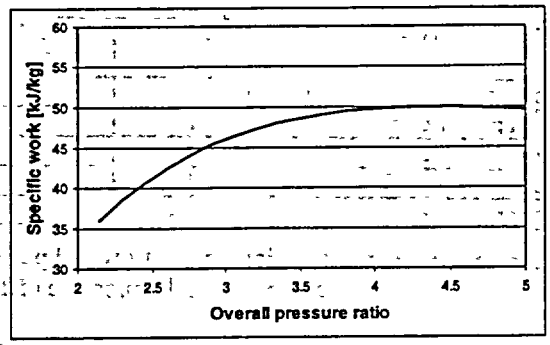

Fig 4. Specific work as function of overall pressure ratio.

The recuperator efficiency is a function of the product of the area and the overall heat transfer coefficient of the recuperator and is therefore a design choice. Since the area and therefore also the price of the recuperator increases exponentially with area, an efficiency of approximately 0.85 was chosen as a good compromise between performance and cost. Figure 3 shows that at a recuperator efficiency of 0.85 the cycle efficiency is a maximum at a pressure ratio of approximately 2.75. Figure 4 on the other hand shows that the specific work is a maximum at a pressure ratio of approximately 4.5. Since both cycle efficiency and specific work are important and since cycle efficiency is not as sensitive to pressure ratio as specific work, it was decided to design for an overall pressure ratio of approximately 4, which is a good compromise between efficiency and specific work.

4. Selection of turbochargers

The operating points of the turbo machines are determined by the system operating point and are expressed in terms of pressure ratio and non-dimensional mass flow, which is defined as

$$\bar{m} = \frac{\dot{m}\sqrt{T_0}}{p_0} \tag{1}$$

where $\dot{m}$ = mass flow rate, T_0 = total inlet temperature and p_0 = total inlet pressure. Table 1 shows the pressure ratio and non-dimensional mass flow for a mass flow of 1 kg/s and a system pressure of 100 kPa at the inlet of the low-pressure compressor.

Turbo unit	Pressure ratio	Non-dimensional mass flow [kg/s√K/bar]
Low pressure compressor	2.0	17.3
High pressure compressor	2.0	8.7
High pressure turbine	1.6	8.1
Low pressure turbine	1.7	12.4
Power turbine	1.4	20.0

Table 1. Operating points of the different turbo machines for a mass flow of 1 kg/s and LP compressor inlet pressure of 100 kPa.

As can be seen from Table 1, the power turbine, although having the lowest pressure ratio, has the largest non-dimensional mass flow. The procedure that was therefore followed was to select the turbocharger with the largest turbine from a range of commercially available units. The turbine of this unit has a non-dimensional mass flow of 10.8 at a pressure ratio of 1.4. This fixes the cycle mass flow at a value of 10.8/20 = 0.54 kg/s at a pressure level of 100 kPa at the inlet to the LP compressor.

Table 2 shows the recalculated non-dimensional mass flows along with the power rating of the different turbo machines for a cycle mass flow of 0.54 kg/s. The scaling of mass flows does not affect the pressure ratios.

Turbo unit	Pressure ratio	Non-dimensional mass flow [kg/s√K/bar]	Power [kW]
Low pressure compressor	2.0	9.3	47.4
High pressure compressor	2.0	4.7	47.4
High pressure turbine	1.6	4.4	48.4
Low pressure turbine	1.7	6.7	48.4
Power turbine	1.4	10.8	27.4

Table 2. Pressure ratio, non-dimensional mass flow and power for a mass flow of 0.54 kg/s and LP compressor inlet pressure of 100 kPa.

With the pressure ratio and non-dimensional mass flows of the other turbines known from Table 2, turbochargers were selected whose turbines match these operating points the closest. The suitability of the compressors was verified with the aid of Flownet, which solves for the speed of the different turbochargers.

5. Modelling of the system with Flownet

Flownet is a general thermal-fluid network analysis code that can model both steady-state and transient flows. Its solver, described elsewhere [1], is based on an Implicit Pressure Correction Method (IPCM) and solves for the conservation of mass and energy at all nodes and momentum in all elements. The code can deal with a wide range of standard network components such as compressors, turbines, pipes, diffusers, valves, heat exchangers and pebble bed nuclear reactors. Flownet can also deal with heat transfer between flow elements and solid structures as well as heat transfer through the solid structures. Important to mention is that heat exchangers are not handled as lumped systems but as distributed systems [2]. This is necessary to more accurately deal with the thermal capacitance of the metal separating the hot and cold streams. Flownet has been extensively validated against experimental results, other codes and analytical solutions.

Input data of compressors and turbines are provided in the form of performance maps, which gives the pressure ratio as function of non-dimensional speed, $N/\sqrt{T_0}$, and non-dimensional mass flow, $\dot{m}\sqrt{T_0}/p_0$, for different geometries such as blade angle. Any number of compressor or turbine stages as well as external loads can be placed on a single shaft and steady-state load balancing can be done by varying either the shaft speed or the master turbine geometry, typically the blade angle. In the case of transient flows Flownet calculates the shaft speed transients by taking the inertia of all rotating parts into account.

Modelling of the cycle by Flownet requires compilation of detail input data for all components such as pipes, diffusers, valves, volumes and heat exchangers. Although space does not allow us to discuss the design of the system in detail the diameters of interconnection piping and the design of heat exchangers will be given.

Pipes that connect the major components have a diameter of 200 mm, except the pipe between the power turbine outlet and the recuperator, which has a diameter of 250 mm. All heat exchangers, including the recuperator, are of a shell-and tube design with one shell pass and one tube pass. In the case of the pre-cooler, intercooler and load rejection heat exchanger the gas flows through the tube side with water flowing through the shell side, while in the case of the recuperator the low pressure hot gas coming from the LP turbine flows through the tube side with the high pressure gas from the HP compressor flowing through the shell side.

The details of the different heat exchangers are given in Table 3.

Heat exchanger	Length between tube sheets [m]	Tube inside diameter [mm]	Number of tubes	Heat transfer area[m^2]	Tube mass [kg]
Pre-cooler	2.1	10.22	575	48	513
Intercooler	1.9	10.22	450	35	363
Load rejection	2.4	10.22	450	43	460
Recuperator	5.8	10.22	1075	255	2728

Table 3. Design of the different heat exchangers.

The Flownet steady-state results for two different pressure levels are given in Table 4.

Component	LP compressor inlet pressure = 100 kPa						LP compressor inlet pressure = 250 kPa					
	P_{in} [kPa]	P_{out} [kPa]	T_{in} [°C]	T_{out} [°C]	Rating [kW]	Speed [rpm]	P_{in} [kPa]	P_{out} [kPa]	T_{in} [°C]	T_{out} [°C]	Rating [kW]	Speed [rpm]
LP Compressor	100.0	200.8	22.9	109.6	51.0	72078	250.0	496.9	26.0	112.1	124.3	71811
LP Turbine	248.5	150.5	628.5	549.0	51.0	72078	611.7	372.1	628.8	549.8	124.3	71811
HP Compressor	198.4	381.9	22.9	102.3	46.7	70009	491.3	938.0	26.1	105.1	114.1	69842
HP Turbine	378.0	249.1	700.0	628.5	46.7	70009	929.2	613.2	700.0	628.8	114.1	69842
Power Compressor	105.0	150.7	21.1	65.9	32.1	39073	262.0	372.1	22.9	66.6	76.8	38707
Power Turbine	149.7	105.0	549.0	498.2	32.1	39073	370.2	262.0	549.8	500.4	76.8	38707
Precooler	101.1	100.5	165.3	22.9	83.9	-	252.4	251.2	155.1	26.0	186.6	-
Intercooler	199.1	198.7	109.6	22.9	50.9	-	492.8	491.9	112.1	26.1	124.1	-
Recuperator hot side	103.0	102.3	498.2	165.3	202.6	-	257.1	255.2	500.4	155.1	515.6	-
Recuperator cold side	381.1	379.4	102.3	438.8	202.6	-	935.9	932.5	105.1	453.3	515.6	-
Load rejection HX	106.5	105.1	65.9	21.1	32.1	-	265.1	262.3	66.6	22.9	76.8	-

Table 4. Steady-state results for two pressure levels i.e. 100 kPa and 250 kPa at the inlet to the LP compressor.

Interesting to note is that the recuperator efficiency is 84 percent in the case of the lower pressure level and 87 percent in the case of the higher pressure level. This is due to the fact that the flow in the recuperator is laminar at the lower pressure level and turbulent at the higher pressure level.

6. Simulation of start-up

The system is started by forcing nitrogen through it by an inline blower placed just before the LP compressor while at the same time adding heat in the heater. The simulation starts with the steady-state solution at a point where the heater exit temperature is 400 °C and the LP compressor inlet pressure is 100 kPa. The heat input is now increased at such a rate that the heater exit temperature increases 50 °C/s until the exit temperature reaches a value of 700 °C where after it is kept constant at this value. During this process the pressure rise across the blower decreases. At the point where the pressure rise becomes zero the by-pass valve across the blower is opened and the blower is isolated from the main loop. From here onwards the system runs on its own.

Figure 5 shows the variation in turbine speeds and Figure 6 the variation in pressures during start-up. The speed of all the turbo chargers increases as expected and steady-state is reached in approximately 100 s. The pressure at the HP compressor outlet increases while the pressure at the inlet to the LP compressor decreases. This behaviour is due to the fact that the inventory is kept constant during the start-up.

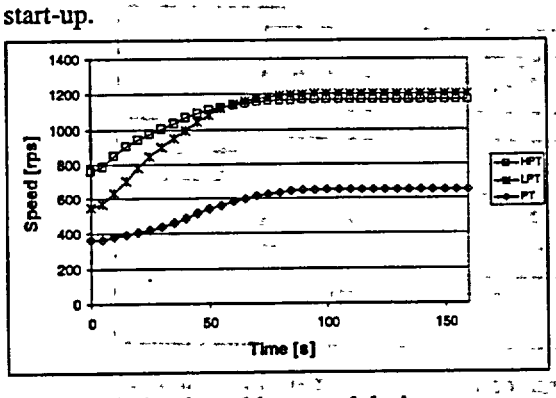

Fig 5. Variation in turbine speed during start-up.

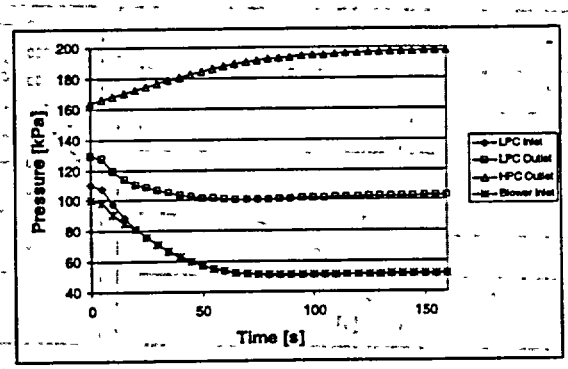

Fig 6. Variation in pressure during start-up

The time step for this simulation was 0.5 s and execution time was approximately 0.2 s per time step on a 700 MHz Pentium III processor.

7. Power control

The power output of the system can be controlled by increasing or decreasing the mass inventory in the system. The issue that needs to be resolved is exactly where to inject or extract the mass. The two most obvious possibilities are either before the LP compressor (position 1, Fig. 2) or after the HP compressor (position 4, Fig 2).

Figure 7 shows the variation in power for the case where the mass is injected and extracted before the LP compressor. The simulation starts at steady-state conditions at a power level of 100 kPa (at position 1) and a heater outlet temperature of 700 °C. At time t = 1 s mass is injected into the system at a rate of 0.1 kg/s for 400 s where after the system is allowed to stabilise for 100 s. Thereafter mass is extracted at a rate of 0.1 kg/s for another 400 s after which the system is again allowed to stabilise. Fig. 8 shows the variation in speed of the three turbochargers during the transient.

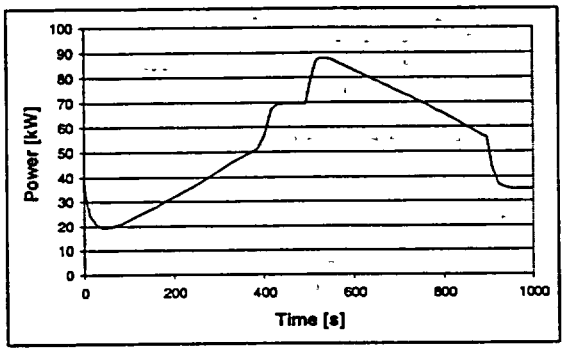

Fig 7. Variation in power when mass is injected and extracted before the LP compressor.

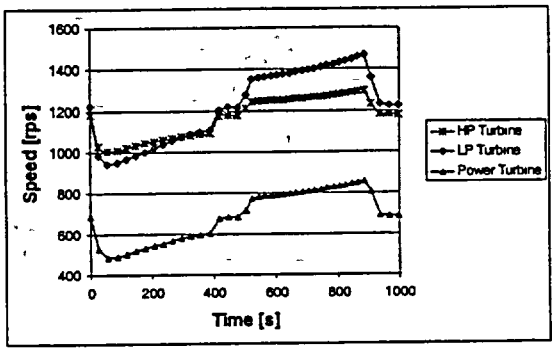

Fig 8. Variation in turbocharger speed when mass is injected and extracted before the LP compressor.

Figure 7 shows that the power first decreases before it starts to increase when mass is injected into the system and visa versa. This behaviour, which is undesirable, is due to the immediate increase in the back pressure of the power turbine when one starts to inject mass before the LP compressor. If mass is injected too fast the system can shut-down.

Figure 9 shows the variation in power for the case where the mass is injected and extracted after the HP compressor. The simulation starts at steady-state conditions at a power level of 100 kPa (at position 1) and a heater outlet temperature of 700 °C. At time t = 1 s mass is injected into the system at a rate of 1 kg/s for 37 s where after the system is allowed to stabilise for 42 s. Thereafter mass is extracted at a rate of 1 kg/s for another 37 s after which the system is again allowed to stabilise. Fig. 10 shows the variation in speed of the three turbochargers during the transient.

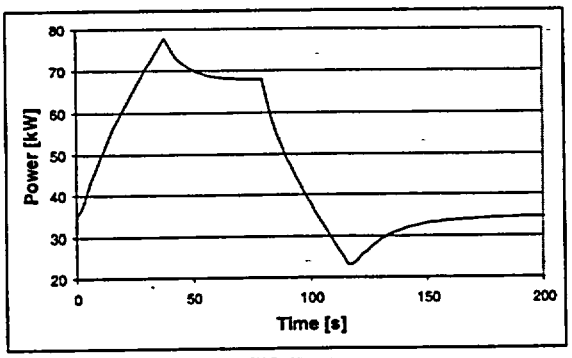

Fig 9. Variation in power when mass is injected and extracted after the HP compressor.

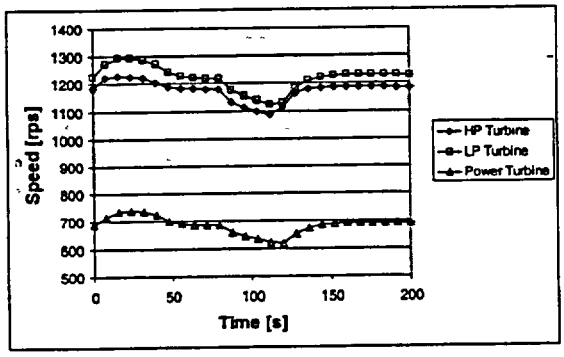

Fig 10. Variation in turbocharger speed when mass is injected and extracted after the HP compressor.

Figure 9 shows that the power output immediately starts to increase when mass is injected after the HP compressor and immediately starts to decrease when mass is extracted. Mass can therefore be injected and extracted at a much faster rate to follow rapid changes in load. Comparing Figures 8 and 10 one

can also conclude that the turbocharger speeds do not fluctuate as much in the case of mass injection and extraction at position 4 as compared to injection and extraction at position 1.

Simulations in this section were done for a time step of 0.2 s and execution time was approximately 0.2 s per time step.

8. Load rejection

Load rejection is done by suddenly opening the bypass valve between the high pressure and low pressure sides, shown in Figure 2. Figures 11 and 12 show the variation in power and speeds of the turbochargers respectively during a load rejection scenario. The initial condition for this scenario is the steady-state solution for a pressure level of 250 kPa (at position 1 in Figure 2) and a heater outlet temperature of 700 °C.

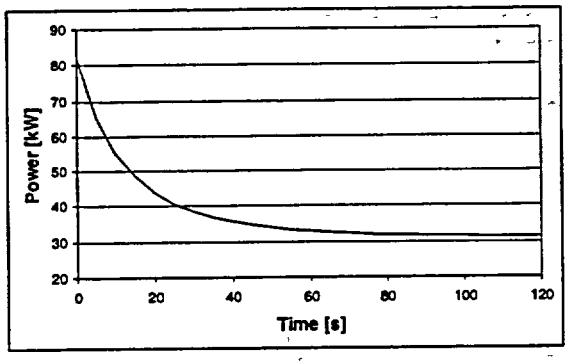

Fig 9. Variation in power during a load rejection.

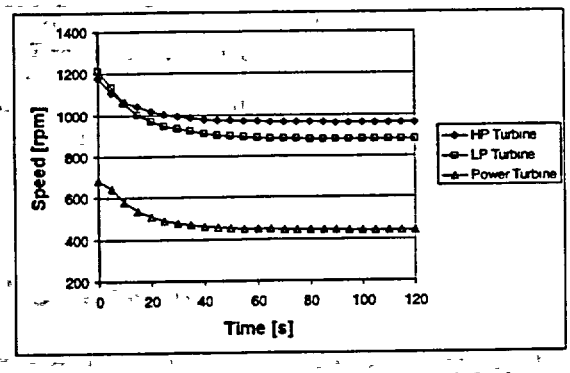

Fig 10. Variation in turbocharger speed during a load rejection.

Figure 9 shows that the power drops from 80 kW to 31 kW (or 61 percent) in approximately 90 s. The valve opening for this case was 15 mm. If the valve opening is increased the system shuts down. Figure 10 shows that the turbocharger speeds also drop significantly during the transient.

9. Conclusion

The design of a physical model of the PBMR with the aid of the thermal-fluid network simulation code Flownet was discussed in this paper. The study showed that it is not only feasible to built a physical model of the PBMR using off the shelve turbochargers, but that all the major operating procedures such as start-up, power variation and load rejection can be demonstrated on the micro model. The study also demonstrated the utility of a powerful simulation tool such as Flownet in the design of the micro model.

10. Acknowledgement

This study was sponsored by PBMR (Pty.) Ltd., a subsidiary of the South African utility ESKOM, and the National Research Foundation. The authors want to thank Mr. Walter Crommelin, a visiting student from TU Delft, for his valuable assistance.

11. References

[1] G.P. Greyvenstein, An implicit method for the analysis of transient flows in pipe networks, *International Journal for Numerical Methods in Engineering*, Vol. 53, pp 1127-1143, 2002.

[2] G.P. Greyvenstein, J.P. van Ravenswaay and P.G. Rousseau, Dynamic modelling of heat, mass and momentum transfer in the Pebble Bed Modular Reactor, *1st International Conference on Heat Transfer, Fluid Mechanics, and Thermodynamics*, 8-10 April 2002, Kruger Park, South Africa.

FLOW DISTRIBUTION OF PEBBLE BED HIGH TEMPERATURE GAS COOLED REACTORS USING LARGE EDDY SIMULATION

YASSIN A. HASSAN and GOKHAN YESILYUT
Department of Nuclear Engineering
Texas A&M University
College Station, Texas 77843-3133
USA

ABSTRACT

The simulation of complex three-dimensional gas flow through the gaps of the spherical fuel elements (fuel pebbles) of Pebble Bed Modulator Reactor is performed. This will help in understanding the highly three-dimensional, complex flow phenomena in pebble bed caused by flow curvature. The flow of this type has distinctive features, which strongly affect the boundary layer behavior. The transition from a laminar to turbulent flow around this curved flow occurs at different Reynolds (Re) numbers. Noncircular curved flows as in the pebble-bed situation need to be investigated. In this study, Large Eddy Simulation (LES) is used in modeling the turbulence to overcome the shortcoming of the Reynolds Average Navier-Stokes approach.

1. Introduction

The High Temperature Gas-cooled Reactor (HTGR) is one of the renewed reactor designs to play a role in nuclear power generation. The high temperature helium gas-cooled nuclear reactor, Pebble Bed Modular Reactor (PBMR) offers inherent safety with high thermal efficiency features as well as flexible fuel cycle with capability to achieve high burnup levels. The combination of coated particle fuel, inert helium gas as coolant and graphite moderated reactor makes it possible to operate at high temperature yielding a high efficiency. Under these conditions, heat transfer in both laminar and turbulent flows varies noticeably around curved surfaces. Curved flows would be present in the presence of contiguous curved surfaces. In the case of an appreciable effect of thermogravitional forces, the Nusselt (Nu) number depends significantly on the curvature shape of the surface. It could change with order of 10 times. The flow passages through the gap between the fuel balls have concave and convex configurations. Here the action of the centrifugal forces manifests itself differently on convex and concave parts of the flow path (suppression or stimulation of turbulence). The flow of this type has distinctive features. In such flow there is a pressure gradient, which strongly affects the boundary layer behavior. The transition from a laminar to turbulent flow around this curved flow occurs at different Reynolds (Re) numbers. Consequently, noncircular curved flows as in the pebble-bed situation, in detailed local sense need to be investigated. To the authors' knowledge there is no detailed complete calculations for this kind of reactor to address this local phenomena. This work is an attempt to simulate the flow behavior within the gaps.

The simulation of these local phenomena cannot be computed with existing conventional computational tools. Not all Computational Fluid Dynamic (CFD) methods are applicable to solve turbulence problems, in complex geometries. As in pebble bed reactor core, a compromise is needed between accuracy of results and time/cost of effort in acquiring the results. Resolving all the scales of a turbulent flow is too costly, while employing highly empirical turbulence models to complex problems could give inaccurate simulation results. In this study, the compromise is achieved by utilizing the large eddy simulation (LES) method. Here, the large scales in the flow are solved and the small scales are modeled. A schematic of the core region used in the LES calculations is presented in Fig. 1. It should be noted that the pattern of the pebble arrangement has several other orientations of the spheres. Figure 1 represents the first attempt to model a core region with this regular pebble arrangement.

2. Computational Modeling Approach

Accurate predictions of the flow and temperature distributions using computational fluid dynamic (CFD) programs depend on several factors as accurate modeling of the geometry, number of cells within the flow domain, mesh quality, selection of the solution technique and the selection of the appropriate turbulence models. In this investigation, the calculations are performed using the CFD code Trio_U [2]. It is a thermo hydraulic calculation modular software package. It includes several turbulence models as k-ε (averaged Navier-Stokes (RANS) type models) and large eddy simulation (LES) models with various subgrid models as Smagorinsky and structure function. This technique was first applied to applications in field of meteorology in the early 1970s. LES seeks to use a combination of direct numerical simulation (DNS) for large scale eddies and models for smaller eddies. It is a suitable compromise between the RANS-type methods and DNS.

Helium gas is passed into the reactor from the top and flows over the fuel pebbles in which a fission reaction is taking place. The helium is heated to a temperature of about 900-Celsius degree and pressure of 7 Mpa inside the reactor. The fuel sphere is 6 cm in diameter. Figure 1 presents the first pattern of 27 spheres with 36 contact points with zero spacing. The peak temperature that can be reached in the reactor core is 1600 Celsius. This is below the temperature of 2000 degrees Celsius that may damage the fuel. The flow parameters are summarized in Table 1. To generate the nodalization scheme an external mesh generator was utilized. This is due to Trio_U has a simple mesh generator which was not capable to create the complex geometry of the pebble bed. Periodic boundary conditions were imposed at the inlet and outlet boundary conditions. The center of the coordinate system is chosen as the center of inner sphere.

Tetrahedral mesh type is used to achieve the complex geometry nodalization and to capture the details of the curved surfaces with sufficient number of nodes. Most of the commercial grid generation tools have the difficulty to handle the points where the curved surfaces are touching as in this model shown in Figure 1. Therefore, artificial spacing is usually applied due to limitations in mesh generation for this kind of three-dimensional complex model. This approach may cause convergence problems. In this study, zero spacing between the pebbles are achieved adjusting the quality of the isotropic nodes over the flow domain using a three-dimensional finite element mesh generator called Gmsh. Mesh description is summarized in Table 2. The maximum time step achieved for 43496 tetrahedral is 0.98 msec due to the CFL condition. One-second simulation took approximately 80 hours CPU time with a 4 processor (400MHz each) Ultra Spark 2 Sun System.

The maximum time step achieved for 43496 tetrahedral is 0.98 msec due to the CFL condition. One-second simulation took approximately 80 hours CPU time with a 4 processor (400MHz each) Ultra Spark 2 Sun System.

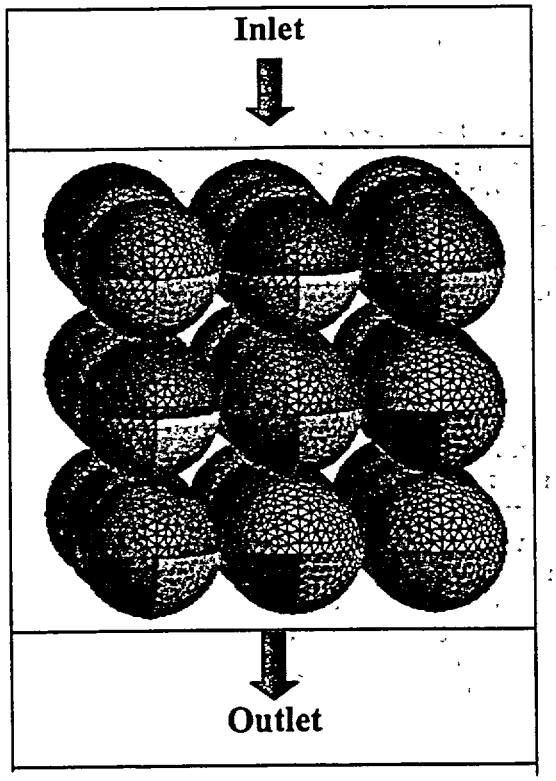

Fig. 1 Simulated Geometry

Table 1 Flow parameters

Electrical power	110	MW
Thermal power	265	MW
Tin	540	^{0}C
Tout	900	^{0}C
Helium Pressure	7	MPa
Mass flow rate	141	Kg/s
Number of fuel pebbles	440 000	
Core Radius	3	M
Core Height	10	M
Velocity (based on total core area)	1.49	M/s

Table 2 Mesh descriptions

Mesh Statistics	
Number of Nodes on Curves	2604
Number of Nodes on Surfaces	10353
Number of nudes in Volumes	10411
Number of Triangles on Surfaces	15834
Number of Tetrahedrons in Volume	43496

3. Turbulence model

Selection of the turbulence model has a great influence on the accuracy of the prediction. To achieve accurate solutions under the complex flow conditions of pebble bed, the large eddy simulation (LES) technique is adopted. In LES the large-scale motions are explicitly resolved while small-scale motions, taking place below the limits of numerical resolution, are represented by a subgrid mode [3]. The underling premise is that the largest eddies are directly affected by the geometry and boundary conditions and can be computed. By contrast, the small-scale turbulence is nearly isotropic and has universal characteristics; consequently, it is more amenable to modeling.

Large-scale field is obtained by applying filtering. A filter provides a formal definition of the averaging process and separates the resolvable scales from the subgrid scales. Filtering is used to derive the resolvable-scale equations. With a generalized filter, the quantity u_i, resolvable-scale filtered velocity, is defined as follows:

$$\overline{u_i(\underline{x},t)} = \iiint G(\underline{x}-\underline{\xi};\Delta)u_i(\underline{\xi},t)d^3\underline{\xi} \qquad (1)$$

The filter function, G, is normalized by requiring that

$$\iiint G(\underline{x}-\underline{\xi};\Delta)u_i(\underline{\xi},t)d^3\underline{\xi} = 1 \qquad (2)$$

Among the many filter functions, the most popular one used in LES research is Gaussian filter and is defined by

$$G(\underline{x}-\underline{\xi};\Delta)=\left(\frac{6}{\pi\Delta^2}\right)^{3/2}\exp\left(-6\frac{|\underline{x}-\underline{\xi}|^2}{\Delta^2}\right) \quad (3)$$

where the filter width Δ is defined by

$$\Delta=(\Delta x\Delta y\Delta z)^{1/3}. \quad (4)$$

In Trio, a homogeneous filter is utilized which is based on the selected numerical method (Barrè et al., 2000) [1]. For incompressible flow, the continuity and Navier-Stokes equations after applying filtering will have the following forms:

$$\frac{\partial \overline{u_i}}{\partial x_i}=0 \quad (5)$$

$$\frac{\partial \overline{u_i}}{\partial t}+\frac{\partial}{\partial x_j}\left(\overline{u_i u_j}\right)=-\frac{1}{\rho}\frac{\partial \overline{p}}{\partial x_i}+\frac{\partial}{\partial x_i}\left[\nu\frac{\partial \overline{u_i}}{\partial x_j}+\frac{\tau_{ij}}{\rho}\right] \quad (6)$$

Smagorisnky model assumes the SGS stress tensor, τ_{ij}, follow a gradient-diffusion process, similar to molecular motion. More detailed of subgrid modeling can be obtained from reference 2.

4. Results and Discussion

Figure 2 presents the location of several studied points. Regions close to the central pebble have been studied in details. Parameters such as velocity and pressure are analyzed. L1-L1', L2-L2', L3-L4' and L4-L4' are lines drawn along the y - direction from inlet to outlet.

L1-L1' => X = 0.03 m Z = 0.00 m
L2-L2' => X = 0.03 m Z = 0.015 m
L3-L3' => X = 0.03 m Z = 0.03 m
L4-L4' => X = 0.0212 m Z = 0.0212 m

Flow parameters have 1/8 symmetry along the x-z plane. As seen in Figure 2, the triangle is one of the 8 symmetric portions of the square surrounding the central pebble at the inlet. P1-P1', P2-P2', P3-P4' and P4-P4' are lines perpendicular to the y - direction as illustrated in Figure 3.

P1-P1' => Y = 0.00 m Z = 0.03 m
P2-P2' => Y = -0.03 m Z = 0.03 m
P3-P3' => Y = -0.06 m Z = 0.03 m
P4-P4' => Y = -0.09 m Z = 0.03 m

Pressure drop along the y-axis at different locations in x-z plane is shown in Figure 4. Total pressure drop along the flow direction is 204 Pa. The pressure difference along the X direction between L1-L1' and L3-L3' is approximately 50 Pa causing cross flow. Pressure drop along the x-axis at different locations on y-z plane is illustrated in Figure 5. The pressure distribution along the x-axis is symmetric. The maximum pressure change is about 75 Pa causing cross flows. Vector velocity plot for velocity within the pebble gaps is presented in Fig. 6. Various ranges of velocity scales are observed. In addition, flow circulation and stagnation are predicted.

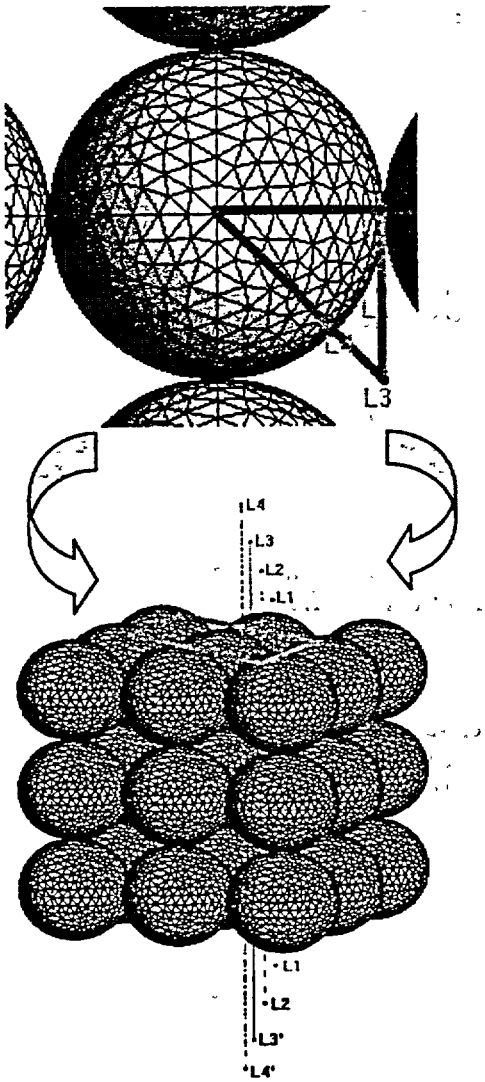

Fig 2: Points L1, L2, L3 and L4 show the location of the presented results.

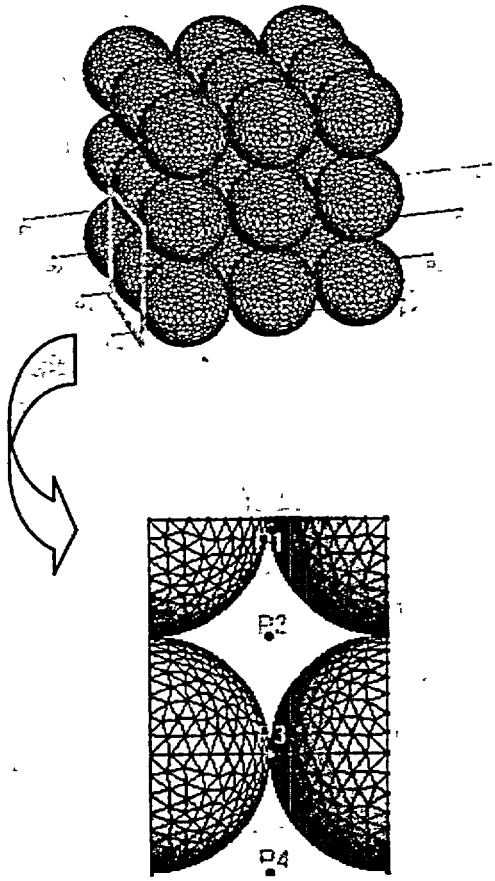

Fig 3: Points P1, P2, P3 and P4 show the location of the presented results.

5. Conclusion

A flow distribution calculation is performed using the state-of-the-art large eddy simulation technique. The complex highly three-dimensional flow in the gaps between the pebble beds is predicted.

6. References

[1] Barre', F., et al., Commissariat A L'Engergie Atomique – Grenoble, SMTH/LDTA/00-n, 2000.

[2] Bieder, U. et al., Commissariat A L'Engergie Atomique – Grenoble, SMTH/LDTA/2001-007, 2001.

[3] Hassan Y. A., et al., International Heat and Mass Transfer, Vol. 44, Issue 21, 2001.

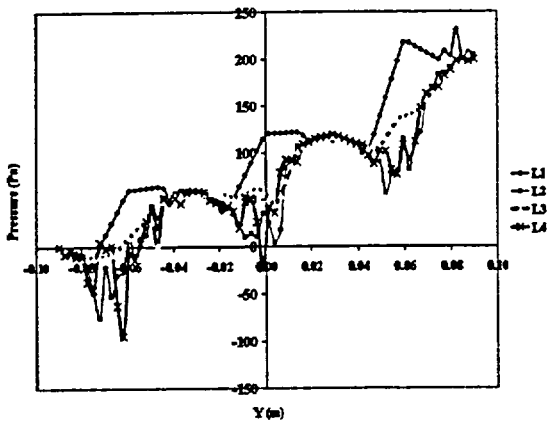

Fig 4. Pressure distribution along y-axis at different locations

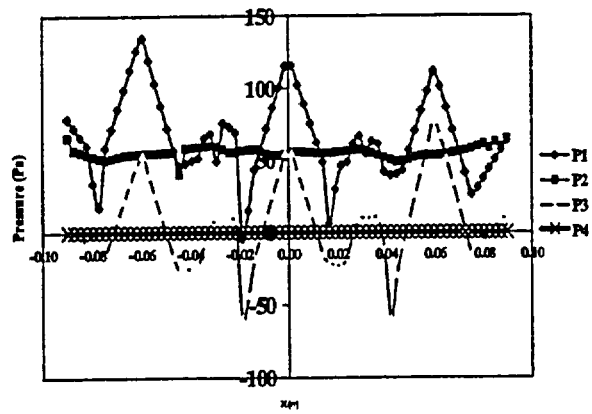

Fig 5. Pressure distribution along X- axis at different locations

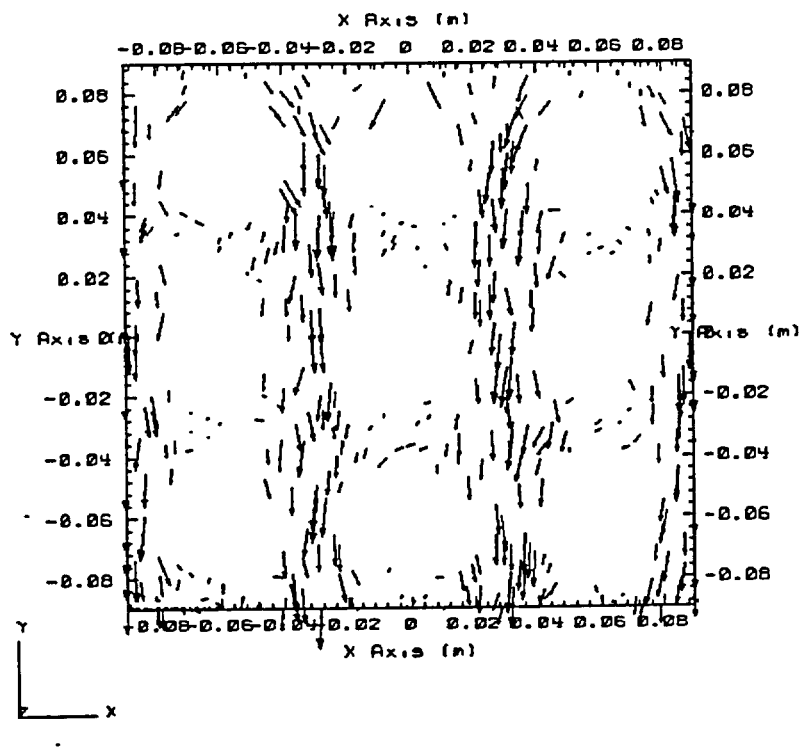

Fig 6. Velocity vector distribution along X-Y plane at Z= 0.085 m

Session 5

Engineering, Design and Applications

DESIGN AND DEVELOPMENT OF GTHTR300

X. YAN, K. KUNITOMI, T. NAKATA and S. SHIOZAWA

Japan Atomic Energy Research Institute
Oarai-Machi, Ibaraki-ken 311-1394, Japan

ABSTRACT

Development and recent successful operations of the HTTR in JAERI are coordinated with programs to study applied systems of the promising reactor technology. One such program being carried out from 2001 to 2008 is design and development of the Gas Turbine High Temperature Reactor, GTHTR300, with objective to allow for demonstration of the plant in 2010s in Japan. GTHTR300 features an original design of fuel cycle based on improved HTTR fuel element and of simplified plant system in pursuit of targeted economics with minimum development requirements. The fuel cycle characterizes on high burnup, low power peaking factor and extended refueling interval. The plant system applies such simplified design features as conventional steel RPV, non-intercooled cycle, horizontal single-shaft gas turbine generator and distributed modular maintenance of the overall plant. Research and development essential to validating the design includes component development and control testing. This paper describes the reference plant design and associated continuing R&D activities in JAERI.

1. Introduction

Development of high temperature reactor technology in Japan has centered in a multitude of research and development activities in JAERI for more than 20 years. The development results in the construction of the 30 MWt High Temperature Engineering Test Reactor (HTTR) in the institute's Oarai Research Establishment. The helium-cooled, graphite-moderated HTTR based on pin-in-block fuel attained the first criticality in November 1998 and has successfully risen to the rated power and 850°C coolant outlet temperature in tests since December 2001. Based on such experience, JAERI lunched an applied program of design and development for GTHTR300 power plant in 2001. The program that is an assigned work by ministry MEXT will be conducted until 2008 with ultimate goals for demonstration of a prototype GTHTR300 in 2010s and for commercialization in 2020s in Japan

Approach to GTHTR300 design is system simplicity and originality with which to yield economical performance at low development cost and risk. The reactor module is rated at 600 MWt and 587/850°C inlet/outlet coolant temperature and employs the same type of fuel proven in the HTTR. It relies on inherent and passive safety system. The reactor pressure vessel which is cooled in an intrinsic flow scheme makes use of conventional steel (SA533). The system design utilizes the simplest possible Brayton cycle, i.e. without cycle intercooling, because our analysis shows that cycle intercooling results in complexities in turbomachinery and system but provides no compelling advantage in busbar cost. The helium turbomachinery in the non-intercooled cycle exhibits superior aerodynamic efficiency by fewer stages and its rotor is lighter, shorter and more rigid, resulting in more robust vibration characteristics. The rotor is laid out horizontally so that demands on bearings are minimized and traditional industrial experience in handling of similarly oriented and sized turbomachinery is applicable. The turbomachinery and heat exchangers are sized and placed separately to permit modular construction and maintenance.

2. Plant Design Description

2.1 Utility/User Requirements

Utility/User Requirements for GTHTR300 are listed in Table 1 and were established in consultation with Japanese utilities and industries to guide the plant design and development so that it is directly responsive to the demand of future nuclear power generating market in Japan.

2.2 System Design

The plant system consists of three basic subsystem modules including the reactor module, the gas turbine generator (GTG) module, and the heat exchangers (HTX) module, as depicted in Fig. 1. The functionally-oriented modules are contained in individual steel vessels situated in separate confinement silos. Partitioning the large plant into properly sized subsystems and arranging them separately facilitates cost-effective modular construction and independently-accessed modular maintenance. For example, the size and weight of the GTG and HTX modules are such that they can be factory built in whole or in large vessel subassemblies and transported to site for erection in parallel, followed by simple piping connection.

Table 1: User/Utility Requirements for GTHTR300

User Requirements	
Item	Requirment
Safety goal	Radioactive nuclides release be prevented by fully passive means, Meet the site evaluation requirement for a current LWR; and additionally, site evacuation shall not be necessary
Site condition	Replacement of LWR site or new site
Seismic condition	The same as that of a next generation LWR
Fuel cycle	Once though (subject to approval of Atomic Energy Commission), fuel burnup more than 100GWd/ton
Nuclear proliferation	High amount of weapon grade Pu shall not be produced
Radiation protection	0.5manSv/ry
Radioactive waste disposal	Liquid: 1/10 of the latest LWR Solid: reuse of fuel blocks if possible
Power level	Modular type 100-300MWe/unit 100-4000MWe/site
Life time	60 years
Availability	More than 90%
Inspection	Once/2 years
Inspection period	< 30 days
Economy	Capital: 40-50 billion ¥/unit or ¥160-200k/kWe) Electricity: ¥4/kWh

In plant cycle, helium is heated in the core to 850°C at 6.84 MPa. It enters the turbine for expansion to convert thermal energy into shaft power needed to drive the compressor and electric generator. The turbine exhaust helium enters the recuperator, wherein its residual heat is recovered in high effectiveness to preheat coolant to the reactor. Having finally been cooled to 28°C by water in the precooler, the helium gas is raised by a pressure ratio of 1:2 to 7 MPa at 136°C by the compressor, preheated to 587°C in the recuperator, and heated in the reactor core to final outlet temperature of 850°C. The cycle thermodynamic conditions are configured to yield peak cycle efficiency for the selected core outlet temperature with the lowest component costs. Table 2 summarizes the plant design and performance data.

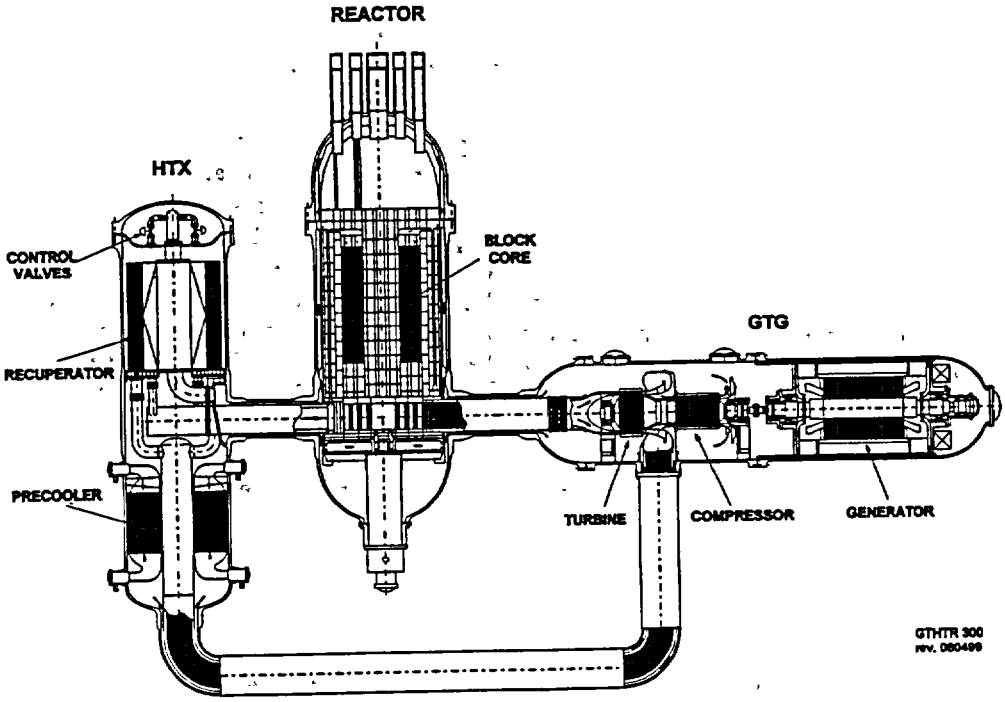

Fig. 1: System Arrangement of the GTHTR300

2.3 Reactor Module Design

The reactor pressure vessel (RPV) is cooled in a flow scheme unique to GTHTR300. The coolant is circulated to and from the core in the inner piping of a pair of coaxial vessel ducts leveled and symmetrically located near the reactor bottom. This unique piping structure makes it feasible to have the core inlet coolant channels embedded in the side reflector and is largely responsible to limiting the temperatures of the reactor lateral structure including the side reflector, core barrel and RPV. Moreover, the compressor-discharged helium at about 140°C and 7 MPa is circulated in the outer annular passage of the same pair of coaxial vessel ducts and through the vessel bottom interior from which a small gas stream is bypassed off the main circulating flow and vented to the annulus between the vessel and core barrel as shown in Fig. 2. It is this small bypass flow that is driven by an intrinsically positive pressure gradient towards the central core and which cools the RPV further as it flows upward in the annulus and enters the central core through top control rod guide tubes. The chart in Fig. 2 is used to determine the 0.5% cooling flow needed to keep the vessel operating temperature in a good margin from the material design limit over the entire operating power range. The vessel operating temperature is also in a regime where irradiation behavior of the vessel steel is sufficiently understood.

Table 2: GTHTR300 Design and Performance Data

Overall Plant	Reactor Power	600 MWt/unit (4 units/plant)
	Reactor pressure vessel	SA533 (Mn-Mo) steel
	Reactor safety system	no active emergency cooling
	Radioactive nuclide retention	confinement
	Plant Cycle	Non-intercooled Brayton cycle
	Power Generation	280 MWe
	Net Power Output	274 MWe
	Net Generating Efficiency	45.60%
	Plant Capacity Factor	90 0%
Reactor Core	Coolant Inlet/Outlet Temperature	587 / 850°C
	Coolant Inlet Pressure	6.92 MPa
	Core Coolant Pressure Loss	60 kPa
	Average power density	5.8 W/cc
	Fuel Element	pin-in-block prism
	Fuel Cycle	LEU once through cycle
	Enrichment	< 20%
	Average Burnup	112 GWd/ton
	Shutdown Refueling	once per 2-6 years
	Refueling Duration	30 days
Turbomachine	Shaft Design Type	horizontal, single-shaft
	Shaft Speed	3600 rpm
	Turbine Inlet Pressure	6.84 MPa
	Turbine Mass Flow	438.1 kg/s
	Turbine Expansion Ratio	1.87
	Number of Turbine Stages	6
	Turbine Polytropic Efficiency	93.0%
	Compressor Inlet Temperature	28°C
	Compressor Pressure Ratio	2.0
	Number of Compressor Stages	20
	Compressor Polytropic Efficiency	90.5%
	Generator Drive	cold-end, diaphragm coupling
	Generator Type	synchronous
	Generator Cooling	7 MPa helium cooled
	Generator Efficiency	98.7%
Heat Exchangers	Recuperator Design Type	plate-fin module x 6 modules
	Recuperator Thermal Rating	1006 MWt
	Recuperator Effectiveness	95 0%
	Recuperator Total Pressure Loss	1.7%
	Recuperator Construction Material	Type 316SS
	Precooler Design Type	helical-coiled finned tube bundle
	Precooler Thermal Rating	323 MWt
	Cooling Water Inlet Temperature	22°C
	Precooler Design LMTD	38°C
	Precooler Tubing Material	carbon steel (STB410)

The GTHTR300 core consists of 90 annular fuel columns, 73 and 48 inner and outer removable

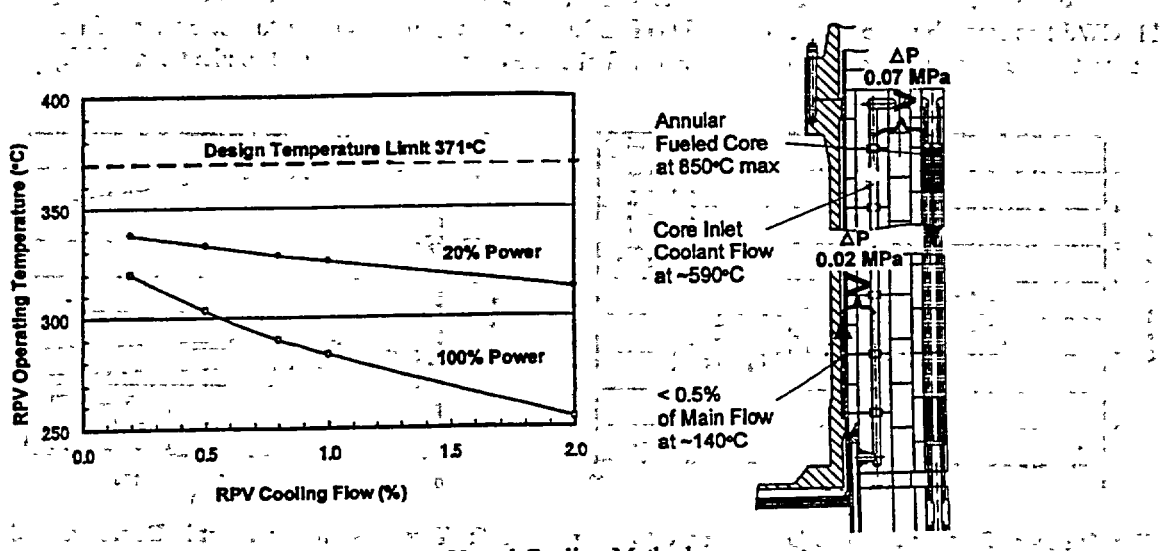

Fig. 2: Reactor Pressure Vessel Cooling Method

reflector columns and 18 outer fixed reflector sectors as shown in Fig.3. Effective core is about 3.6 to 5.5m in inner to outer diameter and 8m in height. The fuel column is stacked in 8 axial layers of fuel elements. The fuel element is a hexagonal graphite block with 57 fuel pins, 405mm across flat and 1000mm in height. The fuel pin is improved in an integral design to pass heat flux more efficient. The fuel pin is made up of stacks of fuel compacts with advanced enlarged coated fuel particles having a diameter of 550μm fuel kernel and a 140μm thick buffer layer for maintaining the integrity of the particles in high burnup conditions.

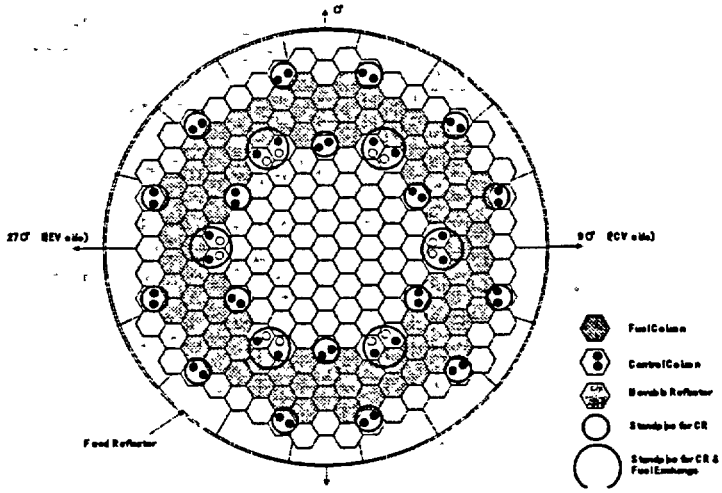

Fig. 3: Cross-Section of GTHTR300 Core

Another unique feature of GTHTR300 core is a two-batch axial fuel shifting scheme combined with strong recovery burnable poisons and some fully inserted power rods. Spent fuel is unloaded from alternate axial layers and the remaining fuel blocks are shifted downward while the new fuel is reloaded in the vacated layers, as illustrated in Fig.4.

The combined properties of the present core nuclear design result in a minimally peaked power profile at an enrichment of 14% only, as shown in Fig.5, and nearly uniform burnup in the core. Such favorable power distribution maintains peak fuel temperatures low in normal operations and keeps the maximum fuel temperature below the 1600°C limit in a loss of coolant accident. The latter is shown in Fig. 6 along with RPV and core barrel temperatures for a depressurized conduction cooldown event. The proposed new refueling scheme plus burnable poisons allows for 1460 days (4 years) of in-core fuel residence with two-batch refueling only and high 112GWd/t average burnup. In sum, the GTHTR300 reactor design is shown to not only retain the inherent and passive safety but also provide low fuel cycle cost and more than 90% plant availability.

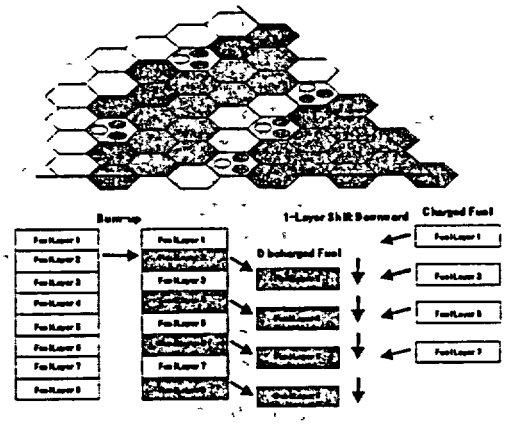

Fig. 4: Two-Batch Axially Shifted Refueling

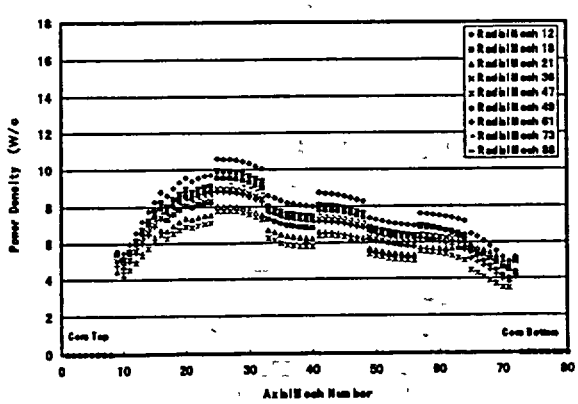

Fig. 5: Power Distribution 100 Days after Refueling

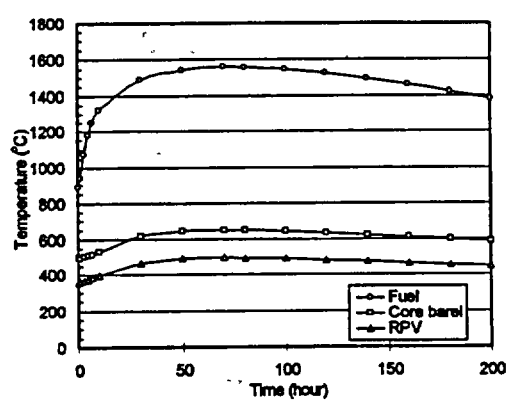

Fig. 6: Temperature Transient in Depressurized Conduction Cooldown

2.4 Power Conversion System Design

Gas Turbine Generator (GTG) Module

Design of the GTG module is shown in Fig. 7. The gas turbine is of axial-flow design consisting of a six-stage turbine and a twenty-stage compressor and drives a synchronous generator on the same shaft at 3,600 rpm. The gas turbine casings are interfaced by solid connections in the GTG module interior. A diaphragm coupling connects the gas turbine and generator shafts and effectively isolates vibration modes and alignment of the two rotor groups. Selection of horizontal rather than vertical rotor orientation simplifies bearing requirements and has the benefits of more conventional design and maintenance practice. With an exception of magnetic bearings, the mechanical design of the turbine and compressor is remarkably similar to that of conventional air breathing gas turbines in that it has similar number of axial stages, similar inlet and outlet geometries, similar rotor bearing span and arrangement, and similar shaft coupling. The aerodynamics of the turbine and compressor is designed based on the same principles and advanced blading features proven in the modern air gas turbines, resulting in high predicated aerodynamic efficiencies, low inlet and outlet losses and balanced axial shaft thrust. Pressurization in the helium-cooled generator cavity does not lead to performance degradation. Instead, the generator is designed to deliver the comparable level of efficiency seen in existing units. The main performance data of the gas turbine and generator were included in Table 2.

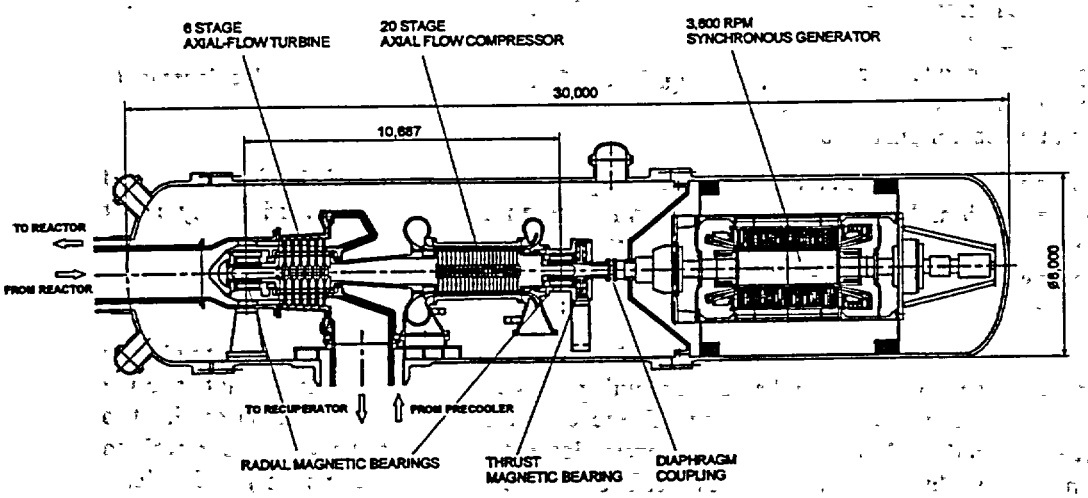

Fig. 7: Gas Turbine Generator Module of GTHTR300

Heat Exchangers (HTX) Module

The HTX module contains the recuperator and the precooler in a vertical steel pressure vessel. The recuperator is made up of six compact plate-fin heat exchanger modules that operate in parallel and are arranged in the upper annulus inside the pressure vessel. The precooler is a helically-coiled finned tube bundle with water circulating in the tubes and helium in the shell. The tube bundle is placed in the lower section of the pressure vessel. The major design data were given for the recuperator and precooler in Table 2. The essential technologies employed in the recuperator and precooler designs have already been developed in Japan.

Power Conversion System Maintenance

The plant system has been laid out with both modular construction and modular maintainability in mind. The latter is particularly critical for maintenance of the gas turbine because by regulations it requires frequently scheduled maintenance removal, more often than all other major power equipment, and because of radioactivity plateout in its metal surfaces. The steps taken in the modular maintenance on the gas turbine are illustrated in Fig. 8. First, a remote tool is inserted into the vessel interior through the opened hatches located on the vessel header and side wall to respectively

disconnect the internal hot gas duct from the turbine intake transition piece and the shaft diaphragm coupling between the gas turbine and generator shafts. After the bolts on the vessel flanges (1A and 1B) and on the lower duct (2) are removed, the building overhead crane is used to lift the gas turbine vessel section as "cartridge" up to the ground maintenance floor. Sealed at both ends, the pressure vessel provides shielding and particle retention from interior radioactivity. No separate case is used and no immediate removal of the machinery from the vessel interior is performed. Instead, the removed gas turbine vessel cartridge is taken to maintenance facility where it is serviced over the time and after radioactive decay. A previously refurbished and fully aligned gas turbine vessel cartridge is immediately installed by the same steps in reversed order. The present maintenance method requires one spare gas turbine vessel cartridge per a four-reactor plant site.

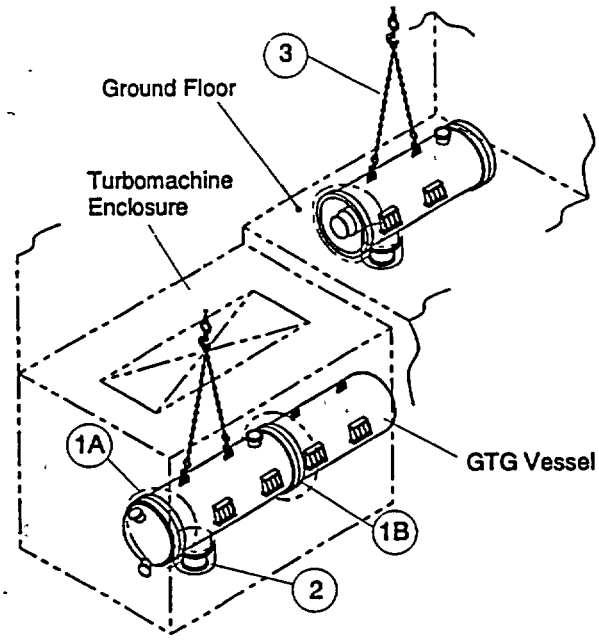

Fig. 8: Gas Turbine Vessel "Cartridge" Replacement

Maintenance removal of the generator is much less frequent and is performed following a removed gas turbine vessel section. The generator core, which is free of radioactivity, is pulled axially out of its own pressure vessel section towards the space vacated by the removed gas turbine vessel section. It is then lifted by building crane up to the ground maintenance floor where hands-on maintenance ensues immediately.

The recuperator modules are accessible and replaceable, if necessary, through the opened top closure of the HTX pressure vessel, following the self-explaining steps as shown in Fig. 9. The tubes in the precooler are serviced from outside of the vessel. The tubes forming individual circuits from inlet to outlet are accessed in the tubesheet inside the nozzles located outside of the vessel side wall to perform ISI on tubes or plugging of a damaged tube. The water in the tubes is completely drainable.

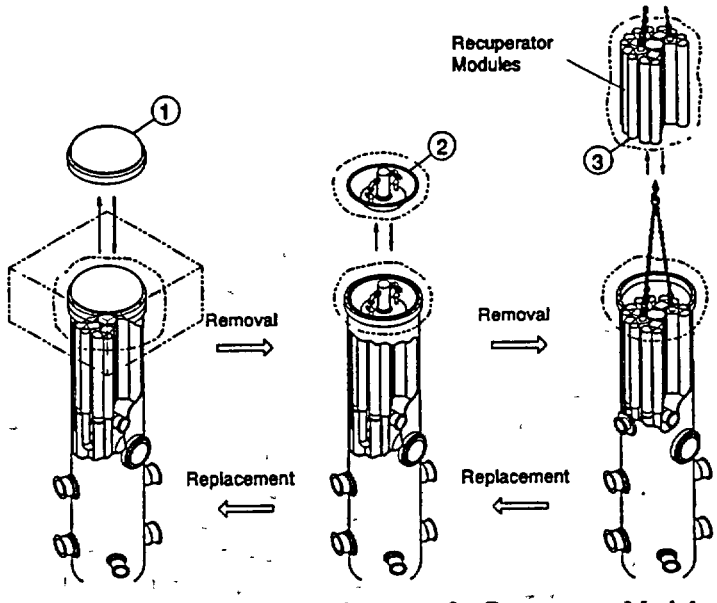

Fig. 9: Steps of Maintenance Replacement for Recuperator Modules

The maintenance replacement activities outlined above for the gas turbine and generator and for the heat exchangers can be amply accommodated within the 30-day period of reactor refueling, without adverse effect on plant availability.

3. R&D Activities

Research and development necessary to verify the GTHTR300 plant design includes performance confirmation test of helium compressor, development of magnetic bearing control algorithm, and control test on a small-scale closed cycle system. The R&D activities are conducted by JAERI in accordance with the plan outlined in Table 3. The compressor model test is intended to confirm the specific aerodynamic features of the compressor design for the full-scale GTHTR300. The key issues are concerned with predicated compressor surge margin, aerodynamic losses near the end wall in the blade flow path as well as inlet and outlet performance. The magnetic bearing development is focused on evaluation of control algorithms through 1/3 scale rotordynamic model testing. Lastly, the small-scale (~10MWt) closed cycle helium turbine system will be built to test the proposed control and protection schemes. The results from the R&D activities will be incorporated in GTHTR300 detailed design which begins in 2002.

Table 3: Design and R&D Schedule for GTHTR300

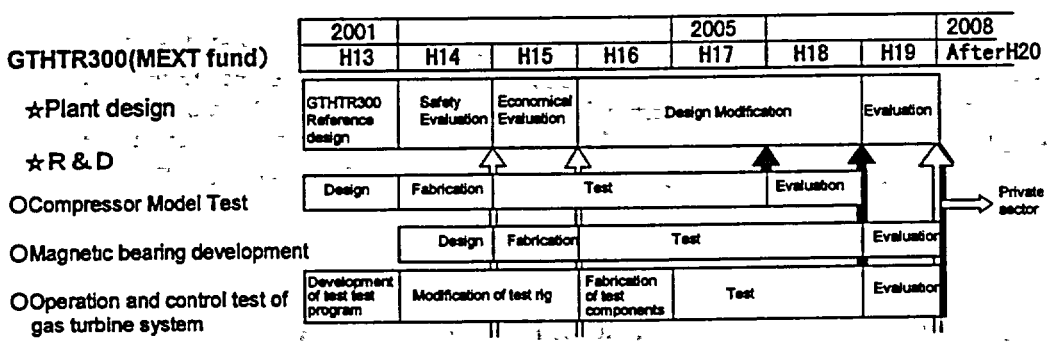

4. Conclusions

GTHTR300 reference design was concluded in fiscal year 2001 and the detailed design comprising safety and economical evaluation and necessary design upgrading by R&D has begun in the current year. The R&D needs to complete validation of the design have been identified and the systematic development activities have been planned and are being executed accordingly. It is through this effort that we hope GTHTR300 as a safe and economical prime mover will respond to the demand for new nuclear power generation in Japan in 2010s.

Acknowledgement

The authors wish to acknowledge the sponsorship of MEXT and the team contribution by a large number of their colleagues in JAERI, industries and utilities in the present program.

Design of a Power Conversion System for an Indirect Cycle, Helium Cooled Pebble Bed Reactor System

C. WANG, R. G. BALLINGER and P. W. STAHLE
Department of Nuclear Engineering
Massachusetts Institute of Technology, 77 Massachusetts Avenue, Cambridge Massachusetts 02139, USA

and

E. DEMETRI and M. KORONOWSKI
Concepts Northern Research and Engineering
39 Olympia Drive, Woburn Massachusetts, 01801, USA

ABSTRACT

A design is presented for the turbomachinery for an indirect cycle, closed, helium cooled modular pebble bed reactor system. The design makes use of current technology and will operate with an overall efficiency of 45%. The design uses an intermediate heat exchanger which isolated the reactor cycle from the turbomachinery. This design excludes radioactive fission products from the turbomachinery. This minimizes the probability of an air ingress accident and greatly simplifies maintenance.

1. Introduction

The desire for reducing CO_2 emissions in the production of electricity along with the trend of increasing world energy consumption has resulted in a renewed interest in nuclear energy. However, for nuclear energy to regain acceptance it must be both economically competitive and safe. Gas cooled reactors have been characterized as being economically competitive and demonstrably safe. With respect to basic nuclear island type, two configurations have been proposed. In the US, Japan and Russia, the prismatic core configuration is the design of choice. In the European community, in particular Germany, and in South Africa and China, the pebble bed core configuration is preferred. In the 1970s and 1980s examples of each design were built and operated in the US and Germany. After a term of lessened interest in the late 1980s and 1990s a number of newer designs are either in the process of design (South Africa-pebble bed) or have been constructed (China-pebble bed, Japan-prismatic) and are now in operation. The South African pebble bed design is intended as a commercial unit while the Chinese and Japanese reactors are considered as test reactors with long term commercial intent.

With respect to the power generation cycle, current commercial designs stress some form of the Brayton cycle using helium as the gas. CO_2 is a consideration for some fast reactor applications but will not be considered in this paper. The advantage of the Brayton cycle being the potential increased efficiency, coupled with a decrease in system complexity and O&M costs. These benefits have yet to be demonstrated in a commercial plant, however. While the Brayton cycle has achieved prominence as the cycle of choice for the new designs, the details of the actual configuration vary. Two cycle types, direct and indirect, have been proposed. Each has its' advantages and disadvantages, the importance of which may depend on the market for which the plant is intended. The direct cycle has the advantage of higher efficiency, simpler control, fewer components, and thus in principle lower cost to construct. Disadvantages of the direct cycle include greater susceptibility to air/water ingress accidents, increased O&M costs due to contamination of the power conversion unit (PCU), an extension of the ASME Section III, Class I pressure boundary to the entire PCU, and the potential safety impact of missile damage from failed PCU components. Arguments for relaxed containment requirements will be harder to make with the direct cycle due to the potential for fission product release to the environment through failure of a single barrier. Advantages of the indirect cycle include

the isolation of the PCU from the primary circuit which minimizes the air ingress and missile accident potential, decreased O&M costs due to an uncontaminated PCU, and a contraction of the Class I boundary area which allows more design flexibility with respect to materials choices. Disadvantages include increased complexity due to the inclusion of an intermediate heat exchanger, significant design issues related to its' design, decreased efficiency, and associated increased plant construction costs. With cost being a significant driver for commercial viability, the potential advantages of the indirect cycle are viewed in many circles as being not worth the cost penalty. As a result, the South African design that is the closest to commercial construction uses a direct cycle.

Beyond the issue of direct vs. indirect configurations, the details of the individual PCU designs are highly variable. Similarities between design concepts include recuperation and intercooling. However, designs differ as to the number of shafts, component orientation (vertical or horizontal), and bearing and seal configurations. A design proposed by General Atomics makes use of a single vertical shaft. The South African design calls for three shafts and a vertical orientation. The use of a single shaft allows for easier control since, unless gearing is used, all of the rotating components turn at the same speed. There is the additional advantage of smaller, higher speed, turbine and compressor designs. However, the single shaft designs require that some form of frequency conversion be used to match the output of the power turbine to the grid. Additionally, the single shaft design requires the use of a very long shaft, which complicates vibration damping. Multiple shaft designs make for easier maintenance since individual components can be removed, and allow the power turbine to turn at synchronous speed. However, this is achieved at the cost of additional piping complexity.

As was pointed out earlier, for any new concept to be accepted it must be able to compete with other sources of energy. These sources will include other nuclear as well as fossil fueled concepts. In general, nuclear sources are very capital cost intensive but balance this with lower fuel costs. Fossil costs are dominated by fuel prices which can be highly variable. Thus, for a nuclear source to be competitive, the construction costs must be minimized. One possible path the achievement of lower capital cost is to make use of factory based modular construction where components can then be delivered to the site and assembled. The extent of modularity in the various plant designs varies and the "jury is still out" as to the realization of cost advantages for modular designs.

In this paper, the design of the power conversion system for an indirect cycle, helium cooled, modular pebble bed reactor (MPBR) system is presented. The design, as will be discussed below, represents the desire to achieve a balance between a system that can actually be built using existing, or very limited and achievable of extension of technology with small cost, while at the same time meeting all existing codes and standards. The goal, within these constraints, was to achieve the maximum efficiency possible. The overall design, shown in Figure 1, is an indirect cycle, three shaft, recuperated and intercooled design with the power turbine turning at synchronous speed.

2. Design Constraints

The design complies with existing codes and standards in the US. The nuclear island of MPBR uses a nuclear reactor design similar to that developed in South Africa. The pressure vessel in this design uses A508/A533 class steel as the reactor pressure vessel (RPV) with an upper temperature limitation of 375°C[1]. This restriction requires a separate cooling system for the hot section components. The application of the ASME code Section III (Class I) results in a temperature limit of 427°C for the intermediate heat exchanger (IHX) pressure vessel and all of the Class I boundary. To satisfy the code requirements and, at the same time, allow for higher turbine inlet temperatures, component cooling and/or thermal breaks are used where required. Component cooling, since it requires the diversion of gas that could be used in power conversion, will result in an efficiency penalty and is thus only used where necessary. A significant advantage of the indirect cycle is the limiting of the Section III Class I boundary requirements to components and piping from the reactor to the IHX. ASME code Section VIII requirements will be used as the basis for the components in the PCU beyond the IHX. Section VIII allows temperatures up to 898°C. In the power conversion unit, the temperatures are usually below this

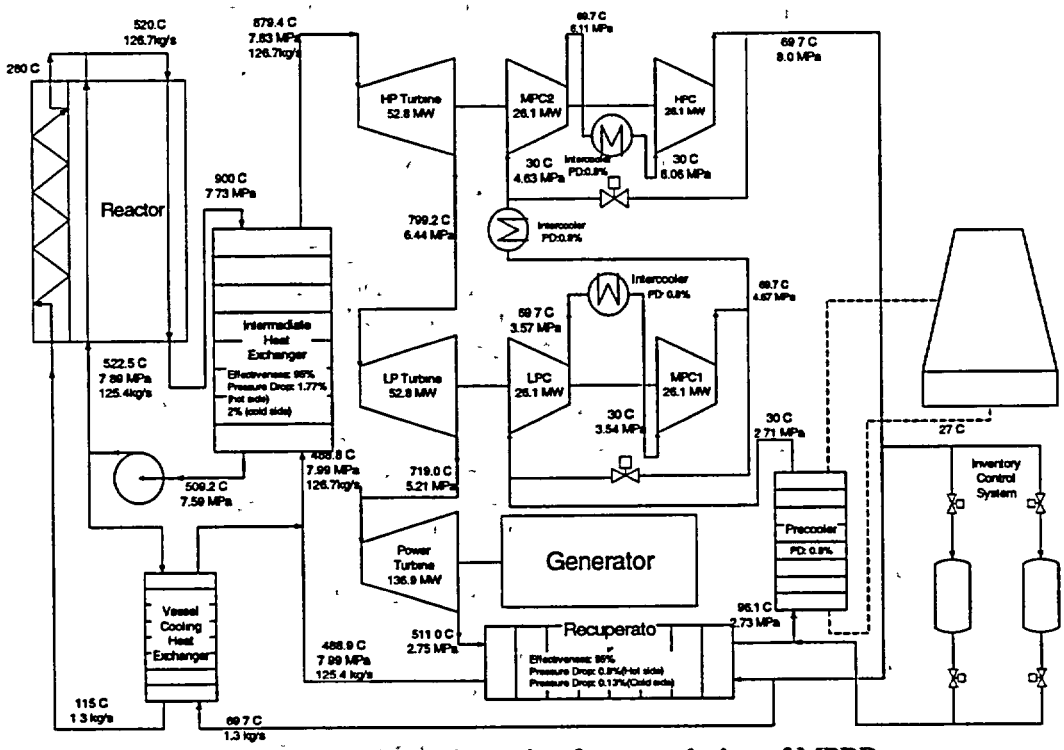

Figure 1 Flow schematic of current design of MPBR

limitation. However, due to concerns for differential thermal expansion, cooling is used for all of the turbine casings and interconnecting piping.

Current open cycle gas turbine technology allows for power levels up to 200MW and beyond. However, experience for design and operation of closed cycle helium turbomachinery is limited. The largest capacity helium turbine built to date is the 50MWe unit in Oberhausen of Germany, which was operated for over 30,000 hours with a turbine inlet temperature of 750°C in a closed cycle plant[2]. After detailed discussions with the manufacturers for turbomachinery, it was determined that the current helium turbine technology will allow powers no higher than 50MW without significant extensions of technology with associated large R&D costs. Not withstanding the claims by many that larger turbines can be easily built, when it comes to an actual commitment by a manufacturer to a design with a guaranteed efficiency, the reality of the difficulty, and associated risk of assuming larger turbines becomes apparent. This constraint necessitated the selection of a multi-spool arrangement for the power conversion unit.

With respect to piping sizes, higher velocity results in smaller piping diameters which will reduce costs. Additionally, minimization of diffuser losses in the turbomachinery, also argues for helium velocity as high as possible. However, when considering the potential for erosion of piping, in the current design, 120m/s is chosen as the piping helium maximum velocity.

With respect to heat exchanger designs, current technology limits the maximum size for compact, plate fin or printed circuit designs.

An additional restriction was applied with respect to plant layout. Our design layout makes use of a horizontal configuration. This configuration was chosen for ease of maintenance and bearing design. The design calls for the use of magnetic bearings. However, while magnetic bearing design technology has greatly matured over the past 10 years, the majority of magnetic bearing experience has been with horizontal configurations. Additionally, while magnetic bearings have been built which

will support the weight of a single shaft design, these bearings have been limited to rotational speeds of several hundred RPM, not the several tens of thousand RPM anticipated for single shaft designs. Thus, again, we have chosen to use technology with maximum industrial experience and minimum extension of technology.

The last constraint concerns the use of modularity. In our design we advocate the maximum use of modular designs for components. This places constraints on the maximum sizes for individual components such as heat exchangers and requires the use of individual modules as building blocks for the IHX, recuperator, and precoolers.

3. Current design

The goal of the design is to provide a plant with high efficiency, low investment, modularity, less cost for maintenance. As the requirement of modularity, the component should be shipped to the plant site by plate car.

Cycle and parameters selection

Advances of technology associated with heat exchanger design, the fabrication of an IHX working under severe conditions such as high temperature and high pressures has become a viable alternative. This has allowed us to choose an indirect cycle design which has the advantages described earlier.

Helium gas is used as the working fluid in both the primary system and the secondary system. While the isolation of the primary from the secondary circuits allows for the choice of a different gas for the secondary side, such as Air, CO_2, Nitrogen or Argon, the penalties in terms of heat exchanger size were deemed to great to balance the potential reduction in issues related to helium containment. Since helium is an inert gas which does not become radioactive and its specific heat is about five times of that of air, it was chosen as the coolant in the primary system. The conductivity of helium is much higher (about a factor of 5 over the relevant range of temperature) than that of air, so heat exchanger sizes would be about half that of an air design at the same conditions [3]. Compared with a steam cycle for the secondary side, the closed gas turbine cycle takes full advantage of the higher inlet temperature which leads to high plant net efficiency. Another potential advantage for the helium secondary cycle is in the area of component degradation. The Light Water Reactor (LWR) and fossil industries have a long history of corrosion related component reliability problems. The use of helium has the promise of eliminating corrosion as an issue.

As indicated earlier, the flow schematic of the current MPBR design is shown in Figure 1. A three-spool arrangement with three-stage intercooling are adopted in the power conversion unit. In the primary system, the helium inlet temperature is 520°C with an outlet temperature of 900°C. The hot helium then goes into the hot side of the IHX, after transferring heat to the power conversion unit, flows to the circulator. The circulator provides the pressure head to overcome the pressure losses through the primary cycle. Thereafter, the helium goes back to the upper plenum of the reactor core to finish the loop. In the secondary system, the helium leaving the cold side of the IHX is expanded sequentially in the high-pressure (HP), low-pressure (LP) and power turbines. The turbine exhaust helium enters the low pressure side of the recuperator and transfers its heat to its high pressure side helium. Before the helium enters a compressor, it is cooled to 30 °C. The helium is compressed to 8MPa by four compressors and then enters the high pressure side of the recuperator. After heat is recovered, the helium flows into the cold side of the IHX. The helium, at a temperature of 879°C leaves the cold side of IHX to start the next cycle once again. The helium pressure in the cold side of IHX is 0.1MPa higher than that of the hot side to prevent radioactive product transfer to the power conversion unit. In order to provide a stream for cooling of the reactor pressure vessel (RPV), a separate vessel cooling heat exchanger is used. On the primary side, helium is blead from the outlet of the circulator and is cooled to 115°C. The cooled gas then enters the annulus cavity between the reactor core barrel and RPV to cool the RPV. On the secondary side of the vessel cooling heat exchanger, cold helium is diverted from the outlet of the high-pressure compressor. Based on the

preliminary calculation, the mass flow rate for cooling the RPV is about 1% of the total mass flow in the primary system. The precooler and intercoolers are helium/water units.

The plant net efficiency depends on the attainable performances of its components and the cycle pressure losses. Improving component performance will increase the plant efficiency. Decreasing the cycle pressure losses will have the same effect. With current compact heat exchanger technology, the IHX and recuperator effectiveness can both be 95% with acceptable size and hence cost. The gas turbine and compressor polytropic efficiency can reach to 92%, and 90% respectively. In the calculation of net efficiency, the following parameters are used: circulator isentropic efficiency 90%, the motor efficiency 98%, and the generator efficiency 98%. Mechanical loss due to bearing friction and windage for the gas turbine to drive the compressor is assumed to be 1%. The cooling tower has the ability to provide water with a minimum temperature 27°C. Thus the precooler and intercoolers can cool the helium to 30°C before entering the compressors. In the primary system, the pressure loss is assumed to be 2% in the reactor, and 1.77% in the hot side of the IHX. In the secondary system, the pressure losses are as follows: 2% in the cold side of the IHX, 0.8% in the low-pressure side and 0.13% in the high-pressure side of recuperator, 0.8% in the each intercooler and precooler. Pressure losses in piping are taken into account in the component losses. The overall radiation loss is 0.2% of the reactor thermal power.

Figure 2 shows the plant net efficiency as a function of the reactor core outlet temperature. For a specific core outlet temperature, there exists a particular overall pressure ratio which results in the maximum plant efficiency. In terms of the optimum points, increasing the core outlet temperature 50°C results in a gain of approximately 1.5% plant efficiency. The effect of IHX effectiveness on the plant efficiency is shown in Figure 3, which illustrates that increasing IHX effectiveness from 90% to 95% would improve the plant efficiency by approximately 0.8%. As described later, increasing IHX effectiveness by 5% would, however, double the IHX and significantly increase cost. Intercooling can reduce the power consumed by compressor and recuperation increases the cycle efficiency[4]. Figure 4 shows the effect of intercooling stage number on plant efficiency. More intercooling stages would increase the plant efficiency but at a price of additional complexity. Reducing the compressor inlet temperature by 3°C improves the plant efficiency approximately 0.5%. However, the compressor inlet temperature is determined by the plant local environment and the performance of helium/water heat exchanger.

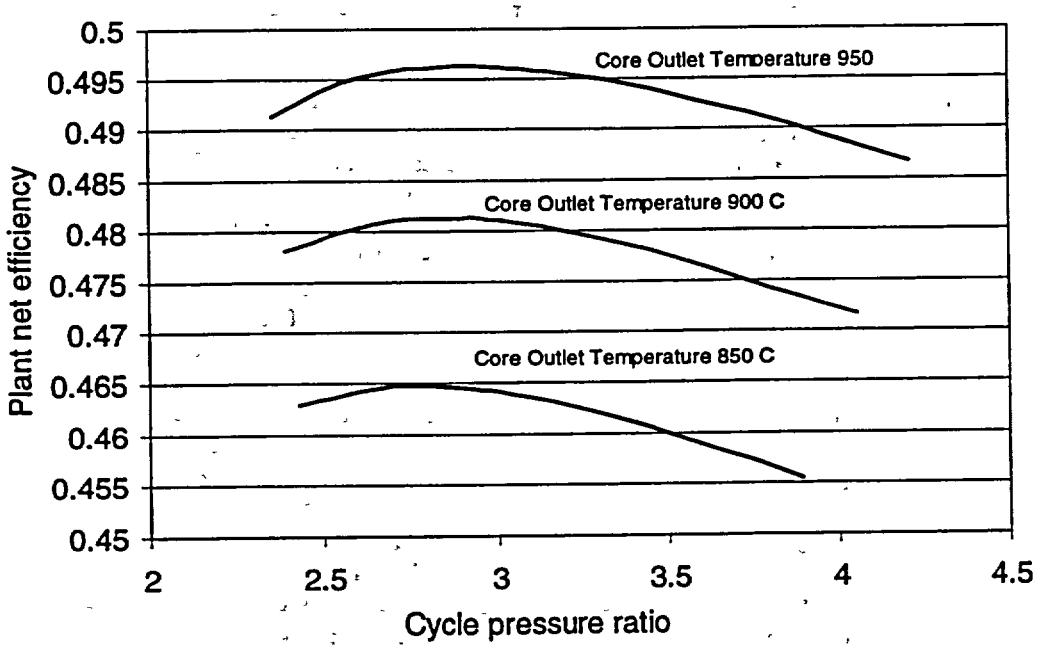

Figure 2 Plant net efficiency with respect to reactor core outlet temperature

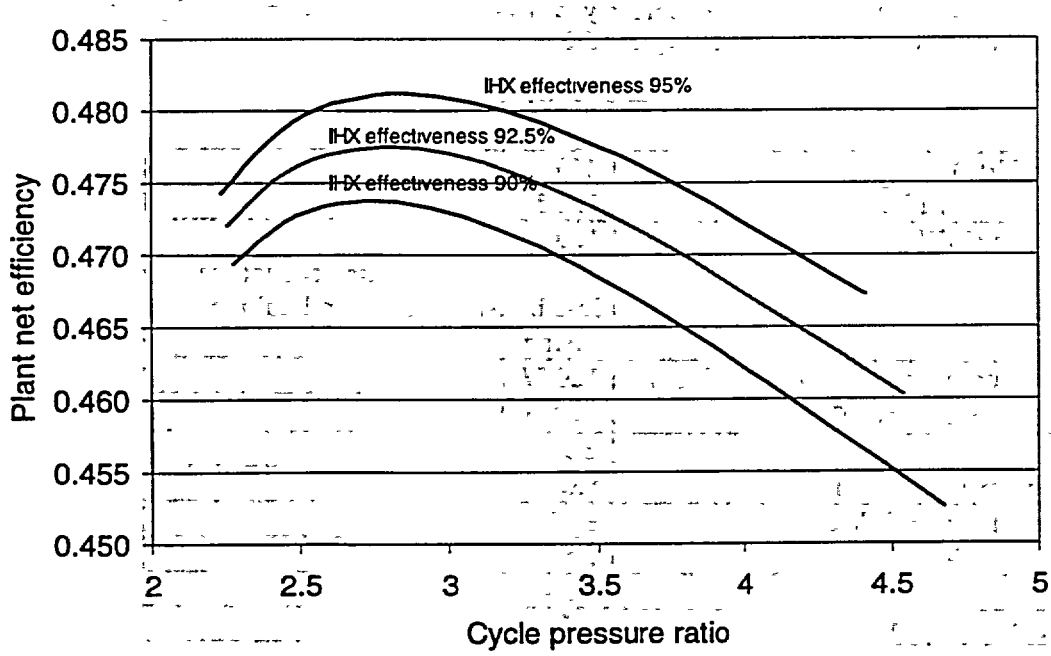

Figure 3 Plant net efficiency with respect to IHX effectiveness

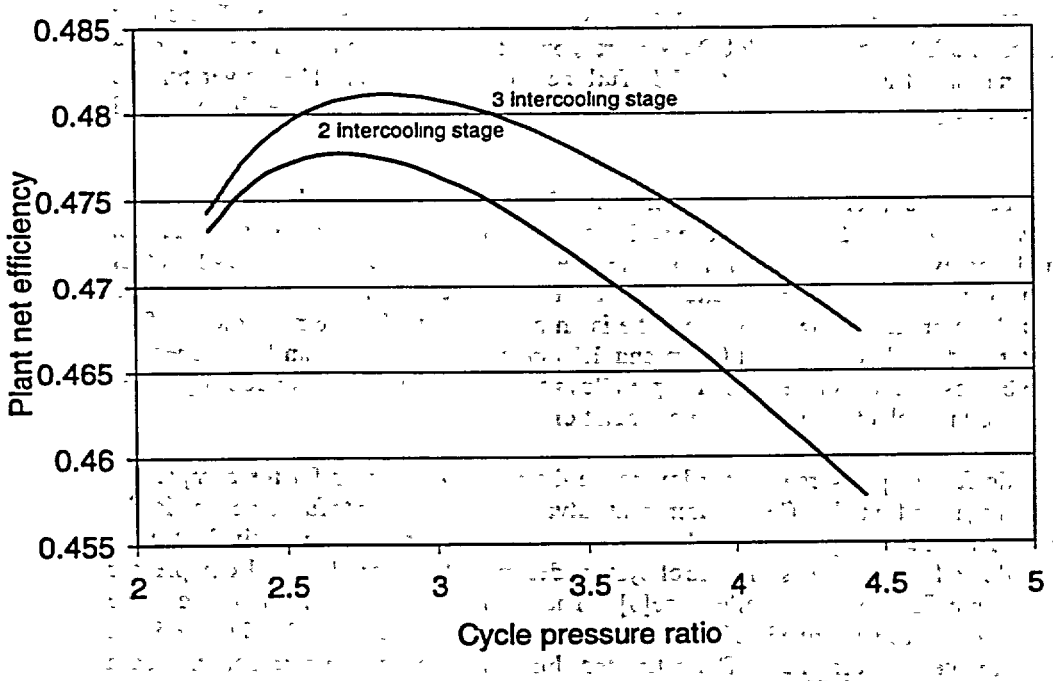

Figure 4 Effects of intercooling stage on plant efficiency

The plant design parameters are summarized in Table 1. The core outlet/inlet temperatures are chosen at 900°C/520°C respectively. The overall cycle pressure ratio in the power conversion unit is 2.96. The gross electrical power and plant net power are 132.5 MW, 120.3 MW respectively. Without considering the energy losses due to cooling the IHX pressure vessel and the casing of the turbines, the plant net efficiency is approximately 48% and takes into account system radiation loss, station

loads, switch-yard loss and RPV cooling. Preliminary analysis indicates that the penalty for component cooling will result in a plant net efficiency of 45%.

Table 1: Plant design parameters

Thermal Power (MWth)	250
Gross electricity power (MWe)	132.5
Net electricity power (MWe)	120.3
Plant net efficiency	48% (Not taking into account the loss by IHX cooling and turbine casing cooling)
Helium mass flow rate(primary/secondary) (kg/s)	126.7/126.7
Core temperature (inlet/outlet) (°C)	520/900
Pressure ratio	2.97
System maximum pressure (MPa)	8.0
Circulator consumed power (MWe)	8.96
Other station loads (MWe)	2.5
Switch-yard loss	0.6%
System radiation loss (MWth)	0.5

Turbomachinery

In the power conversion unit, the three-spool arrangement consists of a HP turbine and a LP turbine driving two compressors separately while a power turbine synchronizes with a generator. The power of the HP turbine and the LP turbine are 52.8 MW in response to the constraints assumed for the design. High rotational speed is allowed for the HP Turbine and LP Turbine. The power turbine rotates at 3600 RPM and a gear box or frequency conversion is avoided. The spools are all horizontal in layout.

The preliminary aerodynamic design has been done for the HP turbine and the high-pressure compressor with rotational speed of 5900 rpm. The preliminary aerodynamic selection criteria are that the machines should possess characteristics with a wide operation range, low losses. Unlike other gases, for helium turbo machines the blade tip circumferential stress becomes the design limitation in the determination of the number of stages. The turbine is an axial type with 50% reaction and four stages. Hub diameter and tip diameter are 1.032m and 1.168m respectively. Mean blade speed is 339.82m/s. Turbine blades will use single crystal super alloys to avoid the necessity of cooling. Vane control is used to extend the high efficiency region of operation.

Since the pressure ratio for compressors is in the low range there are two options for the compressor configurations: centrifugal and axial. The predominant advantage of the centrifugal design is the ability to operate over a wider range of mass flow at a rotational speed than an equivalent axial compressor, which allows for advantages in control system design. However, the axial compressor has potential for higher efficiency and smaller size[5]. The aerodynamic design for a five stage centrifugal compressor has been performed. The blade tip radius for all stages is 0.57m. Figure 5 and Figure 6 show the estimated performance. The estimated dimensions of the compressor include a diameter of 2.5m and length 6.8m. Due to size and weight considerations an effort to design an axial system with higher rotational speed such as 10,000 rpm is under way.

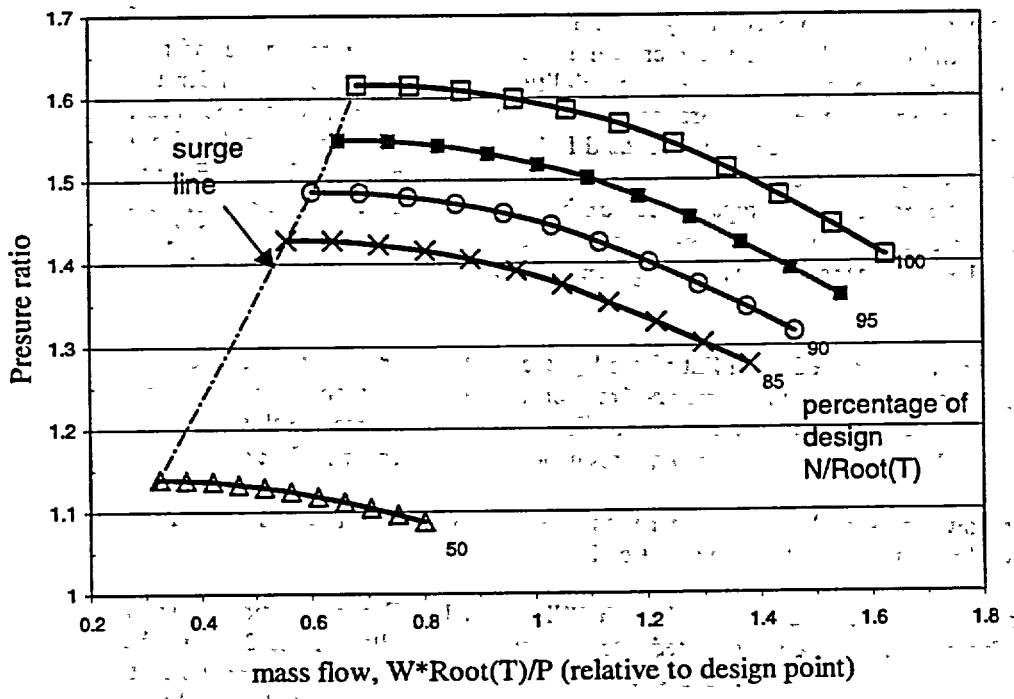

Figure 5: Five-stage centrifugal compressor characteristics

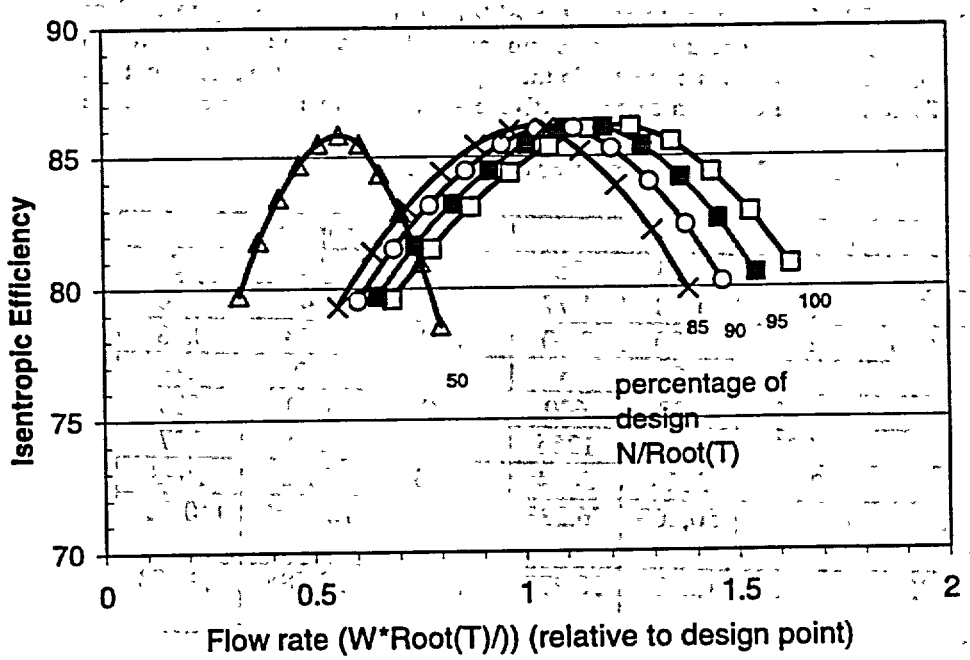

Figure 6 Five-stage centrifugal compressor characteristics

Heat exchangers

The performance of heat exchangers also plays a key role for plant operation and, in fact, are one of the most significant cost variability. The IHX is the critical equipment for implementing the indirect cycle configuration. The selection criteria are their capabilities of operating reliably under the required conditions such as temperature, pressure as well as the features such as compactness, maintenance and cost. The IHX must be able to withstand full system pressure on one side with a complete depressurization of the other side at temperature for at least short periods of time. For the MPBR design we have chosen to use compact heat exchanger technologies for the IHX and recuperator. Compact heat exchanger technologies have achieved a large industrial base [6]. Two options, the Print Circuit Heat Exchanger (PCHE) design and the Plate Fin Heat Exchanger (PFHE), have been considered.

The PCHE heat exchanger is constructed from flat plates by stacked together and diffusion bonded. On the plates, semi-circular channels with diameters 1mm or less are manufactured by chemical etching, hence, the channels become the flow passages. The material of choice the this design is Incoloy 800HT, a high nickel alloy suitable for temperatures up to 900°C under the ASME code.

The PFHE is a counter flow plate-fine heat exchanger with cross flow headers. The fins and parting plates are assembled by a brazing process to form a unit-cell.

The IHX and recuperator have been designed both with PCHE and PFHE configurations. Their features are shown in Table 2. The IHX is separated into 6 modules in parallel. Table 2 shows the IHX dimensions with an effectiveness of 90%, 92.5% and 95%. It is clear that the size, thus the cost, would be double if the effectiveness increases by 5%. At the same design requirement, the weight for PFHE configuration is about half when compared with the PCHE configuration. Figure 7 shows one module of the IHX with the PCHE configuration. The primary hot gas is distributed to the core through the hot side header. After primary gas has been cooled it is vented straight into the cavity between the heat exchanger core and vessel. Then the primary outlet gas flows out of the module from the outer annulus cavity of the coaxial pipe. According to cycle design parameters, the IHX primary outlet temperature is 509°C. In order to meet the ASME code, it is necessary to cool or insulate the IHX pressure vessel. The secondary gas flows into the header and then is distributed into core. After being heated, the secondary gas is collected in the opposite header and then flows out the IHX through a nozzle. Three recuperators with same effectiveness and different pressure losses are have been designed.

Table 2: IHX and Recuperator design data

	IHX			Recuperator		
Effectiveness, %	90	92.5	95	95	95	95
Hot-side pressure loss (%)	1.60	1.68	1.77	0.80	1.40	2.00
Cold-side pressure loss(%)	2.00	2.00	2.00	0.13	0.23	0.33
No. of modules	6	6	6	30	30	30
Module width (mm)	600	600	600	600	600	600
Module length (mm)	885	1013	1255	648	694	727
Module height, (mm)	2773	3014	3454	2745	2042	1693
Est. wt. for Printed Circuit HX configuration (kg)	38,854	50,669	76,233	155,585	126,260	110,821
Est. wt. for Plate-Fin HX configuration (kg)	10,335	13,478	20,278	41,457	33,585	29,478

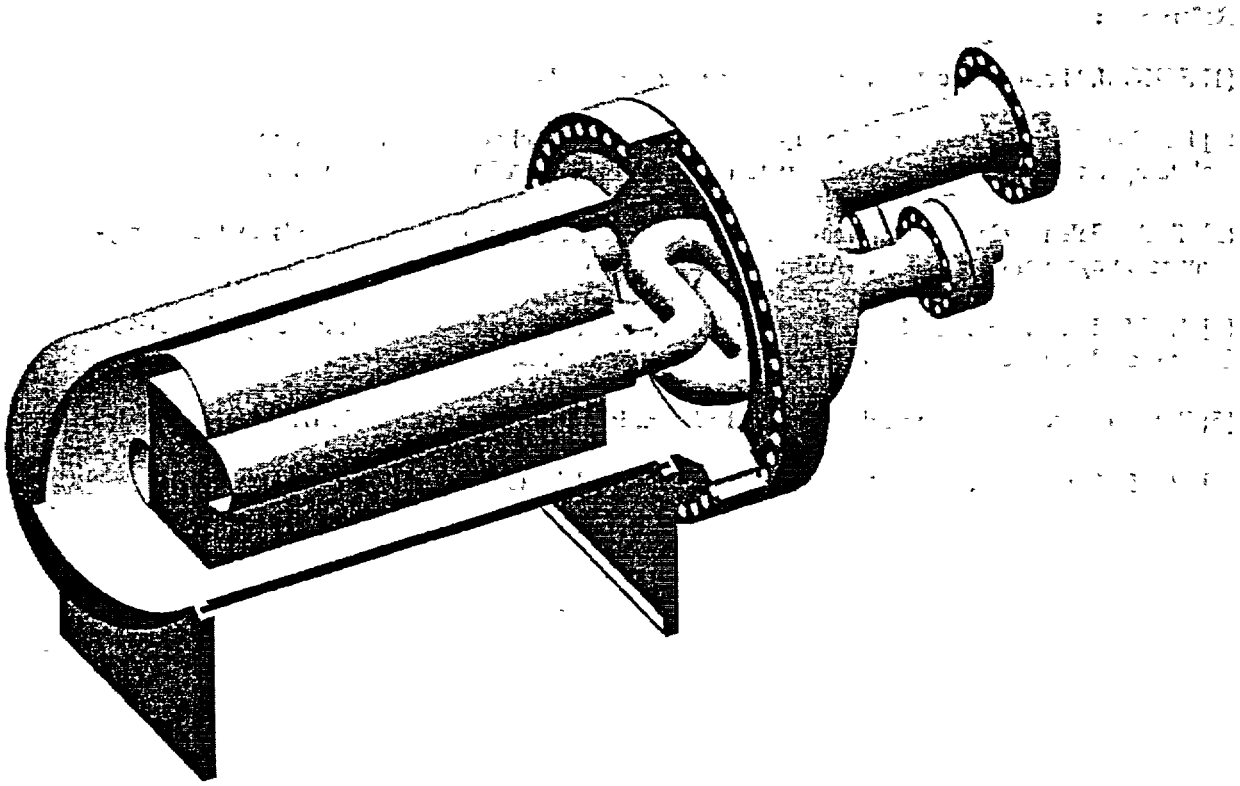

Figure 7: One module of IHX (Printed Circuit Design)

4. Further considerations

As mentioned above, the IHX design is critical to the success of the system. Incoloy 800HT is chosen as the material for IHX. For this material, the differential pressure between the primary and secondary side must be limited to no more than 1.0MPa at high temperature conditions. With a combination of active cooling and insulation, acceptable performance can be achieved during normal operation. However, for extreme transient conditions in which the secondary side has been depressurized while the primary side remains hot and at pressure, the stress-time envelope must be limited to prevent excessive deformation. This may be a significant limitation on plant operation. Removal of this restriction will require the qualification of more advanced material under ASME section III.

The plant efficiency calculation does not take into account the helium leakage occurs in the turbo machines. Leakage will impair the plant efficiency. The leakage rate depends on the sealing technology.

Acknowledgements

This work was performed as a part of NERI Project DE-FG03-00SF22171

References:

[1] ESKOM, "Pre-qualification request—the pebble bed modular reactor"

[2] I. A. Weisbrodt, "Working material—summary report on technical experiences from high-temperature helium trubomachinery testing in germany", IAEA, Vienna, Nov. 1994

[3] T. A. Galen, "Comparison between air and helium for use as working fluids in the energy-conversion cycle of the MPBR", MIT MS thesis, may, 2000

[4] L. M. Lidsky and Y. L. Yan, "Modular gas-cooled reactor power plant designs", ANP'92 International conference on design and safety of advanced nuclear power plants

[5] H. Cohen, etc, "Gas turbine theory", third edition, John Wiley & Sons, Inc. 1987.

[6] W. M. Kays, A. L. London, "Compact heat exchanger", McGraw-Hill, Inc. 1984.

THERMODYNAMIC ASSESSMENT OF PLANT EFFICIENCIES FOR HTR POWER CONVERSION SYSTEMS

W. FRÖHLING and H.-M. UNGER
Institut für Sicherheitsforschung und Reaktortechnik
Forschungszentrum Jülich
52425 Jülich Germany

and

Y. DONG
Institute of Nuclear Energy Technology
Tsinghua University
Beijing 100084 China

We studied thermodynamic aspects influencing the efficiency of 200 MWth-HTR modules, considering steam cycle plants, gas turbine plants with and without intermediate heat exchanger and plants with combined gas turbine/steam cycle. The influence of steam parameters and of reheating is investigated. The investigated parameters with major influence on the efficiencies of gas turbine cycles are the core outlet temperature, polytropic efficiency of the turbomachinery, performance of the recuperator and the cooling temperature. For combined cycles, we have investigated a direct combined cycle with gas turbine and steam generator heated by the exhaust gas of the turbine, and a combined cycle with intermediate heat exchanger. For core outlet temperatures of 900 ^{0}C, and steam temperatures of 600 ^{0}C, respectively, cycle efficiencies between 40.7% and 47.5% have been found, with the indirect gas turbine cycle on the lower bound and the direct combined cycle on the upper bound of the spectrum.

1. Introduction

Conventional power plants – steam cycle, gas turbine and combined cycle plants – are improved continuously. As the HTR can principally be coupled with a variety of those power conversion systems, it was proximate to study the related potential also for the HTR.

Historically, HTR plants have or had steam cycles mainly because they are close to conventional steam plants. New conventional plants have steam temperatures of 600...700°C, for improving the plant efficiency. For an HTR, there are no principal obstacles to be in line with the actual trend, i.e. generate steam with similar temperatures.

Gas turbine cycles are regarded to be attractive for the HTR, mainly because of their potential for a high thermodynamic efficiency. Considerable effort had been invested in the design and experimental R&D for gas turbine cycles, but up to the present such plants were not realized. In the meantime, the progress of gas turbines has stimulated new interest for the gas turbine cycle for the HTR.

Combined cycle plants which connect the gas turbine and the steam turbine have gained increasing importance in conventional power plants. Therefore, we found it reasonable to study the application of this technology for HTR power conversion systems, too.

In our analysis we considered, with restriction to thermodynamic aspects, steam cycles with and without reheater, gas turbine cycles with and without intermediate heat exchanger (IHX), and combined cycles with and without IHX.

2. Main assumptions

The following important parameters and main assumptions have been used in our analyses.
Reactor power and core outlet temperature: We set the reactor thermal power to 200 MW and we

assumed, that a reactor design combining this power and a gas outlet temperature of 900°C can be realized which is compatible with the 1600°C-concept. It requires, that peak core temperatures must not exceed this value in a core heat-up accident.

Temperature difference in the IHX: In the former German nuclear process heat project the design provided an IHX between the reactor and the coal gasifier, with inlet/outlet temperatures of 950/293°C on the primary side and 220/900°C on the secondary side, respectively. This temperature difference in the IHX of 50 K has been experimentally confirmed and we took it as reference value.

Polytropic efficiency of the gas turbomachinery: For optimized gas turbines and compressors, the polytropic efficiency is in the order of 85% to 89%. We set the polytropic efficiency to 85% since the HTR turbine is smaller than conventional large turbines, and the working fluid is helium.

Temperature difference in the recuperator: The performance of the recuperator can be reflected by the temperature difference between the hot and the cold side. In the industrial recuperator design of the HHT project, the average difference was about 25 K, and we selected it as the reference value.

Cooling temperatures in the coolers in a gas turbine cycle: For the coolers, their cooling temperatures will be determined by the state of the art of the coolers and the environment. In the designs of the GT-MHR [1], the PBMR [2] and the MPBR [3], the cooling temperatures are 26, 27 and 30°C respectively. We took 30°C as a conservative reference value.

Live steam conditions: In advanced coal-fired steam power plants, supercritical steam parameters (up to 300 bar and 600°C) are applied. For the HTR steam cycle, we have chosen a live steam temperature of 600°C as a reference, and a live steam pressure of 160 bar for the no reheating steam cycle and 250 bar for the reheating steam cycle, respectively.

Condenser pressure and quality of the exhaust steam: Low condenser pressures (0.03 – 0.04 bar) are desired, but their achievement depends on the site condition. We set the condenser pressure to 0.05 bar in our analyses, typical for wet cooling towers. Normally the quality of the exhaust steam should be higher than 85%. For the German light water reactor convoy plants, the wetness of steam in the low-pressure turbine can be as high as 14%. Thus, in our analyses, 86% has been set as the lower baseline.

Isentropic efficiency of the steam turbine: The isentropic efficiency of an optimized steam turbine is 90% for an advanced power plant. Conservatively, we took a value of 87% in our analyses.

Efficiency of the feedwater pump: According to manufacturers informations, the overall efficiency of the feedwater pump can be 75-85% according to the size. So, we set the efficiency to 75%.

Cycle efficiency and cycle consumption: The cycle efficiency denotes the ratio of the net electricity production, which equals the difference between the generator gross production and the power consumed by the cycle itself to the total nuclear thermal power. In our definition of the cycle consumption, we took only the power use of the helium blower and feedwater pumps into consideration.

3. Results

3.1. Steam cycles

The plant efficiencies of HTR modules with one reheater and without reheater have been calculated. The main thermodynamic conditions can be found in Table 1. The steam cycle without reheater yields, for live steam conditions of 160 bar/600 °C, a plant efficiency – ac-cording to our definition – of 41,5%. In the process with one reheater, live steam of 250 bar/600 °C is expanded in the high pressure turbine section down to 85 bar. Then it is heated up again in the reheater to 600 °C and led to the middle/low pressure section of the turbine. In this case, the efficiency yields 44,3%. The depen-dence on the live steam temperature and pressure is depicted in Fig. 1. For a 1 percentage point gain in effici-ency, the live steam temperature must be elevated by about 60 K, or the pressure by about 50 bar. The figure shows also efficiencies for 177,5 bar /530 °C, the values of the

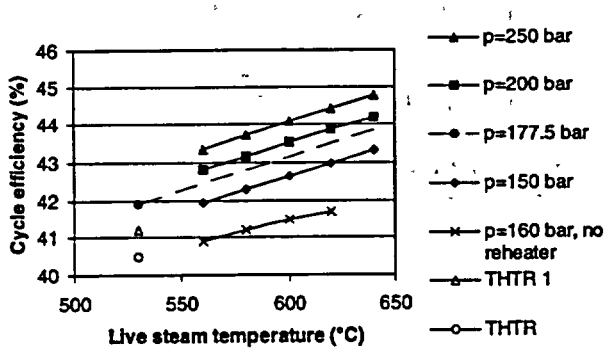

Fig. 1 Cycle efficiencies for steam cycles with and without one reheater

THTR which had one reheater. The point 'THTR' denotes the efficiency as has been published [4]. 'THTR1' denotes our calculation, assuming isentropic efficiencies of 87% for all three sections of the turbine, and a condenser pressure of 0,0685 bar. This was valid for the THTR which had dry air cooling. The difference of about 0,5% between our calculation and the THTR-value is low and can be attributed to some parameters which are not known to us, e.g. the true efficiencies of the three turbomachine sections. For the calculation of the upper point, the condenser pressure was 0,05 bar, all other assumptions equal to point 'THTR1'.

3.2. Gas turbine cycles

The gas turbine cycle has the thermodynamic advantage that it can make direct use of the high upper process temperature of an HTR. We calculated a direct cycle consisting of core, high pressure-, low pressure- and power turbine, recuperator, precooler, low pressure compressor, intercooler, and high pressure compressor. The core outlet temperature affects the plant efficiency significantly, see Fig. 2. When the pressure ratio is fixed and the core outlet temperature is raised by 50 K, the plant efficiency raises by about 2 percentage points. The point for GT-MHR is taken from [1], and point GT-MHR1 shows the result of our calculation with the same assumptions. For the GT-MHR, the cooling temperature of 26 °C is very favorable, and the polytropic efficiency of the turbomachinery is high. For the PBMR [2], the cooling temperature is 27 °C, and with a nuclear thermal power of 265 MW and a generator production of 117 MW the efficiency according to our definition is 44,2%. Based on the design parameters of the PBMR, our calculation gives an efficiency of 44,8%, see point PBMR1 in Fig.2. This agrees sufficiently with the value given in the literature.

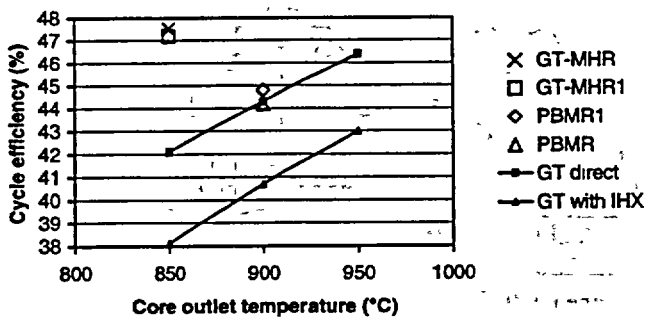

Fig. 2 Cycle efficiency vs. core outlet temperature

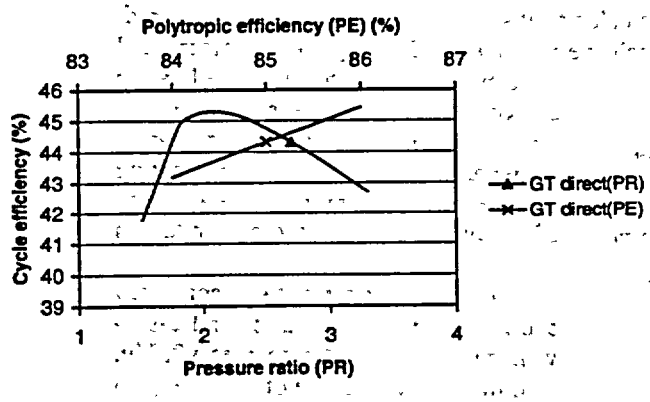

Fig. 3 Cycle efficiency vs. pressure ratio and polytropic efficiency of the turbomachinery for direct gas turbine cycles

Other parameters, besides the core outlet temperature, which can influence strongly the cycle efficiency are the pressure ratio, the polytropic efficiency of the turbomachinery, the performance of the recuperator and the cooling temperature. The cycle efficiency vs. pressure ratio and polytropic efficiency of the turbomachinery is illustrated in Fig. 3. There are however restrictions to use the optimal pressure ratio of around 2,1. With a low pressure ratio the core inlet temperature raises, and if e.g. with respect to the pressure vessel the core inlet temperature must be below 560 °C, a pressure ratio of 2,7 must be taken. The cycle efficiency increases 1 percentage point if the turbomachinery efficiency is elevated by 1 percentage point. If the temperature difference in the recuperator is reduced from 25 K to 20 K, then the cycle efficiency will be increased by 0.7 percentage points. The cycle efficiency will deviate by about 0.5 percentage points if the cooling temperature changes by 3 K.

The main advantage of gas turbine cycles with IHX is the fact, that the whole complicated power conversion unit is clearly separated from the primary circuit, contamination free and with easy access to all components. However, there is a loss of 50 K in the upper process temperature of the secondary cycle. The blower in the primary helium circuit can only be operated up to certain temperature limits. We have chosen 450 ^{0}C as the upper value. As the core inlet temperature is also determined indirectly via the IHX by the pressure ratio in the secondary cicuit, the pressure ratio there must be as high as 4.5, which is much higher than the optimal value. Cycle efficiencies for gas turbine cycles with IHX are depicted also in Fig. 2.

3.3 Combined cycles with gas turbine and steam turbine

The combination of gas turbine and steam turbine leads to the most efficient conventional power plant systems which can reach electric efficiencies next to 58%. Principally, combined cycles are feasible for the HTR, too. From the great variety of possibilities we have selected two cycles: a closed, direct combined cycle and an open combined cycle with IHX.

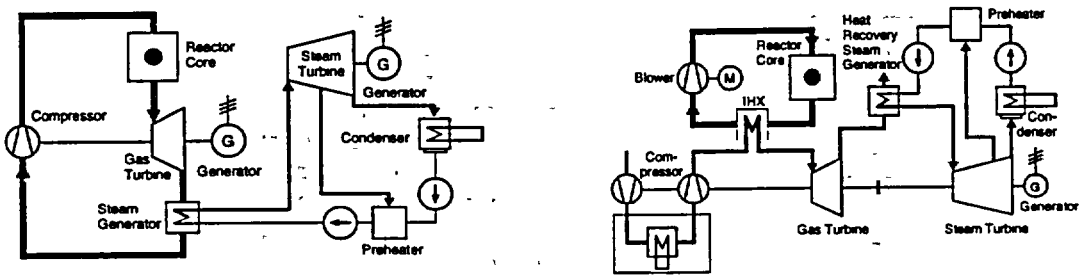

Fig. 4 Combined cycles: direct (above) open with IHX

The direct cycle provides maximum efficiency. The primary circuit consists of the core, a gas turbine, a heat recovery steam generator and a compressor (see Fig. 4). The gas turbine exhaust of 600°C is used for steam generation. With a temperature difference between the off-gas and the steam side of 50 K, a live steam temperature of 550°C can be reached. This cycle obtains an efficiency of 47.5% for 900 ^{0}C core outlet temperature. Within this calculations two aspects have to be considered. On one hand there is the optimum pressure ratio to achieve maximum efficiency. On the other hand there are limits which are affected by the choice of the pressure ratio, e.g. the steam temperature and the operating temperature of the blower. Respecting these aspects, the resulting dependence of the cycle on the reactor temperature is shown in Fig. 5.

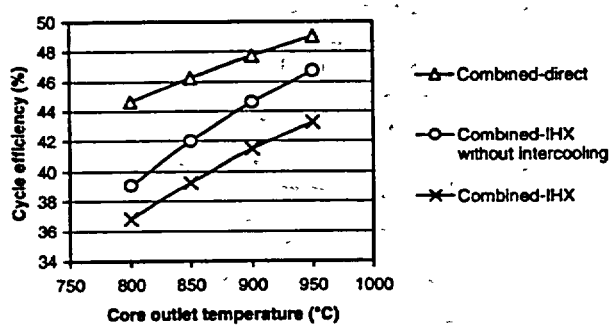

Fig.5 Combined cycles: efficiencies vs. core outlet temperature

An IHX together with a combined cycle has similar advantages and disadvantages, as dicussed in chapter 3.2. Fig. 5 shows the dependence of efficiency on core outlet temperature for two versions of a combined cycle with IHX: One version operates with intercooling between the compressor stages, yielding 41.5% for 900 ^{0}C core outlet tempera-ture. A higher efficiency can be reached by omitting the intercooling. Intercooling has two main effects. Firstly, an intercooler reduces the reactor inlet temperature. Without intercooler, given limits may be exceeded, e.g. for the blower. Also, an intercooler leads to a lower medium compression temperature, which causes less compression power. Secondly, the intercooler rejects heat from the process. For the considered combined cycles with IHX the last aspect has the biggest impact on efficiency. The efficiency without intercooling yields 44.6%.

4. Comparative overview

The potential to improve the efficiency by lifting the reactor core outlet temperature or steam temperature, respectively, is shown in Fig. 6, combining the results of the preceeding sections. All cycles comprising a gas turbine show a similar increase in efficiency if the core outlet temperature is lifted, on different levels for the different processes. The same tendency can be observed for steam cycles, if the live steam temperature is lifted. Fig. 6 shows three groups of cycles, arranged according to the degree of complexity and proof of technology. The cycles with the lowest efficiency, denoted A in Fig. 6, have moderate complexity and predominantly proven technology. Better efficiency is achieved with higher complexity or not nuclear-proven technology, B, and the best theoretical values are achieved with high complexity and not nuclear-proven technology, C. Certainly the core outlet/steam temperatures are by far not the only means to improve the efficiency. Other parameters like the isentropic efficiency of the turbines or of the recuperator are are also of great influence. The calculated efficiencies must be regarded as first-order approximations. It is often observed, that efficiencies „degrade" in parallel to the progress of the design in a real construction project. The overview on efficiencies should stimulate a more comprehensive assessment on power cycles, which must include such important questions like investment costs, or development risks.

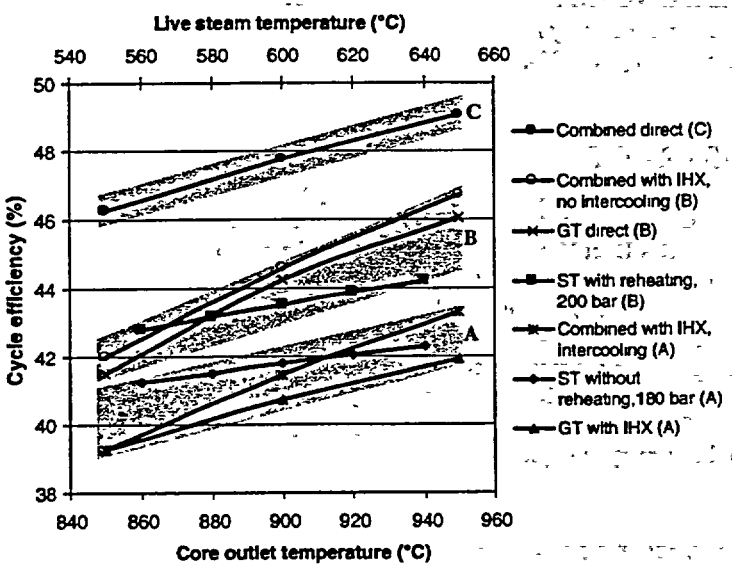

Fig. 6 Overview on efficiencies

Parameter	Steamcycle		Gasturb.c/le		Combined cycle		
	reheater		IHX		IHX		
	no	yes	no	yes	no	yes A	yes B
$P_{nuclear}$, MW	200	200	200	200	200	200	200
$T_{core\ outlet}$, °C	900	900	900	900	900	900	900
$T_{core\ inlet}$, °C	256	256	562	444	286	227	397
P_{blower}, MW	1.7	1.7	_	4.3	_	3.3	4.1
Pressure $Ratio_{total}$	_	_	2.7	4.5	2.5	10	10
$p_{live\ steam}$, bar	160	250	_	_	110	40	40
$T_{live\ steam}$, °C	600	600	_	_	547	408	408
$P_{cycle\ consumption}$, MW	3.5	4.4	0	4.3	0.9	2.5	4 4
P_{net}, MW	82.9	88.2	88.6	81.3	95.0	82.9	89.1
η_{cycle}, %	41.5	44.1	44.3	40.7	47.5	41.5	44.6

A: intercooler between compressor stages, B: no intercooler

Table 1 Main thermodynamic data of the analyzed cycles

5. References

[1] Minatom; DoE; General Atomics; Framatome; Fuji Electric: Executive Summary of Gas-Turbine Modular Helium Reactor Conceptual Design. Framatome, Paris, June 30, 1999

[2] Nicholls, D. R.: Nuclear Engineering International, Dec. 1998, p. 12

[3] Kadak, A. et al.: Modular Pebble Bed Reactor Project, 1st ann. report. MIT, July 1, 1999

[4] HTR-GmbH: THTR-300 MW Kernkraftwerk Hamm-Uentrop, Kurzbeschreibung. Dec. 1983

LOAD ANALYSIS AND SAFETY EVALUATION OF HTR-10's HOT-GAS DUCT VESSEL

HE SHU-YAN, ZHANG ZHENG-MING, YU SU-YUAN
Division of Reactor Structure & Mechanics, Institute of Nuclear Energy Technology, Tsinghua University, Beijing, 100084, China

ABSTRACT

The 10MW high-temperature gas-cooled reactor (HTR-10) is a pebble-bed type reactor. The Reactor Pressure Vessel (RPV) stands side by side with the Steam-Generator Pressure Vessel (SGPV). A horizontal cylindrical Hot-Gas Duct Vessel (HGDV) connects these two vessels and forms the primary loop pressure boundary. The HGDV is the weakest part because it bears complex loads due to the interior pressure and bolt loads as well as additional seismic and installation loads. Therefore, in the HGDV design, the additional loads are reduced to a lower degree which produces a larger safety margin. Analysis shows that, for any loads, the stresses and cyclic loads in the HGDV are relatively low and the leak-before-break requirements can be satisfied. Therefore, the HGDV safety margin is as good as those of the other components in the primary loop pressure boundary.

1. HTR-10's primary loop boundary components and their support system

1.1 Primary loop boundary components

The 10MW high-temperature gas-cooled reactor (HTR-10) is a pebble-bed type reactor. The primary loop pressure boundary consists of the Reactor Pressure Vessel (RPV), the Steam-Generator Pressure Vessel (SGPV) and the Hot-Gas Duct Vessel (HGDV). The RPV stands side by side with the SGPV. The HGDV lies horizontally between the RPV and the SGPV (Fig.1). When necessary, the HGDV can be removed from the two vessels to repair and replace interior components.[1]

1.2 Support system for the primary loop boundary components

The support system is also shown in Fig.1. Besides bearing the weight and the seismic loads of the Primary Loop Boundary Components (PLBC), the support system shall reduce the loads on the HGDV caused by thermal expansion and seismic events. The support platforms for the PLBC are installed at the same level as the HGDV axis. When the PLBC temperature increases, the two ends of the HGDV will have the same thermal displacement in the vertical direction. Therefore, the HGDV will remain horizontal and the bending moments that may be caused by different vertical displacements at the two ends will be minimized.[1]

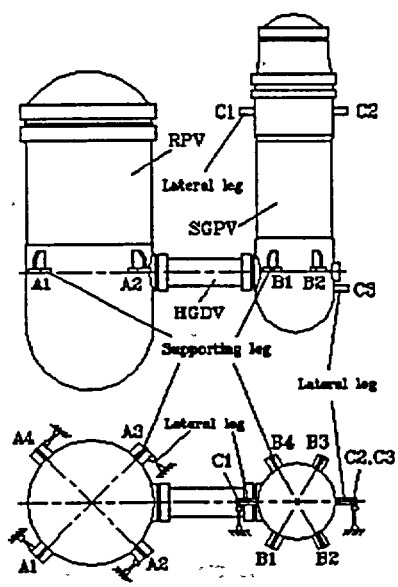

Figure 1. Arrangement and support system of HTR-10 primary loop components

The RPV supporting lugs can only move radially and the RPV centerline is fixed. The SGPV supporting lugs restrain only vertical movement. Three more lateral legs on the SGPV allow the SGPV to move both vertically and axially along the centerline of HGDV. Therefore, the HGDV will move along the HGDV centerline due to the thermal expansion of the

PLBC. The only other thermal load on the HGDV is the friction force generated by the SGPV movement. The temperature change will not generate any bending moment on the HGDV.[1]
For seismic loads, the sway of the SGPV is mainly in the plane determined by the axis of the three vessels. Therefore, the seismic loads on the HGDV can be effectively reduced.[1]

1.3. HGDV main structural parameters

The HGDV is a cylindrical vessel, with the total length of 3325mm, the inner diameter of 900mm, and the wall thickness of 40mm. Its material is SA516-70 and the bolt material is SA540. The HGDV is connected with the RPV and the SGPV by loose flanges that reduce the bending moments on these flanges and the bending stresses on the HGDV caused by the pre-tensioning of the connecting bolts and other facilitates in the PLBC installation. Thirty-two M48×3 bolts, one metal O-ring and one welded Ω-ring are used at each flange couple.[2]

2. HGDV load analysis

Compared with the general pressure vessel, the HGDV has the dual features of pressure vessel and pressurized pipe. During normal operation, the main loads are the interior pressure and the pre-tensioning forces on the flange connecting bolts, which are the same with a general pressure vessel. But, with other large loads on the HGDV such as earthquakes, the restraints at both HGDV ends and the thermal load due to the temperature variation, the HGDV behaves much more like a pressurized pipe. All of the above loads must be considered in the HGDV design.[2]

2.1 Interior pressure and design temperature

The HGDV design temperature, 350°C, is almost uniform during normal operation so the thermal stresses can be neglected. The design pressure is 3.5MPa. Therefore, The circumferential and axial membrane stress in the HGDV shell are $\sigma_{Hm} = 39.4\text{MPa}$ and $\sigma_{Z1} = 19.7\text{MPa}$, respectively.
The total axial force of the bolts generated by the interior pressure is $F_1 = 3.15\text{MN}$. Therefore, the stress in the bolts caused by F_1 is $\sigma_{S1} = 81.9\text{MPa}$.

2.2 Sealing O-ring reaction force

The sealing O-ring, made of Inconel-718 pipe, has an inner diameter of 928mm and specific press of 1.8KN/cm, so the total reaction force of the ring is $F_2 = 0.525\text{MN}$. The stress in the bolts caused by F_2 is $\sigma_{S2} = 13.65\text{MPa}$.

2.3 Friction force

The HGDV move the SGPV along the HGDV centerline as the PLBC expands thermally. The total weight of the SGPV and its internals is 1.05MN. Taking 0.3 as the maximum friction coefficient at the supporting lugs, the maximum friction force to move the SGPV is $F_3 = 0.315\text{ MN}$, and the tension stresses in the HGDV shell and the bolts generated by F_3 are $\sigma_{Z2} = 2.67\text{MPa}$ and $\sigma_{S3} = 8.19\text{MPa}$, respectively.

2.4 Seismic force

Using a 3-D finite element model, the support system is analyzed by linear-elastic transient dynamic calculations. The maximum seismic forces at the two ends of the HGDV for the Safety Shutdown Earthquake (SSE) condition are: bending moment of $M_w = 0.756\text{MN}\cdot\text{m}$, torque of $T_w = 0.161\text{MN}\cdot\text{m}$, shear force of $Q_w = 0.466\text{MN}$, and axial force of $F_w = 0.535\text{MN}$.[3]
The maximum axial tension stresses in the HGDV shell and the connecting bolts generated by M_w are $\sigma_{Z3} = 28.3\text{MPa}$ and $\sigma_{S4} = 66.6\text{MPa}$, respectively. The maximum axial tension stresses in the HGDV shell and the connecting bolts generated by F_w are $\sigma_{Z4} = 4.53\text{MPa}$ and $\sigma_{S5} = 13.9\text{MPa}$, respectively.
The torque and the shear force have very little influence on the HGDV and can be neglected.

2.5 Installation force

During installation, the first step is to connect the HGDV with the RPV with the connecting bolts tensioned to the required pre-tensioning force. At that point, when the HGDV is connected with the SGPV, the center of the two end surfaces of the connecting flanges cannot be exactly aligned, and the two end surfaces can also not be exactly parallel. The two end surfaces will be forced to match by the pre-tensioning force of the bolts. Therefore, a forced displacement and a forced rotation will be generated at the HGDV end surface after installation. The magnitudes of the installation forces will be determined by the installation precision (misalignment of the end surfaces is not more than 0.5mm, and separation angle of the end surfaces is not more than 3×10^{-4}).

Analysis shows that, for the prescribed installation precision, the maximum installation force and stress occur at the joint between the shell and the flange that connects with the SGPV, which coincide with that caused by the seismic loads. This is the most unfavorable case. Therefore, these installation stresses cannot be neglected although they are self-limiting and belongs to secondary stress.

If there is only 0.5mm misalignment and no separation angle between the two end surfaces of the flanges, the maximum axial tension stresses generated in the HGDV shell and the connecting bolts are $\sigma_{Z5} = 11.16\text{MPa}$ and $\sigma_{S6} = 26.24\text{MPa}$, respectively. If the end surfaces have a 3×10^{-4} separation angle with no misalignment, the maximum axial tension stresses generated in the HGDV shell and the connecting bolts are $\sigma_{Z6} = 17.81\text{MPa}$ and $\sigma_{S7} = 41.80\text{MPa}$, respectively.

2.6 Pre-tensioning force of the connecting bolt

If the forces are most unfavorably combined, the maximum possible stress in the connecting bolts is

$$\sigma_S = \sigma_{S1} + \sigma_{S2} + \sigma_{S3} + \sigma_{S4} + \sigma_{S5} + \sigma_{S6} + \sigma_{S7} = 252.3\text{MPa}$$

σ_S is the most conservative pre-tensioning stress, which is too conservative to be used. Compared with the reactor lifetime, SSE will only occur over a short period of time. During this period, the bolts should be strong enough to bear the SSE loads with permission of small helium gas leakage. An excessive pre-tensioning force will generate excessive stress both in the HGDV and in the bolts, which will reduce the component safety. Therefore, the SSE forces were omitted in determining the pre-tensioning force, but fully considered in determining the bolt strength.

Without the bolt stresses σ_{S4} and σ_{S5}, the bolt stress generated by the other forces is

$$\sigma_P = \sigma_{S1} + \sigma_{S2} + \sigma_{S3} + \sigma_{S6} + \sigma_{S7} = 171.8\text{MPa}$$

Taking σ_P as the pre-tensioning stress in the bolts, the total pre-tensioning force of the thirty-two connecting bolts can be calculated as $F_P = 6.61\text{MN}$. The SSE loads will cause the sealing surface to separate partially, but the opening will not exceed 0.05mm. Even for this most unfavorable load, the sealing ability of the O-ring can still prevent the helium gas from leakage.

3. HGDV safety evaluation

3.1 Stress evaluation of the HGDV and the connecting bolts

At the design temperature (350°C), the allowable stress of the bolt material is 240MPa.[5] For the SSE condition, the allowable stress is 288MPa.[4] Therefore, σ_S and σ_P show that the bolt stress is less than its allowable stress limit even for the most unfavorable load.

Stress analysis of the HGDV shell shows that the maximum stress strength, which is in the axial direction, occurs at the outer surface of the shell end closest to the SGPV. If only the pre-tensioning force of the bolts, the interior pressure and the reaction force of the O-ring are considered, the maximum stress strength calculated by the finite element method is $\sigma_0 = 94.5\text{MPa}$.[6] If the forces are most unfavorably combined, this maximum stress strength is $\sigma_1 = 142\text{MPa}$.

The membrane stress strength part of σ_0 is σ_{Z1}. In σ_1, the membrane stress is:

$$\sigma_m = \sigma_{Z1} + \sigma_{Z2} + \sigma_{Z3} + \sigma_{Z4} + \sigma_{Z5} + \sigma_{Z6} = 84.2\text{MPa}$$

At the design temperature, the design stress intensity of the HGDV material is 127MPa [5], which is the limit for the primary membrane stress. For the membrane stress plus bending stress, the limit is 1.5×127MPa=190.5MPa.[4] For the SSE condition, the stress limits are 1.2 times these values,

152MPa and 228MPa, respectively.[4] Comparing these limits with the values in σ_0, σ_1, and σ_m, it can be seen that the HGDV stresses are all within their stress limits.

3.2 Brief description on the Leak-Before-Break property of the HGDV

The HGDV satisfies the prerequisites of Leak-Before-Break (LBB).[7]
The maximum stress in the HGDV is the axial stress at the outer surface. In the LBB analysis, the crack is postulated to be located in this region perpendicular to the direction of the maximum stress. Therefore, the through-wall crack is along the circumferential direction of the shell.
The detectable leak-rate of HTR-10 PLBC is $4m^3$ per hour (for standard conditions). The leak-rate used in the LBB analysis is 10 times the detectable rate.[7] Therefore, for normal operation conditions, the helium gas leak-rate from a penetration crack is $L_v = 40\,m^3/hr$. The helium gas density is $\gamma = 0.179kg/m^3$ at standard condition.[8] The mass leak rate is $L_m = L_v \cdot \gamma = 0.001989kg/s$.
Assuming that the helium gas is ideal gas and the pressure outside the crack is lower than the critical pressure p_c, the gas will flow through the crack and reach critical velocity at the exit.[9] This velocity, which is the sound velocity outside the crack, can be calculated as $V_c = \sqrt{\kappa p_c v_c}$, where v_c is the critical specific volume at the crack exit, $\kappa = C_p / C_v$ (C_p and C_v are the gas specific heats at constant pressure and constant volume). For a monatomic gas like helium, $\kappa = 1.667$.
For the HTR-10 operating condition, the critical helium gas pressure ratio is

$$\beta_c = \frac{p_c}{p_1} = \left(\frac{2}{\kappa+1}\right)^{\frac{\kappa}{\kappa+1}} = 0.4871$$

where $p_1 = 3.0MPa$ is the operating pressure. Then $p_c = p_1 \times \beta_c = 1.4613MPa$.
Inside the crack, the helium gas is at 250°C and 3.0MPa, so the specific volume is then $v_1 = 0.3612m^3/kg$.[8] The specific volume of the helium gas at the crack exit reaches its critical value $v_c = v_1\left[\frac{p_1}{p_c}\right]^{1/\kappa} = 0.5561m^3/kg$. The sound velocity outside the crack can be calculated as $V_c = 1164m/s$. Therefore, the crack open area is $A = L_m v_c / V_c = 0.96mm^2$.
Increasing the stress perpendicular to the crack growth direction increases the crack opening area. If the crack opening area is constant at A, smaller stress will mean longer crack. Therefore, for the calculation of the crack half-length, the shell axial stress generated only by the normal operating pressure (3.0MPa) is adopted, which is $\sigma_n = \sigma_{Zi} \div 3.5 \times 3 = 16.89MPa$.
With the opening area A and the stress σ_n, the crack half-length is $a_0 = 40.4mm$.[10]
The stability criterion of the crack are: (1) The half-length of the circumferential through-wall crack in the shell is $2a_0$;[7] (2) The maximum possible axial stress in the shell is σ_1.
The smaller axial stress σ_n is used to calculate the crack half-length, while the maximum possible axial stress is used to analyze the crack stability, which is apparently very conservative.
Following the linear-elastic analysis method referred in Ref. [11,12,13], The stress intensity factor can be calculated as $K_I = 80.5MPa\sqrt{m}$. The fracture toughness of the HGDV material for the operating condition is larger than $200MPa\sqrt{m}$.[14] Therefore, the postulated through-wall crack is stable. The elastic-plastic analysis of the crack led to the same conclusion.[10]

3.3 HGDV fatigue crack growth

The maximum cyclic load in the reactor lifetime is related to the changes of the interior pressure. The fatigue crack growth caused by cyclic load can be calculated in accordance with Ref. [14]. For the HTR-10 PLBC, any credible fatigue crack growth in the lifetime is very small. The largest credible crack in the HGDV is the through-wall crack with the half-length of a. Assuming that the interior pressure changes from 0 to 3.0MPa 1000 times as the reactor goes from cold start up to normal

operating, the crack growth is not more than 0.5mm. For the combined action of the various cyclic loads, the corresponding growth is not more than 1mm during the reactor lifetime. This small fatigue crack growth is sufficiently safe for the HTR-10 PLBC.

4. Conclusions of the HGDV safety evaluation

The safety of HGDV are guaranteed by the following measures: (1) The PLBC support system design minimizes the additional loads on the HGDV caused by normal operating and seismic conditions. (2) The prescribed installation precision of the PLBC is relatively strict; therefore, the additional installation loads are small. (3) The structure stress strength has a relatively large safety margin.
Following conclusions can be obtained: (1) The stresses in the whole structure are relatively small. The stress margins of the shell and the connecting bolts are very large. (2) The HGDV satisfies the LBB criterion; therefore, the possibility of brittle fracture can be excluded. (3) The cyclic stresses are very small. For any credible crack, the crack growth rate is extremely low. During the reactor lifetime, the crack growth can be neglected.

References

[1] He, S.Y., 1995, Design specification of HTR-10's Primary Loop Boundary Components, INET Report
[2] He, S.Y., 1996, Design specification of HTR-10's Hot-Gas Duct Vessel, INET Report
[3] Zhang, Z.M., 1998, Seismic analysis of HTR-10's Primary Loop Boundary Components, INET Report
[4] ASME Section III, Subsection NB, 1989
[5] ASME Section III, Subsection APPENDIX 1, 1989
[6] Zhang, Z.M., 1996, Stress analysis of HTR-10's Hot-Gas Duct Vessel, INET Report
[7] USNRC SRP3.6.3 (draft), 1988
[8] Ma, Q.F. et al, 1986, Practical manual for thermophysics, Beijing
[9] Pang, L.M., 1982, Engineering thermodynamics, Beijing
[10] Klecker, R., Burst, F.W., Wilkowshi, G., 1986, NRC Leak-before-break (LBB NRC) analysis method for circumferential through-wall cracked pipes under axial plus bending loads, NUREG/CR-4572
[11] Sanders Jr., J. L., 1982, Circumferential through-wall cracks in cylindrical shells under tension, J. Appl. Mech., 49, 103-107
[12] Sanders Jr., J. L., 1983, Circumferential through cracks in a cylindrical shell under combined bending and tension, J. Appl. Mech., 50, 221
[13] Paris, P.C., Tada, H., 1983, The application of fracture proof design methods using tearing instability theory to nuclear piping postulation circumferential through wall crack, NUREG/CR-3464
[14] ASME Section XI, Subsection APPENDIX A, 1989

ACACIA-INDIRECT: A SMALL SCALE NUCLEAR POWER PLANT FOR NEW MARKETS

D.F. DA CRUZ, J.B.M. DE HAAS and A.I. VAN HEEK
NRG, P.O. Box 25, NL-1755 ZG Petten, The Netherlands

ABSTRACT

A 60 MWth, 23 MWe pebble bed HTR plant with indirect Brayton cycle is proposed for the applications of heat and power cogeneration or distributed electricity generation. The reactor will be cooled by helium, whereas for the secondary cycle nitrogen is proposed as a heat carrier. Economic performance is being optimized by simplification of the nuclear part and by the exclusive use of commercially proven systems in the energy conversion part. Cogeneration and maximised electricity production will be the two applications discussed. The pebble bed reactor will be of the cartridge type, refuelled off-line only once every three years. Excess reactivity will be controlled by burnable poison in the reflector. Optimization of burnable poison distribution will be discussed for two core geometries, a cylindrical and an annular one. It is shown that in an annular core burnable poison can be distributed in such a way that the reactor will be able to operate for three years with a sufficiently small overreactivity margin.

1. Introduction

Until now, nuclear power has been successful in the market of large scale electricity generation. Other markets, like heat and power cogeneration or distributed electricity generation in developing countries are still waiting to be penetrated by the uranium based energy source.

For these applications, the power level required per location will be much smaller than for the existing nuclear plants. ACACIA-Indirect (AdvanCed Atomic Cogenerator for Industrial Applications), a 60 MWth, 23 MWe (max.) nuclear plant design with indirect Brayton cycle is proposed. The reactor will be of the pebble bed type, because of the high level of inherent safety that can be attained. Economic performance is being optimized by both simplification of the nuclear part and by the exclusive use of commercially proven systems in the energy conversion part. For the reactor, no on-line fuelling or defuelling systems are envisaged, as the pebble bed reactor will be of the cartridge type, refuelled off-line only once every three years. Excess reactivity will be controlled by B_4C as burnable poison in the reflector only, so no new fuel pebbles with burnable poison need to be developed.

Whereas the reactor will be cooled by helium, nitrogen is proposed as a heat carrier for the secondary cycle because of its similarity with air. In this way, a conventional air based gas turbine can be applied, while at the same time excluding the scenario of air ingress through heat exchanger leak.

Optimization of core geometry and burnable poison distribution will be discussed, as well as cogeneration and maximised electricity production as two plant applications.

2. Plant design

A 60 MWt helium cooled pebble bed reactor is coupled with a secondary nitrogen cycle through a He/N_2 heat exchanger. Two applications are analysed [1]: one for cogeneration of electricity and process steam, and one for electricity generation only. In the last case this is done by a combined cycle of a gas turbine and a steam turbine. Table 1 highlights the main features of the plant, and in figure 1 the component arrangement is depicted for the cogeneration plant. The reactor and energy conversion components are placed into four modules, one nuclear one and three non-nuclear ones. The reactor pack houses the reactor, the He/N_2 heat exchanger (nitrogen heater) and the helium blower. The hot nitrogen is transferred to the gas turbine pack, where it drives the gas turbine. The turbine also drives the two compressors of the intercooled cycle, and a generator delivering 18.8 MWe. After leaving the

turbine, the gas, now cooled down to 516°C, flows to the adjacent heat cogeneration unit. Here it is directed through four heat exchangers in a row: the heat recovery steam generator, the recuperator, the feedwater heater and the precooler. By now, the gas has been cooled down to 28°C, and is sent back to the gas turbine pack for intercooled compression. Before being sent back to the nitrogen heater it is preheated in the recuperator to 299°C. For the combined cycle electric plant, the hot steam leaving the heat recovery steam generator is expanded in an additional steam turbine coupled with a second generator, giving an additional 5.2 MWe.

Table 1 Main features of ACACIA indirect cycle plant, in cogeneration mode and in electricity-only mode.

	Baseline cogeneration	Combined cycle
Reactor power (MWt)	60	
Core inlet/outlet temperatures (°C)	352/900	
Net electrical power output (MWe)	18.1	23.2
Gas turbine output (MWe)	18.8	18.8
Steam turbine output (MWe)	-	5.2
Process steam production (t/h, 425°C/ 4.14 MPa)	27.8	-
Net power generation efficiency (% max.)	30.1	38.7
Net total thermal efficiency (%)	70.0	38.7

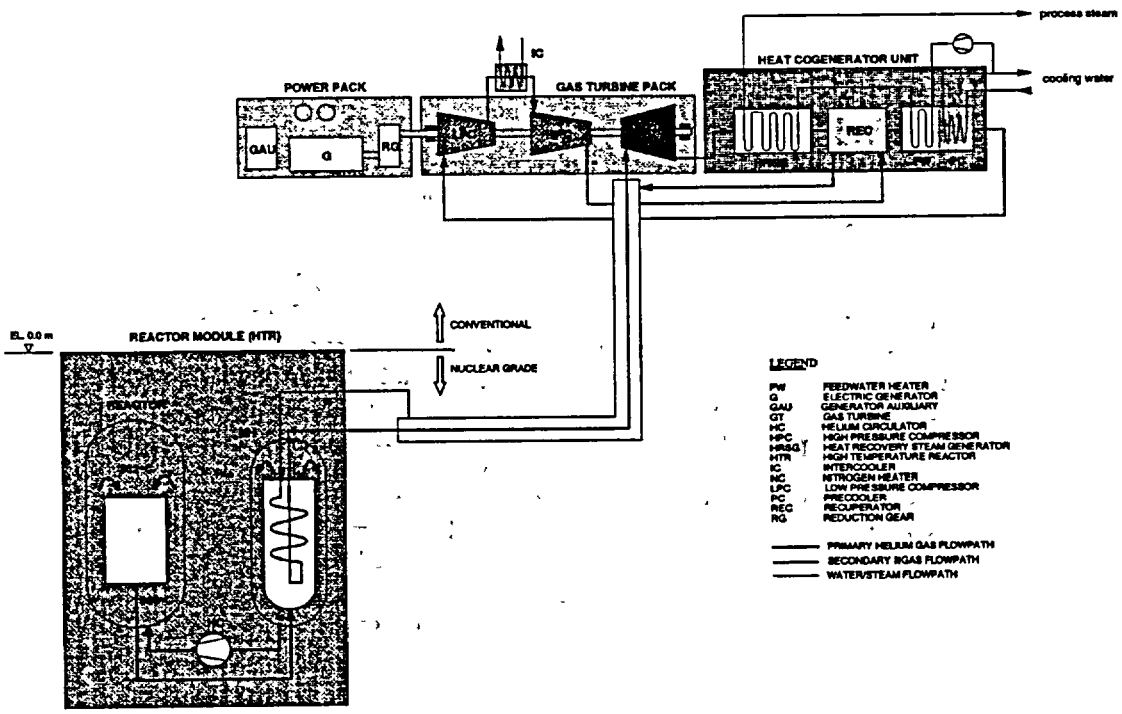

Fig.1 ACACIA cycle design for cogeneration of electrical power and process steam.

The core outlet temperature is set 900°C, which is below what has been or will be demonstrated by the fuels in AVR, HTR-10, HTTR, etc. No safety hazard of water or steam ingress into primary system exists, since all water and steam circulation is remotely located in the third loop. The nitrogen heater is essentially pressure balanced with a slightly higher secondary pressure to ensure that no fission products will enter the secondary system in case of leaking tubes. The reactor vessel will be kept below 370°C, so normal SA533 steel can be used. The nitrogen heater can be designed as compact as an HTR steam generator, by selecting a large temperature difference of 50°C between the primary and

secondary inlet and outlet fluids, an optimal pressure balance inside and outside of the tubes and a minimal tube wall thickness.

Whereas for direct cycle systems a helium turbine needs to be developed and commercialized, a simplification goal in this study is adaptation to conventional or existing components and systems so that the available experience becomes sufficient enough to minimize any significant R&D requirements and deployment risks.
The past and current system and component technologies that support the present N_2 closed cycle are identified below:

- A number of past closed cycle air gas turbine generators were built for up to 30 MWe in Europe, the U.S. and Japan; Some of the plants were operated for up to 100,000 -150,000 hrs.
- More modern gas turbine technologies developed in conventional gas turbines such as dry gas shaft seal, high temperature blade materials, aerodynamic and rotor dynamic modeling will greatly improve the closed cycle experience of the past.
- Conventional gas-to-water coolers and heat recovery steam generator.
- Conventional or retrofitted steam turbine and auxiliaries.
- The present design study has identified little or no R&D requirements for the ECS of the HTR indirect cycle plant and that all major equipment can be obtained based on available experience or from off-the-shelf products (technology references will be provided as required).

3. Core design

The cartridge core is the ultimately simplified pebble bed core besides the recirculation, OTTO and PAP cores [2]. The core is loaded at once with fresh pebbles, and then operated for three years without refuelling or fuel shuffling. After this period the entire core is replaced. The associated loss of fuel utilization efficiency will be offset by a reduction of capital and O&M costs.

A core study has been made as an investigation about the parameters needed to obtain a pebble core with an as flat as possible reactivity behaviour as function of the time between two fuel reloads. This flatness is needed to have a sufficiently small and constant excess reactivity to be controlled by control rods or gas flow. The idea is to use the pebble fuel composition as proposed for the PBMR plant, with 8.1% enrichment and 9 g of heavy metal per fuel element. Excess reactivity will be controlled by B_4C as burnable poison in the reflector. A parameter study regarding core geometry, poison location and concentration is discussed in this section.

The technique of using burnable poison in the reflector of a pebble bed reactor has been proposed in the paper by Van Dam [3]. Instead of a 1-D 2-groups diffusion approximation we used a 2-D 16-neutrongroups approach. The 16-groups nuclear data were condensed from 172-groups cell calculations, based on JEF2.2 data, in which the double heterogeneity of the pebbles was taken into account. For a 60 MW reactor two geometries were modelled in the WIMS/SNAP-code, a cylindrical and an annular one. The first has a pebble bed core with radius 1.45 m and height 6.50 m (average core power density 1.4 MW/m^3) leaving 0.5 m of void on top of the bed till the top reflector.

The cylindrical core is surrounded by a graphite side reflector of 1.0 m thickness and an effective top and bottom reflector of 2.0 m, based on the earlier direct cycle ACACIA design with PAP fuelling [4]. In the side reflector zones were applied to which burnable boron could be added. Results of these calculations for different initial boron concentrations (1, 50, 75 and 100 ppm of natural boron) and as function of the number of full power days can be seen in fig. 1.

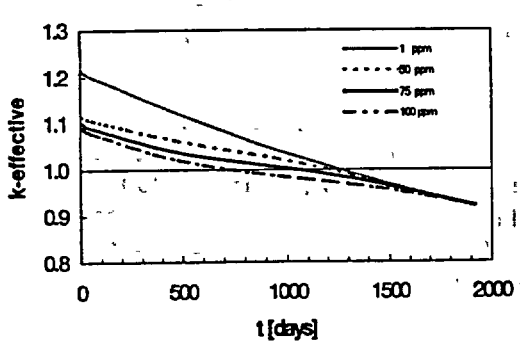

Fig 1. Reactivity as function of the number of full power days for different boron concentrations in the side reflector.

From this figure it can be seen that for a cylindrical core the excess reactivity can be suppressed but will keep a to steep descending tendency during cartridge lifetime, while reducing the lifetime too much. Another disadvantage of poison in the side reflector will be the partial suppression of the control rod worth in the reflector because of the lowered thermal flux importance by the poison in this region.

To obtain an annular core an inner reflector of solid graphite, with radius 0.6 m was placed in the centre of the core. To maintain the same averaged power density the core was elongated to 7.5 meter. In fig. 2 the borated regions in the inner and outer (side) reflectors are indicated by the dashed lines. The effect of poisoning respectively the bottom, inner and outer reflector has been examined.

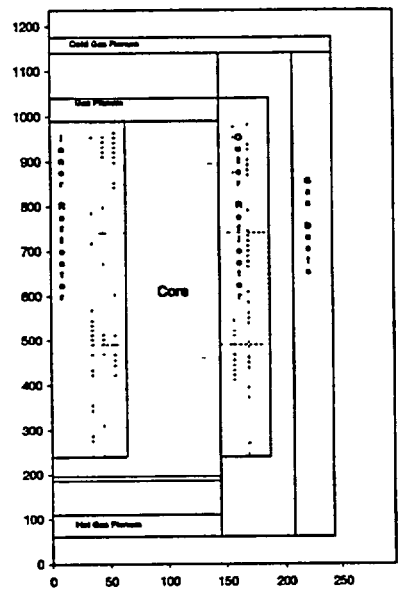

Fig 2. Sketch of the ACACIA model with annular core.

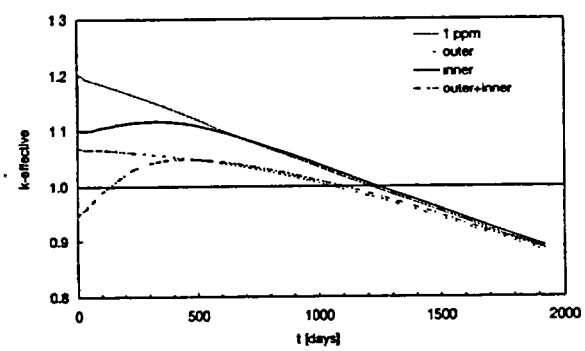

Fig 3. Reactivity effect for 50 ppm boron in the different reflector regions.

Boron in the bottom reflector did not give a significant effect because of the small absorbing area compared to the reflector surface. This did not show as a tool to tailor the reactivity curve.

To compare the influence on the reactivity due to boron in the outer or inner reflector, calculations have been done for 50 ppm boron in the borated regions of the inner or outer and both reflectors. The results are given in fig 3. The references case for 1 ppm or natural boron impurity has been given as well. It can be seen that the influence of the inner reflector is stronger especially in the begin of the lifetime, this is due to the "flux trapping" in the inner core resulting in a high thermal flux importance but also in a faster depletion of the boron in the region.

The required effect of reflector poisoning was found for the annular core with inner reflector poisoning only. From the results given in fig 4 it can be seen that increasing the boron content leads to a flattening the reactivity curve, until there is so much boron that the reactivity increase due to the boron depletion can not keep pace with the decrease by the fuel depletion. For a boron concentration of about 150 ppm the reactivity curve is almost flat until about 1000 full power days. It can also be seen that the period where $k_{eff}>1$ increases as well with the boron concentration.

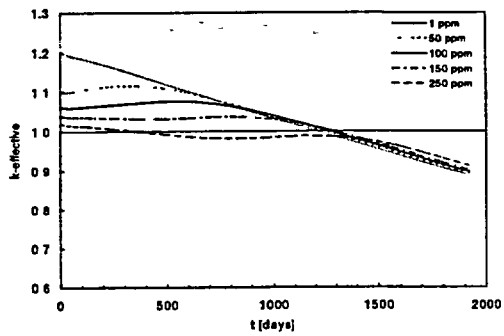

Fig 4. Reactivity as function of boron concentration in the inner reflector.

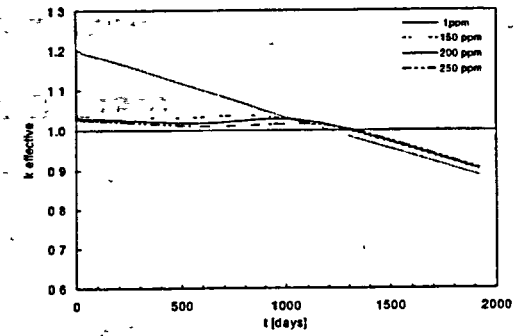

Fig 5. Reactivity as function of different boron contents in the middle section of the inner reflector.

The possibility of axial zoning of the burnable poison in the inner reflector has been investigated as well, see fig. 5. The inner reflector was divided into three zones; the two outer zones were given a concentration of 150 ppm whereas the middle zone was given up to 250 ppm. A further overall lowering of the reactivity curve can be observed. This figure together with fig. 4 shows that there are tools to obtain an almost flat reactivity curve with a core lifetime of about 3 years. In this stage flatness is more important than the absolute difference from k_{eff} =1 because this can be solved by geometrical means.

In the continuation nuclear data will be generated with boron concentrations within the bandwith obtained with this study. These nuclear data will be used in the full 3-D reactor code PANTHERMIX with thermal-hydraulic feedback for the calculation of neutron fluence, power and temperature fields.

4. Conclusion and Prospects

A pebble bed HTR plant for small scale markets with an indirect Brayton cycle and cartridge core has been designed. As the secondary medium is nitrogen, all energy conversion system components are conventional and existing, so R&D requirements and deployment risks are minimized.

The cartridge core will be entirely reloaded once every three years. Core geometry will be annular with with burnable poison in the inner reflector. Poison concentration and location have been chosen in such a way that core overreactivity remains sufficiently small and constant over an operating period of three years.

Thermal-hydraulic and transient analysis is planned to be done for both the core and the entire plant system.

5. References

[1] Longmark Power International Inc., HTR^{icc}, Indirect Cycle Cogeneration, Contract of NRG, 2001.

[2] E. Teuchert, H. Gerwin and K.A. Haas, Simplification of the Pebble Bed High Temperature Reactor, International Specialist's Meeting on Potential of Small Nuclear Reactors for Clean and Safe Energy Sources, Tokyo, October 23-25, 1991.

[3] H. van Dam, Long-term Control of Excess Reactivity by Burnable Poison in Reflector Regions, Annals of Nuclear Energy 27, 63-69, April 2000.

[4] E.C. Verkerk, Dynamics of the Pebble-Bed Nuclear Reactor in the Direct Brayton Cycle, PhD Thesis, Delft University of Technology, 2000.

THE CONCEPT DESIGN OF THE POWER CONVERSION UNIT FOR HTR-10 WITH DIRECT GAS CYCLE

S. YU, Z. ZHANG, Z. WU, Y. XU, Y. SUN

INET, Tsinghua University, Beijing, 100084, China

ABSTRACT

The second phase of 10MW High Temperature Gas-cooled Reactor Test Module (HTR-10) is supported by the Chinese Ministry of Science and Technology and one of its major tasks is to develop a direct helium gas turbine cycle for HTR-10 in the next 5 years. The direct helium turbine cycle coupled with the HTR-10 significantly simplifies the plant system design and should bring considerable cost benefits. The paper sketches the recent concept design for direct gas cycle of HTR-10 and its components, operating modes and interface systems.

1. Introduction

The direct helium turbine cycle coupled with a high temperature gas-cooled reactor is presently being developed in several countries[1], for example, the PBMR and GT-MHR projects. The direct cycle configuration significantly simplifies the plant system design and should bring considerable cost benefits[2]. The proposal of coupling of a direct helium cycle to the 10MW High Temperature Gas-cooled Reactor Test Module (HTR-10) has been approved as one of the major tasks by the Chinese Ministry of Science and Technology for the next 5 years.

The HTR-10 reactor, in its current system configuration, is coupled with a steam turbine power generation unit through a steam generator [3]. Space is reserved inside the SG pressure vessel for a gas turbine that will be installed later for future R&D tasks. After successful operation and initial experiments on HTR-10, the test reactor facility will be reconfigured for research and development work on gas turbines. It would only require the dismantling of the existing helium circulator[4]. Recent developments in gas turbine equipment, high-efficiency heat exchangers and electromagnetic bearings have enabled the development and design of reactor plants combining a safe modular gas-cooled reactor and a power conversion system based on the high-efficiency gas-turbine Brayton cycle. The components of a gas turbine cycle, such as the turbine, compressor, magnet bearings, and plate-and-fin recuperator could be found worldwide. The major challenge for the direct helium gas turbine cycle for HTR-10 would be an integrated test. The questions concerning radioactivity deposition on the turbine blades, the influence of turbine shaft over-speed, as well as the system configuration, could be answered in the tests. HTR-10 will be a very attractive reactor to perform these tests.

2. Diagram and the Concept Design

Based on thermodynamic analysis of the plant gas-turbine cycles, the HTR-10 PCU principal diagram with a direct gas turbine is shown in Fig. 1. The PCU working fluids are high purity helium (primary

coolant and gas-turbine cycle working body) and the PCU cooling system water, – chemically demineralized water. The HTR-10 PCU has the following main equipment:

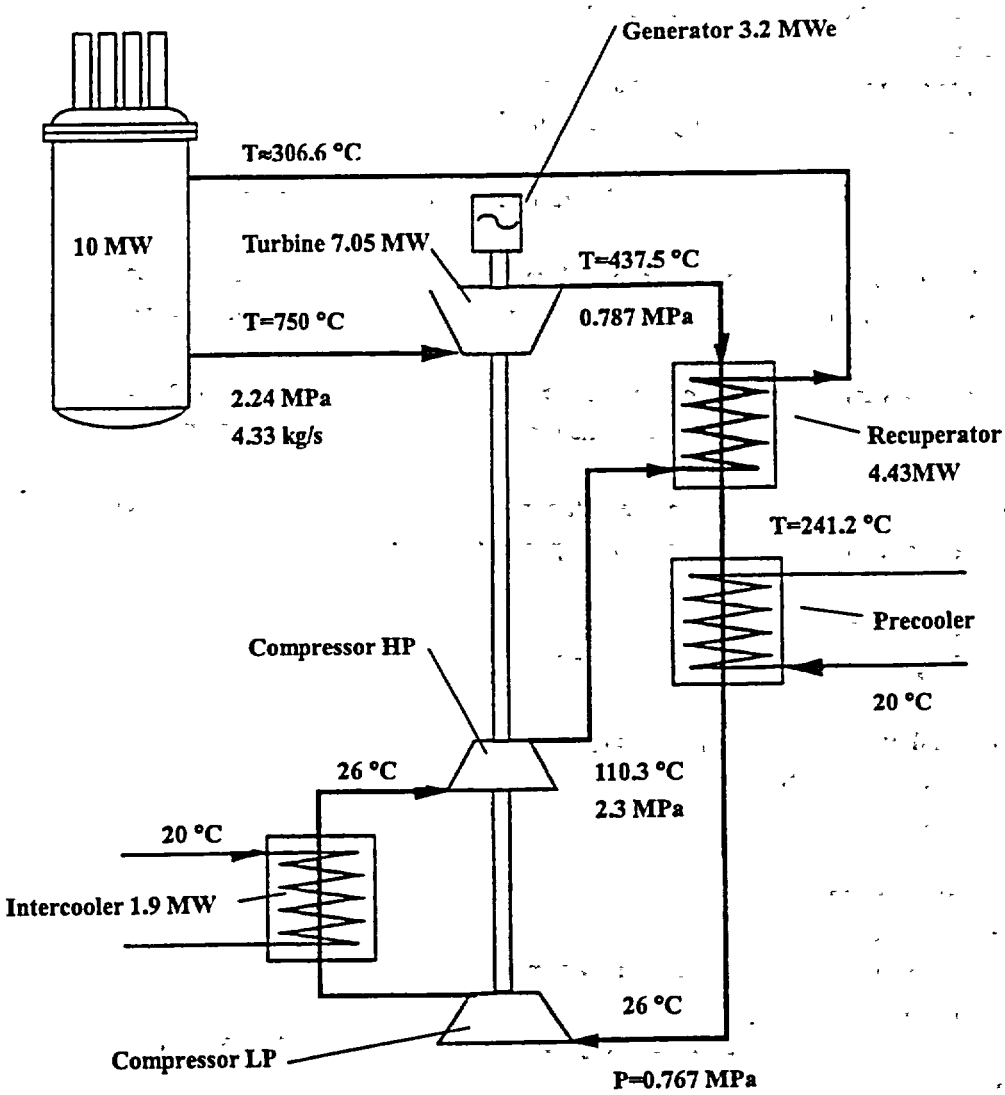

Fig. 1 HTR-10 PCU principal diagram with a direct gas turbine

- turbomachine on electromagnetic suspension consisting of high and low pressure compressors, turbine and generator;
- heat exchange equipment which includes recuperator, precooler and intercooler and generator gas-cooler;
- vessel structures and gas ducts.

Helium is circulated over the primary circuit by the compressors operating both at power operation, owing to helium expansion in the turbine, and in the modes of start-up, shutdown and cooling through

the PCU, owing to generator operation in motoring mode fed by external grid through the frequency converter. During operation, PCU fulfils its functions in the following operating modes:

- putting to operation;
- power variation within the control range;
- load drop and its maintaining at the level sufficient for house load power supply;
- putting out of operation;
- shutdown reactor maintaining in the preset temperature state;
- emergency putting out of operation with cooling down through PCU.

PCU parameters control at corresponding control of the reactor parameters is performed by the following systems:

- turbomachine control and protection system by opening bypass shut-off-control valves (at abrupt decrease of electric load, maintaining load at the house load level, during emergency putting out of operation with cooling down through PCU);
- pressure control system by varying coolant mass in the primary circuit (at putting in and out of operation, electric load decrease or increase, emergency putting out of operation with cooling down through PCU);
- frequency converter by varying the turbomachine rotational speed (at putting in and out of operation, shutdown reactor maintaining in the preset temperature state).

The PCU interfacing systems are the following:

- reactor system (including cross vessel and "hot" gas duct);
- vessel system;
- turbomachine control and protection system, including a set of shut-off and control valves;
- electromagnetic bearings control system;
- generator excitation system;
- frequency converter;
- PCU coolers leak detection system;
- PCU isolation valves system;
- primary circuit protection against overpressurization system;
- PCU cooling water system;
- helium service system, including helium purification system and helium mass control system;
- vacuuming system;
- house load power supply system;
- liquid drainage system;
- air vent and conditioning system in RP compartments;
- fuel and component handling, installation and maintenance equipment;
- RP compartment system;
- automated process control system.

3. Status of the HTR-10 PCU

Currently, the direct helium gas turbine cycle to the HTR-10 is being studied and evaluated. An agreement has been signed between INET and OKBM of Russian to develop the preliminary design for the HTR-10 reactor power conversion unit. A concept layout for a direct gas turbine cycle is shown in Fig. 2.

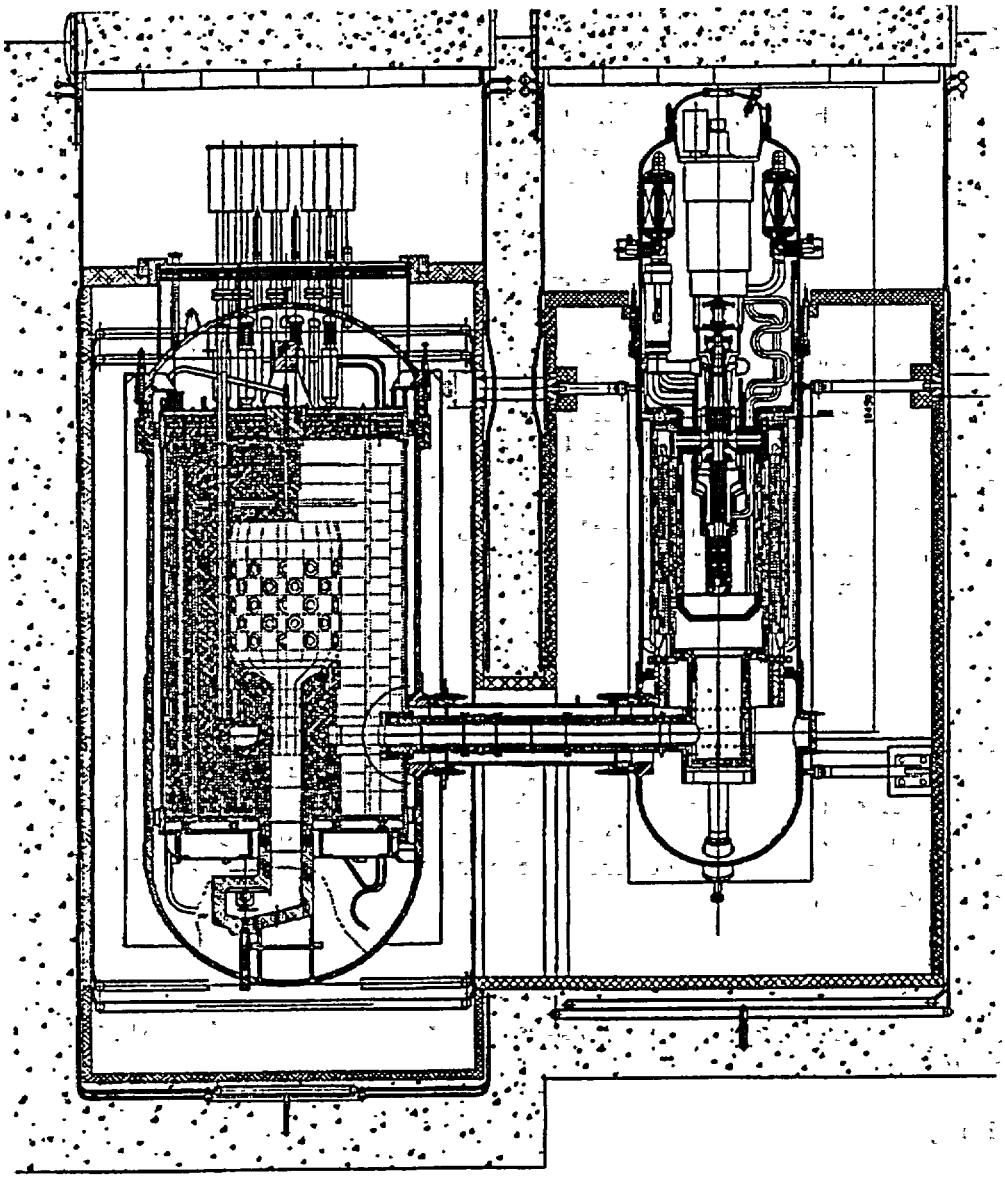

Fig. 2 The concept design of HTR-10 PCU with a direct gas turbine

4. References

[1] International Atomic Energy Agency, 2001. Current Status and future development of modular high temperature gas cooled reactor technology, IAEA-TECDOC-1198

[2] Nicholls, D. 1998. ESKOM sees a nuclear future in the pebble bed, Nuclear Engineering International, vol.43, no.533, pp.12-16.

[3] Xu Yuanhui, 1999. High Temperature Gas-cooled Reactor Program in China. Proceedings of the 4th Nuclear Energy Symposium March 15-16, Taoyuan, China, 25-32.

[4] Zhong Daxin, Qin Zhenya, 2001. Overview of the 10MW High Temperature Gas-cooled Reactor Test Module. Proceedings of the Seminar on HTGR Application and Development March 19-21, Beijing, China, 194-206.

5. Acknowledgement

Authors appreciate the discussion with scientists from OKBM, SLAC and CTI on the project.

BURNUP DEPENDENT CORE NEUTRONIC ANALYSIS FOR PBMR

Y. CECEN, U. COLAK, O. K. KADIROGLU
Hacettepe University, Department of Nuclear Engineering
06532, Beytepe, Ankara, Turkey

ABSTRACT

The strategy for core neutronics modeling is based on SCALE4.4 code KENOV.a module that uses Monte Carlo calculational methods. The calculations are based on detailed unit cell and detailed core modeling. The fuel pebble is throughly modeled by introducing unit cell modeling for the graphite matrix and the fuel kernels in the pebble. The core is then modeled by placing these pebbles randomly throughout the core, yet not loosing track of any one of them.
For the burnup model, a cyclic manner is adopted by coupling the KENOV.a and ORIGEN-S modules. Shifting down one slice at each discrete time step, and inserting fresh fuel from the top, this cyclic calculation model continues until equilibrium burnup cycle is achieved.

1. Introduction

PBMR is of interest to many developing countries trying to harness the benefits of nuclear power for their economical development. One of the interesting properties of this type of reactor is the flexibility of the burnup cycles. In order to investigate the burnup behavior of such a system a model has to be created in such a way that it should simulate the real system. Pebbles randomly resting on top of each other in the core cavity raise problems in the deterministic analysis methods. One has to use Monte Carlo techniques to model such a system.

2. Modeling

The modeling for the core of a PBMR is made in two steps. The first step is to model the fuel pebble and the next step is to model the core.

2.1. Pebble Modeling

TRISO particles, arranged in a triangular pitch, is considered and a unit cell representing such a geometry is assumed. The distance between the particles are taken such that there will be around 15000 particles in a 5cm pebble made out of a homogeneous mixture of graphite and TRISO particles. Using such a triangular unit cell, with 8.4% enriched UO_2 kernels, coated with different layers of graphite and SiC, a cross section set for the unit cell is obtained by using SN spectrum calculation code. A 6 cm pebble is modeled by using this newly created material and 0.5 cm thick graphite layer encompassing it.

2.2. Core Modeling

The core of the PBMR is assumed to be made of three radial zones [1]. The inner zone, with a radius of 77 cm, is the central reflector zone composed of pure graphite balls. Adjacent to it is the mixing zone with a thickness of 33 cm, composed of graphite and fuel pebbles mixed with equal ratios. The outer zone is the fuel zone extending to a thickness of 65 cm. Furthermore the mixing zone is divided into 3 and the fuel zone is divided into 6 regions whereas the axial length of the core is divided into 7 regions.

3. Calculations

The criticality calculations for BOC and Xe equilibrium are performed for three cross section libraries available at the SCALE package [2]. The results of these calculations are presented in Table 1. It is observed that 27 group ENDF-IV library yielded more realistic results when compared with the Hansen-Roach and 44 group ENDF-V libraries. The reactivity data cited in literature [3] guides us to choose 27 group cross section library since other libraries yield subcritical systems at the stated enrichment and power levels and Xe buildup.

The k_{eff}, group fluxes and fission densities per region is calculated for the BOC and Xe equilibrium cases. From the group fluxes integral group parameters for thermal, resonance and fast spectrums are obtained and inputed to ORIGEN-S [4] along with the power distribution.

Burnup calculations yielding the Xe, Sm, Pm and I concentrations along with actinide concentrations of Pu-239, U-236, Pu-240 and Pu-241 are performed. These new isotopes are then inserted into the kernels at the center of the TRISO particles and a new cross section set is calculated as described above. It is seen that in two full power days Xe equilibrium is achieved .

Considering the discharge rate of the fueling system of a PBMR, a burnup step of 6, 10 and 15 full power days are tried but 10 day burnup steps are taken as the optimum value. Every 10 days one seventh of the core is shifted downwards ejecting the bottom layer and inserting a new layer of fresh fuel pebbles on the top layer.

4. Results

TABLE I. Core k_{eff} values at BOC and Xe equilibrium for different cross section libraries

	Hansen-Roach	27group ENDF-IV	44group ENDF-V
BOC	1.0382 ± 0.0004	1.0463 ± 0.0004	1.0344 ± 0.0004
Xe equilibrium	1.0191 ± 0.0005	1.0252 ± 0.0005	1.0165 ± 0.0005

For each burnup step of 10 full power days the criticality of the PBMR is calculated and the results are presented in Table 2.

TABLE II. Core k_{eff} values for different burnup steps

Burnup step	Core k_{eff}
BOC	1.0463 ± 0.0004
Xe equilibrium	1.0252 ± 0.0005
Step 1	1.0312 ± 0.0010
Step 2	1.0254 ± 0.0010
Step 3	1.0231 ± 0.0010
Step 4	1.0202 ± 0.0010
Step 5	1.0171 ± 0.0010
Step 6	1.0121 ± 0.0010
Equilibrium Cycle	1.0123 ± 0.0009

The power peaking factors for BOC, Xe equilibrium and equilibrium core are presented in figures 1 to 3.

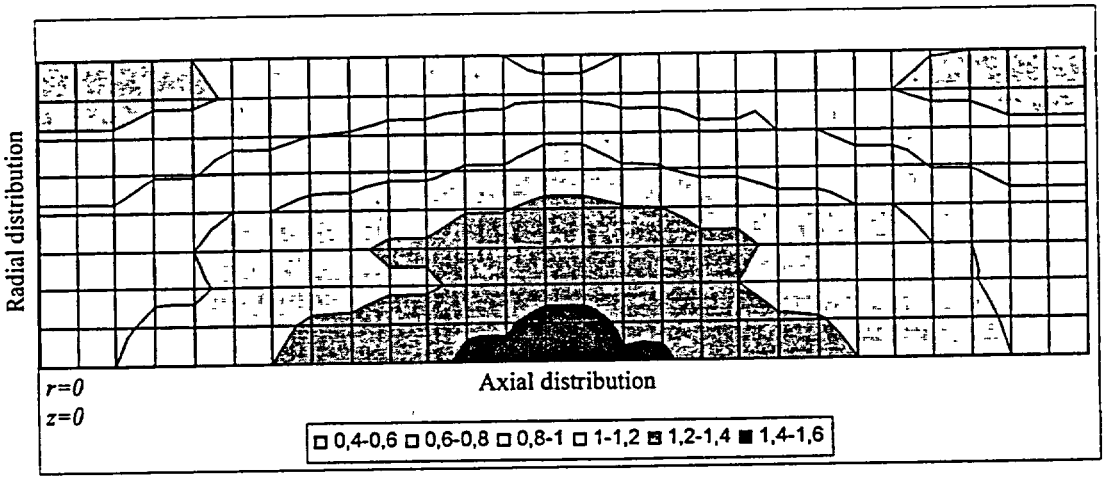

Fig 1. Power distribution at BOC

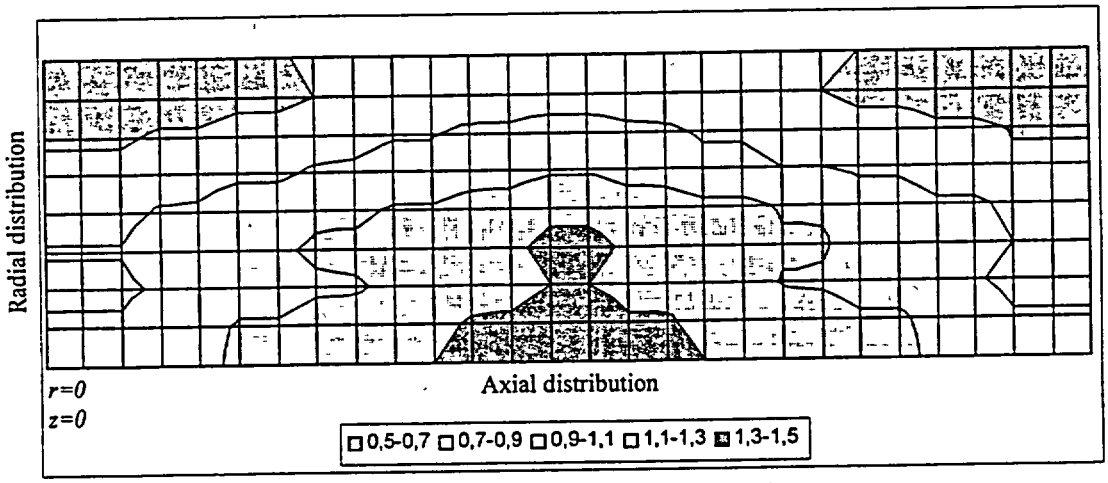

Fig 2. Power distribution at Xe equilibrium

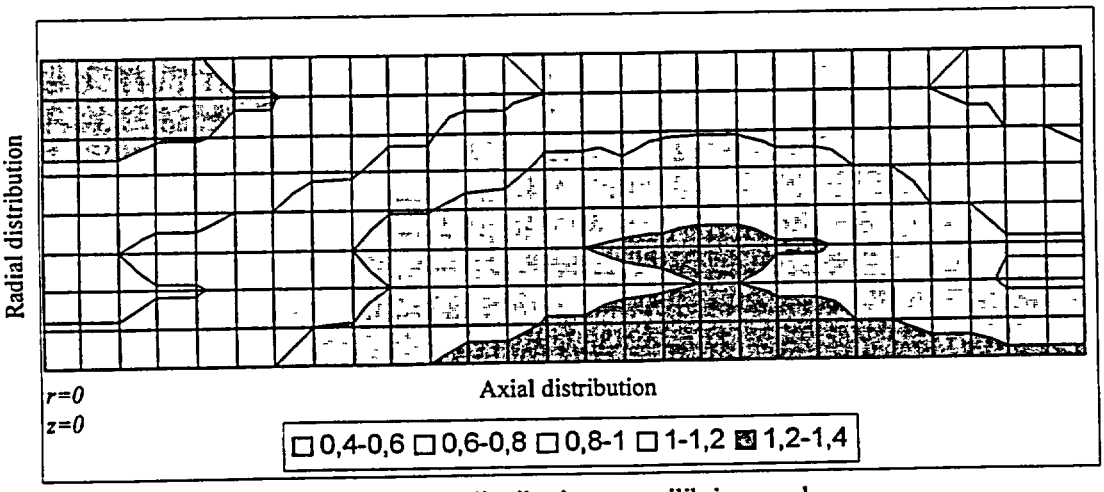

Fig 3. Power distribution at equilibrium cycle

In this approach an approximation is made by assuming that only fresh fuel is inserted to the top of the reactor core. In reality fuel with low burnup will be reused instead of a fresh fuel pebble. Also the flow lines of pebbles within the core with different downward velocity is not taken into account for the sake of simplicity. These approximations introduce errors which will be tackled in the future work.

5. References

[1] U. E. Sikik, H. Dikmen, Y. Çeçen, Ü. Çolak, O. K. Kadiroglu, "Thorium and plutonium Utilization in PBMR", Proceeding of the Advanced Reactors with Innovative Fuels, (ARWIF-2001) Chester, UK, 22-24 Oct. 2001.

[2] L. M. Petrie, N. F. Landers "KENOV.a: An Improved Monte Carlo Criticality Program With Supergrouping", NUREG/CR-0200, Revision 6, Volume 2, Section F11, ORNL/NUREG/CSD-2/R6, September 1998.

[3] "Review of the Pebble Bed Modular Reactor (PBMR) Plant" Current Status and Future Development of Modular High Temperature Gas Cooled Reactor Technology, p.21, IAEA-TECDOC-1198, 2000.

[4] O. W. Hermann, R. M. Westfall, "ORIGEN-S: Scale System Module to Calculate Fuel Depletion, Actinide Transmutation, Fission Product Buildup and Decay, and Associated Radiation Source Terms", NUREG/CR-0200, Revision 6, Volume 2, Section F7, ORNL/NUREG/CSD-2/V2/R6, September 1998.

DR. OSMAN KEMAL KADIROGLU

Dipl. Engineering (1968)	Istanbul Technical University School of Mechanical Engineering
M.S. (1972)	MIT Nuclear Engineering Department
Sc. D. (1976)	MIT Nuclear Engineering Department
1980-present	Hacettepe University Nuclear Engineering Department

YIGIT CECEN
Born in 1976

Nuclear Engineering (2000)	Hacettepe University Nuclear Engineering Department
M.S. (2002)	Hacettepe University Nuclear Engineering Department
2000-present	Hacettepe University Nuclear Engineering Department

ECONOMIC STUDY OF SEAWATER DESALINATION FOR 300MW(E) HIGH TEMPERATURE GAS-COOLED REACTOR (HTR) BY REVERSES OSMOSIS (RO)

L. Tian, J. Guo and Y. Sun, Institute of Nuclear Energy Technology,
Tsinghua University, China

Paper will be handed out separately